2010

Membrane-bound Matrix Metalloproteinases Influence Reactive Synaptogenesis Following Traumatic Brain Injury

Kelly Warren
Virginia Commonwealth University

Membrane-bound Matrix Metalloproteinases Influence Reactive Synaptogenesis Following Traumatic Brain Injury

A dissertation submitted in partial fulfillment of the requirements for the degree of Doctor of Philosophy at Virginia Commonwealth University.

by

Kelly Michelle Warren
B.S. Kinesiology, James Madison University, 2000
M.P.T. University of Saint Augustine for Health Sciences, 2002

Director: Linda L. Phillips, Ph.D.
Professor
Anatomy and Neurobiology Department

Virginia Commonwealth University
Richmond, Virginia
July, 2010

Acknowledgement

"Learning is a treasure that will follow its owner everywhere" ~ Chinese proverb

First and foremost, I would like to acknowledge and thank my mentor and friend Dr. Linda Phillips. Over the past 5 years she has respectfully challenged me to grow both professionally and personally. I marvel at her unending energy and determination when developing and answering new questions. Through her example I have learned that the mind must never be stagnant, but rather must maintain a high level of curiosity to thrive. She has also taught me the importance of hard work, self-responsibility and honesty inside and outside of the classroom and laboratory. Her dedication to teaching and scientific inquiry will inspire me to excel in both areas throughout my career as an educator. Thank you for your wisdom, advice, support and friendship.

I would also like to thank the ladies of the lab, Nancy, Raiford and Lesley. Not only have I learned invaluable techniques in the lab, but I have thoroughly enjoyed developing friendships with each and every one of you. This experience would not have been the same without you there along the way. Thank you all for your time, expertise, laughter, and banter. I will miss you all dearly.

To my remaining committee members Dr. Tom Reeves, Dr. Robert Hamm, Dr. Helen Fillmore, and Dr. John Povlishock, thank you for your guidance and mentoring over the past 5 years. I felt so fortunate to have such a well-rounded committee of

scientists and educators who were willing to take time to share their expertise. Each of you added a unique perspective that enhanced my development as a scientist and educator. Thank you for your constant encouragement and willingness to assist whenever I called upon you.

Finally I would like to thank my parents and brother for their undying love and support. I know they never expected to have a “professional student” on their hands when I entered the world, but they have accepted and encouraged my intellectual curiosity over the past 32 years without question or concern. I am truly blessed to have a family who is so supportive of my goals and dreams. I am who I am and where I am because of you all. I love and thank you.

Table of Contents

List of Tables vii
List of Figures viii
List of Abbreviations xi
Abstract xiv
Chapter 1: Introduction 1
Traumatic Brain Injury 2
Incidence, Demographics, and Classification 2
TBI Pathophysiology 5
Neuroplasticity and TBI 8
Plasticity Within the Injured Hippocampal Formation 12
Hippocampal Structure 12
Hippocampal Function and Response to Injury 17
Injury-Induced Synaptogenesis 19
Adaptive vs. Maladaptive Plasticity 21
Matrix Metalloproteinases 24
General Classification, Structure, and Function 24
Membrane-bound MMPs 30
Membrane-bound MMPs and the Nervous System 36
MT5-MMP 37
ADAMs 46
ADAM-10 and the Nervous System 54
Cadherins 61

Classic Cadherins 61
N-cadherin and the Nervous System 65
Experimental Hypotheses 77
Chapter 2: Classification of MT5-MMP, ADAM-10 and N-cadherin during Adaptive and Maladaptive Injury-induced Synaptogenesis 79
Abstract 80
Introduction 81
Methods 88
Results 96
Discussion 121
Summary 136
Chapter 3: MMP Inhibition Improves Synaptic Efficacy and Stabilization during Injury-induced Synaptogenesis 138
Abstract 139
Introduction 141
Methods 145
Results 155
Discussion 176
Summary 188
Chapter 4: General Discussion 189
Summary of Results 190
Roles of Membrane-bound MMPs in Synaptogenesis 192
Understanding Maladaptive Synaptic Plasticity 197
Potential Benefits of MMP Inhibition on Recovery 198
Signaling Pathways and Plasticity 199
Future Directions 204
Final Remarks 209
References 210

Appendices 261
Appendix A 261
Appendix B 264
Appendix C 274
Appendix D 283
Appendix E 285
Vita 288

List of Tables

1.1 Microarray Analysis of MT5-MMP, ADAM-10, and N-cadherin Transcripts at 7d post-UEC and TBI+BEC 116

List of Figures

1.1 Hippocampal Structure and Circuitry 14

1.2 Matrix Metalloproteinase (MMP) Structure and Subgroups 29

1.3 A Disintegrin and Metalloproteinase (ADAM) General Structure 51

1.4 Classic Cadherin Structure and Interaction with Cytoplasmic Proteins 64

1.5 Cleavage Products of N-cadherin..... 76

2.1 Proposed Synaptic and Peri-synaptic Protein Localization 87

2.2 Potential Hippocampal Molecular Forms of MT5-MMP, ADAM-10 and N-cadherin Observed in Protein Analysis..... 100

2.3 Hippocampal MT5-MMP, ADAM-10 and N-cadherin Protein Expression following UEC..... 102

2.4 Hippocampal MT5-MMP, ADAM-10 and N-cadherin Protein Expression following TBI+BEC 106

2.5 Molecular Layer Localization of ADAM-10, MT5-MMP, and N-cadherin with GFAP at 7d following UEC 110

2.6 Molecular Layer Localization of ADAM-10, MT5-MMP, and N-cadherin with GFAP at 7d following TBI+BEC..... 112

2.7 Quantitative RT-PCR Molecular Layer mRNA Expression of MT5-MMP, ADAM-10, and N-cadherin at 7d post-UEC and TBI+BEC 119

3.1 Comparison of MT5-MMP, ADAM-10, and N-cadherin Hippocampal Protein Expression: TBI+BEC-untreated and TBI+BEC-treated animals at 15d..... 158

3.2 Representative field potentials evoked in the Schaffer collateral afferent input to CA1 161

3.3 Effects of TBI+BEC injury and GM6001 treatment on LTP and LTD..... 164

3.4 Effects of TBI+BEC injury and GM6001 treatment on PFF 169

3.5 Effect of TBI+BEC injury and GM6001 treatment on Cognitive Recovery..... 172

3.6 Effect of TBI+BEC injury and GM6001 treatment on Dendritic and Synaptic Cytoarchitecture at 15d 175

Appendix A Figures 261

A-1 Unilateral Entorhinal Cortex Lesion Stereotaxic Sites 262

A-2 Craniectomy Sites and Fluid Percussion Injury Device 263

Appendix B Figures 264

B-1 Co-migration of MT5-MMP and TIMP-2 in Protein Analysis 265

B-2 Hippocampal Protein Expression of Additional MT5-MMP Forms following UEC 266

B-3 Hippocampal Protein Expression of Additional ADAM-10 Forms following UEC 267

B-4 Hippocampal Protein Expression of Additional N-cadherin Forms following UEC 268

B-5 Hippocampal Protein Expression of Additional MT5-MMP Forms following TBI+BEC 269

B-6 Hippocampal Protein Expression of Additional ADAM-10 Forms following TBI+BEC 270

B-7 Hippocampal Protein Expression of Additional N-cadherin Forms following TBI+BEC 271

B-8 Representative β-actin Load Control for Protein Analysis 272

B-9 Downstream Intracellular Signaling as a Result of N-cadherin Processing by ADAM-10 273

Appendix C Figures 274

C-1 Molecular Layer Localization of ADAM-10 with GFAP at 2 and 15d following UEC 275

C-2 Molecular Layer Localization of ADAM-10 with GFAP at 2 and 15d following TBI+BEC 276

C-3 Molecular Layer Localization of MT5-MMP with GFAP at 2 and 15d following UEC 277

C-4 Molecular Layer Localization of MT5-MMP with GFAP at 2 and 15d following TBI+BEC 278

C-5 Molecular Layer Localization of N-cadherin with GFAP at 2 and 15d following UEC 279

C-6 Molecular Layer Localization of N-cadherin with GFAP at 2 and 15d following TBI+BEC 280

C-7 Representative Minus Primary Controls for ADAM-10, MT5-MMP, and N-cadherin immunostaining with GFAP 281

C-8 Representative Molecular Layer Localization of MT5-MMP, ADAM-10, and N-cadherin with microglial markers CD-11/Iba-1 282

Appendix D Figures 283

D-1 Molecular Layer Co-localization of MT5-MMP RNA transcript with GFAP 7d post-UEC 284

Appendix E Figures 285

E-1 Hippocampal Protein Expression of β-catenin following TBI+BEC 286

E-2 Molecular Layer Protein Expression of β-catenin following TBI+BEC 287

List of Abbreviations

ABP……...AMPA binding protein

AD……..…….....Alzheimer's Disease

ADAM…….……...A Disintegrin and Metalloproteinase

ADAMTS……..……. ……..ADAM with a Thrombospondin type 1 motif

AMPA…….....α-amino-3-hydroxyl-5-methyl-4-isoxazole-propionate

APP……...Amyloid Precursor Protein

ATP…….....Adenosine Triphosphate

BBB……Blood Brain Barrier

C/A……..…….Commissural/Associational

CD……...Cytoplasmic Domain

CN……..Central Nervous System

CREB……....cAMP Response element Binding

CSF……. ……..Cerebral Spinal Fluid

CSPG……..Condroitin Sulfate Proteoglycan

CT……...Computer Tomography

CTD……Crossed Temporodentate

CTF…….....C-Terminus Fragment

DG……..Dentate Gyrus

DRG……..Dorsal Root Ganglion

DSPG……..Dermatan Sulfate Proteoglycan

dTBI……..……Diffuse Traumatic Brain Injury

DTI……..……..Diffusion Tensor Imaging

EAA……Excitatory Amino Acids

EC……Entorhinal Cortex

ECM……..Extracellular Matrix

EDTA……Ethylenediamine Tetraacetic Acid

EGF……...Epidermal Growth Factor

EM…..……..Electron Microscopy

ERK……...……Extracellular Signal-Regulated Kinase

FAK……..Focal Adhesion Kinase

fEPSP……..……..…...Field Excitatory Postsynaptic Potential

fMRI……..……..…..Functional Magnetic Resonance Imaging

FPI……...……Fluid Percussion Injury

GC……...Granule Cell

GCS……Glasgow Coma Scale

GFAP……Glial Fibrillary Acidic Protein

GPI……..……Glycosylphosphatidylinositol

HFS……..……..……..……High Frequency Stimulation

HLD……..……Hemopexin-like Domain

HSPG……..……..…….Heparin Sulfate Proteoglycan

ICP……..Intracranial Pressure

IHC……..…….... Immunohistochemistry

IML……..…..Inner Molecular Layer

JMD……..……Juxtamembrane Domain

KO……..……Knock-out

LOC……...Loss of Consciousness

LPS……..……..……...Lipopolysaccaride

LTD……..Long-term Depression

LTP……..Long-term Potentiation

ML……..…….Molecular Layer

MMP…….... Matrix Metalloproteinase

MS…….……..Multiple Sclerosis

MT-MMP……..…Membrane-type Matrix Metalloproteinase

MWM…….……Morris Water Maze

NMDA…….……*N*-methyl-D-aspartic acid

NT…….……N-Terminus Fragment

OML…….Outer Molecular Layer

PD……..…Parkinson's Disease

PET……..…Positron Emission Tomography

PNS……..…..Peripheral Nervous System

PPF……..……..…….Paired-pulse Facilitation

PSD…….…Post-synaptic Density

PTA……..….Post-traumatic Amnesia

RIP…….…….Regulated Intramembrane Proteolysis

SCI…….……..……...……Spinal Cord Injury

TBI……...Traumatic Brain Injury

TBI+BEC……..……Moderate Central Fluid Percussion + Bilateral EC lesions

TGN……..……..Trans Golgi Network

TIMP……Tissue Inhibitor of Metalloproteinase

TMD…….Transmembrane Domain

UEC……..……..….Unilateral Entorhinal Cortex

VACC……..……..…Voltage Activated Calcium Channels

WB…….…….Western Blot

WT……..…Wild-type

Abstract

MEMBRANE-BOUND MATRIX METALLOPROTEINASES INFLUENCE REACTIVE SYNAPTOGENESIS FOLLOWING TRAUMATIC BRAIN INJURY

By: Kelly Michelle Warren, MPT

A dissertation submitted in partial fulfillment of the requirements for the degree of Doctor of Philosophy at Virginia Commonwealth University

Virginia Commonwealth University, 2010

Major Director: Linda L. Phillips, Ph.D., Professor,
Anatomy and Neurobiology Department

Traumatic brain injury (TBI) produces axonal damage and deafferentation, triggering injury-induced synaptogenesis, a process influenced by matrix metalloproteinases (MMP) and their substrates. Here we report results of studies examining the expression and potential role of two membrane-bound MMPs, membrane-type 5-MMP (MT5-MMP) and a disintegrin and metalloproteinase-10 (ADAM-10), along with their common synaptic substrate N-cadherin, during the period of reactive synaptogenesis. Protein and mRNA expression of MT5-MMP, ADAM-10 and N-cadherin were compared in two TBI models, one exhibiting adaptive plasticity (unilateral entorhinal cortex lesion; UEC) and the other maladaptive plasticity (fluid percussion injury + bilateral EC lesions; TBI+BEC), targeting 2, 7, and 15d postinjury intervals. In adaptive UEC plasticity, membrane-bound MMP expression was elevated during synaptic degeneration (2d) and

regeneration (7d), and normalized at 15d. By contrast, N-cadherin expression was significantly decreased at 2 and 7d after UEC, but increased during 15d synaptic stabilization. In maladaptive plasticity, 2d membrane-bound MMP expression was dampened compared to UEC, with persistent ADAM-10 elevation and reduced N-cadherin protein level at 15d. These results were supported by 7d microarray and qRT-PCR analyses, which showed transcript shifts in both hippocampus and dentate molecular layer (ML) for each model. Parallel immunohistochemistry revealed significant MT5-MMP, ADAM-10 and N-cadherin localization within ML reactive astrocytes, suggesting a glial synthetic or phagocytotic role for their processing during recovery. We also investigated the effect of MMP inhibition on molecular, electrophysiological, behavioral and structural outcome at 15d following TBI+BEC. MMP inhibitor GM6001 was administered at 6 and 7d postinjury, during elevated MT5-MMP/ADAM-10 expression and synapse regeneration. MMP inhibition showed: 1) reduced ADAM-10 and elevated N-cadherin protein expression, generating profiles similar to 15d post-UEC, 2) attenuation of deficits in the initiation phase of long-term potentiation, and 3) improved hippocampal dendritic and synaptic ultrastructure. Collectively, our results provide evidence that membrane-bound MMPs and N-cadherin influence both adaptive and maladaptive plasticity in a time and injury-dependent manner. Inhibition of membrane-bound MMPs during maladaptive plasticity produces more adaptive conditions, improving synaptic efficacy and structure. Thus, targeting MMP function and expression have potential to translate maladaptive plasticity into an adaptive process, facilitating improved recovery.

Chapter 1

Introduction

TRAUMATIC BRAIN INJURY

Incidence, Demographics, and Classification

Traumatic brain injury (TBI) is defined as any external force applied to the head that disrupts the normal function of the brain. Each year, approximately 1.7 million Americans sustain different severities of TBI, often leading to long-term and life-altering physical, cognitive and/or psychosocial impairments. Of these 1.7 million cases, approximately 1.365 million are admitted, treated and released from an emergency department, 275,000 are hospitalized, and it is estimated that 52,000 cases result in fatalities (Faul et al., 2010). In addition to these staggering statistics, another cohort of TBI sufferers are never seen or treated by a medical professional, therefore indicating an even larger number of annual TBI incidents. In the United States (US), children aged 0-4 years, adolescents 15-19 years and adults over the age of 65 years are among the groups most likely to sustain a TBI. In each of these age groups, males have a higher TBI rate than females, which is often attributed to inherent risky behaviors (Faul et al., 2010). The leading causes of TBI include falls, motor vehicle accidents, violence/assault, and sports-related head injuries (NIH, 1999). TBI incidents each year in the US outnumber cases of multiple sclerosis, breast cancer, and spinal cord injury combined, making it one of most pervasive medical epidemics facing our society today (Weber and Maas, 2007). Due to the complicated and patient-specific nature of TBI, evidence-based diagnostic methods and consistency of standards of care have been difficult to define and implement across medical institutions. Consequently, TBI remains a “silent epidemic” that requires continual laboratory and clinical investigation with the common goal to limit the severity and incidence of persistent deficits that affect the millions of Americans who are living with the consequences of TBI today.

TBI is classified as either mild, moderate, or severe, however the diagnosis and treatment of patients who fall within this spectrum is not always clear. Within these broad groups, patients can be further classified based on the type of TBI sustained, including open vs. closed head injury, contusions, hematomas, ischemic damage, diffuse axonal injury, and blast injury to name a few. Based on these categories, patients are often classified as either having a focal or diffuse injury, however these two types of injury are not exclusive and often found to coexist and contribute to morbidity (Graham et al, 2000). All aforementioned sub-classifications are determined upon admission, after patients are put through a battery of tests designed to further delineate mechanism of injury, determine prognosis, and guide treatment. Postinjury details, such as duration of loss of consciousness (LOC) and post-traumatic amnesia (PTA), are collected and used as initial prognostic indicators. A longstanding component of the initial and ongoing post-traumatic assessment is the Glasgow Coma Scale (GCS), which was designed in the 1970's to quantify injury severity and outcome by scoring eye opening, motor and verbal responses (Teasdale and Jennett, 1974). Today, the GCS is still an integral part of initial and follow-up patient assessment however it cannot stand alone in the postinjury care process, and additional specific tests are necessary to properly classify TBI severity and outcome. With technological advances, greater emphasis has been placed on the use of different imaging techniques such as computer tomography (CT), magnetic resonance imaging (MRI), functional MRI (fMRI), positron emission tomography (PET), and diffusion tensor imaging (DTI) to improve classification through identifying different postinjury pathologies and structural changes. Hospitalized TBI patients also may undergo intracranial pressure (ICP) and Brain Tissue Oxygen

monitoring as a more sensitive method of determining injury classification, extent and prognosis. Additionally, the measurement of brain biomarkers in serum and cerebral spinal fluid (CSF) samples continues to show great promise in improving diagnostic accuracy following TBI (Povlishock and Katz, 2005). Despite the number of tests and measurement that have been developed, consistency between medical institutions remains poor, and a universally accepted protocol for TBI classification, diagnosis, and treatment has yet to be created.

However, current broad categories of mild, moderate, and severe TBI carry their own set of postinjury impairments. Depending on the level of severity, patients may experience acute and chronic neurological, cognitive, behavioral and social consequences. Neurological consequences of TBI may include acute impairments in sensory, motor, and autonomic functions, followed by long-term problems such as movement disorders, seizures, visual impairments and sleep disorders (NIH, 1999). Cognitively, patients may experience postinjury memory impairment and difficulty with attending to different tasks for periods of time. If the frontal lobe is involved in the injury, higher executive skills such as judgment, insight, abstract thinking and information processing may be affected. Often times, TBI patients exhibit behavioral and social deficits including increased aggression, agitation, hyper-sexuality, and lack of social inhibition. Collectively, these consequences leave patients and their families/caregivers feeling lost, hopeless, and overwhelmed well after the actual TBI incident. Proper coordination of medical care and involvement in physical, occupational and speech therapies, family/caregiver training, and social reintegration programs greatly improve outcomes and quality of life following TBI.

TBI Pathophysiology

In order to appreciate the complexity of TBI pathophysiology it is important to review the elements which contribute to injury mechanism. As indicated above, TBI is caused by an external force applied to the cranium that causes damage to the brain. The amplitude, timing, and direction of the force directly relates to the amount and type of mechanical stress placed on the brain tissue and subsequent injury. It is well accepted that the primary traumatic insult involves exposure to mechanical force that exceeds normal tolerable limits of the affected tissue, therefore leading to structural damage. Mechanical damage caused by the primary injury event triggers a series of secondary injury responses that invoke additional downstream cellular responses and tissue damage. The timing and severity of the secondary injury response depends on the primary injury, as well as the state of the tissue prior to the initial insult. Age and repetitive traumatic brain injuries have been shown to influence the extent of secondary injury response and recovery.

Multiple *in vivo* and *in vitro* studies have identified a number of intracellular events that follow the initial traumatic insult. Within the CNS, this response involves not only neurons, but also astroglia and other supportive cells, microvasculature, and extracellular matrix molecules, all capable of responding during either primary or secondary phases of injury. Subsequent to the frank membrane breakdown, principal pathology develops in metabolic pathways, particularly those related to adenosine triphosphate (ATP) production. Mitochondria are highly vulnerable and part of the secondary injury cascade affecting both aerobic and anaerobic mechanisms (Verweij et al., 2007; Liftshitz et al., 2003; Gilmer et al., 2009). In addition, TBI elicits a significant

immune response throughout the brain, directly releasing upstream modulators of cell signaling such as chemokines and cytokines (reviewed by Lenzlinger et al., 2001; Israelsson et al., 2008; Lloyd et al., 2008). These molecules are also intimately involved in stabilization of the neuronal/vascular interface within the injured brain, ultimately affecting cerebral blood flow, intracranial pressure (ICP) and O_2/CO_2 exchange. Historically, the primary mechanical disruption of neuronal membrane has been linked to massive pre-synaptic depolarization and the excessive release of excitatory amino acids (EAA), especially glutamate and aspartate (Hayes et al., 1992; Yoshino et al., 1992; Palmer et al., 1993). EAA release activates excitatory neurotransmitter receptors, such as the *N*-methyl-D-aspartate (NMDA) type, allowing for dramatic post-synaptic intracellular shifts in Na^{2+}, K^{+} and Ca^{2+} ions (Faden et al., 1989; Katayama et al., 1990; Hayes et al., 1992; McIntosh et al., 1994; Wolf et al., 2001). Such excessive neuroexcitation has been recognized as a major contributor to injury-induced structural and functional impairments. Other studies have also probed the role of dopamine as a modulator of the neuroexcitatory cascade following TBI (Zhu et al., 2000; Massucci et al., 2004; Wanger et al., 2005; as reviewed by Bales et al., 2009). In an attempt to attenuate the impaired excitatory/inhibitory imbalance generated by TBI, animal studies first applied *N*-methyl-D-aspartic acid (NMDA) antagonists as postinjury therapy, showing protective effects against injury-induced deficits and the facilitation of recovery following TBI (Faden et al., 1989; Hayes et al., 1992; Hamm et al, 1993; Phillips et al., 1998). Although NMDA antagonism showed therapeutic efficacy in animal models of TBI, translation to the clinic has proven difficult, further indicating the complexities and variation among human TBI cases (Muir, 2006). More recently, dopamine agonists,

which significantly attenuate the negative effects of excessive neuroexcitation following rodent TBI (Dixon et al, 1999; Kline et al., 2004; Wanger et al., 2005 and 2007), are being applied in clinical trials (as reviewed by Warden et al., 2006). Pharmacologically targeting these different neuropathological mechanisms has potential to improve outcome following human TBI.

Mechanical neuronal insult induced by TBI also leads to secondary deafferentation and, in severe cases, neuronal death. Following injury, a subpopulation of vulnerable neurons also sustains mechanoporation of their axolemmae. This process is mediated by ionic imbalance, Ca 2+ influx, mitochondrial failure, breakdown in axonal transport and cytoskeletal compaction, ultimately resulting in the disconnection of affected axons. These secondary events are observed in both animals and humans, and are signaled by a number of molecular pathways activated by the primary insult (Erb and Povlishock, 1991; Povlishock et al., 1992). In certain cases, postinjury membrane damage can generate both necrotic and apoptotic neuronal death, ultimately resulting in the loss of susceptible neurons (Farkas and Povlishock, 2007). Ultrastructural analysis of these dying neurons revealed profiles with pyknotic nuclei, swollen mitochondria, vacuolated cytoplasm, and membrane disruption (Dietrich et al., 1994). With diffuse TBI (dTBI), neuronal loss can be demonstrated in the neocortex, hippocampal fields, dentate gyrus, thalamus, and at scattered sites throughout the caudate/putamen (Farkas and Povlishock, 2007). While the mechanically-induced membrane disruption associated with TBI is generally believed to trigger neuron death cascades, it is important to note that intact cells with damaged axons are capable of delayed membrane resealing, therefore eschewing death and exhibiting the potential for

regeneration (Farkas et al., 2006). The process of regeneration actually begins with axonal disconnection at the site of injury, resulting from impaired axonal transport, neurofilament degradation and cytoskeletal compaction (Pettus et al., 1994; Maxwell et al., 1997; Stone et al, 2004). Several hours to days following injury the proximal damaged axon segment swells and the distal segment is disconnected, undergoing Wallerian degeneration (Povlishock, 1992; Povlishock and Pettus, 1996; Kelley et al., 2005; Buki and Povlishock, 2006). The ultimate effect of such degeneration is the loss of pre-synaptic terminals at neurons targeted by these damaged axons (Erb and Povlishock, 1991). This produces deafferentation of post-synaptic sites, inducing the process of reactive synaptic plasticity at those sites. Because TBI produces diffuse axonal injury in the context of a complex pathology, it is difficult to study a focal group of affected axons and their deafferented targets. Our focus has been to better understand the potential for recovery following such diffuse axonal injury by using a model which generates this complex pathology in the presence of focal deafferentation. The effects of TBI-induced axonal injury on synaptic recovery can then be examined in the context of adaptive neuroplasticity.

Neuroplasticity and TBI

Historically, it was believed that the brain was a hardwired structure, lacking the capacity to undergo neurogenesis or structural alterations beyond the period of its development. However, over the course of the last century this theory shifted as evidence emerged that demonstrated the concept of “plasticity” within the nervous system, or neuroplasticity. Neuroplasticity refers to the ability of the nervous system to be altered though processes including neurogenesis and synaptogenesis, often in

response to some type of activity, experience, or even injury (Keyvani and Schallert, 2002). Injury-induced deafferentation is well documented to induce a regenerative neuroplasticity within the central nervous system (CNS), producing both new terminal sprouts from damaged axons and reforming new synaptic connections (Lynch et al., 1976; Scheff et al., 1977; as reviewed by Steward, 1989; Deller et al., 1996). Depending upon the injury location and severity, this response may result in favorable recovery (adaptive neuroplasticity) or unfavorable recovery (maladaptive neuroplasticity). The process of synaptic neuroplasticity induced by CNS injury is termed reactive synaptogenesis. In rodent models, reactive synaptogenesis occurs over a two week period following injury, stepping through a series of phases which include early degeneration, subsequent regrowth and final stabilization of affected synapses. Injury-induced synaptogenesis within the hippocampus will be discussed in detail below. Relative to TBI, animal models which reproduce mild and moderate injury, along with diffuse axotomy, tend to achieve adaptive recovery over time after injury (Phillips and Reeves, 2001; Clausen et al., 2005; Gurkoff et al., 2006). It is assumed that this occurs because sufficient spared axons sprout into deafferented areas and form new synapses to restore function. Conversely, more severe combined TBI pathology clearly results in maladaptive recovery, where fewer synaptic connections are replaced and those generated appear dysfunctional (Phillips and Reeves, 2001; Phillips et al., 1994). These animal studies suggest that the extent of adaptive and maladaptive present following human TBI may be correlated with injury severity and the extent of recovery possible. Although certainly not exclusive, we have shown that modulation of the extracellular synaptic environment by matrix metalloproteinases (MMPs) occurs

during both adaptive and maladaptive plasticity, and may be a critical to the enhancement of recovery following TBI.

Surrounding supportive cells, particularly local astrocytes, are also affected by the primary TBI insult, which is evident by the morphological and functional changes that they undergo. Normally, astrocytes support CNS homeostasis through maintaining ionic balance, interfacing with vessels to stabilize the blood-brain barrier (BBB), providing nutrition for neurons, and recycling neurotransmitters (Wilhelmsson et al, 2006). Following brain injury, astrocytes undergo a transformation to become "reactive", which is characterized by cellular hypertrophy and hyperplasia, thickening and elongation of main cellular processes, and increased glial fibrillary acidic protein (GFAP) expression (Baldwin and Scheff, 1996; Amaducci et al, 1981; Wilhelmsson et al, 2006). These morphologically distinct astrocytes often infiltrate the pericontusional region and may act to either inhibit or promote recovery. Although infiltrating reactive astrocytes form a "glial scar" which inhibits regeneration in the nervous system (Liuzzi and Lasek, 1987; Silver and Miller, 2004; Goldshmit and Bourne, 2010), they have also been shown to protect adjacent uninjured tissue from further secondary damage and decrease the inflammatory response (White and Jakeman, 2008; Sofroniew, 2005, Su et al., 2009; Rasouli et al., 2009), therefore revealing dual roles. As a result of injury, reactive astrocytes can alter their expression of ion transporters, neurotransmitter receptors, as well as matrix proteins and proteases which can be membrane bound or secreted into the extracellular space (Wells et al., 1996; Muir et al., 2002; Falo et al., 2006; Belanger and Magistretti, 2009). Depending on the injury severity, the expression of these proteins can determine the role of local reactive astrocytes in the regulation of

brain pH and neuroexcitability and their influence during injury-induced plasticity (Laird et al., 2008). For example, secreted and membrane-bound MMPs are upregulated in reactive astrocytes postinjury, and can influence plasticity through interaction with their extracellular matrix (ECM) substrates or synaptic junction modulation (Falo et al., 2006; Kim et al., 2005). Secreted ECM molecules, such as proteoglycans, are critical to the formation of the glial scar and often are vulnerable to MMP processing after CNS injury (Pizzi and Crowe, 2007). Reactive astrocytes also play a direct role in the neuroplastic response by phagocytic removal and degradation of damaged tissue (Sofroniew, 2005). In some injury models, reactive astrocytes fail to express inwardly reflecting K^+ channels, therefore compromising their ability to buffer extracellular K^+, maintain ion homeostasis and dampen neuronal excitation (Bordey and Sontheimer, 1998; D'Ambrosio et al., 1999; Bordey et al., 2001). Clearly, the astrocytic response following TBI appears to be injury specific and shows the capacity to either facilitate or impede neuroplastic recovery. Despite their often opposing functional roles, reactive astrocytes are important players in the pathophysiology of TBI. The magnitude and direction of astrocytic response may correlate with injury severity and outcome, therefore making them potential therapeutic targets to facilitate adaptive synaptic plasticity.

Based on this brief review, it is evident that postinjury neuropathology is a complex and dynamic series of events that can result in a wide range of cellular damage and dysfunction. While each element of the postinjury process is important, here we choose to focus on the recovery component of injury-induced synaptogenesis, particularly within the hippocampus of the injured brain.

PLASTICITY WITHIN THE INJURED HIPPOCAMPAL FORMATION

Multiple studies have shown that CNS injury induces a synaptogeneic response, particularly in regions of high plasticity, such as the subventricular zone, dentate gyrus and hippocampus (as reviewed by Taupin, 2006). While there is extensive literature describing activity, experience and injury-induced plasticity in these different regions, the focus of this review will be the injury-induced synaptogenesis within the hippocampus.

Hippocampal Structure

The hippocampus is comprised of two interlocked U-shaped sectors that lie deep within the temporal lobe and are surrounded by entorhinal (EC), parahippocampal and perirhinal cortices. The fascia dentata (or dentate gyrus) and the hippocampal formation (CA1-CA3 laminae) interlock to form a structure that contains a limited number of neuron types that are tightly packed into distinct layers (Fig. 1.1). Intrinsic and extrinsic afferent inputs synapse in dendritic fields of the dentate and hippocampus proper, linking the hippocampus to other limbic structures including the amygdala, cingulate gyrus, mammilary bodies thalamus, EC, and septal nuclei. The organized limbic circuitry (discussed below) and functions of the hippocampus are due, in part, to the structural organization of the dentate gyrus and hippocampal formation (reviewed by Amaral et al., 2007).

The tri-laminar dentate gyrus is made up of granule, molecular and polymorph (hilar) layers, and resembles an arrowhead with suprapyramidal and infrapyramidal blades. The granule cell layer contains small, densely packed excitatory granule cells along with scattered inhibitory dentate pyramidal basket cells at the interface of the

Figure 1.1 Hippocampal Structure and Circuitry. Schematic representation of hippocampal structure and circuitry, including dentate gyrus (DG) and hippocampal fields CA3- CA1. Primary afferent inputs include lateral and medial perforant path (LPP; MPP) projections from the entorhinal cortex (EC) and secondary inputs from contralateral associational-commissural (CA) projections. The tri-synaptic loop circuit includes PP projections to DG granule cell dendrites, which send mossy fiber (MF) projections to the CA3 field. CA3 pyramidal neurons send contralateral AC projections and primary Schaffer collateral (SC) projections to CA1 pyramidal cell dendrites, which send efferents to the subiculum (Sb) and on to the lateral and medial EC (LED; MEC).

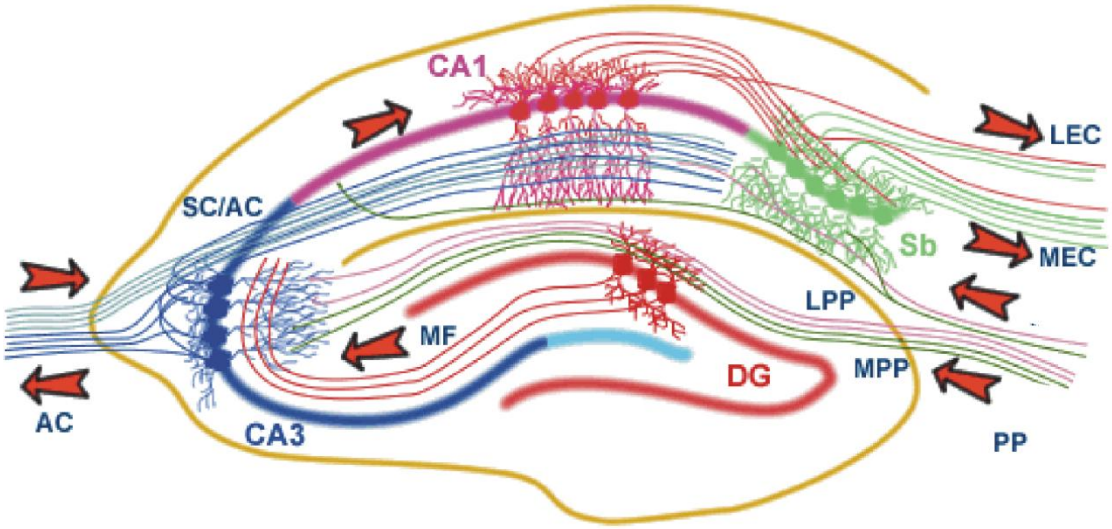

granule and polymorph layers. The spiny apical dendrites of granule cells extend into the molecular layer, their outermost processes reaching the hippocampal fissure. These dendrites receive primarily excitatory input from the EC through the perforant (ipsilateral EC) and crossed temporodentate (CTD; contralateral EC) pathways, as well as Commissural-Associational (C/A) and septal projections. The granule cells give rise to axonal projections called mossy fibers that travel through the hilar polymorph layer and terminate in the CA3 field of the hippocampus. Along the mossy fiber course, these axons extend collateral afferents to synapse on the proximal dendrites of the hilar mossy cells, basal dendrites of the pyramidal basket cells and GABAergic interneurons. The mossy fibers serve as the initial segment of the hippocampal 'trisynaptic loop", linking granule neurons with CA3 and CA1 pyramidal neurons.

The hippocampal formation is comprised of two main sectors of pyramidal neurons, *regio superior* and *regio inferior*. The *regio superior*, or CA1 field, contains multiple rows of medium-sized to large pyramidal neurons, whose apical dendrites receive their principal input from the Schaffer collateral axons. The Schaffer collateral projections arise from large pyramidal neurons located within the *regio inferior*, or CA3 field. The apical dendrites of CA3 neurons receive afferent mossy fiber projections from the dentate granule cell layer. CA1 and CA3 fields are arranged in organized layers similar to those observed in the dentate gyrus, however, additional layers are identified based on the specific features of pyramidal cell input. These layers include (dorsal to ventral) the *alveus*, *stratum oriens*, *stratum pyramidale*, *stratum radiatum*, and *stratum lacunosum/moleculare*. The *alveus* contains pyramidal cell axons that are either directed towards the fimbria or subiculum. The *stratum oriens* contains pyramidal and

basket cell basal dendrites and septal afferents. The *stratum pyramidale* is made up of pyramidal cell somas, whose proximal and distal apical dendrites are localized in the *stratum radiatum* and *lacunosum/moleculare*, respectively. There is an additional layer, *stratum lucidum*, within the CA3 field which is situated between the *stratum pyramidale* and *stratum radiatum* that contains the mossy fiber projections (as reviewed by O'Keefe and Nadel, 1978).

While there are intrinsic connections within the dentate gyrus and hippocampus proper and between contralateral hippocampal structures, there are also a number of extrinsic inputs and outputs that link the hippocampus to other brain regions. Hippocampal afferent inputs and efferent outputs are primarily associated with the circuit of Papez, and include a number of cortical and subcortical connections. Subcortically, the hippocampus makes connections with the anterior nucleus of the thalamus, hypothalamic mammillary bodies and septal nucleus of the basal forebrain through the fornix, as well as direct connection with the amygdala (Bird and Burgess, 2008). The presubiculum is another subcortical structure that projects to the hippocampus through the EC. Additionally, many cortical afferent inputs are connected to the hippocampus through the EC including the perirhinal and parahippocampal cortices, the superior and middle frontal gyri, superior temporal and cingulate gyri, precuneus, lateral occipital cortex, occipitotemporal gyri and subcallosal cortical regions (Bird and Burgess, 2008; Haines, 2004). Collectively, these subcortical and cortical connections link the hippocampus to a number of functional CNS networks, including the neuroendocrine, olfactory and visual systems.

Hippocampal Function and Response to Injury

Based on its structural organization and extensive CNS connections, the hippocampus has received significant attention in the research community over the past decades. The hippocampus is among a number of limbic brain structures involved in emotional, motivational and learning/memory processes. Within the limbic system, it is believed that the hippocampus plays a major role in long-term memory, however, this is limited to specific types of memories. While much debate continues to focus on hippocampal function, most researchers agree that declarative memories are controlled by the hippocampus (Anderson et al., 2007; LaFerla et al., 2007). Declarative memories are those based on facts (semantic) or events/episodes (episodic). Within the category of declarative memory, many theorists agree that the hippocampus is critical for coding and storage of episodic, rather than semantic memory (Good, 2002; Bird and Burgess, 2008). Additionally, animal and human studies both show that the hippocampus plays a role in spatial memory and navigation, as well as temporal lobe amnesia (Morris et al., 1982; Good, 2002).

Beyond basic neuroscience, many studies have focused on the role of the hippocampus in neuropathologies such as Alzheimer's disease (AD) (Ball et al., 1985), epilepsy (Kuruba et al., 2009), and TBI (McCarthy, 2003). A common element in all three conditions is the resultant loss of cognitive function. Following TBI, the hippocampus is highly vulnerable to cellular damage, a feature considered to be directly linked with the long-term cognitive deficits observed clinically. Despite theoretical differences as to the role of the hippocampus in such memory loss, its structural organization has fostered a more recent, detailed study of synaptic neurophysiology,

including parameters such as unidirectional excitatory transmission and synaptic efficacy (Anderson et al., 2007). Initial studies of hippocampal electrophysiology lead to the discovery of synaptic long-term potentiation (LTP), which evolved into the prominent cellular model for the processing of functional learning and memory (Bliss and Collingridge, 1993). Subsequent LTP studies showed that the capacity to evoke such potentiation was directly associated with the structural and functional efficacy of the underlying hippocampal synaptic junctions (Steward, 1982 and 1989; Reeves and Steward, 1986). Further investigation found LTP to be a common synaptic link between memory processing and injury-induced neuroplasticity (Reeves et al., 1997; Phillips and Reeves, 2001; Tang and Zhang, 2002; Reeves et al., 2003; Su et al., 2009), serving to generate a prototype for associating synaptic recovery after TBI with positive cognitive outcome. In the present studies, we have utilized hippocampal LTP as an outcome measure to complement molecular, structural and behavioral endpoints, looking for direct links between ECM/MMP driven mechanisms and functional synaptic recovery after TBI.

While TBI studies of the hippocampus have principally focused on the loss of neurons and attenuating cell death, we now know that the affected circuitry is efficient in its plasticity and, given the right conditions, has the capacity to reorganize and promote significant cognitive recovery (Dietrich et al., 1994; Hicks et al., 1996; Sifringer et al., 2007). Although more investigation into the complexity of TBI pathology is certainly warranted, we feel that the hippocampus is a critical site for understanding neuroplasticity after brain injury based on its well organized and understood circuitry. Given that the hippocampus exhibits significant synaptic plasticity in response to stimuli

such as activity, experience or injury, we have focused on understanding more about its capacity for synaptic reorganization after TBI. While the literature is vast documenting activity- and experience-associated plasticity within the hippocampus, here we will review the area of our focus, reactive or injury-induced synaptogenesis.

Injury-Induced Synaptogenesis

Injury-induced or "reactive" synaptogenesis is a process whereby the nervous system replaces lost synaptic inputs through growth of local spared afferents into a dennervated zone (Steward, 1989). As previously described, a traumatic insult to the brain induces a series of secondary-injury events that often terminate in axonal disconnect and diffuse deafferentation. Such deafferentation triggers a local synaptogenic response, where sprouting of spared axon terminals provide new pre-synaptic input into the denervated region. Reorganized post-synaptic sites emerge in concert with these axonal sprouts to complete new synapses. While replacement by proximal spared fibers would most direct, rodent unilateral EC lesion studies show that homotypic fiber sources are preferred (i.e., CTD fibers from intact contralateral EC), and that other sprouting axons (i.e., C/A projections) may travel up to 20-40 μm into the damaged dentate gyrus to replace degenerated axonal terminals (Steward, 1989).

The unilateral entorhinal cortex (UEC) lesion model has been used in multiple studies to characterize the spatial and temporal profile of reactive synaptogenesis. UEC eliminates 80-90% of the EC afferent fibers projecting to the dentate molecular layer, and, over time, synaptogenesis leads to significant structural and functional recovery. The time course of this process is often described in three distinct postinjury phases. During the first phase of degeneration (1-5d), damaged axon terminals are

removed and degraded by reactive glia, while post-synaptic structures are morphed in shape, often collapsing at their base into the underlying dendritic shaft. This is followed by the regenerative phase (6-15d), which involves collateral sprouting of spared axons into the deafferented zone, concomitant with the reformation of post-synaptic spines and junctions. Finally, a stabilization/maturation phase (15-30^{+}d) follows, where nascent synapses are either stabilized or pruned away, re-establishing a close match to the original synaptic profile (Steward and Vinsant, 1983). At the end of these three phases, synaptic junctions return to a pattern mimicking the uninjured side and synaptic function is restored. It is important to note that while the above timeline is relevant for the UEC model in adult rat hippocampus/dentate gyrus, variations will exist between species, injury type, ages, and brain regions. Therefore, it is important to investigate the time course of injury-induced synaptic reorganization in each experimental design.

UEC studies also provide evidence of selective pre- and postsynaptic target specificity and competition between spared sprouting fibers. Within the hippocampus the C/A afferent projections synapse in the inner third of the dentate molecular layer, while the outer two thirds of the molecular layer contains EC perforant path afferents. Additionally, the CTD sends projections to the dentate outer molecular layer from the contralateral EC (Fawcett et al, 2003). When the ipsilateral EC is 80-90% ablated, these projections are replaced by CTD, C/A and septal afferents in a hierarchical fashion. Elimination of the C/A projections entirely, leads to septal afferent growth, but no EC afferent re-growth, further indicating reinnervation specificity and competition (Cotman, 1979; Nadler et al, 1980). Additionally, there is dramatic dendritic plasticity within each molecular layer zone that aids in the restoration of pre-injury synaptic

density (Deller and Frotscher, 1997; Fawcett et al, 2003). Although these results illustrate changes in a single model, the spatial and temporal reorganization displayed in the adaptive UEC are fundamental to our understanding the differences between adaptive and maladaptive plasticity post-TBI.

Adaptive vs. Maladaptive Plasticity

Based on the above review, the UEC induction of reactive synaptogenesis can be considered a model of adaptive (successful) plasticity, producing functional recovery. This recovery involves restoration of synaptic cytoarchitecture, dendritic laminar organization, and re-emergence of functional efficacy, demonstrated by both electrophysiological and behavioral measures (Reeves and Smith, 1987; Losche and Steward, 1977). Therefore, contrasting the UEC conditions with other TBI models which fail to show synaptic recovery can be quite beneficial. Maladaptive plasticity can occur when the process is dysregulated, generating disordered neuropil and aberrant synaptic structure, a situation which is consistent with the severe cognitive impairments seen in human TBI patients (Phillips et al, 1994, 1997). Our lab has developed an animal TBI model of maladaptive plasticity that combines the excessive neuroexcitation of the cFPI with targeted deafferentation of bilateral EC lesions (TBI+BEC). This model was developed to mimic the complex synaptogenic aspects seen in human TBI, and is studied in concert with the UEC model of adaptive plasticity. Comparing cellular and molecular response within these two models provides a better understanding the underlying mechanisms that contribute to poor synaptic reorganization. Our overall goal is to characterize recovery-dependent differences in molecular expression during injury-

induced synaptogenesis and develop therapeutic interventions that will improve functional recovery following TBI in humans.

Both adaptive and maladaptive plasticity are influenced by the type and timing of injury, ensuing neuropathology, and the expression, activity, and interaction of different cellular and matrix proteins that contribute to synaptic reorganization. Of particular interest is the upregulation of matrix metalloproteinase (MMP) family members and their paired substrates in different nervous system diseases, including TBI (Yong, 2005; Rosenberg, 2009). In CNS neuropathologies, MMPs modulate of the extracellular environment through proteolysis of not only free ECM molecules, but also proteins which are integral to synaptic adhesion and functional activity (Rosenberg, 2002, 2009; Kim et al., 2005; Falo et al., 2006; Komori et al., 2004; Wang et al., 2000). Prior studies have shown that the gelatinases MMP-2 and -9 contribute to BBB breakdown and exacerbate posttraumatic edema through degradation of the vessel basal lamina (Truettner et al., 2005; Vilalta et al., 2008; Vajtr et al., 2009). MMP-9 also plays a role in glial scar formation and cytoskeletal reorganization during axonal regeneration following spinal cord injury, as well as contributing to TBI neuronal damage and increased infarct size after stroke (Hsu et al., 2008; Wang et al., 2000; Romanic et al., 1998). In the context of this dissertation study, our lab has shown that altered MMP-3 expression is correlated with disorganized ultrastructural synaptic profiles and spatial learning deficits after TBI+BEC insult (Kim et al., 2005; Falo et al., 2006). MMP-3 appears to influence the development of synaptic pathology and behavioral impairment through its target ECM protein agrin, which contributes to receptor organization within the synapse (Falo et al., 2008). Earlier studies showed hippocampal upregulation of MMP-2, -3, and -9

expression/activity within the TBI+BEC, paralleled by increased levels of the MMP ECM substrates collagen IV, chondroitin sulfate proteoglycan (CSPG) and tenascin (Phillips and Reeves, 2001; Kim et al., 2005). More recently, members of the membrane-type MMP family and the A Disintegrin and Metalloproteinase (ADAM)/ A Disintegrin and Metalloproteinase with a Thrombospondin type 1 motif (ADAMTS) subgroup have been shown to interact with ECM and synaptic molecules during injury-induced synaptogenesis (Komori et al., 2004; Mayer et al., 2005; Yang et al., 2006). While these studies linking MMPs to TBI and synaptogenesis are small in number, it is apparent that MMPs and their paired ECM substrates play an important role in neuroplastic recovery. However, it is also recognized that their interaction must be tightly regulated to promote successful synaptic repair. It is our overall hypothesis that unregulated MMP/substrate interaction contributes to maladaptive post-injury reorganization and persistent functional impairments following TBI. Therefore, it is important to continue to investigate MMP/substrate interaction as it relates to the processes of adaptive and maladaptive injury-induced synaptogenesis.

The following section reviews the general structural and functional features of the MMP family of enzymes, and takes a closer look at how two membrane-bound MMPs, membrane-type 5 MMP (MT5-MMP) and ADAM-10 can potentially influence the postinjury plasticity process through proteolytic interaction with synaptic adhesion molecule, Neural Cadherin (N-cadherin).

MATRIX METALLOPROTEINASES

General Classification, Structure, and Function

MMPs constitute a large family of highly regulated zinc and calcium dependent proteolytic enzymes that play important roles in both development and disease states. In either secreted or membrane-bound forms, MMPs are collectively capable of degrading virtually all components of the ECM, as well as cleaving other proteinases, proteinase inhibitors, growth factors, chemotactic molecules, growth factor binding proteins, cell surface receptors and cell adhesion molecules (Cawston and Wilson, 2006; Ahmad et. al, 2006; Nagase and Woessner, 1999; Maskos and Bode, 2003; Cunningham et. al, 2005; Conant and Gottshall, 2005). MMPs first gained recognition in 1962, when Gross and Lapiere detected collagenolytic activity in involuting tadpole tales, and revealed collagenase-1 (MMP-1) as the first member of the MMP family. Subsequent studies revealed new members of the MMP family, often with overlapping substrate preferences. Until recently, MMPs had been placed into groups such as collagenases, gelatinases, and stromelysins, based on these similar substrate preferences. With technological advances, distinct structural variations within these groups and overlap in substrate specificity led scientists to rethink MMP classification.

A total of 25 vertebrate MMPs have been identified and grouped into the following 7 subsets, primarily based on domain organization: (1) Minimal domain: MMP-7, MMP-26; (2) Simple hemopexin domain (collagenases, stromelysins, and others): MMP-1, MMP-3, MMP-8, MMP-10, MMP-12, MMP-13, MMP-18, MMP-19, MMP-20, MMP-22, MMP-27; (3) Gelatinases: MMP-2, MMP-9; (4) Furin activation, secreted: MMP-11, MMP-28; and Vitronectin insert: MMP-21; (5) Transmembrane

MMP/Membrane-type (MT-MMP; Type I Transmembrane): MMP-14 [Membrane-type-1(MT1-MMP)], MMP-15 (MT2-MMP), MMP-16 (MT3-MMP), MMP-24 (MT5-MMP); (6) Glycosylphosphatidylinositol (GPI) anchored (Type I Transmembrane): MMP-17 (MT4-MMP), MMP-25 (MT6-MMP); (7) Cys/Pro rich with Ig-like domain (Type II Transmembrane): MMP-23 (Fig. 1.2) (Cawston and Wilson, 2006; Yong, 2005; Stamenkovic, 2003). Studies reveal that among these subsets and groups, despite distinct tissue expression patterns of individual MMPs, structural and functional overlap and interaction occurs, thus revealing a complexity that was once thought to be absent in MMPs (Cawston and Wilson, 2006; Sternlicht and Werb, 2001). In addition to the standard eight subsets, there are other families of enzymes that share structural and functional similarities with MMPs, and are loosely included within the MMP family, such as the ADAMs motifs. This sub-family of molecules will be discussed in further detail in a later section.

Structurally all MMPs are multi-domain proteins, with each domain serving a specific function. Secreted and membrane type-MMPs (MT-MMPs) contain the following common domains, unless otherwise noted: (1) N-terminal signal domain, which is removed upon insertion into the endoplasmic reticulum; (2) Propeptide domain (~80 amino acids) containing a “cystine switch” which helps maintain latency by blocking the catalytic zinc active site, and is cleaved to activate MMPs; (3) highly conserved Catalytic domain (~170 amino acids) containing three histadine residues bound to a zinc ion, calcium ions, and a conserved methionine residue, forming a structurally supportive “Met-turn” motif beneath the zinc ion active site; (4) Hinge region, which varies in length and composition and is involved in substrate specificity (absent in

MMP-7, -23, -26); and (5) C-terminal domain known as the hemopexin-like domain (~200 amino acids), or HLD, which is also thought to be involved in substrate specificity (absent in MMP-7, -23, -26) (Hernandez-Barrantes et. al, 2002; Nagase et. al, 2006; Sternlicht and Werb, 2001; Stramenkovic, 2003). Additional insert sequences are present and further dictate function in certain secreted and membrane-bound MMPs. Vitronectin and fibronectin-type II domain inserts are found in MMP-21; and MMP-2 and -9, respectively, while furin recognition sequences (RR(K/R)R) are found at the C-terminus of the propeptide domain in all MT-MMPs and MMP-11, -28, -21, and -23 (Maskos and Bode, 2003; Nagase et. al, 2006; Cawston and Wilson, 2006; Fillmore et al, 2001). According to current *in vitro* literature, this sequence allows for these specific MMPs to be activated intracellularly by serine proteases of the pro-protein convertase class (i.e.-furin) (Pei and Weiss, 1995; Illman et al., 2003; Sato et al., 1996; Kang et al., 2002). Despite slight subgroup variations, these general structural components create the foundation of the MMP family, and contribute to their multi-functional nature.

As is true in all of science, structure dictates function. MMPs are highly involved in tissue remodeling and reorganization during both development and disease, such as spinal cord injury (SCI), TBI, AD, stroke, Parkinson's disease (PD), and Multiple Sclerosis (MS) (as reviewed by Rosenberg, 2002, 2009; Yong et al., 2001; Nagase et. al, 2006). Proper regulation of MMP function helps maintain a balance between tissue breakdown and preservation, and primarily occurs by three different mechanisms. The first line of MMP regulation involves transcriptional control. Generally, MMPs are expressed at low levels, but can be transcriptionally upregulated in response to increased tissue remodeling and events such as inflammation, injury, and cancer

progression (Nagase and Woessner, 1999). Synthesis of all MMPs as inactive zymogens (proMMP form) also serves as a regulatory mechanism. Therefore, in order to achieve full function, MMPs must be activated by removal of the pro-domain (Sounni and Noel, 2005; Sternlicht and Werb, 2001). Finally, MMP activity can be regulated by a collection of endogenous tissue inhibitors of metalloproteinases (TIMPs), which bind and inactivate all MMPs in a 1:1 (MMP: TIMP) ratio. Currently there are four identified TIMPs (TIMP-1, -2, -3, -4), each of which has different affinities for individual MMPs. These regulatory mechanisms act to balance MMP activation and inhibition, therefore maintaining normal development and remodeling in a healthy state (Nagase et. al, 2006; Cawston and Wilson, 2006).

While endogenous mechanisms are in place to ensure a physiological balance of secreted and membrane-bound MMP activity, regulation of MMPs has been shown to become unbalanced during pathological states. Within the CNS, detrimental effects of persistent MMP activity include tumorigenesis, BBB disruption, neuroinflammation, demyelination, and neuronal death. Therefore, MMPs have been shown to occur in neuropathologies such as SCI, TBI, AD, stroke, PD, MS (Rosenberg, 2002, 2009; Yong et al., 2001). Laboratory and clinical studies have the used blocking/knockdown techniques and synthetic inhibitors in an attempt to control persistent MMP activity in these different neuropathologies. Blocking antibodies, knockout or knockdown methods (transgenic mice, short interfering RNA), antisense methods, and pharmacological MMP inhibitors have all been used to not only investigate the roles of MMPs but to also limit disease progression and improve recovery. For example, administration of broad-

Figure 1.2 Matrix Metalloproteinase (MMP) Structure and Subgroups. a) Variable structure of MMPs including general domains (signal peptide, propeptide, catalytic, hinge region, and haemopexin) and unique inserts/domains (furin cleavage site, type II fibronectin repeats, MT-loop, transmembrane domain, cytoplasmic tail, N-terminal signal anchor, cysteine array, Ig-like domain, and GPI anchor; b) Seven subgroups based on MMP structure. Note membrane-type MMPs possess additional structural domains/inserts that dictate position and function.

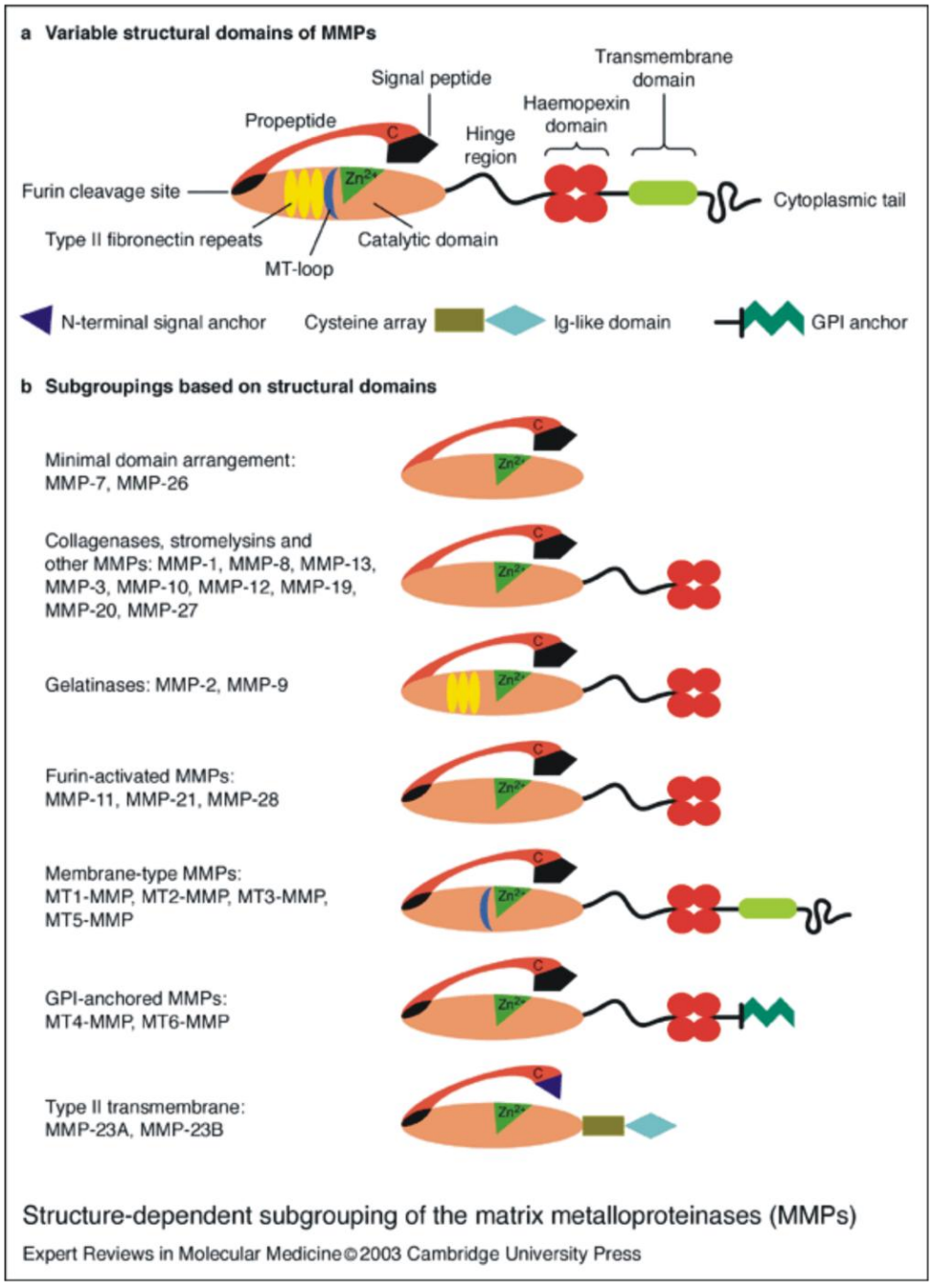

Structure-dependent subgrouping of the matrix metalloproteinases (MMPs)

spectrum MMP inhibitor GM6001 in a stroke model produced a significant reduction in infarct size following focal ischemia (Amantea et al., 2007). Acute administration of GM6001 improved functional recovery following SCI and significantly limited the amount of apoptotic brain damage following TBI (Noble et al., 2002; Sifringer et al., 2007). In most laboratory studies, inhibition or knockdown of overexpessed and active MMPs at appropriate times has limited their detrimental effects and pathology progression. Clinical MMP inhibition studies have not produced the same results, and have often been stopped early due to poor side effects in patients. Both laboratory and clinical studies have historically focused on the inhibition of secreted MMPs such as MMP-2, -3, and -9. However, the role of membrane-bound MMPs in development and disease has gained increased attention over the past decade due to the subgroup's unique structural features and ability to be an upstream mediator of other MMP activity.

Membrane-bound MMPs

Within the family of MMPs important structural differences have been uncovered, especially between the secreted and membrane-bound MMPs. Membrane-bound MMPs possess unique structural features that dictate cellular localization and enzymatic function. It is important to note the structural features that set this group apart from soluble MMPs, in order to better understand the roles they play in physiological and pathological processes.

A truly unique feature of membrane- bound (membrane-type; MT) MMPs is the presence of a membrane anchoring domain following the HLD. This domain consists of a stem region (~30 amino acids) and a hydrophobic tether region (~20 amino acids). The tether region either exists as a transmembrane domain (TMD) with a short

cytoplasmic tail, as in MT1-, MT2-, MT3-, and MT5-MMP, or as a GPI anchor, as in MT4- and MT6-MMP (Hernandez-Barrantes et. al, 2002). The cytoplasmic tail in all MT-MMPs, except MT4-MMP, may serve as a possible phosphorylation site, as is contains a cystine residue, with adjacent tyrosine and serine residues (Parks and Mecham, 1998).

All MT-MMPs, with the exception of MT4-MMP, contain an additional 8-amino acid insertion between β-strand II and III that forms a "MT-loop" within the catalytic domain, that is essential for proMMP-2 activation (Sounni and Noel, 2005; English et. al, 2001). The ability of MT-MMPs to activate proMMP-2 is best illustrated by the research focused on MT1-MMP activation of pro-MMP2. The activation occurs through a series of specific bonds, where MT1-MMP, TIMP-2, and proMMP-2 form a ternary complex on the cell surface (Itoh and Seiki, 2005; Itoh, 2006; Itoh et. al, 2001). The process begins with the expression of an active, full length MT1-MMP protein (~60 kDa) on the cell surface binding to TIMP-2 at the "MT-loop". Three dimensional analysis of the "MT-loop" structure reveals a pocket-like region which matches up with the Tyr-36 residue in the AB loop on the N-terminal domain of TIMP-2 (Fernandez-Catalan et. al, 1998). Mutations of MT1-MMP's "MT-loop" alter enzymatic activity of proMMP-2, further indicating its functional importance (Fernandez-Catalan et. al, 1998). The binding of TIMP-2 inhibits any catalytic activity of MT1-MMP, which appears to be functioning more as a docking station rather than an enzyme in this situation. TIMP-2 possesses a C-terminal domain with a high affinity for the HLD domain of proMMP2. The proMMP-2 "substrate" docks to the C-terminus of TIMP-2 and forms the ternary complex (Strongin et. al, 1995; Maskos and Bode, 2003). The binding of these three proteins is insufficient

to activate proMMP-2, thus an adjacent TIMP-free MT1-MMP is needed to initiate the first pro-MMP-2 cleavage. The primary cleavage site in proMMP-2 is not typically susceptible to MMPs, but a series of loops within the MT1-MMP catalytic domain may act to embrace this site and allow cleavage (Maskos and Bode, 2003). Following the initial cleavage, an additional MMP-2 molecule removes the remaining propeptide domain from the intermediate MMP-2 to yield a mature and fully-active MMP-2 molecule (Deryugina et. al, 2001). While the majority of the current literature of is focused on MT1-MMP, other MT-MMPs are believed to carry out the same function (MT2-MMP, MT3-MMP, and MT5-MMP). The unique "MT-loop" feature further implicates this subgroup of MMPs in physiological and pathological processes that require MMP-2 activity.

As previously mentioned, all MT-MMPs have a furin recognition sequence at the C-terminus of the propeptide domain, which serves as a cleavage site for activation (as reviewed by Cawston and Wilson, 2006). A second site in the propeptide, described as a stretch of 5 homologous amino acids, is present in addition to the furin recognition sequence in all MT-MMPs. This site may be essential to enzymatic functioning and act as an intramolecular chaperone by maintaining protein conformation (Fillmore et. al, 2001; Cao et. al, 2000). Collectively, these structurally characteristics make MT-MMPs unique proteolytic enzymes within the MMP family (see again Fig 1.2).

Based on advances made in uncovering these structural variations, MT-MMPs have emerged as important new players in ECM regulation due to their unique cellular localizations, structure, and involvement in a variety of physiological and pathological processes, such as tissue remodeling, tumor growth and metastasis, angiogenesis,

synaptic plasticity, and even activation of secreted proMMPs (Sato and Seiki, 1996; Jaworski, 2000, as reviewed by Sounni and Noel, 2005). Although MT-MMPs possess functions similar to those of secreted MMPs, and cleave some of the same substrates, such as collagen, gelatin, laminin, glycoproteins and proteoglycans, they do possess structural and functional characteristics which set them apart from their secreted counterparts (Hernandez-Barrantes et. al, 2002). In contrast to secreted MMPs, which can migrate away from the cell to affect distant targets, MT-MMPs are specialized to affect a very focal area of the pericellular microenvironment. As a result of their focal concentration, MT-MMPs have additional unique functions, some of which have direct and indirect effects on secreted MMP activity.

In general, MT-MMPs contribute to the proteolysis of ECM components and the activation of proMMPs (proMMP-2, -13) or other zymogens (ADAMTS-4 p68), as well as influence a variety of extracellular and intracellular signaling pathways, alter cell-to-cell and cell-to-matrix relationships, control gene expression, and promote cell survival, migration and invasion, and angiogenesis, during phases of health and disease (Hernandez-Barrantes et. al, 2002; Sounni and Noel, 2005; Deryugina and Quigley, 2006). MT-MMPs are able to influence the above processes because of the different structural domains that make them unique. The most distinguishing feature of an MT-MMP is its position within the plasma membrane. Prior to inserting in the membrane, most often the furin recognition sequence is cleaved by proprotein convertase in the Golgi during protein trafficking, and the MT-MMP becomes activated intracellularly. Blocking MT-MMP intracellular activation has been shown to be a prerequisite for MT-MMP membrane insertion and position. For example, when intracellular MT1-MMP

activation is blocked *in vitro*, MT1-MMP fails to be trafficked to the membrane and remains localized proximal to the Golgi compartment (Wu et al., 2007). This level of intracellular regulation is thought to allow for proper protein folding and activation prior to membrane insertion, therefore ensuring that when the enzyme is upregulated, it is ready to function when and where it is needed in a timely manner. There is also evidence of alternative methods of MT-MMP activation, including autoproteolysis, cleavage by a non-furin protease and extracellular activation by plasmin (Okumura et. al, 1997). This characteristic of primary intracellular activation is in contrast to most secreted MMPs which are primarily activated extracellularly.

Following activation, the cytoplasmic tail (domain) may be an important player in intracellular events such as trafficking and cell surface localization of the MT-MMP, therefore affecting MT-MMP functions such as sheddase activity and subsequent cell migration (Nakahara et. al, 1997). For example, in cancer cells MT1-MMP is localized at higher concentration in lamellipodia and invadopodia, possibly due to cytoplasmic tail activity (Nakahara et. al, 1997). This specific localization of MT1-MMP leads to an increase in pericellular ECM degradation and surface receptor cleavage, therefore enhancing cell migration (Hotary et. al, 2000; Mori et. al, 2002; Nakahara et. al, 1997). The mechanism of cell migration is not fully understood, but may involve MT1-MMP directed shedding of the membrane glycoprotein CD44, a widely expressed major hyaluronan receptor involved in cell-cell interactions, adhesion, and migration. Releasing the ectodomain of CD44 from the cell surface may alter the cell-matrix adhesion properties and permit cell migration (Naor et. al, 1997). In order to fully promote cell migration, MT1-MMP must also be internalized by a clathrin-dependent

pathway, a process that is also mediated by the cytoplasmic tail (Anilkumar et. al, 2005). Other MT-MMPs may also be able to influence cell migration in a similar fashion. In addition, the cytoplasmic tail may influence cell signaling pathways, as well as MT-MMP dimerization and trafficking (as reviewed by Souni and Noel, 2005; Wang P et. al, 2004).

Once tethered to the membrane, the transmembrane or GPI anchor domains are responsible for maintaining the position of MT-MMPs, which in turn concentrates proteolytic activity to specific regions of the cell surface (Sternlicht and Werb, 2001). In this position, the catalytic domain is the integral structural component, and is necessary to carry out many MT-MMP functions. MT-MMPs membrane localization, along with influence from the cytoplasmic tail domain, may also affect cell signaling pathways that involve cell survival, migration and invasion, and angiogenesis. In pathological states, the spatial relationship of MT-MMPs and their cell surface substrates facilitates cleavage and shedding of either whole or fragmented proteins, resulting in modification of cell signaling pathways (Itoh and Seiki, 2006). An example of this is the indirect activation of epidermal growth factor receptor (EGFR) signaling by MMP-2, -9 and MT1-MMP. EGFR activation affects downstream oncogenic pathways, such as the Sac, Ras, and extracellular signal-regulated kinase (ERK) pathways, and may also lead to increased expression of MT1-MMP in cultured glioma cells. This suggests that EGFR and MT1-MMP may function together as mediators of glioma malignancy (Roelle et. al, 2003). MT-MMPs may also be involved in intracellular signaling through interaction with integrins. Integrins are cell adhesion molecules that mediate bi-directional signal transduction through the plasma membranes of neighboring cells. Interaction between

MT1-MMP and αvβ3 integrin promotes cell adhesion and migration *in vitro* through the phosphorylation of the focal adhesion kinase (FAK) pathway (Deryugina et. al, 2002). In addition, MT2-MMP plays a role in the protection of tumor cells *in vitro* by altering apoptotic signals, therefore suggesting that it may protect tumor cells in vivo as well (reviewed by Deryugina and Quigley, 2006). Through these signaling pathways and other mechanisms, MT-MMPs play very crucial roles in pathological states (Wang R et. al, 2004).

Apart from its membrane-bound activities, the catalytic domain of some MT-MMPs can be cleaved autocatalytically or non-autocatalytically, thereby releasing it into the surrounding microenvironment as a soluble enzyme. Shedding of the catalytic domain from the membrane may be a point of MT-MMP regulation, and possibly result in further pericellular proteolysis and alteration of enzyme-inhibitor balance through TIMP binding (Osenkowski et. al, 2004; Hernandez-Barrantes et. al, 2002; Wang and Pei, 2001). Further investigation of cleaved and shed MT-MMP catalytic domains is needed to better define how they function as soluble proteinases.

Membrane-bound-MMPs and the Nervous System

Although MMPs are highly involved in both physiological and pathological events throughout the body, their involvement in nervous system development, remodeling, and repair remains at the forefront of scientific investigation. During nervous system development, MMPs are involved in dendritic and axonal formation and growth, synapse formation and stabilization, neuronal and glial migration, and structural reorganization. (Komori et. al, 2004; Sekine-Aizawa et. al, 2001; Monea et. al, 2006; Jaworski, 2000). In addition to their roles in development, MMPs act as major players in

a variety of neuropathological processes such as cancer, neurotoxicity, neuroinflammation, cerebral ischemia, TBI, AD, and MS (Sekine-Aizawa et. al, 2001; Sounni and Noel, 2005; Cunningham et. al, 2005; Yong et. al, 2001; as reviewed by Rosenberg, 2002). While several soluble MMPs (e.g., MMP-2, -3, -9) have been shown to influence these processes, membrane-bound MMPs have emerged as important players based on their localization and ability to concentrate enzymatic activity. Here we will detail a specific membrane-bound MMPs, MT5-MMP, in relation to central nervous system development and plasticity.

MT5-MMP

Nearly a decade ago, the fifth member of the MT-MMP subset was cloned, sequenced, characterized, and appropriately named MT5-MMP (MMP24) (Pei, 1999; Llano et. al, 1999). Structurally, MT5-MMP shows the greatest homology with MT3-MMP, followed by MT1-MMP and MT2-MMP, maintaining overall sequence identities at 64.4%, 53%, and 52.1%, respectively (Pei, 1999). Llano et al (1999), found similar homology between MT5-MMP and MT3-MMP at 63%. The molecular mass is ~65 kDa for the full inactive form of MT5-MMP, ~58 kDa for the full active form, ~52 kDa for the transmembrane-lacking form, and 28-34 kDa for shed forms (Pei, 1999; Sekine-Aizawa et. al, 2001, Wang X et. al, 1999).

A few structural variations are present in MT5-MMP, and may influence its functional abilities. Llano et al (1999) found a series of repeated sequences (CCG, CTG, and GCG) in the signal and propeptide domains of MT5-MMP. These sequences generate stretches of 8 Pro residues and 6 Leu residues in the signal sequence, and 6 Ala residues in the propeptide domain, therefore making the N-terminal region of MT5-

MMP significantly longer than the other membrane-bound MMPs. In the human genome, these nucleotide sequences are highly unstable and therefore usually polymorphic, which may suggest the existence of MT5-MMP protein variants with alternative structures and functions (Llano et. al, 1999; Ross and Fillmore, 2007). Another variation is present within the stem domain of MT5-MMP in mouse, rat, and human, where there is an additional furin recognition site, RRKERR. The RRKERR motif is necessary for cleavage and shedding of the soluble MT5-MMP form (Wang and Pei, 2001). Rapid shedding or fragmenting of MT5-MMP appears to be common at physiological temperatures, perhaps due to enzymatic instability (Pei, 1999; Wang X et. al, 1999). These structural differences influence MT5-MMP's functional role within the nervous system.

Aside from structural additions, MT5-MMP has a very unique pattern of tissue expression when compared to the other membrane-bound MMPs, which are expressed in a variety of tissue types (Bernal et. al, 2005). MT5-MMP appears to be preferentially expressed in both rodent and human nervous systems, with mouse and human MT5-MMP 95% homologous (Pei, 1999; Sekine-Aizawa et. al, 2001; Conant and Gottschall, 2005). Within the rat brain MT5-MMP accounts for ~60% of all non-gelatinase type MMPs, whereas MT1-MMP and MT2-MMP account for 22.7% and 13%, respectively (Sekine-Aizawa et. al, 2001). Through reverse transcriptase polymerase chain reaction (PT-PCR) technology, MT5-MMP expression has been tested in a variety of tissues. Although expression remains the highest in the developing and adult brain and spinal cord, weak expression has been detected in tissues such as testis, liver, bone,

pancreas, lung and kidney (Pei, 1999; Llano et. al, 1999; Sekine-Aizawa et. al, 2001; Bernal et. al, 2005).

Expression of MT5-MMP in the developing and adult CNS is primarily in regions that exhibit high neuronal plasticity, such as the hippocampus, olfactory bulbs, dentate gyrus (DG), ventricular zone, and cerebellum (Jaworski, 2000; Sekine-Aizawa et. al, 2001; Hayashita-Kinoh et. al, 2001). MT5-MMP has also been detected in PNS structures such as, isolated dorsal root ganglion neurons (DRG) and the trigeminal ganglion (Jaworski, 2000; Hayashita-Kinoh et. al, 2001). Within these regions, MT5-MMP is primarily expressed in neurons, including cerebellar purkinje and granule cells, hippocampal and cortical pyramidal cells, and granule cells in the DG (Hayashita-Kinoh et. al, 2001; Sekine-Aizawa et. al, 2001). In the developing rat cerebellum, MT5-MMP is specifically localized in the soma and dendrites of Purkinje cells (Sekine-Aizawa et. al, 2001). Within isolated DRG cells of the developing mouse, MT5-MMP is localized in the soma and growth cone of neurites (Hayashita-Kinoh et. al, 2001). The localization and expression patterns of MT5-MMP in the nervous system suggest that MT5-MMP may be involved in normal development, morphogenesis, and neural plasticity. In addition, MT5-MMP is indicated in neuropatholgies such as AD, brain cancer, and neurotrauma (Sekine-Aizawa et. al, 2001; Ahmad et. al, 2006; Llano et. al, 1999; Pei, 1999; Wang P et. al, 2004; Komori et. al, 2004).

MT5-MMP's role in development has been investigated in both the rat and mouse nervous systems (Sekine-Aizawa et. al, 2001; Jaworski, 2000; Hayashita-Kinoh et. al, 2001). Using *in situ* hybridization, MT5-MMP mRNA is first detected in the rat at embryo day 16 (E16), and is clearly expressed in neocortical areas by E20. Levels peak

at postnatal day 0 (P0), and although there is a steady decline into adulthood, MT5-MMP remains highly localized to regions of postnatal plasticity (Jaworski, 2000). In Purkinje cells of the postnatal rat cerebellum, Western blot analysis reveals a gradual increase in MT5-MMP protein levels between P1 and P35, with a dramatic increase during P14-35. Immunohistochemistry supports these observations at different postnatal time points. At P5, MT5-MMP is expressed in mature post-mitotic neurons within the inner granule cell layer, especially in the soma. At P14, a time-point during which dendritic trees are developing, MT5-MMP protein is highly present in dendrites. MT5-MMP remains present in developed dendritic trees and cell bodies at P35, and is densely expressed within the Purkinje cells, as far out as postnatal week 10 (P10W) (Sekine-Aizawa et. al, 2001). A varied expression pattern of MT5-MMP mRNA is observed within the developing mouse cerebellum. Northern blot analysis reveals weak MT5-MMP mRNA expression at E14. Levels increase in the mouse cerebellum from E18 through P0, at which time levels drop sharply and are practically undetectable at P30 (Hayashita-Kinoh et. al, 2001). During this timeline of mouse development, several neocortical morphogenic events are occurring, including active neurogenesis, neuronal migration and differentiation, neurite outgrowth, and synaptic pruning (Brumwell and Curran, 2006). Collectively, MT5-MMP's pattern of expression during rat and mouse brain development suggests that it may be involved in nervous system morphogenesis and plasticity, possibly through ECM degradation and remodeling.

In the adult brain, MT5-MMP is an important player in both physiological and pathological processes. As a member of the MMP family, MT5-MMP has inherent proteolytic abilities, and is active within the nervous system. MT5-MMP cleaves and

fully degrades gelatin, chondroitin sulfate proteoglycans (CSPG), heparin sulfate proteoglycans (HSPG) and dermatan sulfate proteoglycans (DSPG), and partially degrades fibronectin *in vitro* (Hayashita-Kinoh et. al, 2001; Wang X et. al, 1999; as reviewed by Hernandez-Barrantes et. al, 2002). *In situ* zymography shows MT5-MMP gelatinolytic activity in post-mitotic cells migrating to the cerebellar inner granule layer in P9 mice, and in adult cerebellar Purkinje and granule cells. In mouse DRG cells of the PNS, recombinant MT5-MMP degrades CSPG and HSPG, both of which play an inhibitory role in neurite outgrowth (Hayashita-Kinoh et. al, 2001). Cleavage of some proteoglycans is thought to release reservoirs of factors such as amphoterin and pleiotrophin, which may promote neurite outgrowth (Quinn et. al, 1999). MT5-MMP is responsible for this proteolytic activity *in vitro*, because the activity is blocked by MMP inhibitors such as ethylenediamine tetraacetic acid (EDTA), BB94 and TIMP-2 (Hayashita-Kinoh et. al, 2001; Wang X et. al, 1999). MT5-MMP appears to be unable to degrade laminin and type I collagen (Wang X et. al, 1999). The degradation of specific MT5-MMP substrates may contribute to normal tissue remodeling and reorganization, as well as influence synaptic plasticity within the nervous system.

In addition to playing a role in normal tissue reorganization, MT5-MMP may be involved in pathologies such as cancer and AD. The activation of proMMP-2 by MT1-MMP/TIMP-2 is a key event in a variety of human carcinomas, including brain cancer. As previously mentioned, MT5-MMP is capable of activating proMMP-2 *in vitro*, and is believed to function similarly to MT1-MMP (Wang X et. al, 1999; Pei, 1999; Llano et. al, 1999). Therefore, MT5-MMP activation of proMMP-2 could play a role in tumor cell migration and invasion within the brain. It is speculated that MT5-MMP forms a

homodimer, similar to that of MT1-MMP, during proMMP-2 activation as previously described. This is supported by *in vitro* immunoprecipitation experiments that reveal what is thought to be a dimerized MT5-MMP 130 kDa form (Pei, 1999). In human tissue samples, MT5-MMP mRNA is significantly over-expressed in brain tumors such as astrocytomas, anaplastic astrocytomas, and glioblastomas (Llano et. al, 1999). Recently, investigators have tried to target different proteins that interact with MT5-MMP, as a possible means of treating these types of cancer. For instance, activation of proMMP-2 appears to take place at the cell surface, therefore mechanisms that regulate MT5-MMP position and localization on the membrane may also be involved in cancer progression. Typically, MT5-MMP proteins are internalized from the membrane and sent back through the Trans Golgi Network (TGN), and are then retrieved and repositioned on the cell surface. Mint-3, which is capable of binding membrane proteins, is required for retrieval of internalized MT5-MMP back to the membrane, through interaction with the EWV motif in the carboxyl-end of MT5-MMP. Theoretically, if Mint-3 were inhibited or knocked down, fewer internalized MT5-MMP proteins would be repositioned in the membrane, less proMMP-2 would be activated, and tumor cell migration and invasion would diminish (Wang X et. al, 2004). Further investigation into the actual mechanism and efficiency of proMMP-2 activation by MT5-MMP is needed to gain greater insight into its role in human carcinomas of the nervous system.

In addition to involvement in cancer progression, MT5-MMP may also play a role in neurodegenerative diseases, such as AD. One of the hallmarks of AD is the presence of senile plaques, which primarily consist of mis-folded aggregates of amyloid β (Aβ), a proteolytic product of amyloid precursor protein (APP). MT5-MMP interacts

with both Aβ and APP in the brain. In human brains, MT5-MMP is co-localized with Aβ deposits near senile plaques, suggesting that cells may utilize MT5-MMP proteolytic abilities to remove fibrillar forms of Aβ peptides (Sekine-Aizawa et. al, 2001). MT5-MMP also induces cleavage and shedding of APP from the membrane *in vitro*, but only in the presence of the adapter protein Fe65. MT5-MMP sheds a 120 kDa APP fragment from the membrane and induces Fe65-dependent transactivation, where Fe-65 remains bound to the cytoplasmic tail of APP and is translocated to regulate gene expression associated with APP (Ahmad et. al, 2006). While Fe-65 is considered a scaffolding or adapter protein rather than a transcription factor, it has been found to influence protein expression and interact with a number of molecules, including APP, that are involved in nervous system development and tissue specific functions (Araki et al, 2004). In relation to APP, MT5-MMP may either function to decrease the amount of Aβ aggregates and possibly protect against AD, or it may contribute to the progression of AD by cleaving APP into smaller fragments, ultimately leading to senile plaque formation. Further investigation will help characterize MT5-MMP's involvement in AD.

Aside from membrane bound activities, MT5-MMP may possess the ability to process ECM components and other proteins as a soluble species (Pei, 1999). When membrane-bound, MT5-MMP has a very short half-life, of ~ 30 min at 37°C *in vitro*, and is constantly being shed at rates higher than other MT-MMPs. The full length membrane-bound form is autocatalyzed into smaller fragments, which are released into the pericellular space. Of these fragmented species, the ~28 kDa fragment retains the catalytic domain, and therefore may have new proteolytic abilities within the extracellular space (Wang X et. al, 1999). The activity of the cleaved catalytic domain

of MT5-MMP is not fully understood, but may ultimately expand MT5-MMP's substrate profile *in vivo*.

Based on previously discussed expression pattern within highly plastic regions of the brain, and specific localization in developing neurites and dendritic processes, MT5-MMP is also thought to play a very important role in neural plasticity, or synaptogenesis, within the CNS and peripheral nervous system (PNS) following injury. In the PNS, injury induced plasticity involves both collateral and regenerative axonal sprouting into the damaged or denervated regions (Fawcett et. al, 2003). Following a peripheral nerve injury, such as transection of the sciatic nerve, it is normal to observe nerve fiber sprouting into Lamina II of the dorsal horn of the spinal cord. MT5-MMP knockout mice are unable to structurally reorganization sprouting Aβ-fibers within the dorsal horn of the spinal cord following sciatic nerve injury (Komori et. al, 2004). However, wild-type (WT) MT5-MMP mice exhibit the typical injury induced neuronal plasticity. As a result of the lack of axonal sprouting into Lamina II, which contains a high percentage of nociceptive neurons, MT5-MMP knockout (KO) mice also do not develop the neuropathic pain with mechanical allodynia that typically accompanies such an injury. Mechanical allodynia is feature of neuropathic pain, and is evoked by non-noxious mechanical stimuli. The lack of Aβ-fiber sprouting and mechanical allodynia in KO MT5-MMP mice suggests that MT5-MMP plays an important role in laminar reorganization following peripheral nerve injury (Komori et. al, 2004). MT5-MMP may influence reorganization through ECM degradation, or possibly through interaction with cell signaling pathways involved in nerve fiber outgrowth and migration to the appropriate target.

Following CNS injury, certain neurons retain their ability to sprout and form new synaptic connections within injured regions to enhance functional recovery, a process commonly referred to as reactive synaptogenesis (Hamori, 1990; Fawcett et. al, 2003; Phillips and Reeves, 2001). MMPs and their substrates are major contributors to the process of reactive synaptogenesis, which involves collateral sprouting and synaptic reorganization and stabilization (Yong et. al, 2001; Fawcett et. al, 2003). MT5-MMP is emerging as an important player in developmental and injury induced synaptogenesis. One mechanism of synapse modulation may involve the interaction between the enzyme-substrate pair of MT5-MMP and cadherin, which has mainly been studied *in vitro* (Monea et al, 2006). Cadherins are cell-cell adhesion molecules that are present at a number of cell junctions, including synapses (Takeichi and Abe, 2005). Specifically, cadherins are present in extending dendritic filopodia and mature synapses of cultured hippocampal pyramidal cells (Togashi et. al, 2002). During synaptogenesis, cadherins are active in pre- and post-synaptic terminals and help guide and stabilize new connections (Takeichi and Abe, 2005). Interestingly, blockage of cadherin activity at the synaptic junction results in abnormalities in synaptic formation, suggesting that cadherins also regulate morphological changes within dendritic spines (Togashi et al, 2002). MT5-MMP shares a similar localization pattern to that of cadherin, and is present at the growth cone tips of developing cortical neurons, in both axons and dendrites, and remains present in the synapses of mature neurons, when bound to the palmitoylated α-amino-3-hydroxyl-5-methyl-4-isoxazole-propionate (AMPA) receptor binding protein (ABP). Palmitoylated ABP, which can be linked to cell-adhesion complexes, guides MT5-MMP to these locations and facilitates the interaction between

MT5-MMP and cadherins at the synapse (Monea et al, 2006). Therefore, MT5-MMP may also affect synaptic stability though interaction with cadherins and other cell-cell adhesion complexes. Based on the current literature, MT5-MMP is considered an important factor in the process of synaptogenesis. However, additional *in vivo* and *in vitro* studies are needed to fully understand MT5-MMP's role in both developmental and injury-induced synaptogenesis.

ADAMs

ADAMs are type I transmembrane proteins of the adamylisin family that posses both proteolytic and adhesive functional capabilities (Black and White, 1998; White et al., 2003). Due to similar domain structures and proteolytic capabilities, ADAM proteins are included within the MMP family of proteases previously described. Currently, 40 gene members of the ADAM family have been identified, 21 of which are thought to be functionally active in humans (Duffy et al., 2009). The ADAM genes are divided into sub-families, based on their ability to exhibit or not exhibit proteolytic activity, and then further divided into smaller subsets based on specific tissue/cell expression (testis specific vs. non-testis specific). ADAMs that exhibit proteolytic activity in humans include, ADAMDEC-1 (decysin), ADAM-8, -9, -10, -12, -15, -17, -19, -20, -21, -28, -30, and -33. The remaining human ADAM proteases, ADAM-2, -7, -11, -18, -22, -23, -29, and -32 lack one or more essential features in the catalytically active site, and are therefore grouped into the non-proteolytic sub-family (Edwards et al, 2008; White et al., 2003). These two sub-families are further divided based on tissue/cell expression patterns. Studies have shown that ADAMs are expressed during development in different tissue and cell types throughout the body including, testis, lungs, intestines,

muscle, central and peripheral nervous system tissue, somatic tissue, bone, and hematopoietic cell types (Edwards et al., 2008). Although the majority of expression studies investigate levels during development, selective ADAMs do remain present and functional throughout adulthood.

Structurally, ADAMs are traditionally composed of eight basic domains: 1) N-terminal signaling-domain; 2) pro-domain; 3) metalloproteinase domain; 4) disintegrin domain; 5) cysteine-rich domain; 6) EGF-like domain; 7) membrane-spanning domain; and 8) cytoplasmic domain (Fig. 1.3) (Black and White, 1998). While most domains are present in all ADAMs, studies have indicated that in special cases some either remain inactive or are absent entirely. Despite slight variations in structure, these general domains each have individual functions that dictate the role(s) ADAMs play during biological and pathological states.

The N-terminal signaling domain is responsible for directing the protein through the secretory pathway. The pro-domain, much like that of the MMPs, maintains enzyme latency through the same cysteine-switch mechanisms previously detailed, and also acts as an intramolecular chaperone (Roghani et al., 1999). Removal of the pro-domain by a proprotein convertases (i.e.-furin or PC7) in the secretory pathway produces an active enzyme (Lum et al., 1998; Anders et al., 2001). The metalloproteinase and disintegrin domains are the most studied of the ADAM domains, and are respectively responsible for the protease and adhesive properties that characterize most ADAMs. The metalloproteinase domain contains a Zn^{+2} dependent catalytically active site that is held latent by the pro-domain. Sixty percent of ADAMs possess this domain, which contains the same HEXGHXXGXXHD sequence found in the catalytic domains of most

MMPs, indicating the ability for proteolytic activity (Takeda, 2009). Major substrates that are proteolytically processed by the metalloproteinase domain include, signaling ligands and their receptors, cell-cell adhesion molecules, cell-matrix adhesion molecules, cytokines, and growth factors (White et al., 2003; Seals and Courtneidge, 2003). The disintegrin domain contains a 14 amino acid stretch (CRXXXXXCDXXEXC) called the "disintegrin loop" which is believed to be responsible for integrin interaction and therefore the adhesive property of many ADAM molecules (White et al., 2003). Interaction with integrins has been shown to influence cell adhesion and cell-cell interactions. It is important to note that not all ADAM family members have protease and/or adhesive capabilities.

Unlike the metalloproteinase and disintegrin domains, the cysteine-rich domain is present in all ADAM molecules, and is found to be continuous with the disintegrin domain. It has recently been described as having two segments, a "wrist" (C_w) and "hand" (C_h). While C_w is continuous with the disintegrin domain, C_h is the most divergent and variable segment in the ADAM structure and therefore posses what has been termed a hyper-variable region (HVR). The HVR is believed to be involved in substrate specificity, and may play a role in substrate binding to facilitate ectodomain shedding of the substrate by the metalloproteinase domain, therefore influencing protease activity (Takeda, 2009). As a whole, the cysteine-rich domain has also been shown to interact with different molecules to promote cell spreading and migration (Hooper and Lendeckel, 2005). The function of the EGF-like domain, which is absent in both ADAM-10 and -17, is not well understood in the current literature, but is thought to act as a rigid spacer connecting and orienting the metalloproteinase/disintegrin/cysteine

domains to the membrane-spanning domain (Takeda, 2009). The membrane-spanning domain tethers the ADAM protein to the cell surface, which makes these molecules very similar to the MT-MMPs. Therefore, they are presented with a limited pericellular environment which ultimately concentrates their activity to a specific zone. It is important to note that although the majority of ADAMs are found tethered to the cell surface, ADAM-11, -12, -17, and -28 are susceptible to slicing that eliminates the membrane-spanning domain (Cerretti et al, 1999; Roberts et al, 1999; Howard et al., 1999; Galliano et al., 2000). These sliced variants are released as soluble proteins, and able to act at a distance from the cell surface. It is not yet fully understood if all ADAMs are susceptible to this type of alternative splicing. Nonetheless, the production of membrane-bound and soluble ADAM forms permits both focal and diffuse extracellular activity. Among the membrane-bound ADAMs, the cytoplasmic domain varies in both length and composition and is often subject to alternative splicing. At least one Src homology region-3 (SH3) binding site is present on the cytoplasmic domain for serine/threonine or tyrosine phosphorylation. Phosphorylation of these sites and/or binding of other proteins to the cytoplasmic domain have been shown to influence ADAM maturation, trafficking, membrane localization, proteolytic activity, and association with cytoskeletal elements (Seals and Courtneidge, 2003). Taken together, the general domains of ADAM molecules permit a variety of functions that have been shown to influence processes in development and pathology.

Fig 1.3 A Disintegrin and Metalloproteinase (ADAM) General Structure. Schematic representation of ADAM structure including prodomain, metalloproteinase domain, disintegrin domain, cysteine-rich region, EGF-like domain, transmembrane domain, and cytoplasmic tail domain.

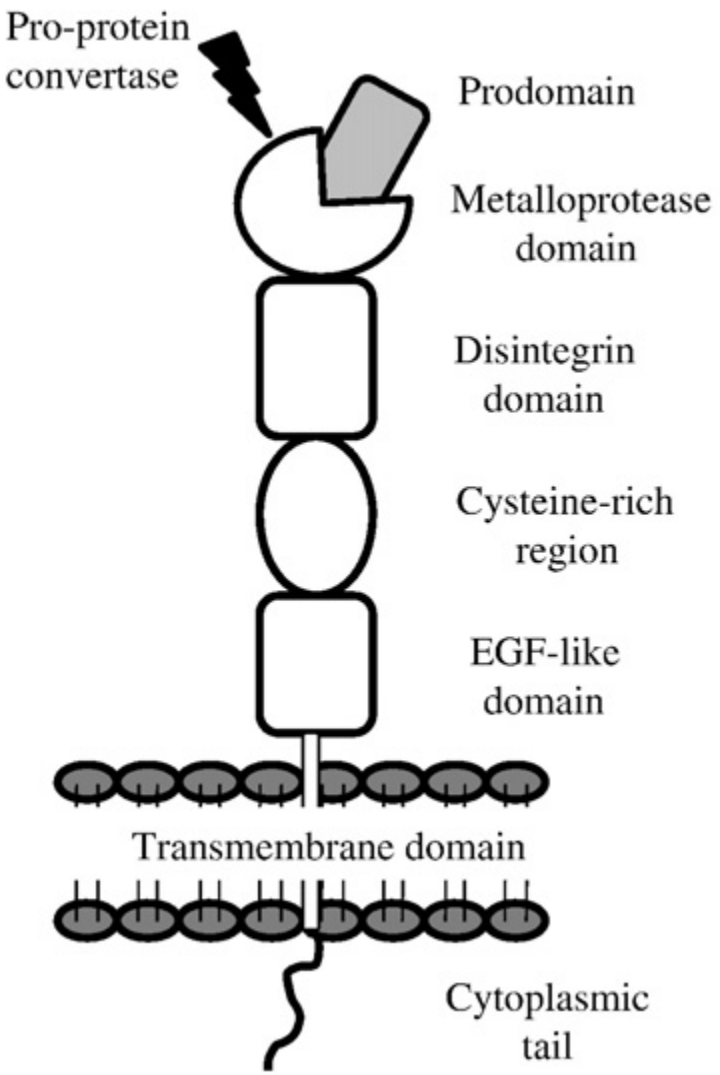

Duffy et al., 2009

Functionally, ADAM proteins are known primarily to proteolytically process the ectodomains of a variety of cell surface receptors and signaling molecules, and are often referred to as “sheddases". Secondary to protease abilities, ADAMs possess adhesive properties that also influence their functional roles during biological processes. Expression patterns implicate ADAMs in biological processes such as neuronal cell migration, axon guidance, cell adhesion, fertilization, neurogenesis, myogenesis, branching morphogenesis in lung, and heart and bone development (as reviewed by Hooper and Ledeckel, 2005). ADAMs have also been shown to play important roles in disease states including, cancer, rheumatoid arthritis, AD, Muscular Dystrophy, cardiac disease, and Multiple Sclerosis (Hooper and Lendeckel, 2005).

It is evident that ADAMs play important functional roles in development and pathology. During biological processes, ADAM activity has been shown to promote both extracellular and intracellular signaling (Reiss et al., 2005; Janes et al., 2005; Borggrefe and Oswald, 2009). Ectodomain shedding of growth factors or cytokines by ADAMs can stimulate and/or inhibit extracellular signaling pathways, which in turn influence a number of biological processes. This ectodomain cleavage of substrates by ADAMs has also been shown in many cases to be a prerequisite for intracellular signaling, involving molecules such as Notch and β-catenin (Pan and Rubin, 1997; Marambaud et al., 2003). This process, referred to as Regulated Intramembrane Proteolysis (RIP) is a sequential proteolytic cascade that involves the primary ectodomain cleavage of a membrane-bound protein, followed by a secondary cleavage within the membrane by intramembrane-cleaving molecules such as presenilins (Brown et al., 2000; Buckingham, 2003). The secondary cleavage can lead to subsequent

processing of intracellular fragments which act in intracellular signaling pathways to influence gene transcription. Currently, ADAM-10 is the primary RIP molecule in the ADAM family (Saftig and Hartmann, 2005). In addition to extracellular and intracellular signaling, ADAMs also influence cell adhesion and migration through binding to integrins and modulation of cell-cell and cell-matrix connections, respectively. Cell adhesion and migration can also be affected by cleavage of cell adhesion or ECM molecules. Therefore, in many cases, the metalloproteinase and disintegrin domains can work in concert to influence different biological processes.

Successfully carrying out these functions requires a certain level of regulation. ADAMs are tightly regulated by a variety of means. Regulation of these biological processes often involves controlling the protease activity, which can be influenced by adjacent and downstream domains. Structural modifications such as Pro domain removal and alternative splicing of cysteine-rich and cytoplasmic domains can drastically affect the activity of ADAMs. Binding of surrounding adapter proteins to or phosphorylation of the cytoplasmic domain may also impact protease activity. Due to the homology of the catalytic site between MMPs and ADAMs, several ADAM family members have been shown to be regulated by the binding of endogenous TIMPs. While much regulation is in place to limit the proteolytic activity of ADAMs, other lines of regulation act to promote sheddase activity. For example, ADAM-mediated shedding can be stimulated as a result of G-protein coupled receptors or protein kinase C (PKC) activation, changes in intracellular Ca2+ levels, and natural or experimental stimuli. Additionally, alterations to ADAM cell surface placement and localization can influence sheddase activity as well as change the pericellular environment of potential substrates

(Reiss and Saftig, 2009). These levels of regulation of ADAMs influence the spatiotemporal expression and function of ADAMs, which is necessary during biological processes. Loss of ADAM regulation has the potential to disrupt ADAM/substrate balance, and may lead to the progression of disease.

The importance of ADAMs in development and disease has been confirmed however specific nuances for each ADAM family member remain to be fully detailed. While ADAMs within small subsets may have overlapping structural and functional characteristics, it is important to delineate specific biological roles. For the purposes of this study, we have chosen to highlight ADAM-10, and emphasize its expression and activity patterns within the nervous system.

ADAM-10 and the Nervous System

ADAM-10 was first isolated in 1989 in bovine brain myelin samples, but did not get its original vertebrate designation until 1996 (Howard et al., 1996). Today, ADAM-10 has been identified as an essential protein in a number of vertebrates and is considered the principle 'RIPing' sheddase of cell surface proteins such as APP and Notch. Among the family of ADAMs, ADAM-10 shares the greatest sequence homology with ADAM-17 (Maskos et al., 1998). Both ADAM-10 and -17 lack the EGF domain and calcium I and III binding sites in the disintegrin domain, and possess additional disulfide bonds within their metalloproteinase and a shorter C_h segment in the cysteine-like domains (Takeda, 2009). Due to their sequence similarities, ADAM-10 and -17 have been shown to play compensatory roles in both development and disease. While structural and functional similarities exist between ADAM-10 and -17, ADAM-10 appears to be expressed at

higher levels in the nervous system, therefore suggesting a greater role in nervous system development and disease (Marcinkiewicz and Seidah, 2000).

Early vertebrate studies investigated expression patterns of ADAM-10 in developing and mature systems. During development, ADAM-10 mRNA was found to be expressed ubiquitously throughout the dermatome, myotome, epidermis, gut ectoderm, epithelial tissue of the kidney and liver, heart and in neural crest cells of the chick embryo (Hall and Erickson, 2003). In the developing mouse brain, ADAM-10 mRNA was detected at E13 in cranial ganglia, and at E17 and P4, primarily concentrated within the superficial cortical layers and hippocampus. In adult mouse brain, ADAM-10 mRNA expression was dampened, however more specifically localized to pyramidal cells in cortical layers II-VI, throughout the CA1 hippocampal region, dentate gyrus, and dorsal thalamus, and within non-neuronal cells including oligodendrocytes within the corpus callosum and choroid plexus cells (Marcinkiewicz and Seidah, 2000). In human tissue, ADAM-10 was found to be highly expressed throughout the brain, in both neurons and glial cells, as well as in mesenchymal stem cells, placenta, bone marrow and blood myeloid cells, and bladder (Karkkainen et al., 2000; Marcinkiewicz and Seidah, 2000; Edwards et al, 2008). These expression patterns suggested a potential functional importance of ADAM-10 within the developing and adult nervous systems. Further functional studies confirmed ADAM-10 as the principle sheddase involved in the Notch signaling pathway, and revealed it to be among a small group of ADAMs responsible for α-secretase cleavage of APP. Although substrates Notch and APP have dominated ADAM-10 literature, there are additional potential substrates, including Ephrins, CD44, L1 adhesion molecule, N-cadherin, and

EGF, that may also influence nervous system physiology and pathology (Janes et al., 2005; Nagano et al., 2004; Mechtersheimer et al., 2001; Reiss et al., 2005; Sahin et al., 2004). In the following sections, selective ADAM-10 substrates will be highlighted to demonstrate the involvement of ADAM-10 in development and disease.

ADAM-10 involvement in the Notch signaling cascade has garnered much investigation due to the importance of Notch in a number of biological processes. Within the nervous system, Notch is present from birth to death, and actively influences processes including neurogenesis, axonal and dendritic growth, synaptic plasticity, and neuronal death. Notch has also been implicated in different neuropathologies, including ischemic stroke, AD, PD, Huntington's disease, and brain cancer through the Notch signaling pathway (Lathia et al., 2008). Therefore, understanding ADAM-10/Notch interaction not only gives insight to nervous system development and maintenance, but it may also shed light on possible treatment options for the involved neuropathologies. The Notch signaling pathways involves the binding of the Notch receptor to its appropriate ligand (Delta-like, Jagged in mammals), which induces a set of proteolytic cleavages, the release of an intracellular Notch fragment, and subsequent regulation of gene transcription. The released intracellular domain of Notch does not bind directly to DNA but rather acts as a transcriptional coactivator by binding recombination signal sequence-binding protein Jκ (RBP-J) and activates the transcription of genes that contain binding sites for RBP-J (Borggrete and Oswald, 2009). Notch target genes include: transcription factors such as Hes and Hey proteins; developmental and immune genes such as CD25 and GATA3; genes associated with cell survival, proliferation, and migration such as c-myc and cyclinD1; and a variety of others such as NFκB2, bcl-2,

and ADAM-19 (as reviewed by Borggrefe and Oswald, 2009). The downstream effects of Notch signaling on both development and disease are widespread, and partially dependent on ADAM activity. ADAM-10 is capable of cleaving Notch at its first cleavage site, which in turn allows for additional cleavage by γ-secretase and release of an intracellular fragment (Pan and Rubin, 1997; Borggrefe and Oswald, 2009). Without the ADAM-mediated cleavage event, Notch deficiency would occur, leading to a breakdown in gene transcription and downstream CNS processes. Interestingly, ADAM-10 knockout mice exhibit multiple developmental malformations, including defective CNS and heart development, vasculogenesis and somitogenesis, similar to those seen in other Notch deficiency models such as Notch1/Notch4 and presenilin1/presenilin2 double knockout mice (Hartmann et al., 2002; Krebs et al., 2000; Herreman et al., 1999). Based on these finding and observations it can be posited that ADAM-10 and Notch interaction is essential for CNS development, and may also be important in CNS disease processes.

Amyloid precursor protein (APP) is another well-studied substrate of ADAM-10 that is involved in cell motility and axonal vesicular transport under normal conditions (Sabo et al., 2001; Kamal et al., 2001). Like Notch, APP is susceptible to proteolytic processing by a variety of secretases, and releases fragments that can act on downstream gene targets. Within the brain, APP can be processed by α- (ADAM-10, -17), β- (BACE1), and γ- (presenilin) secretases, and each cleavage product acts differently. Cleavage of APP by ADAM-10 results in the release of an extracellular APPsα fragment, which has been shown to be neuroprotective and promote neuroplasticity (Bell et al., 2008). This preliminary cleavage induces an intramembrane

γ-secretase cleavage and release of an intracellular fragment believed to have nuclear signaling functions. In contrast, cleavage by β-secretase results in the release of an Aβ fragment that has been associated with AD plaques, neurotoxicity, and abnormal neurite size (LaFerla et al., 2007; Sastre, 2010). Due to the protective qualities of the APPsα fragment and the detrimental nature of the Aβ fragment within the brain, ADAM-10 has recently been targeted in AD studies. In human post-mortem studies, ADAM-10 mRNA was detected by northern blot analysis in AD brains throughout the frontoparietal cortex (Marcinkiewicz and Seidah, 2000). ADAM-10 also showed moderate granular and vesicular staining in pyramidal and non-pyramidal neurons in cortical layers I-V and also around diffuse neuritic plaques (Bernstein et al., 2003). Recall that MT5-MMP was also found to localize around neuritic plaques, which may indicate functional overlap between the two membrane-bound MMPs. While ADAM-10 was present in AD brains, protein expression was significantly reduced when compared to age matched controls, indicating that perhaps a reduction in ADAM-10 results in decreased APPsα release, therefore giving way to Aβ processing and AD progression. *In vivo* AD/ADAM-10 studies support this hypothesis. When AD mice were crossed with mice that moderately overexpressed ADAM-10 (APPV7171/ADAM10mo), results indicated decreased Aβ peptide levels, reduced plaque formation and improved LTP and cognitive scores when compared to singly transgeneic AD parent mice (Postina et al., 2004). In a separate study looking at excitotoxic stress induced by kainate injection, moderate ADAM-10 expression was shown to provide neuroprotection against excitotoxic stress in AD parent mice, but failed to protect against seizures and neurodegeneration. Additionally singly transgeneic dominant negative ADAM-10 mice

showed shorter seizing times and less neuronal cell death and glial cell invasion following kainate injection when compared to wild-type mice. These results suggest that while overexpression of ADAM-10 may limit excitotoxicity in mice that also overexpress APP, inhibition of ADAM-10 may be beneficial in controlling seizure activity and neuroinflammation in this model (Clement et al., 2008). While these studies indicate a role for ADAM-10 in APP processing, it should also be noted that when ADAM-10 is deleted in cells, APP processing still occurred (Deuss et al., 2008). Although these are *in vitro* results, it is important to recognize the functional overlap between ADAM-10 and other ADAMs or MMPs.

While much of the work done to investigate ADAM-10 interaction with ephrins has been conducted in *Drosophila* it may still reveal an important functional relationship that has potential influence on vertebrate nervous system processes. Ephrins act with Eph receptors to form bi-directional signaling systems between membrane proteins involved in tissue compartmentalization processes such as somitogenesis, angiogenesis and axonal guidance (Saftig and Hartmann, 2005). Within the nervous system, axonal guidance requires axon repulsion, which is activated when Eph receptor/ephrin connections are disrupted (Pasquale, 2005). Studies indicate that ADAM-10 is capable of ephrin ectodomain cleavage, and disruption of Eph receptor/ephrin binding. In *Drosophila*, KUZ (ADAM-10 orthologue) was found to be required for proper axonal extension during development (Fambrough et al., 1996). These observations were further investigated in primary cultured neurons that showed ectodomain cleavage of ephrin-A2 when full-length KUZ was present and inhibited cleavage when dominant negative KUZ was present (Hattori et al., 2000). ADAM-10

was also found to associate with Eph3A and cleave ephrin-A5 to ensure signal termination and complex internalization in cultured cells (Janes et al., 2005). These and other studies implicate ADAM-10 as a primary sheddase of ephrins within the nervous system, and suggest an important role for ADAM-10 in plasticity changes associated with axonal guidance and nervous system development.

Finally, ADAM-10 can be tightly linked to nervous system development and plasticity through interaction with N-cadherin. This interaction is similar to that between MT5-MMP and N-cadherin. N-cadherin, which will be discussed in greater detail in the following section, is a transmembrane synaptic adhesion molecule that homophilically binds across the synaptic cleft to connect and stabilize pre- and post-synaptic elements (Benson and Tanaka, 1998). In addition to maintaining synaptic structure and integrity, N-cadherin is important for synaptic efficacy and signaling. ADAM-10 has been shown to regulate cell surface expression and availability of N-cadherin through ectodomain shedding (Uemura et al., 2006; Reiss et al., 2005). Release of the extracellular N-cadherin fragment has been shown to promote neurite outgrowth (Paradies et al, 1993; Utton et al., 2001). N-cadherin ectodomain shedding not only promotes neurite outgrowth and modulates the synaptic stability extracellularly, but it also triggers downstream intracellular cytoskeletal changes and transcriptional events through the activity and translocation of β-catenin (Reiss et al., 2005).

While MT5-MMP and ADAM-10 mediated N-cadherin cleavage, along with the downstream events will be detailed in later sections, these studies may be taken as evidence that these membrane-bound MMPs play a critical role in the process of synaptic plasticity. To better understand the potential effects of N-cadherin proteolytic

cleavage, the following section will review characteristics of classic cadherins and highlight N-cadherin's role in the nervous system.

CADHERINS

Classic cadherins

Classic cadherins constitute a well-established family of Ca^{+2} dependent, cell adhesion molecules, with as many as 20 members in a single vertebrate species (Takeichi and Abe, 2005). Cadherins are classified as single-pass transmembrane, type I glycoproteins that typically form strong homophilic bonds in the presence of Ca^{+2}, and are known to be associated with adherins junctions in a variety of cell types (Heupel et al., 2008; Benson and Tanaka, 1998). Cadherin mediated cell-cell adhesion plays an important role in development and maintenance of tissue integrity in multicellular organisms (Halbleib and Nelson, 2006). In addition to their adhesive properties, cadherins dynamically influence different intracellular signaling pathways that in turn affect downstream transcriptional events during embryological and adult processes (McCusker and Alfandari, 2009).

Structurally, these cell-adhesion molecules possess a large extracellular segment, made up of tandemly repeated extracellular cadherin domains (Fig 1.4). Based on extracellular domain number and organization, classic cadherins are further subdivided into two distinct groups: type I/II or type III cadherins. Type I/II cadherins are found solely in vertebrates and ascidians and possess five extracellular domains. Of the five extracellular domains, the distal most is responsible for specific binding, which is typically homophilic. However, heterophilic binding can occur through formation of *cis*-

and *trans*-heterodimers between similar cadherins (Shan, WS et al., 2000). This group can be further divided into type I: epithelial (E-), neural (N-), placental (P-), and retinal (R-) cadherins, and type II cadherins, which are designated numerically (ex: Cadherin-11). Type I cadherins possess a conserved HAV (histadine alanine valine) adhesion recognition sequence that is crucial for homophilic cadherin interactions (as reviewed by Suzuki and Takeichi, 2008; Noë et al., 1999). Type II cadherins lack this HAV sequence, and are often found to bind heterophilically between cells. Finally, type III cadherins exist in invertebrates and vertebrates such as fish and birds, but are not found in mammals. In contrast to type I/II, their extracellular segment typically possess greater than five extracellular domains, as well as a unique primitive class cadherin domain (PCCD) that is situated between the extracellular domains and the plasma membrane (Oda and Tsukita, 1999; Tanabe et al., 2004).

Despite variations in extracellular arrangement, all classic cadherins possess a highly conserved intracellular segment that contains juxtamembrane and cytoplasmic tail domains. The juxtamembrane domain (JMD) contains a GGGEED sequence that permits interaction with members of the p120 catenin family. The JMD also plays an important role in cell-cell adhesions and cell physiology by influencing cadherin clustering, cytoskeletal modifications, and the influx of calcium (Benson et al., 2000; Brusés JL, 2006). The cytoplasmic tail domain (CD) serves as a binding site for catenins, such as β- and γ-catenin. This protein cluster is linked to the actin cytoskeleton through α-catenin to not only ensure structural integrity of the tissue and full adhesive activity, but also to influence intracellular signaling pathways (see again Fig. 1.4) (Togashi et al., 2002; Lilien et al., 1999).

Figure 1.4 Classic Cadherin Structure and Interaction with Cytoplasmic Proteins. Classic cadherin structure includes tandemly repeated extracellular (EC) domains, a membrane spanning domain, and an intracellular domain that is further divided into juxtamembrane and cytoplasmic tail domains. The intracellular domain interacts with cytoplasmic proteins such as β- and α-catenin, which anchor cadherin to the actin cytoskeleton.

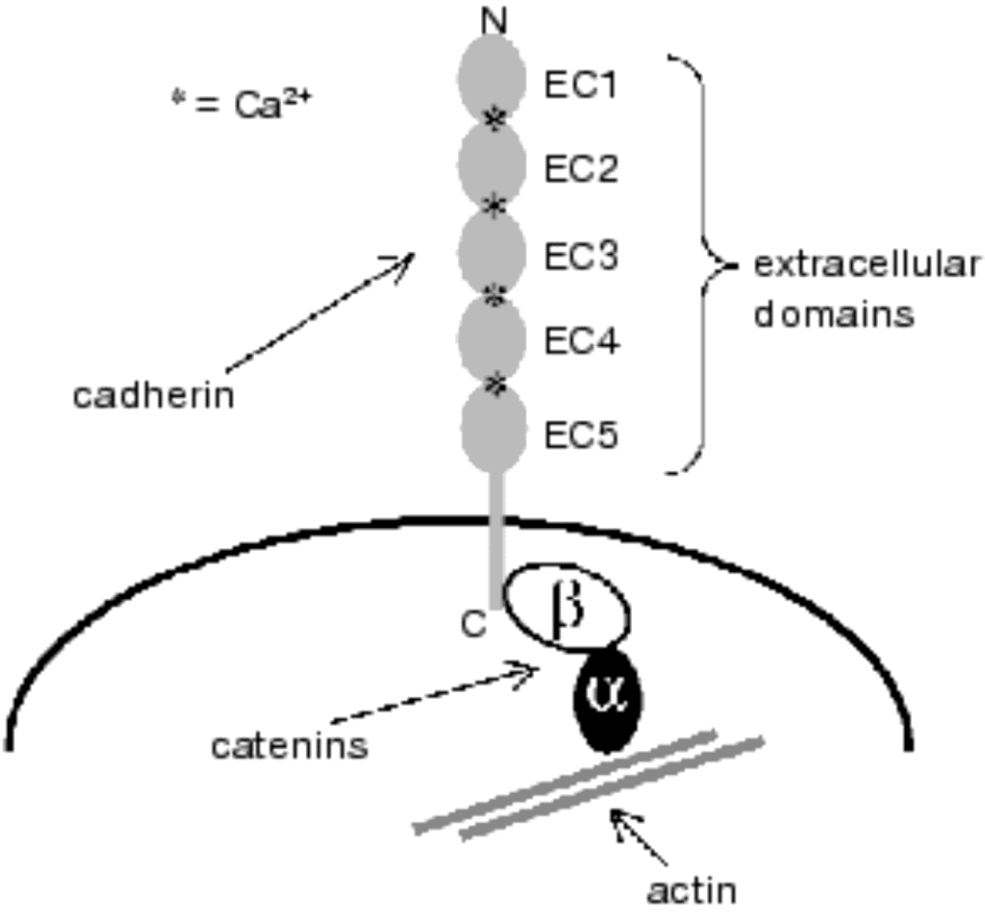

Ivanov et al., 2001

Having knowledge of the general structure and function of classic cadherins allows us to understand the role they play in tissue development, maturation and maintenance. While cadherins influence a variety of processes throughout an organism's lifespan, their role in nervous system development and disease has garnered tremendous attention and fostered important scientific inquiry. In order to highlight the importance of cadherins in the nervous system, we will shift the focus of this review to the role that N-cadherin plays in nervous system development, neurophysiology and neuropathology.

N-cadherin and the Nervous System

Successful nervous system development requires coordinated temporal and spatial synthesis, regulation, and interaction of a number of essential proteins. Of these proteins, N-cadherin (130 kDa) is one of the first present during the onset of nervous system development. *In vivo* studies show that N-cadherin mRNA is typically expressed in two phases, an early embryonic phase and a late embryonic/postnatal phase. In the early embryonic phase, N-cadherin mRNA is ubiquitously expressed throughout undifferentiated neuroepithelium. During this phase the neuroepithelium is proliferating in the ventricular zone and the first neurons begin differentiation in the marginal zone (lamina I) of the cerebral cortex. During the late embryonic/postnatal phase, when more neurons have differentiated and fiber tracts begin to form, N-cadherin mRNA expression becomes restricted to particular subsets of neurons in cell-rich layers or lamina within specific regions of the brain. These specific brain regions include: deep neocortical layers, internal nuclear layer of the retina, parietal cortex, olfactory bulb, cerebellum, and several limbic system structures such as the

hippocampus proper and dentate gyrus (Bekirov et al., 2002; Redies and Takeichi, 1993). Within the rat hippocampus, the highest observed N-cadherin mRNA expression occurs from postnatal day 0-2, within cell-rich areas such as the granule cell layer of the dentate gyrus and the pyramidal cells of CA1 and CA3 fields. It has also been observed that although N-cadherin is initially localized to both inhibitory and excitatory synapses, with time it selectively localizes to excitatory synapses within the hippocampus (Benson and Tanaka, 1998). In addition to neuronal localization, N-cadherin mRNA has also been shown within the neuropil of the dentate gyrus molecular layer, which is suggestive of astrocytic or oligodendrocyte localization (Bekirov et al., 2002). This observation is consistent with both *in vivo* and *in vitro* studies that have shown N-cadherin mRNA within supportive cells of the nervous system, such as glial and Schwann cells (Wilby et al., 1999; Letourneau et al., 1990). In the postnatal/adult phases of life, the distribution of N-cadherin is basically maintained, while its intensity of expression tends to decrease with age.

N-cadherin expression patterns indicate that it is functionally important during nervous system development, and remains necessary into later phases of life. Studies show that N-cadherin is functionally involved in neural tube morphogenesis, development of left to right asymmetry through the Wnt signaling pathway, and formation of the alar region of the midbrain, hindbrain and posterior spinal cord (Lele et al., 2002; Thiery JP, 2003). Interestingly, null-N-cadherin homozygotes display multiple nervous system defects, including malformations of somites and the neural tube, and typically die by day 10.5 of gestation due to heart defects (Thiery JP, 2003; Lou et al., 2001). Despite the cause of death, the nervous system malformations observed in

these animals would ultimately be detrimental to the process normal development, thus indicating the importance of N-cadherin during this stage.

As nervous system development persists neurons differentiate, migrate to their final destination and extend axonal and dendritic processes in order to form synaptic connections and circuits within the brain. Once established and throughout their existence, synapses experience a variety of modifications and changes. Together these processes can be characterized as either activity-independent, which includes the "hard wired" events leading up to and including synaptogenesis, or activity-dependent, which can also include synapse formation as well as further synaptic modification (ex: strengthening; weakening; deletion). N-cadherin plays important and distinct roles in both activity-independent and dependent processes.

During the activity-independent phase of development, N-cadherin is upregulated and recruited to both pre- and post-synaptic compartments, as well as along axonal shafts. Specifically, N-cadherin is recruited and inserted into the membrane of the symmetrical zone on the synapse, or puncta adherentia, which lies laterally to the asymmetric synaptic neurotransmitter release zone (Uchida et al., 1996). Studies show that recruitment of N-cadherin to these compartments during development is important for neurite outgrowth, axon target recognition, pre-synaptic assembly, dendritic spine morphogenesis, and synaptic formation and specificity (Jontes et al., 2004; Bozdagi et al., 2000; Lilien et al., 1999). In addition to a synaptic role, N-cadherin controls growth cone migration to Schwann cells, therefore influencing the process of axon myelination (Letourneau et al., 1990).

The aforementioned processes are guided and/or influenced by specific structural components of N-cadherin. Studies have investigated the role(s) extracellular and intracellular domains of N-cadherin play in these processes. As previously mentioned, the extracellular domain of cadherin is necessary for cell-cell adhesion. It is not only responsible for the physical bond formed between cells, in this case neurons, but also is important for recruitment of N-cadherin to proper sites within the neuronal compartments. Studies that look at the effect of mutant N-cadherin in both young and old neurons illustrate the importance of the extracellular domain. For example, in older neurons, with pre-established synaptic contacts, extracellular domain deletion did not lead to synapse disassembly, but instead resulted in dendritic spine morphology changes (elongated or bifurcated spines) and significantly smaller synapses. In both sets of neurons, although less dramatic in older transfected neurons, disruption of pre-synaptic vesicle recycling and Synapsin and PSD-95 distribution was observed (Togashi et al., 2002). These findings highlight the importance of the N-cadherin's extracellular domain for proper synaptic assembly, and potentially function.

The intracellular domain of N-cadherin can also influence activity-independent events during neural development and synaptogenesis. Recall that the intracellular domain possesses two distinct regions, the JMD and CD. These regions serve primarily as binding sites for different synaptic proteins that are essential for synaptic formation and function. A majority of these synaptic proteins belong to the catenin family. The interaction between catenins and N-cadherin's intracellular domain is not only essential for the creation and maintenance of synaptic structure, but also important for intracellular signaling.

It is important to note that the JMD and CD have distinct roles when it comes to carrying out these essential synaptic functions. The JMD has been shown to influence processes such as neurite outgrowth, functional coupling between pre- and post-synaptic elements, synaptic adhesion, and synaptic stabilization through cadherin clustering. These events are believed to involve the coupling and uncoupling of p120 catenin to/from its surface (as reviewed by Brusés, 2006). The relationship between the JMD and p120 catenin has also been implicated in intracellular signaling. When p120 becomes uncoupled from the JMD, it has been shown to influence transcription through nuclear translocation and subsequent interactions with a zinc finger transcription factor (Daniel and Reynolds, 1999).

The CD appears to have more of a structural role during neural development and synaptogenesis, through its interaction with catenins and the actin cytoskeleton. Studies have implicated the CD/catenin complex in events such as neurite outgrowth, pre-synaptic vesicle assembly, dendritic spine stabilization, and synaptic adhesion and maturation (as reviewed by Brusés, 2006; Benson and Tanaka, 1998). Proper orientation of N-cadherin, β-catenin, αN-catenin and cytoskeletal components is necessary for these events to occur successfully. Multiple studies have shown that alterations to any one of the complex proteins during synaptogenesis in young neurons can lead to dendritic morphological changes and synaptic destabilization (Togashi et al., 2002; Abe et al., 2004; Bozdogi et al., 2004). More mature neurons tend to be affected less by these changes, which may indicate compensation by similar cadherins/catenins. The CD is also involved in intracellular signaling, primarily through interaction with β-catenin which is influenced by phosphorylation. β-catenin is in a dephosphorylated

state while bound to the CD, but is released into the cytoplasm when phosphorylated (Lilien et al., 1997). Uncoupled β-catenin, which is well established as a Wnt signaling molecule, has the potential to influence a variety of signaling pathways and downstream transcription (McCusker and Alfandari, 2009). For example, β-catenin can combine with the Tcf/LEF family of transcription factors to alter gene expression (Huber et al., 1996; Moon et al., 2004). It is clear that both the JMD and CD play important roles in synaptic formation, structural integrity, and intracellular signaling during activity-independent developmental and synaptogenic events.

Beyond development, N-cadherin has been found to be involved in activity-dependent events, mainly activity-dependent synaptic plasticity. Activity-dependent synaptic plasticity is a dynamic process that involves periods of neural activity at the synapse that have the potential to change synaptic structure and strength, and is essential to normal brain function. Activity-dependent plasticity is also crucial in synaptic circuitry rewiring following CNS injury (Benson et al., 2000). Neural activity has been shown to increase adhesive forces of N-cadherin and also recruit more N-cadherin to existing and nascent synapses at different stages of synaptic plasticity (Tanaka et al., 2000; Bozdogi et al., 2000). Decreasing or increasing neural synaptic activity using pharmacological agents can also alter the expression and localization of catenins that are associated with N-cadherin intracellularly (Abe et al., 2004). Recall that the alteration of any of the cadherin-catenin components has been shown to correlate with changes in synaptic structure and function.

The experimental model most often used to illustrate N-cadherin's involvement in synaptic plasticity is LTP. To understand N-cadherin's role in synaptic plasticity, it is

important to first describe the LTP model. LTP is the cellular model of long-lasting synaptic plasticity that is believed to contribute to learning and memory (Nagy et al., 2006). Because the hippocampus is crucial for learning and memory formation, hippocampal slice preparations is the dominant model used in these experiments, where the CA3 field Schaffer collateral afferent fibers are stimulated, and recordings of field excitatory postsynaptic potentials (fEPSP) are taken from the dendrites of the CA1 field (Squire, 1992). The high frequency stimulation administered to the slice triggers strong depolarization of neurons, which can lead to both short and long-lasting synaptic plasticity. Short-lasting plasticity is fast and occurs during the induction and early phases of LTP (E-LTP), often lasting for approximately 60 minutes post-stimulation. E-LTP does not require new protein synthesis, but rather relies on modification to the synapse using existing and available stored proteins (Malenka and Bear, 2004). Long-lasting plasticity is slower to develop, occurs during the late phases of LTP (L-LTP), and involves gene transcription and protein synthesis, as well as the formation of new synaptic connections. L-LTP can last hours to days, and sometimes weeks post-stimulus (Benson et al., 2000; Bozdogi et al., 2000). N-cadherin has been shown to play important and distinct roles in both E-LTP and L-LTP.

Based on the synaptic localization of N-cadherin and its role in synaptic assembly and adhesion, it is clear to see how it can influence short- and long-term activity-dependent synaptic plasticity. Alterations in short-term synaptic plasticity properties have been demonstrated in N-cadherin knockout embryonic stem cells, which displayed functional impairments in high-frequency pre-synaptic vesicle exocytosis (Jüngling et al., 2006).

In the case of E-LTP, which includes LTP post-stimulus induction, studies have shown an important role for N-cadherin. In hippocampal slices pre-treated with N-cadherin blocking antibodies, antagonists, or recombinant fragments, E-LTP either fails to be induced or displays a decreased E-LTP response that quickly returns to baseline (Tang et al., 1998). N-cadherin also has been shown to be important in strengthening of existing and assembly of new synapses during L-LTP. In a study by Bozdogi et al., spCAMP induced LTP resulted in a significant increase of N-cadherin protein levels at synaptic labeled puncta (2000). In contrast to N-cadherin LTP studies, cadherin-11 knockout mice display enhanced LTP in hippocampal neurons that appeared structurally sound. This finding suggests that cadherins may influence different signaling cascades that contribute to synaptic plasticity, and that there are unique roles for cadherins localized within this region (Manabe et al., 2000).

How does N-cadherin strengthen synapses during neural activity? A possible mechanism involves the association for N-cadherin with N-methyl-D-aspartic acid (NMDA) type glutamate receptors (NMDAR). Following strong stimulation of NMDAR, N-cadherin dimerizes and becomes increasingly resistant to being processed by MMPs. Dimerization promotes strong synaptic adhesion and therefore allows additional synaptic changes to take place without compromising synaptic stability (Tanaka et al., 2000). However, another study indicates that neural activity may decrease N-cadherin adhesive forces due to changes in [Ca^{+2}]. It is well established that a threshold of neural stimulation causes an influx of Ca^{+2} through NMDAR channels, and leads to a decrease [Ca^{+2}] at the synaptic cleft. This decrease in extracellular Ca^{+2} limits the available Ca^{+2} needed for homophilic N-cadherin binding, therefore weakening its

adhesive properties and permitting structural remodeling. It is estimated that [Ca^{+2}] drops from 1.3mM to 0.8-.03 nM upon LTP induction, which in some cases may be sufficient to weaken N-cadherin synaptic adhesion (Heupel et al., 2008). Despite varying reports, opposing N-cadherin responses to neural activity may be due to involvement of different signaling pathways that are activated during specific stages of development and disease.

Neural activity can also lead to N-cadherin extracellular domain cleavage by enzymes such as MT5-MMP and ADAM-10, an event that is triggered by NMDAR stimulation (Fig 1.5) (Monea et al., 2005; Reiss et al., 2005; Uemura et al., 2006). Extracellular domain cleavage decreases N-cadherin's adhesive capabilities across the synapse, which may be beneficial during period synaptogenesis when the flexibility of synaptic elements is necessary. Release of a 90 kDa N-cadherin N-Terminal Fragment (NTF) into the extracellular space can influence different biological events. For example, NTF can associate with ECM molecules and potentially influence cell adhesion and neurite outgrowth. In addition, extracellular cleavage of N-cadherin activates a cascade of events that results in additional cleavage and signaling intracellularly (McCusker and Alfandari, 2009). Intracellular C-terminal Fragment 1 (CTF1; 40 kD), which contains the transmembrane and entire intracellular domain of N-cadherin, is generated following NTF shedding. CTF1 is further modified by Presenilin-1 (PS-1), which releases the intracellular domain from the transmembrane domain, and is renamed CTF2 (35 kD) (Uemura et al., 2006). CTF2 can interact with both β-catenin and cAMP response element-binding (CREB) binding protein (CBP) to prevent their degradation, and in turn either promote or limit gene transcription (Marambaud et al.,

2003; Reiss et al., 2005). While the exact function(s) of these fragments remains elusive, it is clear that neural activity alters N-cadherin structure and function, and in turn affects different synaptic processes.

Based on the current literature, N-cadherin serves a number of functions during synaptogenesis and throughout the life of a synapse. N-cadherin is important during activity-independent events, such as neurite outgrowth and axon targeting, and during activity-dependent events such as synaptic plasticity and intracellular signaling. Many of these studies have focused on the role(s) of N-cadherin during normal nervous system development and neurophysiological events. There appears to be a need for further investigation of N-cadherin expression and function during various neuropathologies, such as TBI. Therefore, we have designed this study to investigate the interaction between N-cadherin and two membrane-bound MMPs, MT5-MMP and ADAM-10, during injury-induced synaptogenesis following TBI.

Figure 1.5 Cleavage Products of N-cadherin. MMP extracellular cleavage of full-length (130 kDa) N-cadherin releases a 90 kDa N-terminal fragment (NTF). Extracellular cleavage is followed by intracellular processing of N-cadherin. Intracellular fragments include a ~40 kDa C-terminal fragment 1 (CTF1) and a second ~35 kDa fragment (CTF2).

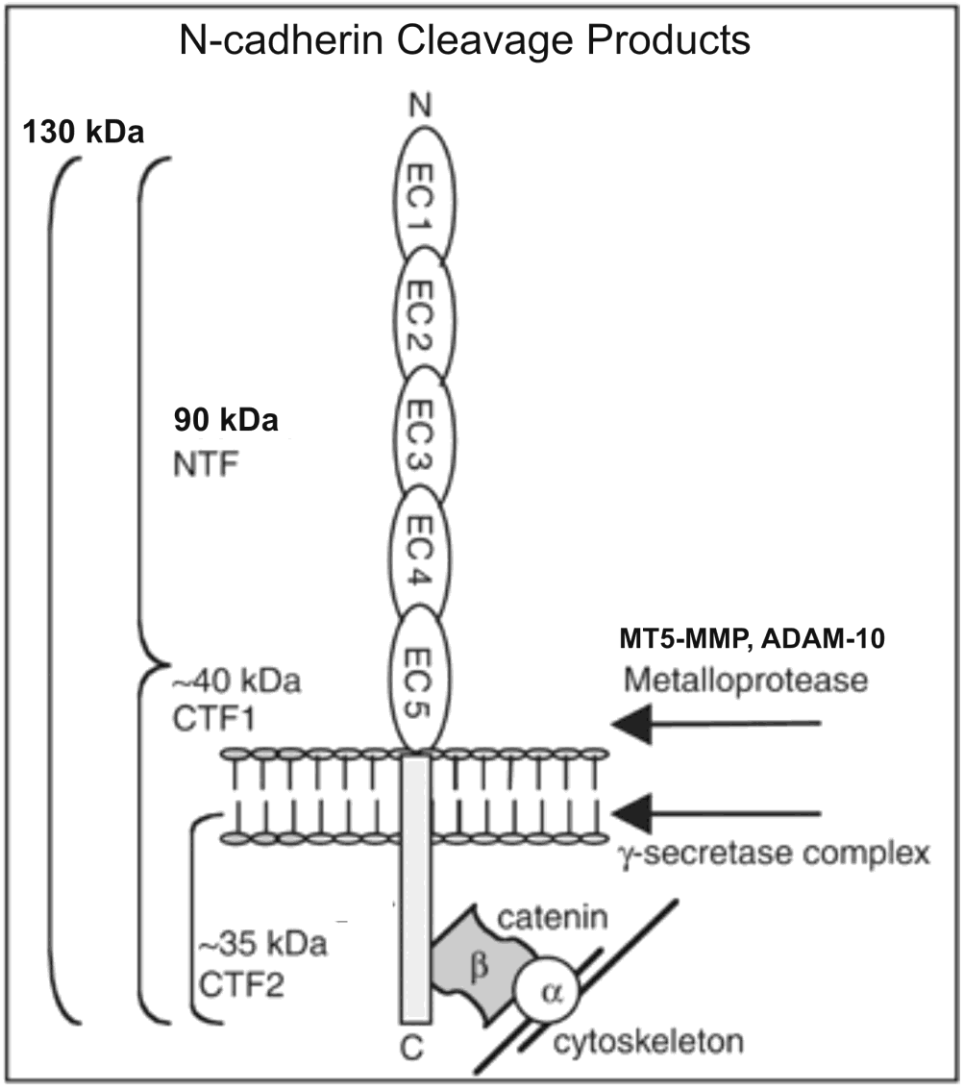

Reiss et al., 2005

EXPERIMENTAL HYPOTHESES

The following set of experiments and their results are divided into two main chapters. The first chapter describes the spatial and temporal hippocampal expression of MT5-MMP, ADAM-10, and N-cadherin in models of adaptive (UEC) and maladaptive (TBI+BEC) synaptogenesis. The second chapter describes the effects of *in vivo* pharmacological MMP inhibition on protein expression, physiological response, synaptic structural integrity and cognitive behavior during maladaptive synaptogenesis induced by (TBI+BEC). The general hypotheses for both sets of experiments are:

Hypothesis 1: Hippocampal MT5-MMP, ADAM-10 and N-cadherin protein and mRNA expression will be altered in UEC and TBI+BEC models during each phase of reactive synaptogenesis (2, 7, and 15d postinjury). The comparison of spatial and temporal expression profiles for MT5-MMP, ADAM-10 and N-cadherin will reveal differences between models of adaptive (UEC) and maladaptive (TBI+BEC) plasticity, identifying aberrant changes linked to the extent of recovery achieved.

To test Hypothesis 1, the spatial and temporal profile of hippocampal protein and mRNA expression was characterized using Western blot analysis, immunohistochemistry and qRT-PCR over select postinjury time intervals (2, 7, and 15d for protein; 7d for mRNA).

Hypothesis 2: MMP inhibition during periods of enhanced MT5-MMP/ADAM-10 expression will alter N-cadherin protein levels, as well as improve both synaptic efficacy and structure during synapse stabilization when examined 15d post-

TBI+BEC. These effects on synaptic plasticity will be reflected in progressive abrogation of injury-induced cognitive deficits when tested at 12-15d postinjury.

To test Hypothesis 2, TBI+BEC cases were treated with either MMP inhibitor GM6001 or vehicle at 6-7d postinjury. The GM6001 treated and vehicle groups were then sacrificed during the period of synapse stabilization at 15d after injury. Hippocampal protein expression was determined using Western blot analysis, while synaptic function was analyzed by *in vitro* electrophysiological measures, and synaptic cytoarchitecture determined using electron microscopic techniques. A separate group of TBI+BEC animals was subdivided for either the same GM6001 or vehicle treatment and tested for cognitive performance in the Morris Water Maze at 12-15d postinjury.

Chapter 2

Classification of MT5-MMP, ADAM-10 and N-cadherin during Adaptive and Maladaptive Injury-Induced Synaptogenesis

ABSTRACT

Traumatic brain injury (TBI) leads to long-term impairments, often resulting from excessive neuroexcitation and axonal insult within vulnerable brain regions (Okonkwo and Povlishock, 2003; Povlishock and Katz, 2005). Axon damage produces deafferentation and triggers an injury-induced synaptogenic response, involving matrix metalloproteinase (MMP) interaction with paired substrates within the deafferented region. Two such MMPs are Membrane-Type 5 Matrix Metalloproteinase (MT5-MMP) and A Disintegrin and Metalloproteinase-10 (ADAM010), which are highly expressed in the brain and may influence injury-induced synaptogenesis via cleavage of a shared substrate, neuronal cadherin (N-cadherin) (Reiss et al., 2005; Monea et al., 2006). The present study examined the spatial and temporal profiles of hippocampal protein and mRNA for MT5-MMP, ADAM-10 and N-cadherin. Models of adaptive (unilateral entorhinal cortex lesion; UEC) and maladaptive (combined central fluid percussion with bilateral entorhinal cortex lesion; TBI+BEC) plasticity were contrasted in order to identify differences in the expression of these matrix proteins during reactive synaptogenesis. Rats were subjected to UEC or TBI+BEC and hippocampal protein extracts prepared at 2, 7, and 15d postinjury. Western blot results showed significant elevation of MT5-MMP and ADAM-10 expression at 2 and 7d in both models, however, model differences were observed at 15d. Each enzyme was decreased at 15d after UEC, but only MT5-MMP showed reduction following TBI+BEC, while ADAM-10 exhibited a persistently elevated expression . Adaptive UEC recovery reduced N-cadherin at 2d, which returned to control levels at 7d, and increased expression at 15d. Maladaptive plasticity induced by TBI+BEC also caused a significant decrease N-cadherin at 2 and 7d, but failed to show

the increase at 15d as was seen with UEC. Preliminary qRT-PCR experiments sampling 7d deafferented molecular layer revealed increases in UEC transcript for MT5-MMP and ADAM-10 consistent with the observed protein change, while in TBI+BEC only ADAM-10 transcript was altered, with an elevation matching 7d protein rise. N-cadherin mRNA showed an increase at 7d after UEC, prior to 15d protein increase. By contrast, N-cadherin transcript was not altered at 7d after TBI+BEC, supporting absence of any rise in N-cadherin protein. These inter model differences support distinct roles for each molecule in generating the maladaptive plasticity observed post-TBI+BEC. In parallel immunohistochemical experiments, MT5-MMP, ADAM-10 and N-cadherin showed strong signal within reactive astrocytes of the deafferented dentate molecular layer, suggesting either a glial synthetic or phagocytotic role for processing matrix proteins during recovery. Collectively, these results reveal spatio-temporal differences in MT5-MMP, ADAM-10 and N-cadherin expression when adaptive and maladaptive synaptic plasticity are compared, identifying specific molecules and times which might be targeted for improvement of synaptic recovery following TBI.

INTRODUCTION

Traumatic brain injury (TBI) is a widespread, commonly under-diagnosed neuropathology that affects roughly 1.7 million people each year in the United States alone (Faul et al., 2010). Following TBI, many patients experience long-term physical, cognitive, and/or psychosocial impairments, which arise as a result the primary traumatic insult, as well as the subsequent cascade of secondary neuropathological

events (Povlishock and Katz, 2005; Langlois et al., 2006). These secondary events often result in diffuse axonal damage, neuronal death, and deafferentation within the damaged brain region (Povlishock and Christman, 1995; Hayes et al., 1992; Okonkwo and Povlishock, 2003). In an attempt to repair the damaged tissue and regain function, the brain exhibits properties of synaptic plasticity, where surrounding non-injured neurons sprout to create new synaptic connections. However, the success of functional recovery is based on a variety of factors, including the complexity and severity of the injury.

Experimental models of TBI have been designed to mimic the neuropathology and downstream reactive synaptogenesis observed following injury in humans. Following experimental TBI successful synaptic reorganization is evident, and postinjury events can be divided into three specific phases: degradation of injured axons (1-5 days post-lesion); regeneration of new synapses (6-15 days post-lesion); synaptic maturation (15-30+ days post-lesion) (Steward and Vinsant, 1983). Of these models, the unilateral entorhinal cortex lesion (UEC) is well-established as a model of adaptive injury-induced synaptogenesis within the hippocampus (Steward et al., 1988). The UEC eliminates 80-90% of the afferent fibers that synapse in the outer molecular layer (OML) of the rat dentate gyrus. It is an appropriate model for studying adaptive injury-induced synaptogenesis, because it results in predictable remodeling of the deafferented zone and recovery. However, plasticity and functional recovery in the human TBI patient is less organized and predictable, and therefore the use of more complex and clinically relevant models is warranted. In an attempt to reproduce the complex neuropathology and persistent cognitive deficits similar to those seen in human TBI, our lab developed a

rodent injury model that combines central fluid percussion with bilateral entorhinal cortex lesions (TBI+BEC). This model results in diffuse neuroexcitatory injury with bilateral focal hippocampal deafferentation, leading to maladaptive synaptic plasticity and persistent structural, functional and behavioral deficits (Phillips et al., 1994; Phillips and Reeves, 2001). By contrasting models of adaptive and maladaptive plasticity (UEC vs. TBI+BEC), we can determine the expression profile of different proteins over time postinjury, focusing on candidates which may be responsible for the failure of successful synaptogenesis and functional recovery seen in the TBI+BEC model.

Of the many proteins that change following injury, matrix metalloproteinases (MMPs) are among those upregulated in several models of central and peripheral nervous system injury (Truettner et al., 2005; Rosenberg et al., 2007; Falo et al., 2006; Komori et al., 2004; Yong et al., 2001). MMPs constitute a large family of zinc and calcium-dependent enzymes responsible for cleavage of a variety of extracellular matrix (ECM) substrates in response to different neuropathologies, including TBI (Sekine-Aizawa et al., 2001; Sounni and Noel, 2005; Cunningham et al., 2005; Yong et al., 2001). During the early postinjury stages, MMPs play important roles in ECM degradation which can foster synaptic reorganization. However, persistent MMP expression and activity has the potential to produce excessive ECM/substrate breakdown and poor synaptic functional recovery following TBI (Suehiro et al., 2004; Rosenberg et al., 1996a, 1996b, 1998, 2001; Kim et al., 2005; Shigemori et al., 2006). To better understand the role of MMPs in synaptic plasticity, we have characterized different MMP/substrate pairs in the adaptive UEC and maladaptive TBI+BEC models. We found that MMP expression after UEC was temporally correlated with different

phases of adaptive synaptogenesis. However, selective secreted MMPs were persistently upregulated during post-TBI+BEC synaptogenesis, and failed to show consistency with expression patterns characteristic to adaptive plasticity (Falo et al., 2006; Kim et al. 2005). These findings reveal the importance of MMPs in the process of reactive plasticity, and suggest that manipulation of their expression may improve functional recovery following injury.

While our lab and others have historically investigated the post-TBI role of secreted MMPs, the role of membrane-bound MMPs had not been studied in TBI synaptic plasticity models. In contrast to their secreted counterparts, membrane-bound MMPs are specifically positioned adjacent to their substrates, which may permit lytic activity at neuronal membrane sites targeted for synaptic function. In this novel study, we characterized the hippocampal protein profiles of two membrane-bound MMPs, Membrane-type 5 matrix metalloproteinase (MT5-MMP) and A disintegrin and metalloproteinase-10 (ADAM-10), along with their mutual substrate neural cadherin (N-cadherin) during the period of reactive synaptogenesis induced by UEC and TBI+BEC. MT5-MMP and ADAM-10 are localized in and around hippocampal synapses and have been shown to cleave N-cadherin. N-cadherin functions at synapses via homologous N-terminus interaction with adjacent cadherins to guide developing synapses and stabilize and strengthen mature connections (Jaworski, 2000; Marcinkiewicz and Seidah, 2000; Takeichi and Abe, 2005; Monea et al., 2006; Reiss et al., 2005). N-cadherin also forms intracellular complexes with catenin molecules, which are ultimately anchored to cytoskeletal structural elements to further ensure synaptic structural integrity (Takeichi and Abe, 2005). Therefore proteolytic extracellular cleavage of N-

cadherin by MT5-MMP and/or ADAM-10 activity may potentially modify synaptic structure and function during injury-induced synaptogenesis.

In the present study, we investigated the spatio-temporal protein profiles of MT5-MMP, ADAM-10 and N-cadherin within the deafferented hippocampus at 2, 7, and 15d postinjury. This time course encompasses the three phases of injury-induced synaptogenesis previously described. We hypothesized that the protein profiles of all three molecules would be significantly altered after TBI, and that these profiles would show differences between adaptive and maladaptive recovery, particularly during the 7-15d period of synapse generation and stabilization. Parallel changes in mRNA production for each molecule were also posited. Finally, we also hypothesized that hippocampal MT5-MMP and ADAM-10 protein distribution would be altered during synaptogenesis, showing an elevation within the deafferented outer molecular layer. This elevation was posited to include increases within reactive astrocytes, positioned in close proximity to synaptic N-cadherin (Fig. 2.1).

Figure 2.1 Proposed Synaptic and Peri-Synaptic Protein Localization. Schematic representation of ADAM-10 (red) localization in post-synaptic density and surrounding glial processes; MT5-MMP (blue) in surrounding glial processes; and N-cadherin (yellow) spanning the synaptic cleft and localized in both pre- and post-synaptic elements. Proximity of MMPs to N-cadherin favors molecular interaction/processing

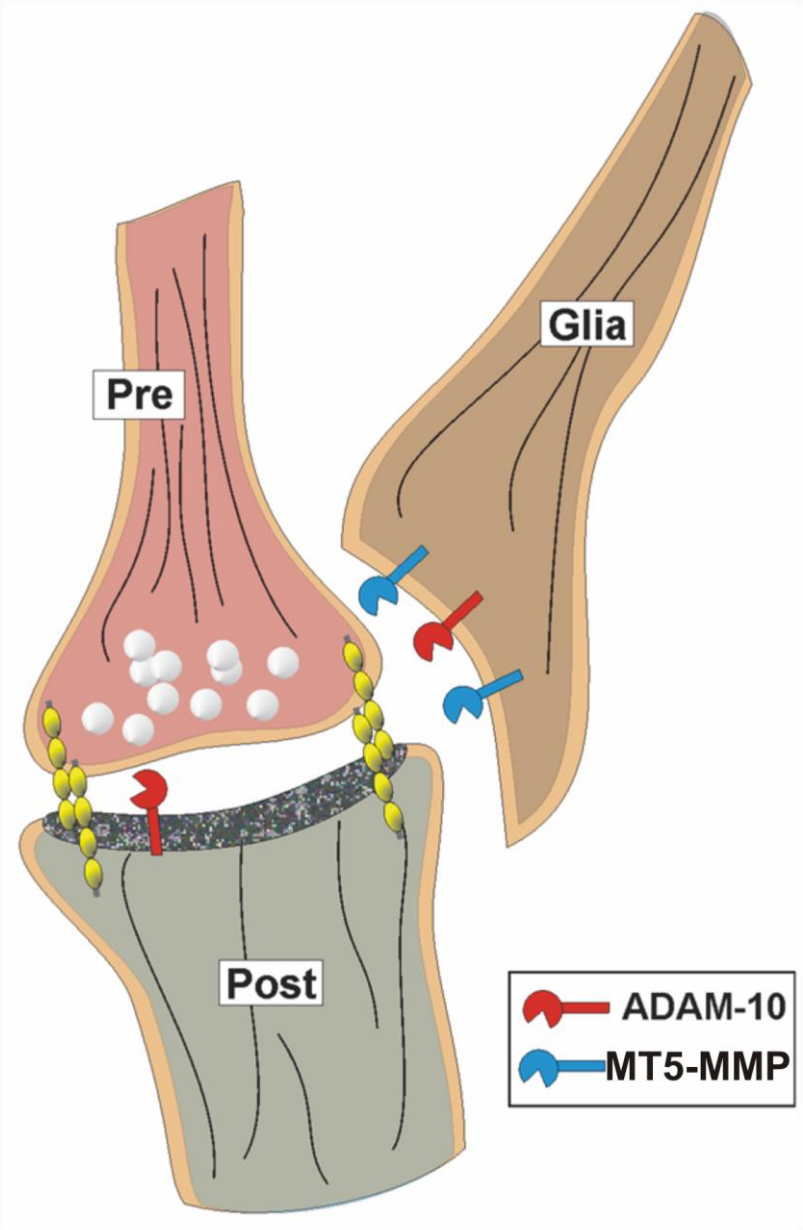

METHODS

Experimental Animals

Adult male Sprague-Dawley rats (300-400g) were used in this study. Two rats were housed per cage, with food and water *ad libitum,* and subjected to a 12 hr dark-light cycle at 22°C. All protocols for injury and use of animals were approved by the Institutional Animal Care and Use Committee of Virginia Commonwealth University. At 2, 7 and/or 15d postinjury time intervals, four randomly divided animal groups were used for biochemical assessment: (1) Unilateral Entorhinal Cortex (UEC, total n=41), (2) Combined Injury (TBI+BEC, total n=58), (3) Sham-injured (total n=53). For all biochemical analysis, the contralateral hippocampus served as a paired-control for the UEC, while sham-injured animals served as controls for the TBI+BEC animals.

Unilateral Entorhinal Cortex Lesion

The entorhinal cortex lesion (UEC) protocol was a modification of the method of Loesche and Steward (1977). A group of rats were anesthetized with isoflurane (4% in carrier gas of 70% N_2O and 30% O_2) delivered via nose cone and placed in a stereotaxic frame for surgical preparation. During all surgeries, animal body temperature was maintained at 37°C via thermostatic heating pad (Harvard Apparatus, Holliston, MA). Additionally, animal heart rate (beats per minute, bpm), arterial oxygen saturation (%), breath rate (breath per minute, brpm), pulse distention (μm), and breath distention (μm) were monitored via pulse oximeter during all surgical preparation (MouseOx; Starr Life Sciences, Oakmont, PA). Briefly, an approximately 3 mm x 5mm portion of the skull was removed on the right side to expose the dura mater superior to the entorhinal cortex. Electrolytic lesions were made by passing a 1.5 mA current (40

second duration) via 0.2 mm Teflon-insulated wire electrode, positioned 10° to the perpendicular plane, at eight separate stereotaxic sites: 1.5 mm anterior to the transverse sinus, and 3, 4, and 5 mm lateral to midline, 2 , 4 and 6mm ventral to the brain surface for the first two lateral measurements (3 and 4mm) and only 2 and 4mm ventral to the brain surface for the last lateral measurement (5mm) (see Appendix A, Fig A-1). After lesioning, the electrode was removed, the scalp was sutured over the surgical site, and Bacitracin was applied. Rats were closely monitored for recovery from anesthesia and lesion and then returned to their home cages.

Surgical Preparation for Central Fluid Percussion TBI

Animals were anesthetized (as above) and placed in a stereotaxic frame for surgical preparation 24hrs prior to injury. Body temperature and physiological measurements were monitored throughout surgical preparation (as above). As previously described (Phillips et al., 1994), rats received a 4.8 mm midline craniectomy midway between bregma and lambda, exposing but not breaching the underlying dura (see Appendix A, Fig A-2). Two steel screws were implanted 1 mm caudal to the coronal suture on the left and 1mm rostral to lambdoidal suture on the right. A modified Leur-Loc hub (2.6 mm inside diameter) was implanted in the craniectomy site and fixed with cyanoacrylate adhesive. Dental acrylic was added around the hub and screws to secure the complex. The scalp was sutured closed to cover hub and Bacitracin was applied to the wound. Rats were monitored for recovery and returned to their home cages.

Central Fluid Percussion TBI

Moderate central fluid percussion injury (2.0±0.1 atm) was performed as described by Dixon et al. (1987). The fluid percussion injury device is made up of a Plexiglas cylinder (60cm long, 4.5 cm diameter) filled with double distilled water. One end of the cylinder has a rubber-covered Plexiglas piston mounted on O-rings, and the opposite end is closed by a metal extra-cranial pressure transducer (Entram Devices, Inc., model EPN-0300-100A). The end of the metal transducer (5mm tube, 2.6 mm inside diameter) has a male Leur-loc fitting that connects to the exposed female Leur-loc hub implanted in the rat skull. A metal pendulum is dropped from a determined height that coincides with injury severity, and strikes the rubber-covered piston, forcing a small injection of 2x distilled water into the closed cranial cavity, briefly displacing brain tissue (see Appendix A, Fig A-2). Injury level is recorded by the extra-cranial transducer, and visualized and reported (atmospheres, atm) on an oscilloscope (Tektronix 5111: Beaverton, OR). Twenty-four hours after surgical preparation, rats were re-anesthetized, connected to the fluid percussion device through the exposed hub, and subjected to injury. Animals were monitored for recovery from anesthesia and injury by observation and timing of multiple reflexes (paw, tail, corneal, righting, pinna), and then returned to their home cages.

Combined Central Fluid Percussion +Bilateral Entorhinal Lesion

Animals that received the combined injury were surgically prepared for fluid percussion injury, and twenty-four hours later received moderate (2.0±0.1 atm) central fluid percussion injury. These animals recovered for another twenty-four hour time period, and were then re-anesthetized and subjected to bilateral entorhinal cortex

lesions (Phillips et al., 1994). Bilateral lesions were performed as described above in UEC protocol (see Appendix A, Fig A-2). After lesioning, electrodes were removed, the scalp sutured, and Bacitracin was applied. Animals were transferred to a recovery cage and monitored for at least 1 hr to ensure adequate recovery, and were then returned to their home cages.

Western Blotting

At 2, 7, and 15d following UEC or TBI+BEC a subset of animals (UEC n=24; TBI+BEC n=39; Sham-injured n=35) were selected for hippocampal protein analysis. Rats were anesthetized (4% isoflurane in carrier gas of 70% N_2O and 30% O_2) and sacrificed by decapitation. Whole hippocampi were removed, homogenized in ice-cold TPER (Pierce), and centrifuged (8,000xg) for 5 min at 4°C. Supernants were removed and assayed for protein concentration (Shimadzu UV-160, Shimadzu Scientific, Columbia, MD; FLUOstar Optima, BMG Labtechnologies, Inc., Durham, NC). For blot preparation, a 1:5 dilution (5 µg sample:20 µg H_2O) of each sample was mixed with XT Sample Buffer/Reducing Agent (Bio-Rad Laboratories, Hercules, CA) and heated at 95°C. Proteins were resolved on a 4-12% Bio-Tris gel (Bio-Rad) and transferred to PVDF membranes. Post-blotted gels were stained and analyzed for even protein load and transfer. Membranes were washed in dH_2O twice and TBS once for 5 min each, and then blocked in 5% milk TBS-Tween (TBS-T) for 1 hour. Membranes were then probed with primary antibody (MT5-MMP rabbit polyclonal n-terminus: 1:1,000, Abcam, Cambridge, MA; N-Cadherin mouse monoclonal c-terminus: 1:1,000, BD Transductions Laboratories, San Jose, CA; ADAM-10 rabbit polyclonal c-terminus: 1:1,000, Sigma, St. Louis, MO) in 5% Milk TBS-T. After overnight incubation at 4°C, blots were washed six

times with Milk TBS-T for 5 min each, incubated in secondary antibody (IgG goat anti-mouse: 1:20,000, Rockland, Gilbertsville, PA; IgG bovine anti-rabbit: 1:20,000, Santa Cruz, Santa Cruz, CA;) for 1 hour, and washed six times with TBS-T for 5 min each. Antibody binding was visualized with enhanced chemiluminescence substrate, SuperSignal (Thermo Scientific, Rockford, IL). Positive blot bands were imaged on the Syngene G: BOX and densitometry was performed by GeneTools (Syngene, Frederick, MD). β-actin (mouse monoclonal: 1:3,000, Sigma, St. Louis, MO) was used as a load control for TBI+BEC Western blot experiments (see Appendix B, Fig B-8), while post-blot staining was used to assess loading consistency for UEC Western blot experiments.

Immunohistochemistry

At 2, 7 and 15d following UEC or TBI+BEC a subset of animals (UEC, n=7; TBI+BEC, n=13; Sham-injured, n=13) were selected for qualitative analysis. Rats were anesthetized with a lethal dose of sodium pentobarbital (90 mg/kg, i.p.) and perfused first with 0.9% NaCl followed by aldehyde fixative (4% paraformaldehyde in 0.1M NaHPO4 Buffer or PBS, pH=7.4). Brains were removed and stored in buffer overnight at 4°C. Coronal vibratome sections (30-40 µm) of the hippocampus and dentate gyrus were prepared for immunofluroescent visualization. Briefly, vibratome sections were pre-incubated in 0.5% peroxidase for 30 min, and washed three times with PBS for 10 min each. PBS was removed, sections were placed in blocking buffer (fish gelatin in PBS + 0.05 % Triton X-100) for 30 min and then incubated overnight at 4° C in primary antibody (MT5-MMP rabbit polyclonal n-terminus: 1:250, Abcam, Cambridge, MA; N-Cadherin goat polyclonal n-terminus: 1:100, Santa Cruz, Santa Cruz, CA; ADAM-10

goat polyclonal c-terminus: 1:500, Santa Cruz, Santa Cruz, CA; GFAP mouse monoclonal: 1:20,000, Millipore, Billerica, MA; CD-11 mouse monoclonal: 1:500, BD Biosciences, San Jose, CA; Iba-1 rabbit polyclonal: 1:250, Wako, Osaka, Japan). Antibody signal was optimized in preliminary experiments, and selected sections were incubated overnight in primary antibody in each experiment. After overnight incubation, sections were washed three times in PBS for 10 min each, and then blocked for 30 minutes in buffer. In a dark room, the secondary fluorescent antibody (Alexa 488 donkey anti-goat or donkey anti-rabbit: 1:1,000; Alexa 594 donkey anti-mouse: 1:1,000, Invitrogen, Carlsbad, CA) was applied for 1-2 hours, followed by three PBS washes for 10 min each. Sections were then float-mounted in PB onto Probe On Plus glass slides (Fisher Scientific, Pittsburgh, PA) and cover-slipped (1.5 um thickness) using Vectashield (Vector Laboratories, Burlingame, CA). Tissue was qualitatively analyzed for MT5-MMP, N-cadherin, and ADAM-10 co-localization with GFAP and CD-11 using the Leica TCS-SP2 AOBS confocal laser scanning microscope.

Microarray Analysis

At 7 d following UEC or TBI+BEC, subsets of animals (UEC n=5; TBI+BEC n=3; Sham n=3) were anesthetized (4% isoflurane in carrier gas of 70% N_20 and 30% O_2) and sacrificed via decapitation. Both whole hippocampal (UEC n=1; TBI+BEC/Sham n=1) and dendrite-rich dentate molecular layer (ML) (UEC n=4 pooled; TBI+BEC/Sham n=2 pooled for each group) samples were prepared. Following decapitation, hippocampi and dissections of enriched dentate molecular layers were quickly frozen in liquid nitrogen. At the time of analysis, RNA extracts were prepared from frozen samples placed directly in Trizol reagent (InvitrogenTM, Life Technologies, Carlsbad,

CA). A subsequent cleanup process with RNAeasy (QIAGEN, Valencia, CA) was performed according to the manufacturer's protocol. RNA purity was judged by spectrophotometry (260, 270, 280 nm). RNA integrity, as well as that of cDNA and cRNA synthesis products, was assessed by running 1µl of each sample in RNA 6000 Nano LabChips® on a 2100 Bioanalyzer (Aligent Technologies, Foster City, CA). Affymetrix GeneChip Rat Genome 230 2.0 Arrays (Santa Clara, CA) were then used to screen for genomic transcript changes, including MT5-MMP, ADAM-10, and N-cadherin mRNA expression (see Dumur et al., 2009 for detailed methods description). Once data was collected, background correction, normalization, and estimation of probe set expression summaries were performed using the log-scale Robust Multi-array Analysis (RMA) method. Identification of altered gene expression for injured compared to control samples was assessed by applying the Significance score (S-score) method. The S-score method uses an error-based model to determine the variances for probe pair signals and follows a normal standard distribution. The procedure produces scores centered at "0" (no change) with a standard deviation of 1. Benjamin-Hochberg correction method was then used to correct for multiple testing and to obtain adjusted alpha-levels for each probe set (MT5-MMP, ADAM-10, and N-cadherin).

qRT-PCR

The 7d UEC and TBI+BEC samples used for microarray analysis were also analyzed using quantitative reverse transcriptase polymerase chain reaction (qRT-PCR) methods to assess gene expression levels for MT5-MMP, ADAM-10 and N-cadherin using TaqMan® chemistry. Probes and primer sets for detection of MT5-MMP (Rn00582114 m1), ADAM-10 (Rn01530753 m1), and N-cadherin (Rn00580099 m1)

were obtained from Inventoried Assays (Applied Biosystems, Foster City, CA). These gene specific probes were labeled in the 5' end with FAM (6-carboxyfluorescein) and the 3' end with a dark quencher. Cyclophilin A from the Pre-developed TaqMan® Assay Reagents (Applied Biosystems) was used as an endogenous control for all samples. Experiments were performed in the ABI Prism 7500 Sequence Detection System (Applied Biosystems) using the TaqMan® One-Step PCR Master Mix Reagents Kit. All samples were tested in triplicate under cycling conditions of 48°C for 30 minutes, 95°C for 10 minutes, 40 cycles of 95°C for 15 seconds, and 60°C for 1 minute. To calculate fold changes in expression levels for each gene, the $2^{-\Delta\Delta Ct}$ method was used. To calculate the efficiency of amplification for MT5-MMP, ADAM-10, and N-cadherin, 10-fold serial dilutions of template samples were run (Dumur et al., 2009)

In situ Hybridization

At 7d following UEC or TBI+BEC, a subset of animals (UEC, n=5; TBI+BEC, n=3; Sham-injured, n=2) were selected for *in situ* hybridization (ISH) analysis. Rats were anesthetized with a lethal dose of sodium pentobarbital (90 mg/kg, i.p.) and perfused first with 0.9% NaCl followed by aldehyde fixative (4% paraformaldehyde in 0.1M $NaHPO_4$ Buffer or PBS, pH=7.4). Brains were removed and stored in buffer overnight at 4°C. Coronal vibratome sections (20-30 µm) of the hippocampus and dentate gyrus were prepared for ISH. Sections were mounted on slides and stored at -20°C until riboprobe preparation was complete. A rat MT5-MMP cDNA was generated by PCR cloning from nucleotides 408-931 of mouse MT5-MMP and using the following primers: F: 5'-ATGTGGCGTCCCTGAT-3', R: 5'-TGAAGTTGTGTGTCTCC-3' (Jaworski, 2000). Sense and antisense riboprobes were generated against a 500bp fragment of MT5-

MMP using digoxigenin (DIG) labeled dNTPs (Roche, Mannheim, Germany) and the MAXI-Script In Vitro Transcription Kit (Ambion, Austin, TX). Probes were hydrolyzed to ~250 nt. Mounted vibratome sections were prepared and hybridized at 65°C as previously described (Yamagata et al., 2002). Briefly sections were fixed with PFA, incubated in Proteinase K, acetylated, permeabilized in 1% Triton-X and hybridized. Bound riboprobes were detected by horseradish peroxidase (POD)-conjugated anti-DIG antibodies and fluorescent staining with Tyramide Signal Amplification (TSA) systems (PerkinElmer, Shelton, CT). For immunofluroescent labeling, sections were blocked and primary antibody applied overnight at 4° C (GFAP rabbit anti-cow polyclonal antibody, DAKO; 1:1000). Secondary antibody was applied to sections, which were coverslipped and sealed. Images were obtained on a Leica TCS-SP2 AOBS confocal laser scanning microscope.

Statistical Analysis

Results were expressed as percent change from paired control samples. The significance of differences in densitometric measures of Western blot immunobinding was analyzed using the Student's t-test. Computer-based SPSS software was used for all analyses. A probability of less than 0.05 was considered statistically significant for all experiments.

RESULTS

Physiological Measurements

During surgical preparation and lesioning, all animals were monitored for heart rate (350 $\pm$ 20bpm), arterial oxygen saturation ($\geq$ 93%), breath rate (45 $\pm$ 5bpm), pulse distention

(15 ± 5μm), and breath distention (12 ± 5μm) with pulse oximeter (MouseOx; Starr Life Sciences, Oakmont, PA). Surgical procedures on all experimental animals produced no significant change in these physiological measures.

Western Blot Analysis

MT5-MMP, ADAM-10, and N-cadherin Protein Forms in Hippocampus

Western blot (WB) results revealed predominant and additional lesser forms of MT5-MMP, ADAM-10 and N-cadherin following UEC and TBI+BEC (Fig. 2.2). A predominant band was present for MT5-MMP at 80 kDa. The active form of MT5-MMP is ~58 kDa, however this band was not detected in our MT5-MMP protein analysis. When the MT5-MMP membrane was re-probed, the 80 kDa band was found to co-migrate with TIMP-2 (~24 kDa), the endogenous inhibitor of MT5-MMP (see Appendix B Fig.B-1). Additionally, a less prominent and unbound TIMP-2 band was observed at 24 kDa. This result suggests that active MT5-MMP was bound to TIMP-2, and like other MT-MMPs, may participate in the downstream activation of other MMPs (e.g.- proMMP-2). An additional 85 kDa MT5-MMP form was present, which has yet to be characterized in the literature, but may represent a glycosylated form. Immunopositive bands for ADAM-10 were observed at 100 kDa, 80 kDa, and 70 kDa. These ADAM-10 bands most likely represent an alternative TIMP-1 bound form (100 kDa), a “pro” or latent form (80 kDa), and a predominant active form (70 kDa), as described in the ADAM-10 literature. Finally, bands for N-cadherin were visualized at 130 kDa and ~40 kDa. These N-cadherin bands represent a predominant full-length form (130 kDa) and

its intracellular fragment that includes the transmembrane domain (~40 kDa), which is produced following ectodomain cleavage.

MT5-MMP, ADAM-10 and N-cadherin Protein Expression Post-UEC

Western blot analysis of whole ipsilateral hippocampal extracts revealed significant injury-induced changes in MT5-MMP, ADAM-10 and N-cadherin protein between 2 and 15d post-lesion, when compared to contralateral uninjured controls (Fig. 2.3). The TIMP-2 associated 80 kDa form of MT5-MMP was significantly elevated at 2 and 7d postinjury (177.23 ±20.77, $p<0.01$; 202.06 ± 21.90, $p<0.01$). The active 70 kDa form of ADAM-10 also showed significant elevation over control at 2 and 7d postinjury (213.15 ± 8.26, $p<0.01$; 200.89 ± 34.62, $p<0.05$). Full length N-cadherin expression was significantly decreased at 2d (68.39 ±6.94, $p<0.01$), and increased at 15d (128.27 ± 9.00, $p<0.05$). At 7d, there was a trend towards a significant decrease in N-cadherin expression (74.23 ± 11.77, $p=0.079$). At all three postinjury intervals, an inverse relationship was noted between both enzymes and N-cadherin, suggesting possible enzyme/substrate interaction during injury-induced synaptogenesis. These results showed an up-regulation of two key MMPs during the degenerative (2d) and early regenerative (7d) phases of synaptogenesis, followed by a return to baseline during the stabilization phase (15d). These changes in MT5-MMP and ADAM-10 protein expression may correlate with changes in enzymatic activity, which could influence the early phases of injury-induced plasticity through interaction with N-cadherin following UEC.

Figure 2.2 Potential Hippocampal Molecular Forms of MT5-MMP, ADAM-10 and N-cadherin Observed in Protein Analysis. Schematic membrane-bound, structural depiction of active (58kDa) and TIMP-2 bound (80kDa) forms of MT5-MMP; TIMP-1 bound (100kDa), pro- (80kDa) and active- (70kDa) forms of ADAM-10; Full-length form (130kDa) and cleaved intramembrane-cytoplasmic fragment (40kDa) of N-cadherin.

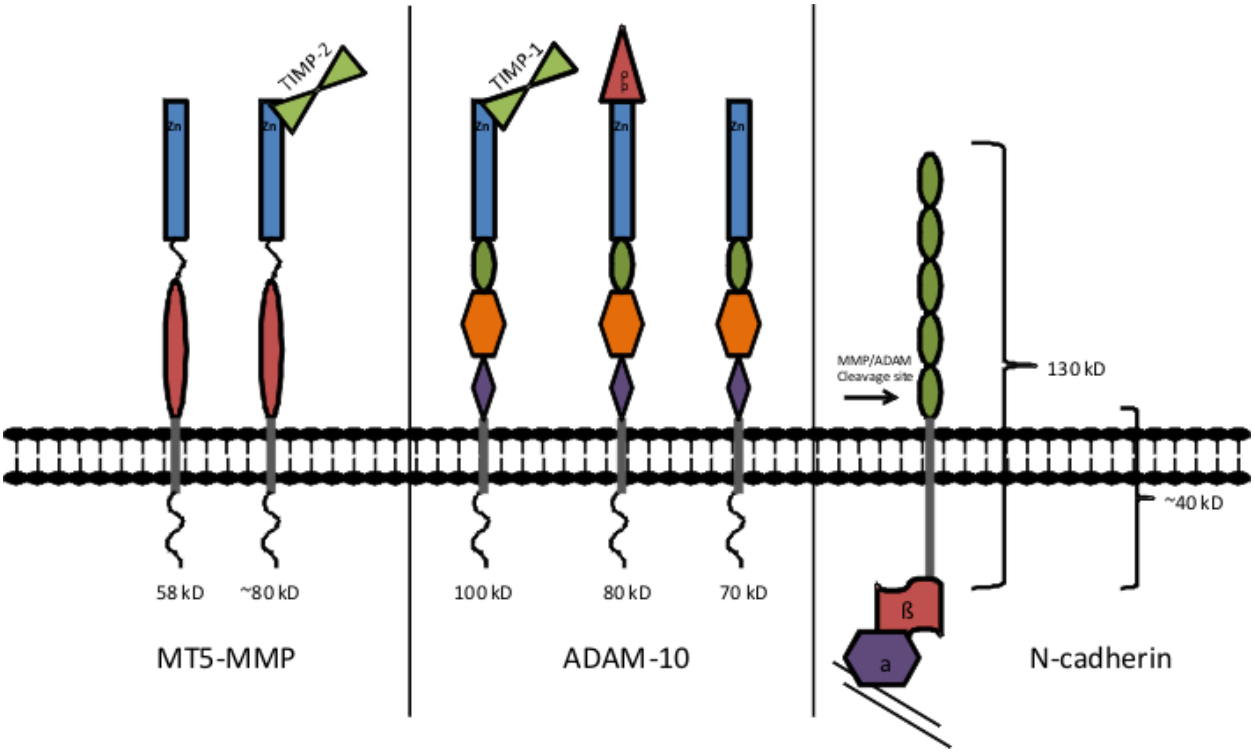

Figure 2.3 Hippocampal MT5-MMP, ADAM-10 and N-cadherin Protein Expression following UEC. Values expressed as percent of contralateral hippocampus over 2, 7, and 15d postinjury time intervals. Following UEC insult, significant increases in MT5-MMP (MT5) and ADAM-10 protein expression were observed at 2 and 7d with normalization of both MMPs at 15d. By contrast, N-cadherin showed significant reduction at 2 and 7d and elevation at 15d. Note inverse relationship between enzymes and substrate over postinjury time course. Representative blots shown below. I=ipsilateral hippocampus (injured); C=contralateral hippocampus (control); 2d: n=4-7; 7d: n=4-7; 15d n=4-6. *$p<0.05$, **$p<0.01$.

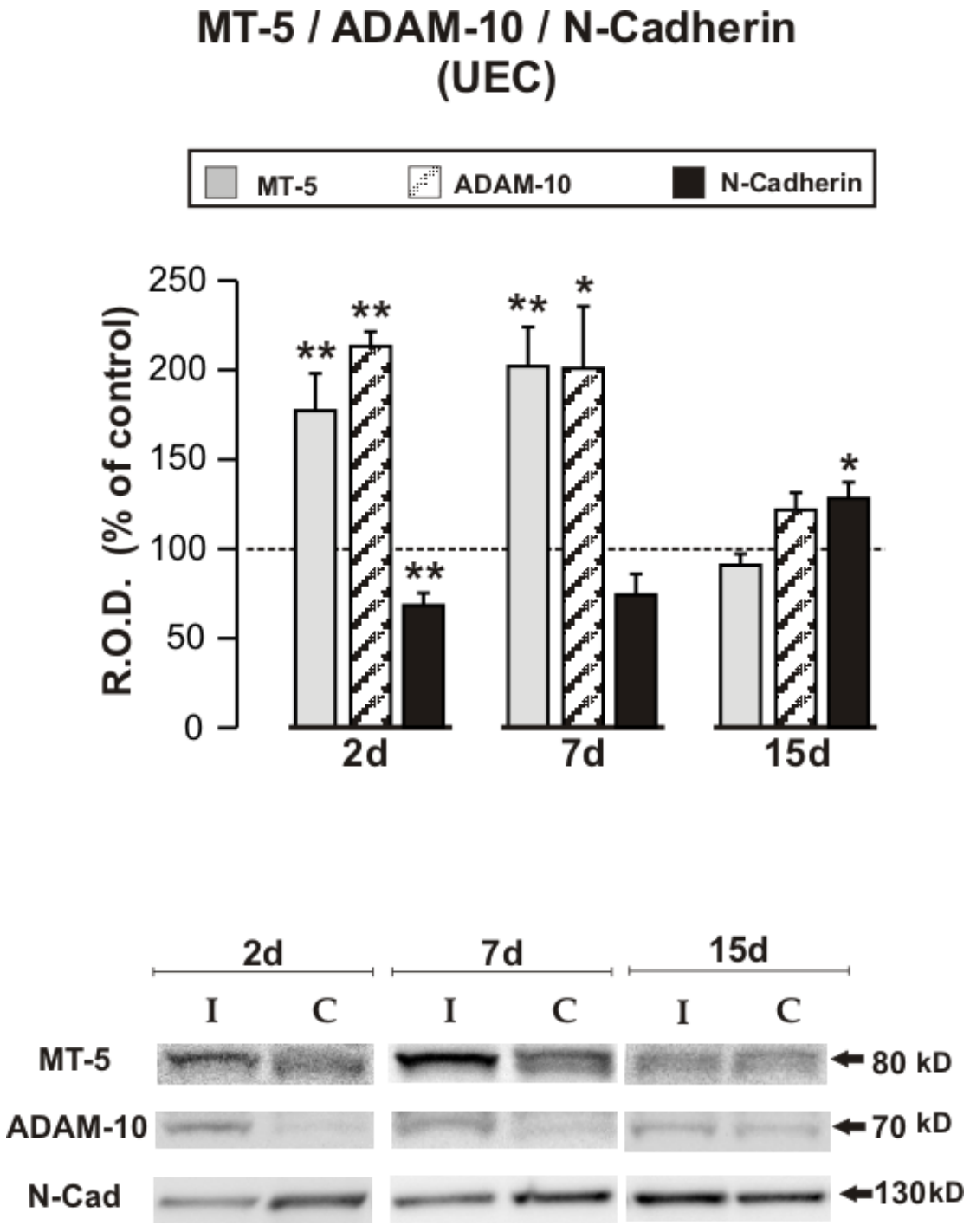

In addition to the predominant protein forms of MT5-MMP, ADAM-10, and N-cadherin, other alternative/minor bands were also visualized following UEC (see Appendix B, Fig B-2 through B-6). Analysis of MT5-MMP showed that an 85 kDa species was significantly decreased over all time points (2d: 19.34 ± 3.15, $p<0.02$; 7d: 22.84 ± 1.92, $p=0.001$; 15d: 60.25 ± 5.79, $p<0.05$) following injury. This 85 kDa form has not been previously reported for MT5-MMP, and may represent an uncharacterized bound form or a post-translationally modified form that migrates differently in the gel system. ADAM-10 protein analysis revealed two additional bands, 100 kDa and 80 kDa. The 100 kDa band, an apparent TIMP-1 bound form, was significantly decreased at all time points (2d: 80.84 ± 1.69, $p<0.01$; 7d: 77.73 ± 5.18, $p=0.05$; 15d: 76.15 ± 6.19, $p<0.05$), as was the latent 80 kDa pro-form (2d: 32.03 ± 3.64, $p<0.01$; 7d: 45.85 ± 10.4, $p<0.01$; 15d: 67.11 ± 6.95, $p<0.05$). These results showed that two regulated forms of ADAM-10, a TIMP-1 bound and latent form, were reduced with deafferentation remaining below control levels through all phases of reactive synaptogenesis. With N-cadherin, we also observed a ~40 kDa fragment at 2 and 15d, which was significantly decreased at 2d (65.27 ± 6.40, $p<0.001$). These results show the presence of a cleaved form of N-cadherin, which may represent a product of acute postinjury ADAM-10 and/or MT5-MMP proteolysis.

MT5-MMP, ADAM-10 and N-cadherin Protein Expression Post-TBI+BEC

Whole hippocampal extracts were also examined to determine changes in MT5-MMP, ADAM-10 and N-cadherin protein expression, when compared to sham control (Fig. 2.4). Western blot analysis revealed significant differences across all groups over the examined time intervals. The 80 kDa form of MT5-MMP was significantly elevated

above sham at 2 and 7d postinjury (126.73 ± 9.85, p=0.05; 195.72 ± 11.01, p<0.001). The 70 kDa active-form of ADAM-10 showed significant elevation over control at all three intervals (2d: 156.34 ±18.18, p<0.01; 7d: 267.17 ±23.54, p<0.001; 15d: 230.78 ± 30.41, p<0.001). Full- length N-cadherin expression was significantly decreased at 2 and 7d (75.11 ± 6.91, p<0.05; 81.03 ±4.80, p<0.05). These results were similar to those found following UEC, including the inverse relationship between enzymes and substrate and similar MT5-MMP protein profiles. Nevertheless, two important differences were observed when comparing adaptive to maladaptive expressional changes. Notably, the significant up-regulation of ADAM-10 across all time intervals and the failure of N-cadherin to significantly increase above control levels at 15d. These results suggest that, of the two metalloproteinases, ADAM-10 and its proteolytic interaction with N-cadherin may preferentially contribute to the maladaptive synaptic plasticity observed 7-15d following TBI+BEC insult.

Consistent with the UEC results, additional WB bands for all three proteins were also visualized after TBI+BEC. For MT5-MMP, an 85 kDa species was found to significantly decrease over all time points (2d: 40.98 ± 6.84, p<0.001; 7d: 46.55 ± 6.46, p<0. 001; 15d: 59.23 ± 5.81, p<0.001) following injury. ADAM-10 protein analysis revealed that a 100 kDa ADAM-10 form was significantly decreased at 2d (82.43 ± 3.36, p<0.001), and returned to sham levels at 7 and 15d. An 80 kDa latent form of ADAM-10 was also significantly reduced, but only at 2 and 15d (52.76 ±7.45, p<0.001; 79.66 ±4.98, p=0.05). These additional forms of both MT5-MMP and ADAM-10 showed similar profiles to those in the UEC study, suggesting that they may be regulated and/or function similarly in both injury models. Although a 40 kDa form of N-cadherin was

Figure 2.4 Hippocampal MT5-MMP, ADAM-10 and N-cadherin Protein Expression following TBI+BEC. Values expressed as percent of sham controls over 2, 7, and 15d postinjury time intervals. Following TBI+BEC, a significant increase in MT5-MMP (MT5) protein expression was observed at 2 and 7d, while ADAM-10 was significantly increased at all time-points. By contrast, N-cadherin showed significant reduction at 2 and 7d, and failed to elevate above control levels at 15d. Note inverse relationship between enzymes and substrate over post-injury time-course. Representative blots shown below. I=Injured; S=Sham (control); 2d: I=6-10, S=8; 7d: I=7-16, S=9-10; 15d I=7-8, S=8; *p<0.05, **p<0.01.

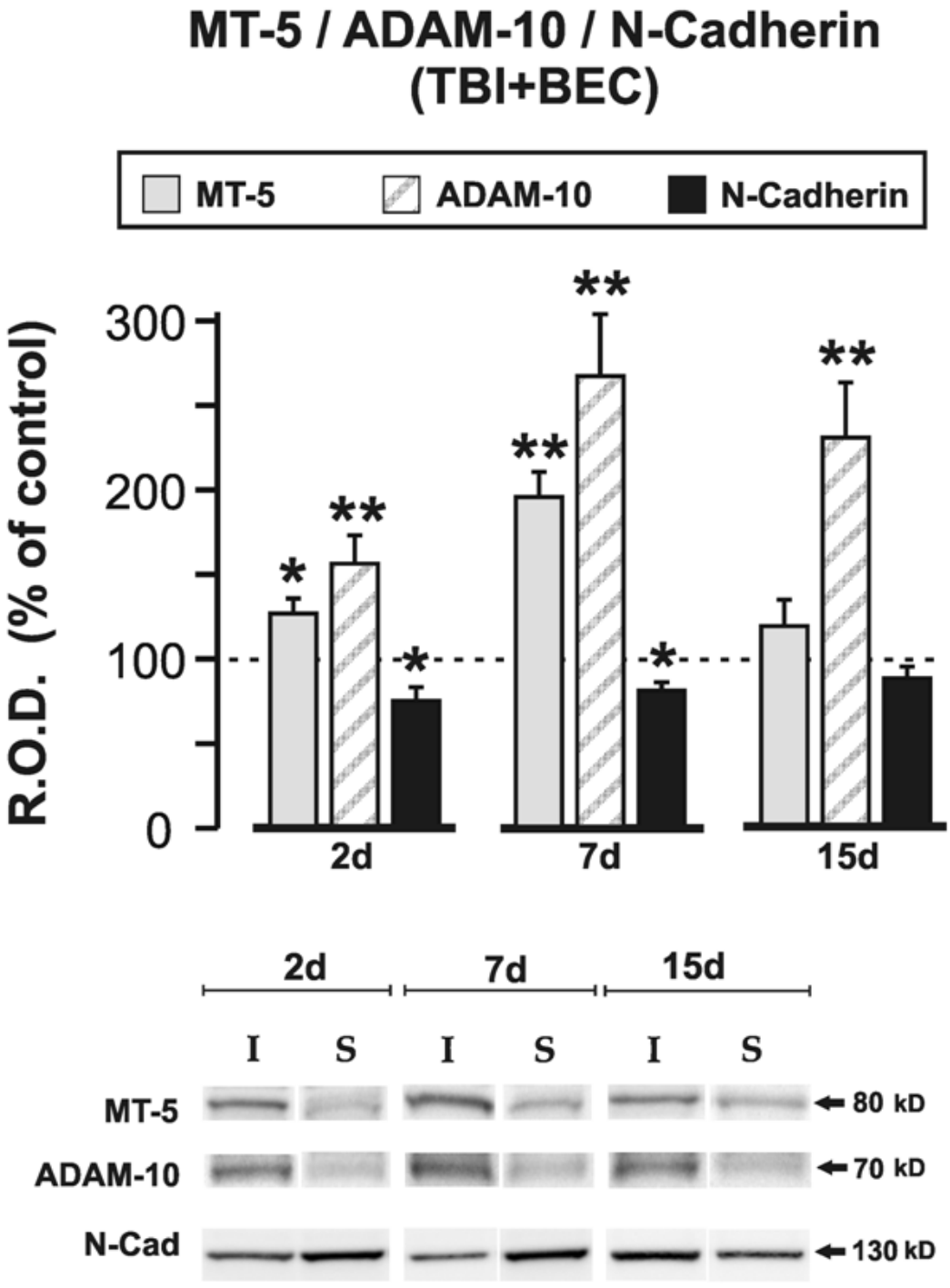

present over all post-TBI+BEC time intervals, there was no significant change from sham, whereas this form was significantly decreased at 2d after UEC. Because this 40 kDa form may be further cleaved into fragments that influence intracellular signaling pathways, such intermodel differences suggest that N-cadherin regulated cell signaling may contribute to the aberrant plasticity observed after the combined insult.

Immunohistochemistry

Immunofluorescent labeling was used to characterize cellular ADAM-10, MT5-MMP and N-cadherin localization, as well as overall protein distribution within the dentate gyrus following UEC and TBI+BEC. Tissue was double stained with MT5-MMP/ADAM-10/N-cadherin and markers for astrocytes (GFAP) and microglia (CD-11/Iba-1). MT5-MMP, ADAM-10 and N-cadherin co-localized with the astrocytic marker in each injury model at 2, 7 and 15d postinjury (Fig. 2.5 and 2.6), but failed to show co-localization with either microglial marker (see Appendix C, Fig. C-8). Images double stained with GFAP and MT5-MMP/ADAM-10/N-cadherin from the 7d postinjury time interval are presented here to show protein localization and distribution. Additional images for the 2 and 15d time intervals are shown in Appendix C (Fig. C-2 through C-6).

ADAM-10 Immunohistochemistry following UEC and TBI+BEC

Confocal imaging of hippocampus showed increased ADAM-10 signal throughout the deafferented molecular layer (ML) of both 7d UEC and TBI+BEC cases when compared with paired controls (Fig. 2.5 and 2.6). The antibody signal was present as diffuse punctate sites within the neuropil, but the primary staining was localized within reactive astrocytes, co-labeled with GFAP. The overall intensity of ADAM-10 was

greater in the combined insult cases. In both models, ADAM-10 uniformly filled the cell bodies and processes of reactive astrocytes. Diffuse staining was also present in glial processes surrounding granule cell (GC) somata. When 2, 7, and 15d cases were compared, the greatest signal and cellular labeling was observed at 2 and 7d postinjury in both models, consistent with WB results showing greatest expression of ADAM-10 at those times. While these experiments cannot confirm whether ADAM-10 is produced by astrocytes or simply being degraded within them, it is clear that astrocytes play a role in the processing of ADAM-10 following during both adaptive and maladaptive synaptogenesis.

MT5-MMP Immunohistochemistry following UEC and TBI+BEC

In contrast to ADAM-10, hippocampal confocal imaging showed a different pattern for MT5-MMP ML distribution in 7d UEC and TBI+BEC animals relative to paired controls (Fig. 2.5 and 2.6). Overall intensity of signal was lower in the UEC than for TBI+BEC, where, in the latter, MT5-MMP showed a strong diffuse staining throughout the ML. Like ADAM-10, the overall intensity of MT5-MMP was also greater in the combined insult cases. In both models the primary signal was again localized within GFAP positive astrocytes. Following UEC, the MT5-MMP signal filled the somata and processes of these reactive astrocytes. By contrast, MT5-MMP labeling in the combined model formed a cluster-like staining pattern within astrocytic cell bodies and their primary processes. A dense punctuate MT5-MMP labeling was seen surrounding granule cells. Comparison of all three postinjury time intervals showed the greatest labeling at 2 and 7d in both models. WB results did show greatest increase in MT5-MMP at 7d, approximately equivalent for each injury. Interestingly, our

Figure 2.5 Molecular Layer Localization of ADAM-10, MT5-MMP and N-cadherin with GFAP at 7d following UEC. Confocal imaging revealed co-localization of ADAM-10, MT5-MMP and N-cadherin with astrocytic marker GFAP in molecular layers. Single-channel confocal images showed pronounced signal within the deafferented OML, with a cell-filling pattern for ADAM-10 and N-cadherin. MT5-MMP displayed a punctate staining throughout the neuropil and clustered signal within reactive astrocytes. Contralateral (control) overlays display a dampened injury response, but similar expression pattern for each protein. ADAM-10, MT5-MMP and N-cadherin (green); GFAP (red). 40x magnification. OML = outer molecular layer; IML= inner molecular layer; GC= granule cell layer. Arrowheads indicate examples of co-localization for each protein.

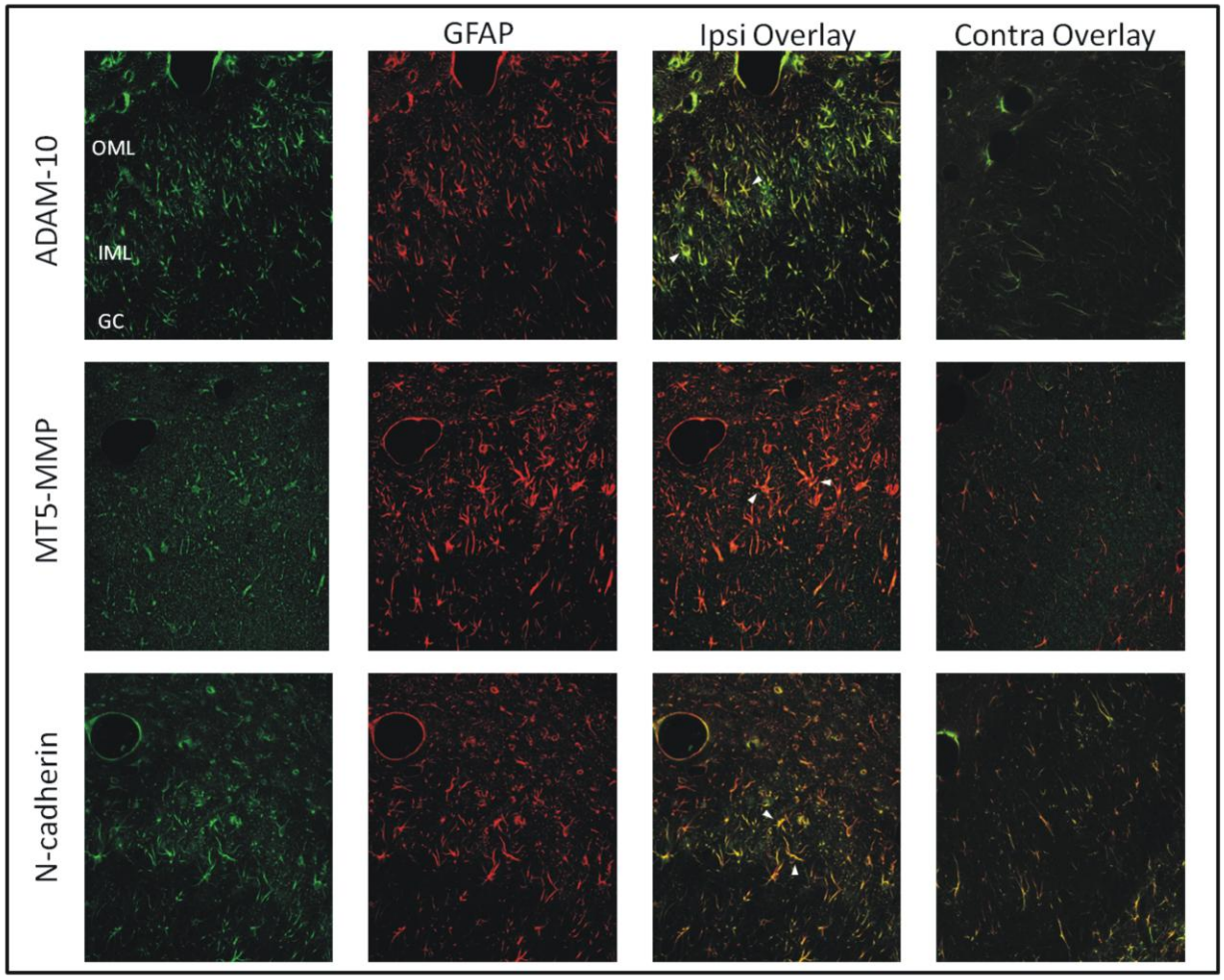

Figure 2.6 Molecular Layer Localization of ADAM-10, MT5-MMP and N-cadherin with GFAP at 7d following TBI+BEC. Confocal imaging revealed co-localization of ADAM-10, MT5-MMP and N-cadherin with astrocytic marker GFAP in combined injured animals. Overlays of injured animals showed pronounced astrocytic response and signal within the deafferented outer molecular layer. ADAM-10 exhibited a cell-filling pattern, while MT5-MMP revealed punctate neuropil staining and somatic clustered intracellular signal reaching into proximal processes. N-cadherin had similar punctate neuropil pattern, and primarily astrocytic somatic clustering. Sham-injured (control) overlays display a dampened injury response, but similar spatial expression pattern. ADAM-10, MT5-MMP and N-cadherin (green); GFAP (red). 40x magnification. OML = outer molecular layer; IML= inner molecular layer; GC= granule cell layer. Arrowheads indicate examples of co-localization.

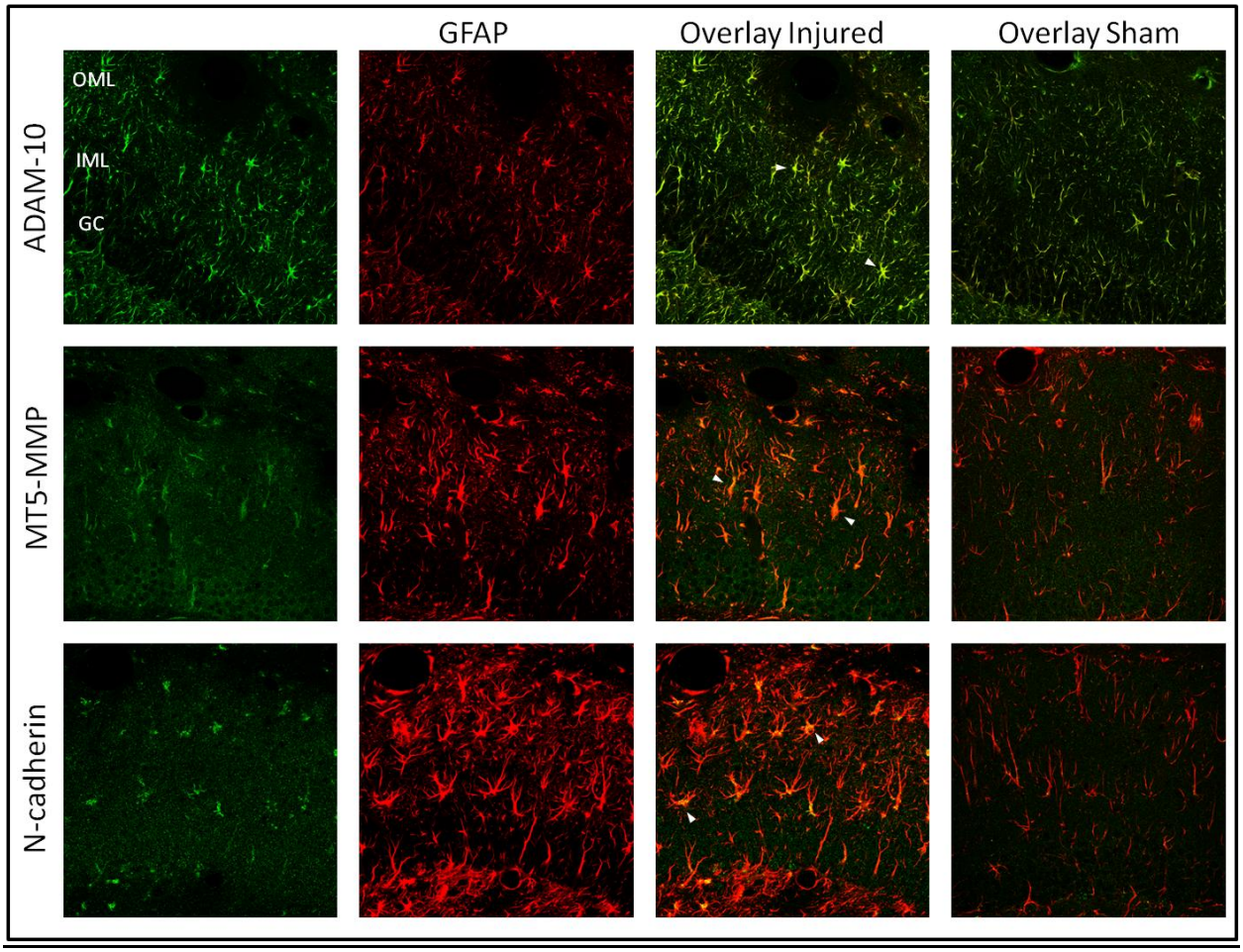

immunohistochemistry supported the higher ML MT5-MMP signal for combined cases. As for ADAM-10, strong glial labeling suggests a possible role of the reactive astrocyte in either MT5-MMP synthesis or phagocytotic processing.

N-cadherin Immunohistochemistry following UEC and TBI+BEC

Confocal imaging of hippocampal N-cadherin revealed more subtle model differences at 7d postinjury (Fig 2.5 and 2.6). Following UEC, N-cadherin and GFAP were co-localized within the ML, with increased signal throughout the deafferented neuropil relative to paired controls. Fine, punctate label was seen around GC somata. The overall pattern of N-cadherin staining was similar for the 7d post-TBI+BEC cases, however, signal was more punctuate and concentrated within the astrocyte cell bodies with minimal process labeling. These subtle model differences may indicate variations in astrocytic processing of N-cadherin during adaptive and maladaptive synaptogenesis. The results of these experiments show an increase in ML expression of N-cadherin at 7d postinjury. This is in contrast to the reduced expression assessed by WB measurements. It is important to note that due to technical limitations, antibody recognizing an N-terminal sequence of N-cadherin was used for immunohistochemical experiments, while a C-terminal recognizing antibody was employed for WB analysis. Application of the different antibodies most likely accounts for differences in N-cadherin expression detected by the two methods. We interpret our WB results as illustrating a decrease in overall C-terminal signal due to MT5-MMP or ADAM-10 cleavage of intact N-cadherin. By contrast, the confocal experiments appear to show cleaved and shed N-terminal fragments of N-cadherin, which are potentially internalized for processing within reactive astrocytes of the ML.

DNA Microarray analysis

At 7d post-UEC and TBI+BEC, RNA extracts of whole hippocampus (UEC n=1; TBI+BEC/Sham n=1) and enriched molecular layer (ML) (UEC n=4 pooled; TBI+BEC/Sham n=2 pooled) were used to generate cDNAs for microarray gene expression screening. The 7d postinjury time interval was selected because it was the period exhibiting greatest WB MT5-MMP and ADAM-10 hippocampal protein expression and we wanted to determine if this protein peak was matched by an elevation in mRNA synthesis. A rise in mRNA expression at 7d would also help us interpret changes in protein expression occurring during the subsequent synaptic stabilization phase of recovery at 15d. For this study, changes in gene expression of ±50% or more from control were considered significant. Results did reveal potential injury effects in some cases, although overall changes in MT5-MMP, ADAM-10, and N-cadherin transcripts at 7d postinjury were not significant using our ±50% cutoff (Table 1). Among the three genes, the most pronounced UEC transcript shift occurred with ADAM-10, where we found a 45% and 47% increase relative to control in ML and hippocampus, respectively. MT5-MMP and N-cadherin transcripts at 7d after UEC revealed no significant change (0-5%). For post-TBI+BEC gene expression, the greatest shifts were seen in ML samples, where ADAM-10 and N-cadherin transcripts increased 20% and MT5-MMP decreased 20% in expression. In the whole hippocampus, ADAM-10 mRNA was 15% higher than control, while MT5-MMP and N-cadherin transcripts were not altered. Microarray results revealed potential transcript changes in both hippocampus and ML for each model. These indications of possible mRNA shifts after injury were subsequently probed and verified in the ML samples using qRT-PCR methods.

Table 1. Microarray Analysis of MT5-MMP, ADAM-10 and N-cadherin Transcripts at 7d post-UEC and TBI+BEC. Transcript values reported as a relative change from control (UEC: contralateral molecular layer or whole hippocampus; TBI+BEC: sham). Post-UEC values show greatest change in ADAM-10 for molecular (+45%) and whole hippocampal (+47%) sample(s), while N-cadherin and MT5-MMP show no change (NC). Post-TBI+BEC values show small shifts in transcript for MT5-MMP (-20%) molecular layer, ADAM-10 molecular layer (+20%) and whole hippocampal (+15%), and N-cadherin molecular layer (+20%) samples. UEC molecular layer n=4 rats, ipsilateral sides pooled and contralateral sides pooled; whole hippocampus n=1 rat ,ipsilateral and contralateral side separately analyzed; TBI+BEC molecular layer n=2 rats, all pooled from both animals; Sham molecular layer n=1rat, two sides pooled; n=2 rats; TBI+BEC whole hippocampus n=1rat , injured hippocampi pooled; Sham hippocampi n=1 rat, two sides pooled.

Table 1. Microarray Analysis in Adaptive & Maladaptive TBI models

UEC

	Molecular layer (n=4, pooled)	Whole Hippocampus (n=1)
MT5-MMP	NC	NC
ADAM-10	1.45+	1.47+
N-cadherin	NC	NC

TBI+BEC

	Molecular layer (n=2, pooled)	Whole Hippocampus (n=1 injured, 1 sham)
MT5-MMP	1.20-	NC
ADAM-10	1.20+	1.15+
N-cadherin	1.20+	NC

Quantitative RT-PCR

Aliquots from the same 7d UEC and TBI+BEC ML RNA extracts used for microarray analysis were subjected to qRT-PCR with specific primers to MT5-MMP, ADAM-10, and N-cadherin mRNA (Fig. 2.7).

MT5-MMP, ADAM-10 and N-cadherin mRNA Expression after UEC

Quantitative RT-PCR analysis of ipsilateral ML samples at 7d post-UEC revealed higher mRNA expression for MT5-MMP, ADAM-10 and N-cadherin when compared to contralateral control. While experimental design prevented statistical analysis in this situation, MT5-MMP transcript did show a modest 31% increase, while ADAM-10 mRNA was elevated 112% over control. These results are temporally consistent with our WB results which showed significant elevation in both MT5-MMP and ADAM-10 protein at 7d postinjury. N-cadherin mRNA had the most pronounced change, a 117% elevation over control, indicating active transcription during a period of reduced N-cadherin protein expression, and just prior to the 15d increase in N-cadherin during UEC synapse stabilization.

MT5-MMP, ADAM-10 and N-cadherin mRNA Expression after TBI+BEC

In 7d TBI+BEC ML samples subjected to qRT-PCR we observed an apparent elevation of ADAM-10 mRNA expression compared to sham-injured control. Transcript was increased by 83% during the period of sprouting and synaptogenesis, consistent with post-TBI+BEC WB protein expression. These results suggest that matched changes in ADAM-10 transcript contribute to the large 7d rise in protein seen after combined insult, and may also support the persistent elevation of ADAM-10 protein at

Figure 2.7 Quantitative RT-PCR Molecular Layer mRNA Expression of MT5-MMP, ADAM-10 and N-cadherin post-UEC and TBI+BEC. Values expressed as a percent of control (UEC: contralateral ML; TBI+BEC: Sham) at 7d following injury. ML samples showed elevated MT5-MMP, ADAM-10, and N-cadherin transcript post-UEC, and only elevated ADAM-10 transcript post-TBI+BEC. Shifts in initial ADAM-10 microarray data (see Table 1) consistent with ADAM-10 ML transcript expression in both models. ML =Molecular Layer. UEC ML n=4 rats, ipsilateral sides pooled and contralateral sides pooled; TBI+BEC ML n=2 rats, all pooled from both animals; Sham molecular layer n=1rat, two sides pooled.

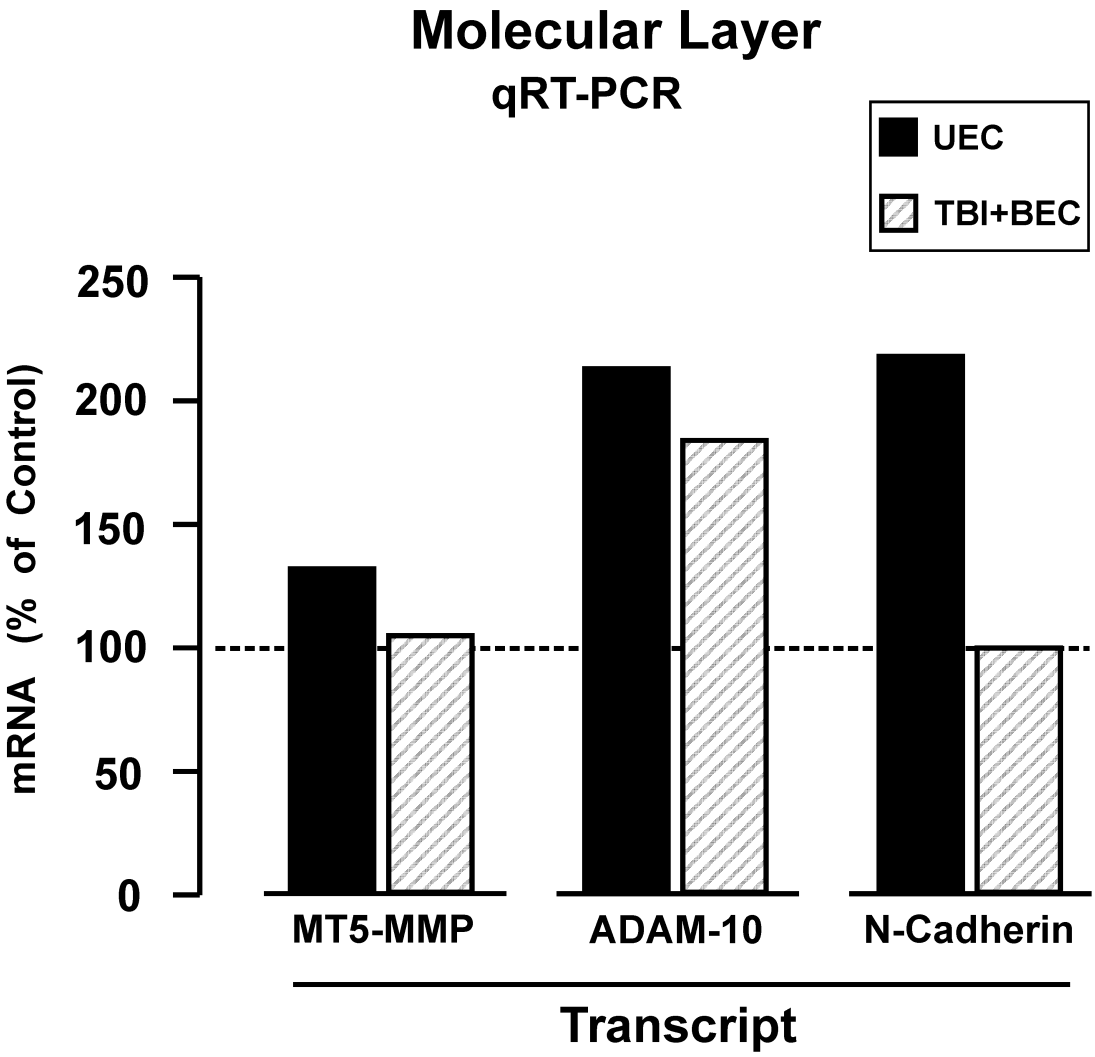

15d with maladaptive plasticity. MT5-MMP and N-cadherin mRNA expression in the ML were not different from control at 7d. These results suggest that if transcript elevation was responsible for the 7d WB rise in MT5-MMP protein, it likely occurred prior to the time of tissue sampling. Absence of change in N-cadherin transcript at 7d after TBI+BEC would be consistent with the observation that the protein was not elevated over controls at either 7 or 15d after injury.

In situ hybridization

MT5-MMP RNA localization at 7d following UEC and TBI+BEC

Preliminary *in situ* hybridization experiments were conducted to determine the cellular site of MT5-MMP synthesis within the hippocampus. The MT5-MMP probe used in this experiment was a gift generously provided by Dr. Diane Jaworski. This probe was designed for the characterization of MT5-MMP expression within the developing brain (Jaworski, 2000). Based on results from immunohistochemical experiments, we predicted that MT5-MMP synthesis occurs within hippocampal glial cells, specifically reactive astrocytes. Preliminary trials using 20-30 μm thick coronal brain sections revealed MT5-MMP anti-sense signal within reactive astrocytes in the deafferented dentate ML at 7d after UEC and TBI+BEC, as indicated by MT5-MMP probe co-localization with astrocytic marker GFAP (see Appendix D Fig. D-1). Anti-sense signal was found predominantly within astrocytic processes and around the cell body perimeter, closely matching the distribution of the protein in our immunohistochemical study. While MT5-MMP signal was present in both injured and control slices, increased labeling and astrocytic response was also observed in both UEC and TBI+BEC animals.

Unfortunately, we also observed non-specific fluorescent signal with the sense control sequence in some of our experiments. This signal was found within the same reactive astrocytes targeted by the antisense label. In troubleshooting this result, we identified several possible sources of the aberrant control signal: 1) the use of different restriction enzymes for cDNA cuts than those of the original published technique, potentially causing non-specific binding of the extended vector DNA sequences, 2) the use of 20-30 µm thick vibratome tissue slices as opposed to thinner 8-10 µm frozen sections, and 3) insufficient permeability of probe into the tissue, generating surface adhesion artifact. We plan to conduct additional experiments to address these possible complications, and will generate clean sense controls before proceeding with further *in situ* hybridization analysis of MT5-MMP, ADAM-10 and N-cadherin mRNA in our injury models.

DISCUSSION

The current study examined the spatial and temporal profile of MT5-MMP, ADAM-10 and N-cadherin protein expression during reactive synaptogenesis (2-15d postinjury) within the dennervated hippocampus. Expression of the membrane type MMPs and their common ECM substrate were compared in two different TBI models, directly contrasting adaptive (UEC) versus maladaptive (TBI+BEC) synaptic plasticity. These protein data were complemented by assessment of mRNA expression for each molecule at 7d postinjury, the period of active sprouting and synapse formation. In our Western blot analyses, we found that MT5-MMP and ADAM-10 protein was elevated at the 2 and 7d postinjury intervals for both models, times marking acute degenerative change and early synaptic growth. The greatest increase in MMP expression was seen

with ADAM-10 at 7d. This data was supported by large 7d elevations in ADAM-10 versus MT5-MMP transcript in both models. We also observed a consistent decrease in N-cadherin expression at 2 and 7d after injury in each model. Notably, the main differences between adaptive and maladaptive plasticity were seen at 15d, when synapse stabilization is underway. Here, adaptive UEC plasticity showed reduced MMP protein and an increase in N-cadherin expression over that of controls. By contrast, the maladaptive plasticity of TBI+BEC was marked by a persistently elevated ADAM-10 protein level and the absence of any rise in N-cadherin expression. Interestingly, immunohistochemistry for each MMP and N-cadherin showed primary localization in reactive astrocytes of the deafferented molecular layer and the intensity of this localization was increased following injury. These results show that membrane-bound MMPs are involved in the both adaptive and maladaptive synaptic plasticity and, given the distinct recovery-dependent differences in MT5-MMP, ADAM-10, and N-cadherin expression, likely participate through interaction with N-cadherin to affect synapse stabilization. Elevated ADAM-10 and reduced N-cadherin expression was most correlated with the maladaptive response. Such enzyme/substrate interactions could critically influence cell-cell and ECM-cell interaction and the organization of intact synapse structure. Overall, these results confirm that membrane-bound MMP response is influenced by the type and complexity of neuropathology induced by TBI.

Postinjury Time Course of Membrane-bound MMPS and N-cadherin Expression

Our Western blot analysis of hippocampal MT5-MMP, ADAM-10 and N-cadherin protein expression during reactive synaptogenesis revealed the following: 1) both membrane-bound MMPs were increased early postinjury (by 2d) and peaked in

expression at the 7d sprouting period, suggesting a prominent role in the earlier phases of recovery, 2) both membrane-bound MMPs were matched by a reduction in their target substrate N-cadherin, observed for adaptive and maladaptive conditions alike, and 3) the principal forms of these proteins indicate different roles for each enzyme, MT5-MMP expressed in a TIMP bound, non active form and ADAM-10 changes primarily linked to the 70 kDa active enzyme. Overall, the profiles of MT5-MMP and ADAM-10 expression in the adaptive UEC model are consistent with our previous analyses of secreted MMPs, where both transcription and translation of MMPs 2, 3 and 9 are rapidly elevated at the onset of synaptogenesis (Kim et al., 2005, Falo et al., 2006). In contrast to those studies, where released MMPs were reduced at later stages of synaptic recovery, our current results suggest that persistent expression of active membrane bound ADAM-10 can aberrantly influence the long-term stabilization of new synapses generated after TBI. A prominent role for ADAM-10 during TBI-induced synaptic plasticity would be expected from the literature, where it has been shown to influence axonal guidance, cortical synapse development and synaptic modulation through interaction with molecules like ephrin, APP, and N-cadherin (Hattori et al., 2000; Bell et al., 2006; Reiss et al., 2005). The active form of this enzyme appears to target the synaptic adhesion protein N-cadherin during the early, more plastic phases of synapse regeneration, but this enzyme/substrate interaction is attenuated during synapse maturation and stabilization. Such interaction would be predicted since reduced adhesion would be required for the morphing of synaptic structure in the acute postinjury period, and elevated N-cadherin needed for transmembrane anchoring of the synaptic junction complex and binding of synaptic proteins to the pre- or postsynaptic

cytoskeleton. The presence of high levels of ADAM-10 would foster the cleavage of N-cadherin at its extracellular/membrane interface, resulting in shedding of the N-terminal sequence into the matrix space. Other studies have also demonstrated that synaptic stabilization and functional efficacy are mediated through N-cadherin extracellular binding, transmembrane placement, and intracellular association with catenin molecules (Gottardi and Gumbiner, 2004). In addition, the intracellular N-cadherin fragmentation can signal the transcription of genes involved in cell survival, migration and synapse adhesion/stabilization (McCusker and Alfandari, 2009). Thus, N-cadherin is involved in synaptogenesis, through direct physical binding and indirect effects on downstream transcription. Our results provide further evidence that these membrane-bound MMPs and N-cadherin are an important enzyme/substrate pairing for successful synaptic reorganization following TBI.

From the literature, MT5-MMP can be linked with neuroplasticity, where reorganization of Aβ fibers after sciatic nerve injury, synaptic modulation through N-cadherin cleavage, and neurite outgrowth with proteoglycan cleavage are all promoted by its activation (Komori et al., 2004; Monea et al., 2006; Hayashita-Kinoh et al., 2001). By contrast, we did not find MT5-MMP in its active form, rather expressed at a higher 80 kDa band, a size predicted for enzyme bound to endogenous inhibitor. Blot re-probing experiments suggest that this high kDa band represents active MT5-MMP bound to its endogenous inhibitor TIMP-2. Such a result opens the possibility that the enzyme may play a very different role from the predicted N-cadherin modulation during reactive synaptogenesis. Rather, TIMP-2 bound MT5-MMP may be part of a ternary complex that activates pro-MMP-2, and leads to downstream gelatinase activity. Activated MMP-

2 would then be available to interact with ECM molecules present in the damaged neuropil to influence early phases of reactive synaptogenesis. We know that shifts from pro- to active MMP forms occur following CNS injury (Ashi et al., 2000; Noble et al., 2002; Li et al., 2009) and that focal activation of these enzymes can occur in a complex formed by TIMP/MT-MMP/pro-MMP binding at the cell membrane (Strongin et. al, 1995; Sternlicht and Werb, 2001; Maskos and Bode, 2003; Nagase et al., 2006). Such focal MMP activation could be particularly important when new synaptic sites are being organized along reforming dendrites within the deafferented molecular layer.

In addition to the significant changes found in predominant forms of MT5-MMP, ADAM-10 and N-cadherin, secondary signals for each protein were also observed following injury. These additional forms showed temporal shifts consistent with the expression of the principal kDa forms. For example, ADAM-10 probed blots contained both 100 kDa TIMP-1 bound and 80 kDa pro-enzyme forms which were significantly reduced in tandem with the elevation of active ADAM-10 enzyme. Further, we also observed a 2d increase in a 40 kDa N-cadherin form, consistent with the intracellular C-terminal fragment produced by ADAM-10 cleavage. Generation of a 35 kDa N-cadherin C-terminal fragment has been associated with intracellular signaling pathways which facilitate gene transcription (Marambaud et al., 2003; Reiss et al., 2005; McCusker and Alfandari, 2009; Jang et al., 2009). While our peptide did not migrate exactly at 35 kDa, it remains possible that injury has generated the same intracellular fragment, although not fully processed for its role in downstream cell signaling. Given the known roles for MMP and N-cadherin interaction, these findings are not surprising, however, they are

novel in the context of reactive synaptogenesis, providing further insight into the time and recovery-dependent roles of these two membrane-bound MMPs.

Model Differences in Membrane-bound MMP and N-cadherin Expression

Direct comparison between adaptive and maladaptive models of reactive synaptogenesis revealed three major differences in MT5-MMP, ADAM-10 and N-cadherin expression. Compared to adaptive synaptic recovery, the maladaptive condition showed: 1) attenuated MT5-MMP and ADAM-10 expression at 2d after injury, 2) a higher level of ADAM-10 protein at 7d, which remained significantly elevated at 15d postinjury and 3) a failure to generate elevated full-length N-cadherin at 15d during synapse stabilization.

Following UEC lesion, TIMP-bound MT5-MMP and active ADAM-10 protein levels were significantly elevated during the acute degenerative (2d) and early regenerative (7d) phases of recovery. With TBI+BEC, a similar 2d rise over control occurred, but was reduced in extent by approximately 28%. Lower enzyme expression at 2d may limit the amount of MMP/substrate interaction required to promote the necessary degeneration and clearance of damaged axon terminals following combined injury. This result is similar to that seen for secreted MMP-3 at 2d, where the TBI+BEC insult generated a lower level of enzyme than the UEC (Phillips et al., unpublished observations). By contrast, at the 7d interval, where axonal sprouting and synapse formation is most rapid, ADAM-10 expression was 25% higher than seen in adaptive recovery, and remained elevated up to 47% over UEC levels at 15d postinjury. Again, this result is in agreement with a persistent elevation of MMP-3 protein at 7d in the

maladaptive TBI+BEC model (Phillips et al., unpublished observations). Together they support a differential response for MT5-MMP and ADAM-10 between the two models. Combined injury pathology had a lesser effect on MT5-MMP, which was most associated with the early periods of debris removal and organization for axonal sprouting. By contrast, maladaptive plasticity was clearly linked to higher ADAM-10 response and a persistent elevation of the enzyme past the time period when it is attenuated in the adaptive UEC model. Such persistent MMP elevation under conditions of failed recovery is in agreement with long-term increase in transcript levels for secreted MMPs 2, 3 and 9 previously reported for the TBI+BEC model (Phillips and Reeves, 2001; Kim et al., 2005; Falo et al., 2006).

Another important model difference was observed regarding the expression of full-length N-cadherin, which showed a significant 15d elevation over control levels during adaptive UEC recovery. This would be predicted for the phase of synaptogenesis when nascent synapses are selectively pruned and junction complexes stabilized by N-cadherin adhesion. A similar elevation of the synaptic protein agrin was described 7d following UEC, which paralleled the reduction of MMP-3 (Falo et al., 2006; Falo et al., 2008). With TBI+BEC maladaptive plasticity, full length N-cadherin was attenuated by 30% at 15d relative to the UEC model, a result predicted from the observation that active ADAM-10 was elevated at the same time point. A persistent ADAM-10 proteolysis of N-cadherin at newly developing synapses would limit synaptic stabilization and possibly alter downstream signals regulating gene transcription critical to recovery. Notably, this same pattern of persistently elevated enzyme and significantly reduced substrate was seen with MMP-3 and its synaptic target agrin

following TBI+BEC (Falo et al., 2006; Falo et al., 2008). Moreover, reduced N-cadherin and agrin protein expression in the maladaptive model is consistent with the poor synaptic reorganization seen in earlier ultrastructural studies (Phillips et al., 1994; Falo et al., 2006).

Model differences were also found with some of the additional forms identified for each protein. The 100kDa TIMP-1 bound and 80kDa pro-enzyme forms of ADAM-10 were significantly reduced at all three postinjury intervals after UEC, however, they each returned to control levels at 7d post-TBI+BEC. While the reason for a normalization of these ADAM forms during the phase of sprouting and synapse formation is not clear, it may represent a compensatory shift towards latent enzyme expression as a control for the extent of ADAM-10 activity generated in the maladaptive model. The one case where a model difference was not observed was the 85kDa form of MT5-MMP which was significantly reduced at all time intervals for UEC and TBI+BEC, suggesting that this MT5-MMP form may play a similar role in the adaptive and maladaptive recovery processes.

Tissue Distribution of Membrane-bound MMPs and N-cadherin after Injury

Tissue localization provides important correlative data for the accurate interpretation of quantitative changes in MMPs and their target substrates during reactive synaptogenesis. Based on current literature, MT5-MMP, ADAM-10 and N-cadherin clearly display spatial expression patterns that would favor interaction at the synaptic interface and support active roles in synaptic reorganization (Jaworski, 2000; Sekine-Aizawa et al., 2001;, Hayashita-Kinoh et al, 2001; Benson and Tanaka, 1998;

Monea et al., 2006; Marcinkiewicz and Seidah, 2000; Marcello et al., 2007). Our immunohistochemical analysis of MT5-MMP, ADAM-10 and N-cadherin support such a relationship in several ways: 1) the deafferented molecular layer in UEC and TBI+BEC cases shows elevation of each enzyme and N-cadherin relative to paired controls, 2) the 7d increase in MMP protein is more profound for the combined insult cases, correlating with the quantitative blot results, and 3) astrocytes are the primary sites of tissue localization for all three proteins, with subtle differences in neuronal distribution noted between MT5-MMP and ADAM-10.

Adaptive and maladaptive synaptogenesis showed several similarities in enzyme and N-cadherin protein distribution. In each TBI model, dentate MT5-MMP, ADAM-10 and N-cadherin were elevated relative to uninjured controls. Proteins showed principal localization within reactive astrocytes in the deafferented molecular layer during all phases of reactive synaptogenesis. This pattern is entirely consistent with our earlier studies with MMPs 2, 3 and 9, where endogenous glia appear to be the primary site for production or processing of these enzymes (Phillips and Reeves, 2001; Kim et al., 2005; Falo et al., 2006). Moreover, secreted MMPs are consistently reported to be localized within the glia affected by a variety of CNS traumas (Rosenberg, 1995). Diffuse neuropil localization is also consistent with the proposed high concentration of these three molecules at synaptic sites either around granule cell (GC) bodies or along their dendrites. A notable difference in membrane-bound MMP distribution between models was the stronger intensity of this latter pattern in the combined cases. This was particularly true for MT5-MMP, which might be explained by it potential role in activation of MMP-2 within the ML extracellular space. More profound damage in the TBI+BEC

model would require greater matrix fluidity to facilitate debris removal. Localization of N-cadherin within reactive astrocytes and throughout the ML supports glial uptake and processing of its cleaved extracellular domain during a time of increased active ADAM-10 expression. Again, the combined maladaptive model showed subtle differences, with slightly more signal in a diffuse pattern relative to cellular localization than the UEC. The TBI+BEC model exhibits slow debris clearance (Phillips et al., 1994), suggesting that perhaps this shift in N-cadherin distribution represents a lesser degree of glial response to phagocytose the cleaved adhesion protein. Over the 2-15d time course, we found a similar pattern of MT5-MMP, ADAM-10 and N-cadherin distribution in the dentate, with the principal difference being relative intensity of signal. This pattern was consistent with model and temporal differences seen in our WB results. N-cadherin was the only exception, where, as described above, we can attribute the higher tissue signal versus lower blot signal to differences in antibody recognition used for the two experiments. As with our other histological time course studies, the more acute increases are followed by long-term decreases as synaptogenesis proceeds. Taken together, these results support local interaction between membrane-bound MMPs/substrates during synaptic remodeling, a site where glial processes intimately interface with pre- and post-synaptic membranes (Benson et al., 2000).

Our immunohistochemical results not only illustrate the spatial profile of these matrix proteins, but also point to a major astrocytic role in their regulation during reactive synaptogenesis. The data suggests that this role may be different as a function of membrane-bound MMPs. A primary clue here was the distinct structural appearance of antibody signal for MT5-MMP and ADAM-10. We found similar punctate somatic and

process labeling in reactive astrocytes for both MT5-MMP and N-cadherin, supporting a common link to phagocytosis and internalization after injury. By contrast, ADAM-10 uniformly filled the astrocyte cell bodies and did not directly match with the N-cadherin pattern. Although most published studies show ADAM-10 localized within neurons, there is also evidence that ADAM-10 may have an astrocytic origin (Kieseier et al., 2003; Bandyopadhyay et al., 2006). While this difference is an interesting observation, our data cannot fully discriminate between the possibilities. It should be noted that our WB data does show major changes in active enzyme, supporting lytic astrocytic activity for ADAM-10 as well.

The magnitude and direction of astrocytic response may be dependent on the severity and complexity of TBI, and therefore influence the level of recovery. Reactive astrocytes can exhibit detrimental, as well as stimulatory effects on injury-induced plasticity. Traditionally, reactive astrocytes are proposed to contribute to the formation of inhibitory glial scars adjacent to damaged tissue, therefore preventing or limiting recovery postinjury (Liuzzi and Lasek, 1987; Rudge and Silver, 1990). Conversely, some studies argue that astrocytic scars play a protective role, restricting additional tissue damage following injury, as well as synthesizing and releasing local cytokines/growth factors (White and Jakeman, 2008; Su et al., 2009). Reactive astrocytes also produce and release MMPs to aid in the removal of damaged tissue/cells from the injured region, a necessary step prior to the regenerative phase of synaptogenesis. We know that MMP-3 expression during post-UEC synaptogenesis contributes to adaptive recovery. However, overproduction and release of MMPs could lead to upregulated activity and additional tissue damage. For example, lytic activity of

both MMP-3 (Kim et al., 2005) and the gelatinases MMPs 2, and 9 (Phillips, unpublished results) is persistently elevated during maladaptive synaptic plasticity, negatively affecting recovery in the TBI+BEC model. In these cases, MMPs are predominantly located within CNS glia and are likely released to influence synaptogenesis. Thus, a tight spatial and temporal regulation of MMP expression appears necessary for adaptive plasticity to occur. Despite their dual role, targeted manipulation of reactive astrocytes during maladaptive plasticity has potential to improve recovery by limiting the overexpression and release of MMPs postinjury.

RNA Expression of Membrane-bound MMPs and N-cadherin During Sprouting and Synaptogenesis

To better understand the profile of postinjury MT5-MMP, ADAM-10, and N-cadherin protein expression, we used microarray and qRT-PCR methods to screen for transcript changes at 7d after UEC and TBI+BEC. Microarray results from whole hippocampus and enriched ML samples revealed the greatest change to be in ADAM-10 transcript, which occurred following adaptive UEC. In contrast, slightly more modest shifts were seen after TBI+BEC. Increased ADAM-10 transcript did not appear to differ between ML and hippocampal samples, further supporting its prominent role in reactive synaptogenesis. These findings are paralleled by increases in hippocampal ADAM-10 protein expression values at 7d for both models and the persistent rise in the enzyme at15d following TBI+BEC. Microarray screening of MT5-MMP and N-cadherin failed to show post-UEC changes in gene expression and only a modest rise in N-cadherin ML transcript with TBI+BEC. While these results do not specifically match our hippocampal WB profile, they do provide details regarding the synchrony of transcription and

translation in these models. No change in ML UEC MT5-MMP and N-cadherin transcript at 7d suggests that these genes are regulated at either earlier or later time intervals to produce the protein changes we have observed. In the maladaptive model, ML gene expression patterns were attenuated, consistent with the slower start for membrane-bound MMP response and slower lysis of synaptic proteins like N-cadherin. The strongest cross-model synchrony of transcript and protein change was seen for ADAM-10, which might be predicted since the 7d time point showed the most increase in protein expression.

Quantitative RT-PCR analysis of the same 7d ML samples, revealed greater changes in MT5-MMP, ADAM-10 and N-cadherin mRNA expression, as is commonly the case when samples are shifted from array to PCR analysis. Elevated ADAM-10 mRNA in both models remains consistent with our hippocampal WB results. Again, this tight synchrony of protein and mRNA expression for ADAM-10 shows that its up regulation is important during dentate synaptic reorganization. The principal asynchrony between message and protein was seen with the combined model MT5-MMP and N-cadherin. As indicated above, we interpret this pattern to mean that our 7d sampling missed an earlier peak in MT5-MMP transcript. Alternatively, the use of ML for the PCR may introduce unknown differences when compared to hippocampal WB results. We also interpret the lack of effect on 7d transcript for N-cadherin in the maladaptive model as an expected result, since the protein does change at the later 15d time point with TBI+BEC. It should be noted that reported protein expression was determined from whole hippocampal samples, while the greatest changes in mRNA expression were derived from ML samples. The fact that 7d whole hippocampal mRNA analysis showed

minimal to no change relative to controls tends to support synthesis of these proteins by non-neuronal cells, such as reactive astroglia concentrated in the deafferented zone, a conclusion consistent with our immunohistochemical and preliminary *in situ* hybridization findings. Taken together, the PCR analysis further supports the involvement of membrane-bound MMPs in the acute phases of synaptic regeneration, as well as the notable persistent expression of active ADAM-10 and reduced N-cadherin during stabilization of nascent synapses.

Role of MT5-MMP, ADAM-10 and N-cadherin in Synaptic Recovery after TBI

The spatial and temporal patterns of MT5-MMP, ADAM-10, and N-cadherin expression during adaptive and maladaptive recovery provide insight into potential mechanisms underlying their role in injury-induced synaptogenesis. While membrane-bound MMPs like MT5-MMP and ADAM-10 may be either directly or indirectly capable of modifying ECM-cell and cell-cell structure within the CNS, they may also act as upstream mediators of plasticity. At this time, our view of postinjury mechanisms is strongly based on evidence that MMP lysis of N-cadherin has downstream effects on plasticity-related events. The present results show that elevation of active ADAM-10 is paralleled by decreased full length N-cadherin expression postinjury. Additionally, a persistent elevation of active ADAM-10 at 15d post-TBI+BEC is correlated with reduced N-cadherin expression when compared to the pattern in UEC, further suggestive of a critical ADAM-10/N-cadherin interaction during synaptogenesis. There is evidence that ADAM-10 and MT5-MMP cleavage of N-cadherin has both extracellular and intracellular downstream effects that can potentially influence synaptic plasticity (Uemura et al, 2006; Reiss et al., 2005; Monea et al., 2006). For example, *in vitro* studies show

ectodomain shedding of N-cadherin releases an N-terminus fragment (NTF) that promotes neurite outgrowth in cultured neurons (Paradies and Grunwald, 1993; Utton et al., 2001). Additionally, MMP-driven ectodomain shedding of N-cadherin is required for its further intracellular cleavage, which releases a 40kDa C-terminus fragment (CFT1), similar to the form we observed in our WB analysis. The release of CTF1 alters the structural integrity of the synapse by changing the intracellular binding properties of the protein, thereby permitting structural synaptic modifications during times of heightened plasticity (i.e., acute degenerative and regenerative phases of reactive synaptogenesis) (Jang et al., 2009). Release of intracellular N-cadherin fragments has also been shown to alter synaptic Ca^{2+} conductance and therefore affect synaptic function. This N-cadherin fragmentation is linked to changes in submembrane interaction with proteins such as the AMPA receptor family and p120 catenin, resulting in a decreased Ca^{2+} conductance (Silverman et al., 2007; Malenka and Bear, 2004; Brusés, 2006; McCusker and Alfandari, 2009; Jang et al., 2009). CFT1 undergoes further processing into a 35kDa fragment (CTF2), which can inhibit the AKT signaling pathway, therefore potentially leading to neuronal death in pathological states (Jang et al., 2009). Additionally, CTF2 may affect synaptogenesis by binding CREB binding protein (CBP) and preventing downstream transcription of CREB-dependent genes that are critical for nervous system function and plasticity (Marambaud et al., 2003; Lonze and Ginty, 2002). Further, CTF2 also associates with the Wnt signaling molecule β-catenin, which promotes transcription of genes that are important for cell proliferation and survival, such as cyclin D1, c-myc, c-jun, and N-cadherin (Reiss et al., 2005). Clearly the literature points to the signaling events produced by the proteolytic processing of N-

cadherin as critical to the efficient reorganization of the synaptic junction. We believe our aggregate data provide evidence that this is true, and that the success or failure of injury-induced synaptic recovery may depend upon MMP directed generation of substrate fragments at specific phases of synaptogenesis. Indeed, the altered ADAM-10 and N-cadherin expression we observed during the later stages of aberrant injury-induced synaptogenesis support this conclusion.

SUMMARY

The current study examined MT5-MMP, ADAM-10 and N-cadherin protein and mRNA expression during adaptive and maladaptive plasticity as a first step in better understanding the role of these matrix molecules in postinjury recovery. It is clear that the neuropathology generated by UEC and combined TBI+BEC are different, and therefore recruit different responses from these membrane-bound MMPs to either foster or inhibit structural and functional recovery. The results presented here raise several questions about postinjury mechanisms that may affect MMP regulation, expression, and, in turn, injury-induced plasticity. Our results implicate MT5-MMP and ADAM-10 as important enzymes in the plasticity process, potentially through activation of other proteases or interaction with N-cadherin. Although we show MT5-MMP and ADAM-10 influence on synaptic plasticity in two different TBI models, it remains unclear what specific event(s) regulate their differential postinjury expression patterns. Future studies are needed to determine MT5-MMP and ADAM-10 functional activity over the time course of reactive synaptogenesis. In addition, detailed behavioral and functional

assessments are necessary to further understand model differences and reveal possible therapeutic targets to improve synaptic plasticity and recovery following TBI.

Chapter 3

MMP Inhibition Improves Synaptic Efficacy and Stabilization during Maladaptive Injury-Induced Synaptogenesis

ABSTRACT

In our prior studies we have reported that a variety of matrix metalloproteinases (MMPs) influence the success of reactive synaptogenesis induced by traumatic brain injury (TBI). The first portion of this dissertation has shown that specific membrane-bound MMPs, MT5-MMP and ADAM-10, are spatially and temporally correlated with adaptive synaptic plasticity, specifically the period of recovery when new synapses are stabilized. The success of this process appears to be linked to reduced MMP levels and elevated expression of their common substrate, N-cadherin, an adhesion molecule critical to the organization and stabilization of the synaptic junction. Such observations suggest that membrane bound MMPs may act in concert with N-cadherin to support functional recovery seen with adaptive synaptic plasticity. Our earlier studies indicate that attenuation of secreted MMP activity at 6-7d postinjury improves the structural integrity of newly formed synapses in the TBI+BEC model of maladaptive synaptogenesis. Here, we posit that inhibition of membrane bound MT5-MMP and ADAM-10, targeting their elevation during onset of regenerative axonal sprouting in that model, will enhance N-cadherin related stabilization of synaptic structure and promote functional recovery. Adult male rats subjected to TBI+BEC (combined fluid percussion + entorhinal lesion insult) were treated with the broad spectrum MMP inhibitor GM6001 (10mg/kg i.p.) or vehicle at 6 and 7d postinjury, targeting both the onset of synapse reorganization and the period of highest hippocampal MT5-MMP and ADAM-10 protein expression. Assessment of drug effect was made at 15d postinjury, the period when these two MMPs and their substrate N-cadherin were most prominently altered during maladaptive plasticity. Relative to sham-injured controls, GM6001 treatment decreased

ADAM-10 protein levels and increased in N-cadherin protein expression. Functional effects of MMP inhibition were also evaluated at 15d postinjury, using brain slices for *in vitro* electrophysiological recordings of long-term potentiation (LTP), long-term depression (LTD), and paired pulse facilitation (PPF) in the Schaffer collateral input to CA1. This pathway was selected based upon its widespread use as a model for probing hippocampal synaptic efficacy, and the fact that its components remain intact following the TBI+BEC insult. Combined injury resulted in the delayed induction of LTP, which was partially restored with GM6001 treatment. By contrast, LTD failed to show any drug-related change. Further, PPF trials showed no significant effects of either injury or drug, suggesting that functional deficits associated with this hippocampal pathway did not involve defects in pre-synaptic terminals. To assess behavioral plasticity following MMP inhibition, a subset of injured-untreated and injured-treated animals were tested for spatial memory performance using the Morris Water Maze. Our results showed the profound, persistent deficits associated with the TBI+BEC model, however, GM6001 treatment failed to alter behavioral outcome. Finally, qualitative ultrastructural analysis of injured animals treated with GM6001 revealed dendritic cytoarchitecture and synaptic integrity consistent with adaptive synaptic recovery, supporting the hypothesis that GM6001 MMP inhibition also protects synaptic structure after TBI. Collectively, these results suggest that membrane-bound MMPs and their substrate N-cadherin interact during reactive synaptogenesis to influence synapse stabilization, contributing to enhanced synaptic function following TBI.

INTRODUCTION

Two principle features of traumatic brain injury (TBI) are excessive neuroexcitation and diffuse axonal injury, which lead to neuronal deafferentation in vulnerable brain regions (Okonkwo and Povlishock, 2003; Povlishock and Katz, 2005). Injury-induced deafferentation results in reactive synaptogenesis, which serves to replace degenerated synaptic connections and restore function. This plasticity is influenced by a number of extracellular matrix (ECM) molecules, including members of the matrix metalloproteinase (MMP) family and their targeted substrates (Phillips and Reeves, 2001). MMPs constitute a large family of zinc and calcium dependent enzymes that are capable of substrate cleavage at cell surfaces, including the majority of ECM shaping molecules (Rosenberg, 2002). Clearly, MMP proteolytic modification of cell-ECM and cell-cell connections is critical for the formation and maintenance of neural circuitry, as well as for synaptic replacement, reorganization, and recovery following TBI (Sternlicht and Werb, 2001; Treuttner et al., 2005; Falo et al., 2006; Szklarczyk et al, 2002). While MMPs promote a variety of plasticity processes including axonal guidance and synaptogenesis during nervous system development and disease, MMP activity is tightly regulated to avoid the negative consequences of excessive lysis (Yong et al., 2001).

Our lab has demonstrated MMP involvement in reactive synaptogenesis following TBI, which suggests an integral MMP role in recovery (Reeves et al., 2003; Kim et al., 2005; Falo et al., 2006). Studies revealed aberrant MMP protein expression and activity when the plasticity process is maladaptive. This work contrasts the adaptive synaptic recovery induced by unilateral entorhinal cortex lesion (UEC) with a

model which combines moderate central fluid percussion injury and bilateral entorhinal cortex lesions (TBI+BEC), resulting in poor synaptic recovery. We posit that these persistent recovery deficits are due, in part, to the unregulated expression and activity of MMPs within damaged brain regions. Therefore, to improve synaptic recovery and uncover potential treatment paradigms for human TBI, we have explored the efficacy of pharmacological MMP inhibition postinjury in producing enhanced synaptic recovery. In the TBI +BEC model, MMP inhibition with the hydroxyamate compound FN-439 at 6-7d postinjury reduced spatial learning deficits and improved synaptic cytoarchitecture (Falo et al., 2006). Interestingly, we also found that FN-439 administration 30 minutes after UEC attenuated both structural and functional recovery at 7d postlesion (Reeves et al., 2003). These results suggest that, while regulated MMP expression and activity is required for successful synaptic recovery, excessive MMP response can attenuate this recovery and result in maladaptive reorganization following brain injury.

Recently, two membrane-bound MMPs, Membrane-type 5 MMP (MT5-MMP) and A Disintegrin and Metalloproteinase-10 (ADAM-10), have emerged as important players in the plasticity process. MT5-MMP and ADAM-10 may influence the outcome of reactive synaptogenesis by targeting the neuronal adhesion molecule, N-cadherin (Monea et. al, 2006; Reiss et al., 2005). In the CNS, N-cadherin ligates pre- and post-synaptic elements extracellularly, stabilizes intracellular synaptic structure, and influences the organization and function of mature synapses (Benson and Tanaka, 1998). MT5-MMP and ADAM-10 are localized in and around synapses, in close proximity to N-cadherin, permitting concentrated proteolytic activity at synaptic junctions (Jaworski, 2000; Marcinkiewicz and Seidah, 2000; Takeichi and Abe, 2005). Interaction

between MT5-MMP, ADAM-10 and N-cadherin has the potential to influence reactive synaptogenesis following TBI through modification of synaptic adhesion and stabilization.

The first study in this dissertation has shown that specific membrane-bound MMPs, MT5-MMP and ADAM-10, are spatially and temporally correlated with adaptive synaptic plasticity, specifically the period of recovery when new synapses are stabilized (Warren et al., 2009). We observed an inverse relationship between levels of enzyme and substrate in both models, as well as recovery-dependent changes in protein expression postinjury. Relative to the adaptive UEC model, maladaptive plasticity showed a reduced MT5-MMP response at 2d postinjury and a persistently elevated ADAM-10 expression at 15d. Synaptic adhesion protein N-cadherin was reduced at 2 and 7d postinjury, but showed elevation above normal levels of expression at 15d with adaptive recovery. With maladaptive synaptogenesis, N-cadherin failed to increase at 15d. We conclude that these altered patterns of 2d MT5-MMP and 15d ADAM-10/N-cadherin expression contribute to the poor synaptic recovery seen in the TBI+BEC model. Further, we posit that the inhibition of MT5-MMP or ADAM-10 activity at 6-7d postinjury, the interval of its maximum expression, will attenuate enzyme expression and elevate N-cadherin at 15d after injury. Moreover, these shifts will reduce structural and functional pathology which characterizes the maladaptive synaptic plasticity of the TBI+BEC model.

In this present study we investigated the effect of MMP inhibition on MT5-MMP, ADAM-10 and N-cadherin protein expression by administering the broad-spectrum MMP inhibitor, GM6001, at 6 and 7d following TBI+BEC insult. Assessment of drug

effect was made at 15d postinjury, the period when these two MMPs and their substrate were most prominently altered during maladaptive plasticity. GM6001 inhibits MMP activity by chelating zinc at the active site of secreted and membrane-type MMPs, including MT5-MMP and ADAM-10. Substrate binding is prevented, rendering the MMPs inactive (Grobelny et al., 1992; Schultz et al., 1992). We chose to use GM6001 in our study based upon its ability to cross the blood brain barrier to inhibit MMPs *in vivo* and published evidence for its *in vitro* inhibition of MT5-MMP and ADAM-10 (Gijbels et al., 1994; Leib et al., 2000; Bendeck et al., 1996; Monea et al., 2006; Reiss et al., 2005). We chose to administer GM6001 at 6 and 7d for several reasons: 1) to target the period where we observed maximal postinjury MT5-MMP and ADAM-10 elevation, 2) to manipulate MT5-MMP and ADAM-10 activity during the period of axonal sprouting and 3) to match our prior protocols which showed enhanced synaptic recovery with FN-439, a MMP inhibitor with high selectivity for secreted MMP-3 (Falo et al, 2006). In these studies we first assessed hippocampal MT5-MMP, ADAM-10 and N-cadherin expression at 15d postinjury with Western blots. In a parallel set of experiments, functional effects of MMP inhibition were evaluated with *in vitro* electrophysiological recordings of long-term potentiation (LTP), long-term depression (LTD), and paired pulse facilitation (PPF) in the Schaffer collateral input to CA1. To assess behavioral plasticity following MMP inhibition, a subset of injured-untreated and injured-treated animals were tested for spatial memory performance using the Morris Water Maze. At the end of behavioral assessment, a subset of animals from each group was prepared for ultrastructural analysis of drug effect on synaptic cytoarchitecture. Our results show that MMP inhibition significantly affected ADAM-10 and N-cadherin protein expression,

improved measures of synaptic efficacy, and enhanced the integrity of hippocampal synaptic ultrastructure.

METHODS

Experimental Animals

Adult male Sprague-Dawley rats (300-400g) were used in this study. Two rats were housed per cage, with food and water *ad libitum,* and subjected to a 12 hr dark-light cycle at 22°C. All protocols for injury and use of animals were approved by the Institutional Animal Care and Use Committee of Virginia Commonwealth University. Rats were randomly divided into three groups and subjected to either: 1) TBI+BEC injured-untreated (n=25), 2) TBI+BEC injured-GM6001 treated (n=20), 3) TBI+BEC injured-vehicle treated (n=10), 4) sham-injury (n=25). Animals were allowed to survive for 15d, at which time subgroups were again randomly selected for biochemical, electrophysiological or ultrastructural assessment. In all analyses, sham-injured animals served as paired-controls and results were expressed as percent change from this group. A subset of injured-treated, injured-untreated and sham-injured rats underwent behavioral testing (MWM) on days 12-15 postinjury before being sacrificed at 15d.

Surgical Preparation for Central Fluid Percussion TBI

Animals were anesthetized (isoflurane 4% in carrier gas of 70% N_2O and 30% O_2 delivered via nose cone) and placed in a stereotaxic frame for surgical preparation 24hrs prior to injury. Body temperature was maintained at 37°C using a thermostatic

heating pad (Harvard Apparatus, Holliston, MA) and physiological parameters (heart rate, arterial oxygen saturation, breath rate/distension and pulse distension) monitored throughout surgical preparation using pulse oximetry (MouseOx; Starr Life Sciences, Oakmont, PA). Rats received a 4.8 mm midline craniectomy midway between bregma and lambda, exposing but not breaching the underlying dura. Two steel screws were implanted 1 mm caudal to the coronal suture on the left and 1mm rostral to lambdoidal suture on the right. A modified Leur-Loc hub (2.6 mm inside diameter) was implanted in the craniectomy site and fixed with cyanoacrylate adhesive. Dental acrylic was added around the hub and screws to secure the complex. The scalp was sutured closed to cover hub and Bacitracin was applied to the wound. Rats were monitored for recovery and returned to their home cages.

Central Fluid Percussion TBI

Moderate central fluid percussion injury (2.0±0.1 atm) was performed as described by Dixon et al. (1987). The fluid percussion injury device is made up of a Plexiglas cylinder (60cm long, 4.5 cm diameter) filled with double distilled water. One end of the cylinder has a rubber-covered Plexiglas piston mounted on O-rings, and the opposite end is closed by a metal extra-cranial pressure transducer (Entram Devices, Inc., model EPN-0300-100A). The end of the metal transducer (5mm tube, 2.6 mm inside diameter) has a male Leur-loc fitting that connects to the exposed female Leur-loc hub implanted in the rat skull. A metal pendulum is dropped from a determined height that coincides with injury severity, and strikes the rubber-covered piston, forcing a small fluid injection into the closed cranial cavity, briefly displacing brain tissue. Injury level is recorded by the extra-cranial transducer, and visualized and reported

(atmospheres, atm) on an oscilloscope (Tektronix 5111: Beaverton, OR). Twenty-four hours after surgical preparation, rats were re-anesthetized, connected to the fluid percussion device through the exposed hub, and subjected to injury. Animals were monitored for recovery from anesthesia and injury by observation and timing of multiple reflexes (paw, tail, corneal, righting, pinna), and then returned to their home cages.

Combined Central Fluid Percussion +Bilateral Entorhinal Lesion (TBI+BEC)

Animals that received the combined injury were surgically prepared for fluid percussion injury, and twenty-four hours later received moderate (2.0±0.1 atm) central fluid percussion injury. These animals recovered for another twenty-four hour time period, and were then re-anesthetized and subjected to bilateral entorhinal cortex lesions (Phillips et al., 1994). Briefly, a small portion of the skull was removed on the right and lefts sides to expose the dura mater superior to the entorhinal cortex (see again Appendix A, Fig. A-2). Electrolytic lesions were made by passing a 1.5 mA current (40 sec each) via 0.2 mm Teflon-insulated wire electrode, positioned 10° to the perpendicular plane, at eight at eight separate stereotaxic sites: 1.5 mm anterior to the transverse sinus, and 3, 4, and 5 mm lateral to midline, 2 , 4 and 6mm ventral to the brain surface for the first two lateral measurements (3 and 4mm) and only 2 and 4mm ventral to the brain surface for the last lateral measurement (5mm) (see again Appendix A, Fig. A-1). After lesioning, electrodes were removed, the scalp sutured, and Bacitracin was applied. Animals were transferred to a recovery cage and monitored for at least 1 hr to ensure adequate recovery, and were then returned to their home cages.

MMP Inhibitor (GM6001) Administration

Inhibition of MT5-MMP and ADAM-10 activity was achieved using a commercially available MMP inhibitor, GM6001 (Millipore, Billerica, MA). This hydroxamate compound chelates the active site zinc atom within a variety of MMPs, preventing substrate binding and rendering the enzyme inactive (Grobelny et al, 1992; Schultz et. al, 1992). Although it targets a broad-spectrum of MMPs, GM6001 has been shown to inhibit both MT5-MMP and ADAM-10 *in vitro* (Monea et. al, 2006; Reiss et. al, 2005). Animals within the TBI+BEC Injured-treated group received GM6001 (10mg/kg i.p.) once daily, at 6 and 7d postinjury, delivered in vehicle consisting of 4% carboxymethlycellulose (CMC sodium salt, Sigma, St. Louis, MO) suspension as described. GM6001 dose, suspension, and delivery was based on previous *in vivo* studies which showed effective inhibition of MMPs in neurotrauma models (Wang and Tsirka, 2005; Sifringer et al., 2007). The timeframe for dosing was selected to coincide with the period where we observed maximal postinjury MT5-MMP and ADAM-10 elevation. A separate injured-vehicle group received 4% CMC with the same dosing paradigm to assess effects of vehicle on biochemical outcome. No significant differences were detected between injured-untreated and injured-vehicle animals (data not shown), therefore the two groups were combined into one for subsequent experimental analyses.

Western Blot Analysis

At 15d following injury, a subset of rats (TBI+BEC injured-treated: n=6; TBI+BEC injured-untreated: n=7-8; sham-injured: n= 8) were subjected to hippocampal protein analysis. Rat were anesthetized with isoflurane (4% in carrier gas of 70% N_2O and 30%

O_2) and quickly decapitated. Whole hippocampi were removed, homogenized in ice-cold TPER (Pierce), and centrifuged (8,000xg) for 5 min at 4°C. Supernatants were removed and assayed for protein concentration (Shimadzu UV-160, Shimadzu Scientific, Columbia, MD; FLUOstar Optima, BMG Labtechnologies, Inc., Durham, NC). For blot preparation, a 1:5 dilution (5 µg sample:20 µg H_2O) of each sample was mixed with XT Sample Buffer/Reducing Agent (Bio-Rad Laboratories, Hercules, CA) and heated at 95°C. Proteins were resolved on a 4-12% Bio-Tris gel (Bio-Rad) and transferred to PVDF membranes. Post-blotted gels were stained and analyzed for even protein load and transfer. Membranes were washed in dH_2O twice and TBS once for 5 min each, and then blocked in 5% milk TBS-Tween (TBS-T) for 1 hour. Membranes were then probed with primary antibody (MT5-MMP rabbit polyclonal n-terminus: 1:1,000, Abcam, Cambridge, MA; N-Cadherin mouse monoclonal c-terminus: 1:1,000, BD Transductions Laboratories, San Jose, CA; ADAM-10 rabbit polyclonal c-terminus: 1:1,000, Sigma, St. Louis, MO) in 5% Milk TBS-T. After overnight incubation at 4°C, blots were washed six times with Milk TBS-T for 5 min each, incubated in secondary antibody (IgG goat anti-mouse: 1:20,000, Rockland, Gilbertsville, PA; IgG bovine anti-rabbit: 1:20,000, Santa Cruz, Santa Cruz, CA;) for 1 hour, and washed six times with TBS-T for 5 min each. Antibody binding was visualized with enhanced chemiluminescence substrate, SuperSignal (Thermo Scientific, Rockford, IL). Immunopositive bands were imaged on the Syngene G:BOX and densitometry was performed using GeneTools software (Syngene, Frederick, MD). β-actin (mouse monoclonal: 1:3,000, Sigma, St. Louis, MO) was used as a load control for Western blot experiments (see again Appendix B, Fig B-8).

Electrophysiological Recording

A randomly selected subset of rats from TBI+BEC injured-treated (n=9), TBI+BEC injured-untreated (n=8), or sham-injured (n=12) groups were prepared for *in vitro* electrophysiological recording. Each rat was anesthetized with 4% isoflurane for 4 min, and the brain rapidly removed. Coronal 450 µm slices were cut into artificial cerebrospinal fluid (ACSF; 2-4 ºC) containing (in mM): NaCl 124, KCl 3, $MgSO_4$ 2, $CaCl_2$ 2, NaH_2PO_4 1.3, $NaHCO_3$ 26, glucose 10; pH 7.4; saturated with 95% O_2/5% CO_2 gas. All slices containing the mid-dorsal hippocampus were saved, which yielded 4 to 6 slices per brain. Slices were then transferred to a holding chamber containing oxygenated ACSF, gradually brought to 34°C, and were allowed to equilibrate under these conditions for at least 1 h prior to recording. For electrophysiological recording, a slice was gently transferred from the holding chamber to a submersion-type recording chamber, and perfused with oxygenated ACSF (34°C) at a rate of 2-3 ml / min.

A bipolar stimulating electrode (teflon-insulated tungsten, with intertip distance (0.2-0.3 mm) was lowered into the stratum radiatum of CA1 in order to stimulate the fibers of the Schaffer collateral system. This hippocampal projection was selected for study in lieu of the perforant path projection to the dentate gyrus, which is bilaterally ablated in the TBI+BEC model. The Schaffer-collateral projection to CA1 also represents a downstream component of the hippocampal trisynaptic loop and is often used for studies of synaptic efficacy after CNS injury. A recording electrode (glass micropipette filled with ACSF; resistance 6-8 MegOhm) was also placed in the stratum radiatum, approximately 0.5-0.7 mm medial to the stimulating electrode, to measure the evoked population excitatory postsynaptic potentials ("field EPSPs" or fEPSPs). The

initial depth of electrodes was approximately 200 micron below the surface of the slice, however, fine adjustments were made in the depths of both stimulating and recording electrodes to achieve maximum fEPSP amplitude.

Unless otherwise noted, stimulation used for evoked potentials was constant current stimulus-isolated square wave pulses (0.20 msec duration) delivered at one pulse each 30 sec (0.033 Hz). All evoked field potentials were amplified (bandpass = d.c. to 5 kHz), digitized at 20 kHz, and stored on hard disk for off-line analysis. For off-line quantification of digitized waveforms, fEPSP slopes were measured as rate of descent over a 0.5 msec interval in the initial negative-going phase of the fEPSP (ClampFit v.8.2 software, Axon Instruments, Inc., Union City, CA).

An input-output function was generated for each slice by varying stimulus intensity in ten equal steps from subthreshold level to the stimulus intensity which evoked a maximum fEPSP. To assure measurement stability, all evoked potentials were repeated 4 times, at each separate level of stimulation intensity, and statistical analyses were performed only on the averaged signals. Following the determination of the input-output function, three paradigms of neural functional plasticity were implemented: long-term potentiation (LTP), long-term depression (LTD), and paired-pulse facilitation (PPF).

Stimulus amplitude was adjusted to evoke a fEPSP response which was 50% of maximum, based on the prior input-output analysis (see above). Using this constant level of stimulation intensity, a 30 minute period of baseline recording was obtained by evoking fEPSPs at a stimulus rate of 0.033 Hz. LTP was then induced by theta-burst high frequency stimulation (HFS) consisting of a total of ten bursts of four pulses at 100

Hz, with 200 msec separating the onset of each burst. The magnitude of LTP was then evaluated for a period of 60 minutes, using the same stimulation parameters (0.033 Hz) as used during the pre-HFS baseline sample. Following the 60 minute period of post-HFS monitoring, LTD was induced using 15 minutes of 1 Hz stimulation. The effects of the 1 Hz stimulation were then evaluated by acquiring responses at the low stimulation rate (0.033 Hz) for 20 minutes.

A subset of rats (n=6) within each group were further assessed for paired-pulse facilitation (PPF). In the PPF procedure, two identical stimulus pulses, subthreshold for target cell discharges (i.e., not evoking population spikes) and separated by either 50, 100, or 150 msec, usually evoke non-identical responses. The second augmented response has been interpreted as due, in large part, to residual Ca^{2+} loaded into pre-synaptic terminals during the first response, which has not been buffered or cleared prior to the second response (Leung and Fu, 1994). Paired-pulse plasticity was calculated at each interpulse interval (50, 100, and 150 msec) using the ratio of the second fEPSP slope to the first ($fEPSP_2/fEPSP_1$).

Morris Water Maze Assessment

The Morris Water Maze (MWM) was used to assess spatial memory function as previously described (Hamm et al, 2001; Phillips et al., 1997). TBI+BEC injured-treated (n=7), TBI+BEC injured-vehicle (n=8) and sham-injured (n=5) groups were subjected to 4 trials per day for 4 days (12-15d post-injury). In each block of trials, rats were placed in the pool, facing the wall and commenced testing once from each of the start locations (north, south, east west ordinates). The order of start locations was randomized and the hidden goal platform was consistently positioned 45 cm from the outside of the pool

wall. A digital camera was mounted above to pool to record all trials. For each trial, rats were given up to 120 sec to find the hidden platform. If the rat failed to reach the platform after 120 sec, it was placed on the platform for 30 sec, removed from the pool, and returned to a heated chamber between trials. All trials were separated by 4 min intervals. A mean daily latency to find the platform (in sec) was calculated for each animal and group mean comparisons were made as described previously (Phillips et al., 1997).

Electron Microscopy

At the end of MWM testing (15d postinjury), a subset of rats (n=3/injured group) were randomly selected for qualitative EM analysis. Rats were anesthetized with a lethal dose of sodium pentobarbital (90 mg/kg, i.p.) and perfused with 0.9% NaCl followed by mixed aldehyde fixative (4% paraformaldehyde and 0.2% glutaraldehyde) in 0.1M Phosphate Buffer (PB), pH 7.2. Brains were then removed and stored in buffer overnight at 4°C. Coronal vibratome sections (40 µm) containing the hippocampus and dentate gyrus were collected in 0.1M PB and prepared for EM processing as previously described (Phillips et al., 1994). Briefly, sections were first placed in 1% osmium (in 0.1M PB, pH 7.2), processed in resin and flat-embedded on plastic slides. After curing, hippocampi were excised and a series of semi-thin (0.5µm) and ultrathin (silver, 600Å) sections cut on a Leica EM UC6i ultramicrotome (Leica Microsystems, Wetzlar, Germany). The semi-thin sections were photographed as a guide for ultrastructural sampling. Ultrathin sections were collected on membrane-coated slotted grids and observed on a Jeol JEM-1230 electron microscope equipped with a Gatan UltraScan 4000SP CCD camera. A series of 5,000 x images were collected at regular intervals

across the dorso-ventral extent of CA1 radiatum and the dentate molecular layer for subsequent qualitative cytoarchitectural analysis.

Statistical Analysis

For Western blot data, results were expressed as percent of control and group means calculated. Changes in protein expression were first evaluated for significance by comparison of relative optical density measures within TBI+BEC injured-untreated and injured -treated samples to that of paired sham-injured control cases. Subsequent comparisons were also made for optical density measures between TBI+BEC injured-untreated and injured-treated cases. The effects of injury and drug treatment on protein level were determined using the Student's t-test.

Electrophysiological results were evaluated with mixed-model ANOVAs, using the MANOVA software routines in SPSS v. 11.5, with between-subjects factor of analytic group (uninjured control, TBI+BEC (untreated), and TBI+BEC (treated)). In LTP analyses, the repeated measures factor was time relative to application of the high-frequency stimulation (theta-burst), and in PPF analyses the repeated measures factor was interpulse interval. Contrasts between specific groups were evaluated using simple effects based on planned comparisons (Keppel, 1991; Levine, 1991).

For behavioral measures, group means were first analyzed using ANOVA, with specific group differences evaluated using the Fisher Least Significant Difference test. A probability of less than 0.05 was considered statistically significant for all experiments. All results are reported as mean $\pm$ SEM.

RESULTS

Physiological Measurements

During surgical preparation and lesioning, all animals were monitored for heart rate (350 ± 20bpm), arterial oxygen saturation (≥ 93%), breath rate (45 ± 5bpm), pulse distention (15 ± 5µm), and breath distention (12 ± 5µm) with pulse oximeter (MouseOx; Starr Life Sciences, Oakmont, PA). Surgical procedures on all experimental animals produced no significant change in these physiological measures.

Western blot analysis

Effect of MMP Inhibition on MT5-MMP, ADAM-10 and N-cadherin Protein Expression

In order to test the effect of MMP inhibition on MT5-MMP, ADAM-10 and N-cadherin expression during the period of synapse stabilization, we sampled hippocampal protein extracts at 15d postinjury. We specifically targeted GM6001 treatment at the 6-7d postinjury interval to affect the period when enzyme levels are highest and N-cadherin substrate decreased. The primary 80 kDa MT5-MMP expression at 15d was neither significantly affected by GM6001 treatment when compared with injured vehicle cases, nor was it different from sham-injured controls (104.55 ± 9.75, p=0.65) (Fig. 3.1). These results suggest that MT5-MMP protein expression was not a major player at 15d postinjury, consistent with our prior Western blot results. However, we did observe a significant drug effect on active 70 kDa ADAM-10 protein expression at 15d postinjury relative to injured-untreated animals (Fig. 3.1). Injured-untreated cases showed an increase (230.78 ±30.41, $p<0.001$), while injured-treated cases were not different from controls (109.74 ±14.86, p=0.64). Further, when

injured-untreated and injured-treated were directly compared, there was a 48% reduction in 70 kDa ADAM-10 following GM6001 which proved to be significant ($p<0.01$). While 15d full length N-cadherin (130 kDa) within the injured groups was not different from sham-injured controls ($p=0.15$), GM6001 treatment significantly elevated 130 kDa N-cadherin in the injured-treated animals when compared with the injured-vehicle cases at 15d (injured-untreated: 88.69 $\pm$ 5.47 $p=0.24$; injured-treated: 122.29 $\pm$ 12.87; $p<0.05$) (Fig. 3.1). Notably, the relative expression of MT5-MMP, ADAM-10 and N-cadherin in the GM6001 treated TBI+BEC cases was now similar to that seen at 15d following UEC, shifting the profile toward that present during adaptive synaptic plasticity.

Further, these results show that GM6001 administration at the time of sprouting and synapse formation selectively affects ADAM-10 during synapse stabilization phases of synaptogenesis. Moreover, significant increase in N-cadherin after GM6001 treatment supports a direct enzyme/substrate interaction between ADAM-10 and N-cadherin during this synapse stabilization.

Blot signal for the additional forms of MT5-MMP (85 kDa), ADAM-10 (100 kDa, 80 kDa) and the 40 kDa N-cadherin fragment following GM6001 treatment was not different from that of the injured-vehicle group at 15d postinjury (data not shown). These results indicate that MMP inhibition did not affect the expression of these additional forms of MT5-MMP, ADAM-10 and N-cadherin.

Figure 3.1 Comparison of MT5-MMP, ADAM-10 and N-cadherin Hippocampal Protein Expression in TBI+BEC-untreated and TBI+BEC GM6001-treated animals at 15d. Values expressed as percent of sham controls. GM6001 treatment at 6 and 7d postinjury significantly decreased ADAM-10 and increased N-cadherin protein expression relative to injured-untreated group when measured at 15d.There was no change noted between groups for MT5-MMP (MT5) expression. Representative blots shown below. I=Injured; S=Sham (control); Injured-Vehicle n=7-8, Injured-Treated n=6, Sham n=8; *p<0.05, **p<0.01

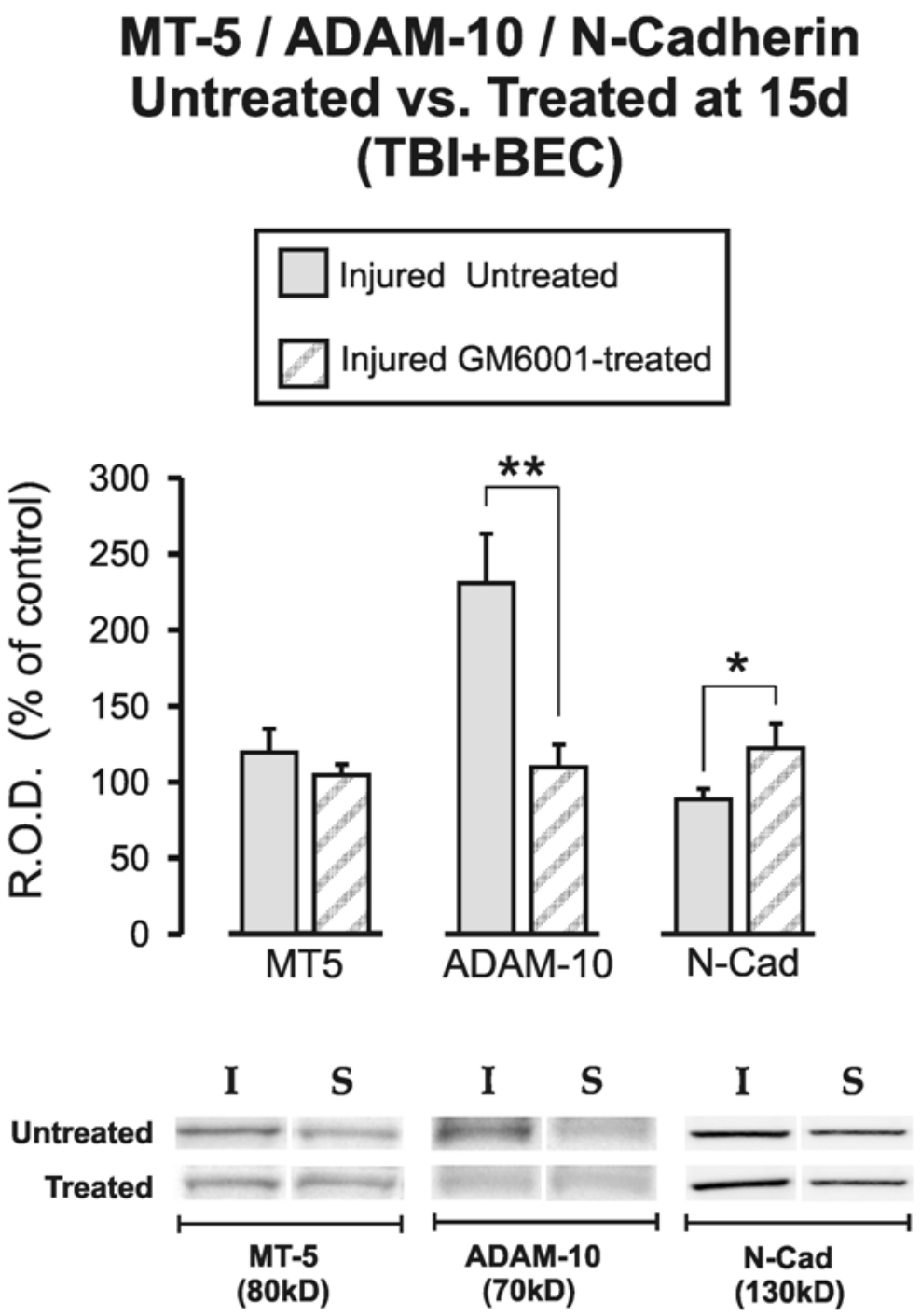

Electrophysiology

Effect of MMP Inhibition on Long-Term Potentiation and Long-Term Depression

Application of the theta-burst high-frequency stimulation (HFS) generally elevated fEPSP slopes during the 60 minute post-HFS period. Example evoked waveforms from each group are shown in Fig. 3.2, illustrating potentials acquired during pre-HFS baseline period, and during the post-conditioning period. Also illustrated is the fEPSP measurement, taken early in the downstroke of the fEPSP. In comparison to fEPSP measurements based on peak amplitude, a slope measurement early in the fEPSP waveform is less affected by population spikes. As indicated in Fig. 3.2, the standardized current intensity (50% of maximum, based on input-output functions) evoked moderate fEPSP waveforms, having small population spikes, or lacking them altogether. After HFS, the evoked fEPSPs often developed large population spikes (see example, marked 'p.s.' in Fig. 3.2). Within the LTP literature, there is a widespread agreement that the 'early-slope' measurement approach reflects current fluxes initiated by the population EPSP, prior to contamination by target cell discharges.

Figure 3.2 Representative field potentials evoked in the Schaffer collateral afferent input to CA1. Traces are shown from a sham control rat, from a TBI+BEC (vehicle) rat, and from a TBI+BEC (GM6001-treated) rat. A sample waveform is shown during the baseline recording period, prior to the application of high frequency stimulation (HFS) used to induce LTP, and from 10 min and 60 min after HFS. Within each row stimulus current was held constant. The method of measuring the initial fEPSP slope is illustrated in two of the baseline waveforms. In addition to usually increasing fEPSP slope, HFS often also induced a population spike (p.s.) which persisted during the post-HFS recording period

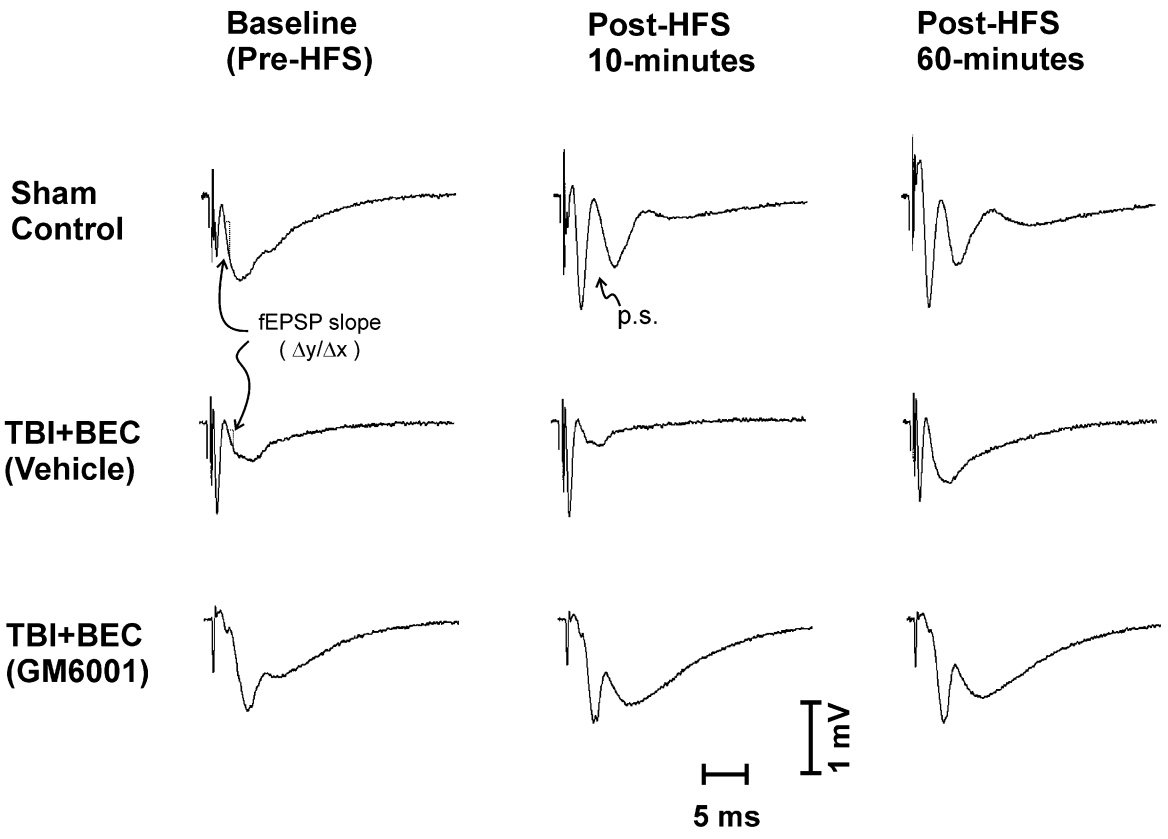

In uninjured control rats, the HFS trains induced a significant 58.0±8.6% increase in fEPSP slope, when averaged across the 60 minute post-HFS monitoring period ($p<0.001$). However, as measured at 15 d after the TBI+BEC injury, LTP was weak and quite variable. Again averaging across 0-60 minutes post-HFS, the TBI+BEC (untreated) group exhibited a 36.1±15.5% elevation of fEPSP slope, but this narrowly missed significance ($p=0.077$). In contrast HFS induced a significant 45.8±10.8% average increase in TBI+BEC (treated) rats ($p<0.01$). Figure 3.3 panel A shows, mean fEPSP slope measurements, normalized to pre-HFS baseline, for each group. These results indicated that the HFS was effective in inducing a functional plasticity: a significant 58% and 46% enhancement for controls and injured-treated rats, respectively, and a (non significant) 36% change in injured-untreated rats. A separate issue was whether these magnitudes of LTP were statistically different among the three groups. As a first approach to this question, we analyzed whether the mean fEPSP, averaged over entire 60 minutes of post-HFS monitoring, was significantly different among the three groups. This analysis indicated that there were no statistically significant differences among any of the three groups ($p=0.198$), probably due to the highly variable responses in rats subjected to TBI+BEC.

Figure 3.3 Effects of TBI+BEC injury and GM6001 treatment on LTP and LTD. (A)**.** Rats with TBI+BEC injuries showed weak and highly variable LTP, significantly below control levels during the first 15 minutes post-conditioning (Period 1 (P1) interval). Time of application of high-frequency stimulus (HFS) trains is marked with filled arrow. Injured rats treated with GM6001 exhibited a level of LTP intermediate between the control and injured-untreated groups. LTD (induction time marked with open arrow) was not significantly altered by injury or GM6001 treatment.). For clarity data points are averages of 2-minute epochs. (B) Mean level of LTP was significantly suppressed in injured rats from 0-15 min post-HFS ($p<0.05$). LTP in GM6001-treated rats was not different from control levels. No significant injury or drug effects were observed from 16-60 minutes post-HFS (P2).

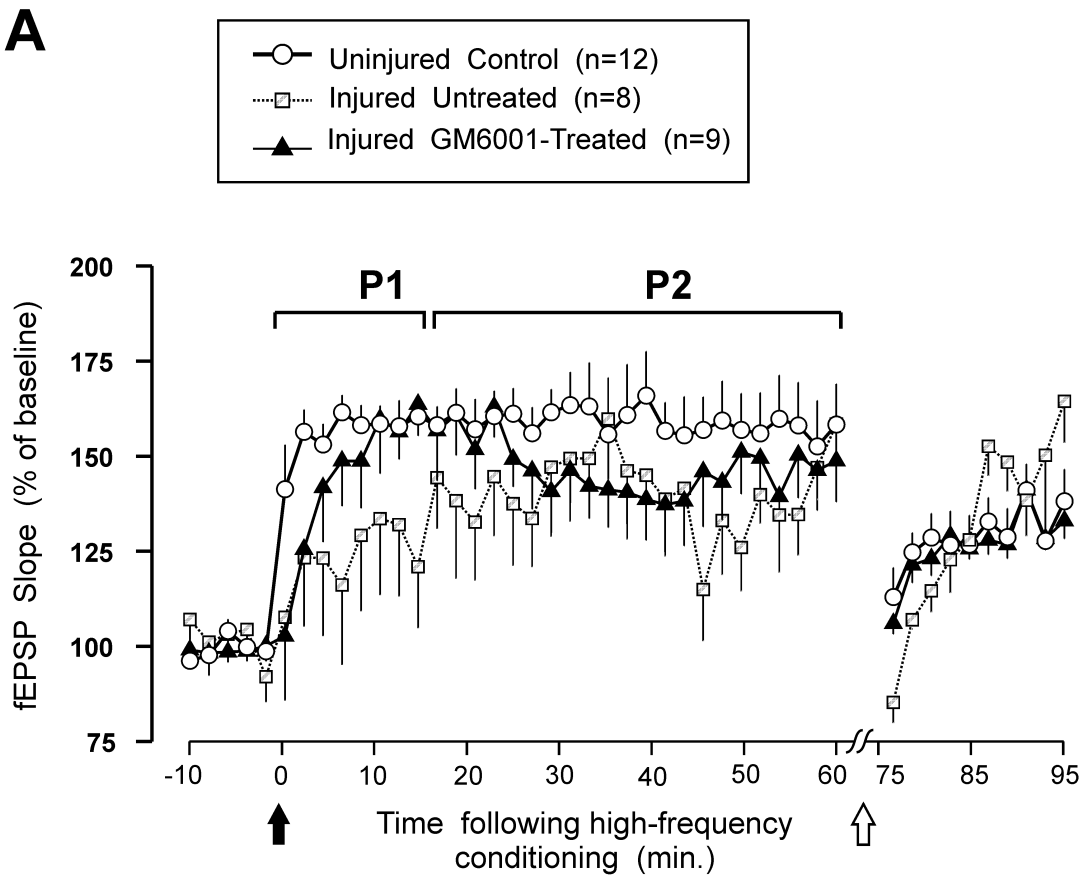

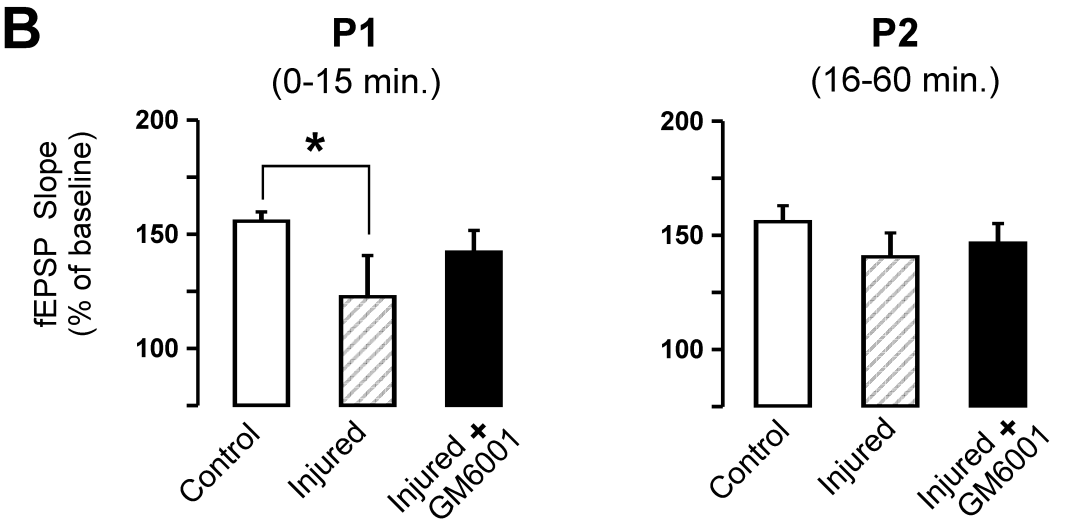

Inspection of Figure 3.3 panel A, suggested a possible systematic difference among groups during the first 15 minutes post-HFS. Specifically, the rate of post-HFS response increases in the injured-untreated group tended to be retarded in comparison to the control and to injured-treated groups. Accordingly, analyses were also conducted separately for this early period (Period 1 = 0-15 minutes post-HFS), and for P2=16-60 minutes post-HFS. While this division is arbitrary, for theoretical reasons it is useful to explore indications that injury or drug treatments may preferentially impact activity-dependent plasticity at early stages. For example, and as discussed below, molecular cascades and structural modifications, initiated by HFS, may be quite labile during the early phases of plasticity, and especially susceptible to neuropathological conditions during this time. Analyses targeted at period P1, revealed that the average LTP induced in TBI+BEC (untreated) rats was significantly below that of uninjured control rats ($p<0.05$) (see Figure 3.3 panel B). In contrast, during this same interval (0-15 minutes post HFS) the level of LTP in TBI+BEC (treated) rats was not different from uninjured controls ($p=0.183$), or from TBI+BEC (untreated) rats ($p=0.323$). To the extent that a significant effect of injury was only observed in the TBI+BEC (untreated), and not in the TBI+BEC (treated), groups, these results are consistent with a neuroprotective effect of GM6001 on LTP induction under these injury conditions. However, any neuroprotective benefit was limited to this early interval, because no statistically significant differences were noted among the groups during 16-60 minutes post-HFS (see Figure 3.3 panel B).

Although application of the low-frequency (1 Hz) stimulation appeared to induce some degree of long-term depression (LTD), the mean fEPSP slopes in all groups

trended back to the potentiated level during the 20 minutes of LTD monitoring (75-95 minutes in Figure 3.3 panel A). Although the TBI+BEC (untreated) group exhibited an especially unstable pattern during this interval, statistical analyses did not reveal any significant between-group differences of mean fEPSP slopes, induced by the LTD procedure.

Effect of MMP Inhibition on Paired-Pulse Facilitation

Studies of LTP have documented the involvement of multiple postsynaptic mechanisms including specific kinase activities, translocation and modification of AMPA receptors, morphological changes to spines and postsynaptic densities, protein synthesis, and gene activation. Less evidence has accumulated for a presynaptic role in LTP induction (e.g., reviewed by Malenka and Bear, 2004), although important questions remain in this area. Because N-cadherin participates in the linkage and stabilization of presynaptic terminals with postsynaptic structures, it is useful to consider if TBI+BEC injury, and GM6001 treatment, alter presynaptic functional plasticity in a manner comparable to their effects on LTP. To approach this issue we also implemented the paired-pulse facilitation (PPF) procedure. While a postsynaptic role in this form of short-term plasticity cannot be entirely ruled out, there is a substantial consensus that, using low levels of stimulus current as presently implemented, PPF is *predominantly* mediated presynaptically. Multiple authors have interpreted the augmentation of the second response to reflect residual Ca^{2+} loaded into presynaptic terminals during the first response (Lomo, 1971; Creager et al., 1980; Zucker, 1989; Leung and Fu, 1994).

In the present study, all groups showed a similar pattern of responses to the paired stimulus presentations. An example set of paired fEPSPs, obtained from a control rat, are shown in Fig. 3.4 panel A. Note the similar amplitude and waveform of the first field potential in each pair. This was expected because 30 seconds were allowed to pass between each paired pulse presentation. This permitted a recovery of the ionic status of the presynaptic compartment, presumably including a return of intracellular calcium to basal levels. Note also that the amplitude and waveform of the second field potential in each pair were contingent on the interpulse interval, with the greatest augmentation of $fEPSP_2$ seen at an interval of 50 msec. Stimulus currents were held constant during this procedure, set individually for each slice to ensure that $fEPSP_1$ was stimulated below the threshold for a population spike. However, it was commonly observed that a population spike was visible in $fEPSP_2$, especially at 50 and 100 msec intervals (see example 'p.s.' in Fig. 3.4 panel A).

At interpulse intervals of 50 msec, $fEPSP_2$ was elevated over $fEPSP_1$ by an average of 69.55$\pm$7.30%, for all slices tested. The mean magnitude of PPF, at the 50 msec interpulse interval, ranged from 81.92$\pm$13.82% (injured untreated) to 59.47$\pm$14.52% (injured-treated), with controls showing an intermediate 67.24$\pm$9.46%. However, these differences did not reach statistical significance. All groups showed the predicted pattern of decreased PPF as interpulse interval was increased to 100, and then to 150 msec (Fig. 3.4 panel B). However, the same lack of statistically significant group differences were noted also at these longer intervals, with overall PPF magnitudes of 51.69% and 33.16% observed at 100 and 150 msec, respectively. Taken together, analysis of the PPF data indicated that neither the TBI+BEC injury nor

Figure 3.4 Effects of TBI+BEC injury and GM6001 treatment on PPF. (A) Representative paired-pulse waveforms for interpulse intervals 50, 100, and 150 msec, from a sham-injured control rat. Dotted portion of waves abbreviates period between evoked responses. In the PPF protocol, stimulus current is set below threshold for population spikes (first response in each pair). Characteristically, the second response is augmented (steeper descent of fEPSP), and a population spike is often induced at interpulse intervals of 50 or 100 msec (p.s. in example). (B) Mean paired-pulse ratios (fEPSP2 / fEPSP1) for the analytic groups exhibited similar decreases as interpulse interval was increased from 50 to 150 msec. Neither the TBI+BEC injury, nor the GM6001 treatment, was associated with a statistically significant effect on PPF

A

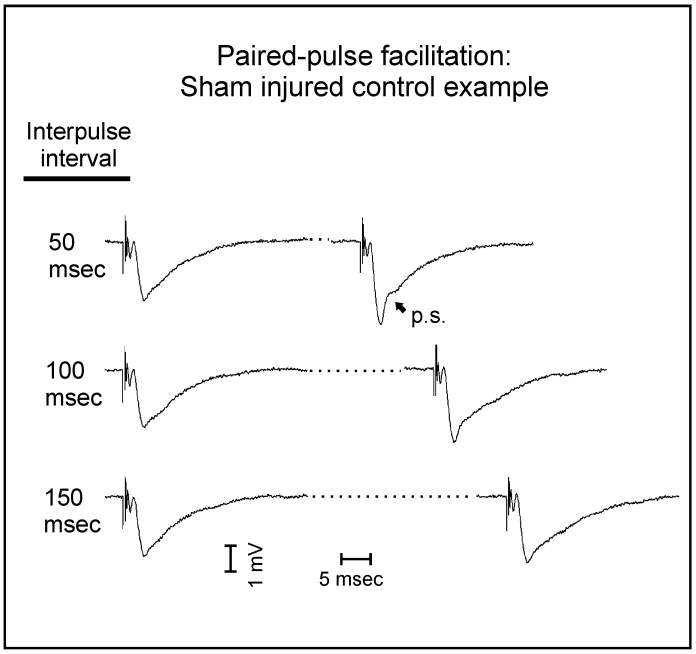

B

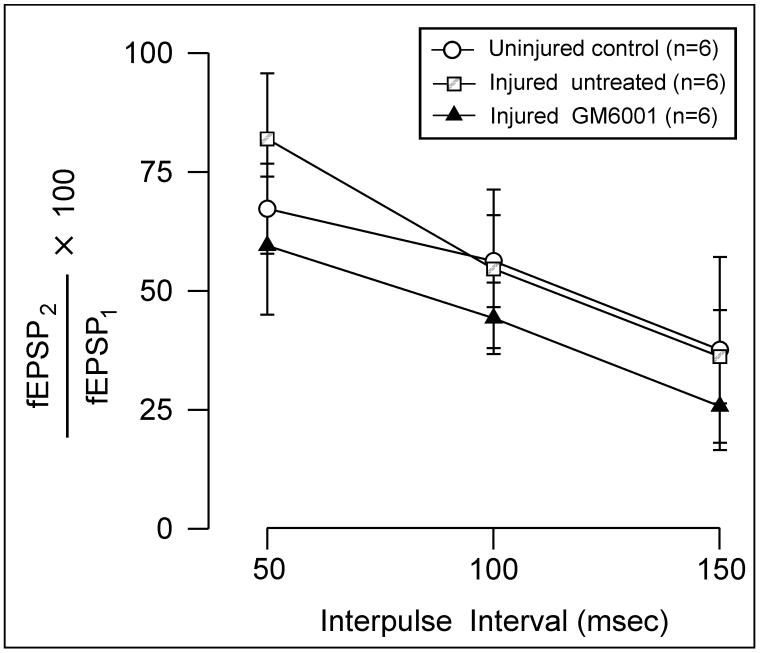

the GM6001 compound significantly altered this form of short-term plasticity (p=0.482).

Morris Water Maze Testing

MMP Inhibition and Cognitive Behavioral Outcome

Cognitive performance of injured-untreated and injured-treated animals was assessed at 12-15d postinjury using the Morris Water Maze (Morris et al., 1981) task (Fig. 3.5). Group latencies (measured in seconds) to locate the hidden platform were analyzed using ANOVA, which revealed significant differences in main effect of group ($p<0.001$). Following ANOVA analysis Fisher Least Significant Difference (LSD) tests were conducted to determine specific group differences. Post Hoc analysis using the Fisher LSD test indicated significant differences between injured-untreated and sham groups, as well as between injured-treated and sham groups ($p<0.001$). GM6001 treatment at 6-7d postinjury failed to produce significant differences in performance between the injured-untreated and injured-treated groups ($p=.294$). These results indicate that the GM6001 dosing used in this study, while altering ADAM-10 and N-cadherin expression and affecting the induction of LTP, did not significantly improve spatial memory deficits associated with maladaptive plasticity.

Figure 3.5 Effect of TBI+BEC injury and MMP Inhibition on Cognitive Recovery. Spatial learning and memory was assessed using the Morris Water Maze task. Pre-trained sham-injured (open circle), injured-vehicle (black square) and injured-treated (gray triangle) groups underwent testing on days 12-15 postinjury. Average latency to goal scores (measured in seconds) for each group are presented across postinjury testing days. Injured-vehicle and injured-treated animals displayed significantly longer latency to goal times when compared to sham-injured animals at all postinjury day intervals, indicating an injury effect. However, MMP inhibition by GM6001 treatment (i.p., 10 mg/kg, 6 and 7d postinjury) did not improve cognitive recovery in the injured-treated group when compared to sham control. $p<0.001$.

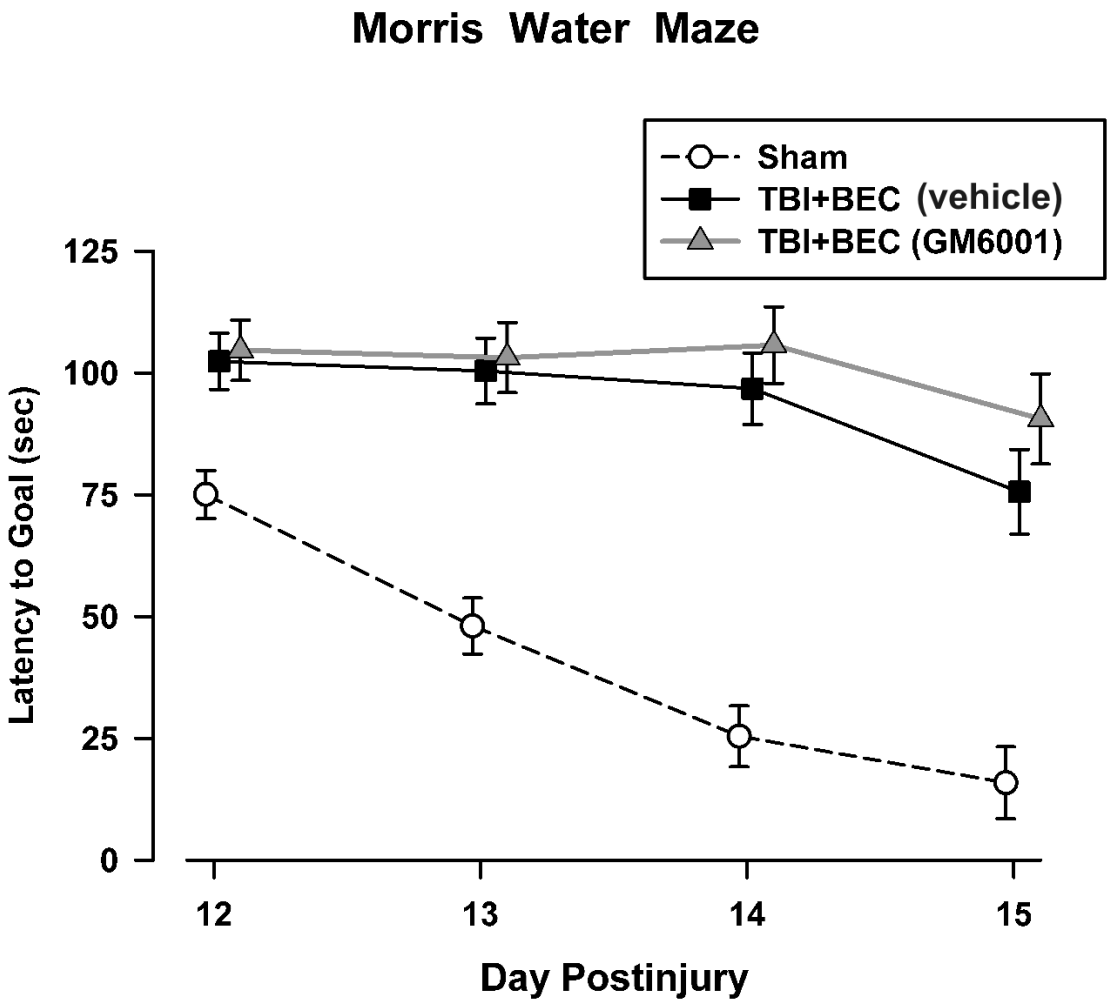

Ultrastructural Analysis

MMP Inhibition and Hippocampal Synaptic Structure

Following MWM assessment, a subset of15d postinjury untreated and GM6001 treated animals were prepared for ultrastructural analysis. Qualitative observations of ultrathin sections from both dentate gyrus molecular layer and CA1 stratum radiatum revealed differences in dendritic and synaptic cytoarchitecture between the two groups. Injured-untreated animals showed evidence of persistent hippocampal dendritic and synaptic pathology (Fig. 3.6). Their dendrites were of small diameter, irregular in form and often containing disrupted cytoskeleton. Synapses appeared immature, with thinned post-synaptic densities and atypically large separation at the synaptic cleft. In contrast, GM6001 treated animals displayed dendritic and synaptic cytoarchitecture more consistent with control 15d postinjury cases. Overall, treated cases appeared to have larger diameter dendrites, with intact cytoskeletal networks. Synaptic profiles revealed well-developed junctions, with mature pre-and post-synaptic organization. Although qualitative in nature, these observations do suggest that MMP inhibition during the initiation of sprouting and synapse formation can foster a shift toward the generation of normal synaptic structure in a model of maladaptive synaptic recovery. While these observations do not follow the absence of GM6001 effect on cognitive outcome, they do compliment our 15d protein and electrophysiological analyses, which show that the MMP inhibitor increases expression of the neuronal adhesion molecule N-cadherin and elicits a reversal of field potential deficits during the induction of LTP.

Figure 3.6 Effect of TBI+BEC injury and GM6001 Treatment on Dendritic and Synaptic Cytoarchitecture at 15d. Ultrastructural profiles of the dentate molecular layer and hippocampal CA1 stratum radiatum following vehicle (A/C) or GM6001 (B/D) treatment. Qualitative assessment of GM6001 cases (B/D) suggest increased dendritic integrity, with larger diameters and more intact cytoskeleton. Synapses appeared more frequently and had normal structural organization (see inset arrows) when compared to vehicle (A/C). The GM6001 profile is consistent with our 15d observations of increased expression of N-cadherin and partial restoration of CA1 LTP following MMP inhibition. Bar = 2µm.

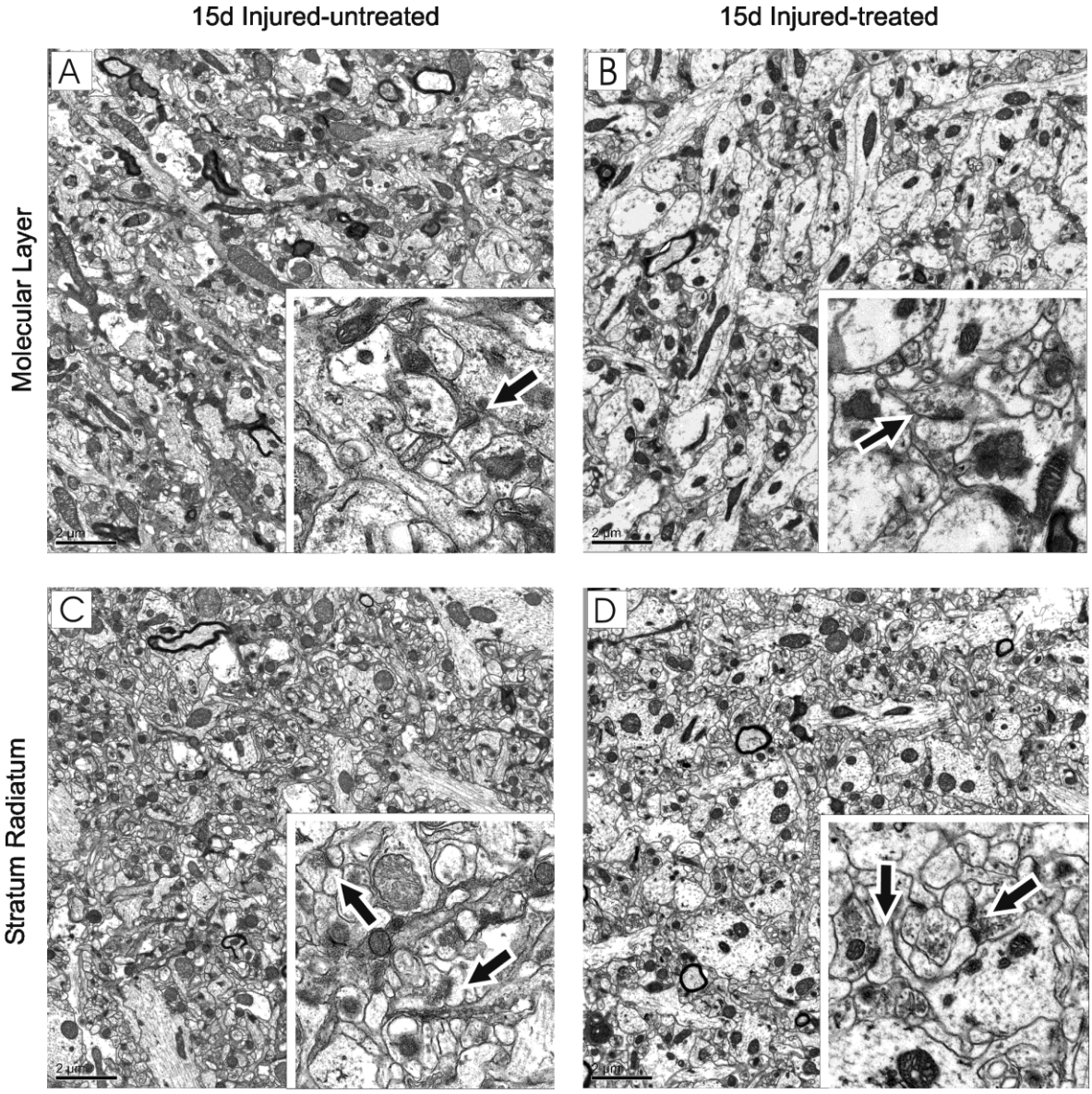

DISCUSSION

The current study examined the effects of MMP inhibition on MT5-MMP, ADAM-10, and N-cadherin protein expression, synaptic function, synapse cytoarchitecture and cognitive recovery in the TBI+BEC model of maladaptive plasticity. Following injury, the broad-spectrum MMP inhibitor GM6001 was administered on days 6 and 7 postinjury, targeting both the onset of synaptic reorganization and the period of most elevated MT5-MMP and ADAM-10 expression. Assessment of drug effect was made by comparing injured-treated and injured-vehicle animals at 15d survival, when stabilization of regenerated synapses begins. Our results showed that GM6001 treatment produced the following: 1) a reduction in ADAM-10 and increase in N-cadherin hippocampal protein expression, generating a profile similar to that found at 15d post-UEC, 2) an enhancement of synaptic efficacy, evidenced by effects on the early induction phase of LTP, and 3) improved structural reorganization of dendritic and synaptic cytoarchitecture. In the present experimental design, GM6001 MMP inhibition failed to produce improvement in cognitive performance. Collectively, this study provides evidence that targeted MMP inhibition promotes a more adaptive environment for reactive synaptogenesis, thereby improving postinjury recovery in the maladaptive condition. In following sections, we will discuss how these results support a prominent role for membrane bound MMPs and N-cadherin in the enhancement of functional and structural synaptic recovery.

MMP Inhibition and Protein Expression

Western blot (WB) analysis at 15d postinjury, the onset of synapse stabilization, revealed that MMP inhibition produced differences in hippocampal ADAM-10 and N-cadherin protein expression. When injured-treated and injured-vehicle groups were compared, drug treatment significantly decreased ADAM-10 protein by 48%, while N-cadherin was significantly elevated by 38%. This resulted in a pattern of relative expression which matched that of the adaptive UEC described in the previous chapter, supporting the hypothesis that appropriate balance of MMP/substrate interaction is key to the final stabilization of regenerated synapses. While we have studied the effects of other MMP inhibitors (e.g., FN-439) on behavioral and structural outcome in the combined model (Falo et al., 2006), this is the first study to show that MMP inhibition has a direct effect on the expression of membrane bound MMPs and N-cadherin during the stabilization phase of synaptogenesis. These results are also consistent with prior studies in our laboratory which show that manipulation of recovery in the combined model alters the expression of MMPs. For example, postinjury administration of the NMDA antagonist MK-801 significantly reduced MMP-2 activity and MMP-3 protein expression (Phillips and Reeves, 2001; Falo et al., 2006).

Our WB results also revealed differential effects of GM6001 on the two membrane bound MMPs. Here, MMP inhibition failed to affect the TIMP-2 bound MT5-MMP protein expression at 15d post-TBI+BEC. This result might be explained by the fact that a majority of MT5-MMP signal was seen at 80 kDa, consistent with TIMP-2/MT5-MMP binding at the catalytic site, likely in the context of proMMP-2 activation. This arrangement would then act to hinder GM6001 binding and inhibition. While MT5-

MMP protein expression remained unchanged at 15d, our current interpretation of MT5-MMP response is supported by prior findings showing shifts in hippocampal MMP-2 protein after TBI+BEC, similar to our observed MT5-MMP changes (Phillips and Reeves, 2001). Based on the concomitant elevation MT5-MMP and MMP-2 at 2-7d postinjury, targeting earlier time points for MMP inhibition of MMP-2 would be warranted to provide further evidence for this proposed relationship, as well as further delineate specific MMP role in postinjury recovery. Taken together, these data support our proposed role for MT5-MMP as an activator of proMMP-2 during the earlier phases of injury-induced synaptogenesis. Our WB results show that MMP inhibition can significantly affect protein expression following injury in a TBI model of maladaptive plasticity, and promote a molecular environment similar to that found with adaptive plasticity.

One important consideration for interpretation of our results would be how inhibition of MMP activity leads to changes in protein expression following injury. Postinjury MMP inhibition may influence protein expression by reducing the capacity for MMPs to modify ECM and cell to cell connections. Such modification would affect the initiation of a number of signaling pathways which regulate cell survival and death, often through altering gene transcription and protein translation. In the context of this study, persistent ADAM-10 lysis of synaptic N-cadherin between 7-15d postinjury may be linked to *anoikis*, or cell death by loss of cell anchorage (Grossman, 2002). Inhibition of this ADAM-10 activity would reduce cleavage of synaptic N-cadherin, maintain synaptic contact, attenuate loss of anchorage, and potentially allow for a more stable transcriptional regulation of ADAM-10 and N-cadherin expression in surviving cells.

Inhibition of MMPs has also been shown to decrease downstream neuronal degeneration and improve recovery in other neurotrauma models, potentially by limiting excessive loss of cell anchorage and preventing *anoikis* (Ashi et al., 2000; Wang and Tsirka, 2005; Zhao et al., 2006; Sifringer et al., 2007). Additionally, injury-induced alteration of ECM and cell to cell connections can provide feed forward signals that influence downstream pathways within the cell and lead to MMP upregulation (Conant and Gottschall, 2005). For example, post-ischemic alterations of hippocampal ECM-cell contacts have been shown to trigger intracellular signaling by protein focal adhesion kinase, $pp125^{FAK}$, which leads to upregulation of MMP-2 and -9 (Zalewska et al, 2003). Potentially, increased MMP expression may lead to continued alteration in ECM/cell interaction, activation of these signaling pathways, and further MMP upregulation. In the context of our Chapter 2 results, this endogenous feedback mechanism may have mediated the injury-induced increases in active ADAM-10 expression that were observed over the postinjury time course. Therefore, postinjury inhibition of MMP activity may further decrease ECM/cell alterations, thereby limiting the effects of downstream signaling through such pathways. This may explain our observations that GM6001 decreased ADAM-10 protein expression at 15d postinjury. Finally, MMP inhibition may influence N-cadherin expression through β-catenin, which can indirectly decrease N-cadherin protein upon its release from the cadherin/catenin complex and subsequent nuclear translocation to act as a transcription factor (McCusker, 2009). Our results suggest that MMP inhibition may help to maintain β-catenin submembrane binding in the cadherin/catenin complex, therefore limiting its release to affect a down regulation of N-cadherin. The result would be enhanced synapse stabilization. While

MMP inhibitors are designed to limit protease activity, our results provide further evidence they can also influence the process of injury-induced synaptogenesis through downstream regulation of the expression of plasticity-associated proteins, and therefore improve recovery.

MMP Inhibition and Synaptic Functional Recovery

In order to examine the effect of MMP inhibition on recovery of synaptic function we conducted a series of *in vitro* electrophysiological experiments including assessment of LTP, LTD and PPF. We chose to record the synaptic response in CA1 stratum radiatum following Schaffer Collateral fiber stimulation. This choice was made for two reasons: 1) the absence of a homotypic perforant path projection in the combined animals subjected to BEC insult and 2) the presence of synaptic reorganization in CA1 dendrites following cFPI alone. Results from these experiments showed an injury effect on the capacity for LTP during the first 15 minutes (P1) following conditioning stimulus. These experiments were the first *in vitro* assessment of LTP, LTD and PPF in the TBI+BEC model and were consistent with our prior *in vivo* studies showing persistent deficits in the capacity to elicit LTP up to 15d postinjury (Reeves et al., 1997). A key finding in the present electrophysiological assessments was that the GM6001 treatment partially restored the injury-induced LTP deficit noted in the first 15 minutes post-conditioning. This suggests that dampening of MMP activity during the 6-7d period of sprouting and synapse formation can improve synaptic function in the context of maladaptive plasticity. While this was the first investigation to examine the effects of MMP inhibition on TBI+BEC synaptic efficacy, the consequences of postinjury MMP inhibition on synaptic function have been examined in the UEC model of adaptive

plasticity. In that study, the MMP inhibitor FN-439 was applied at 30 min after lesion and outcome assessed at 7d postinjury (Reeves et al., 2003). Results showed a reduced capacity to elicit LTP and aberrant spatial reorganization of synapses along deafferented dendrites when compared to vehicle controls. In contrast to MMP inhibition at 7d, the latter study suggests that acute inhibition of MMPs during the degenerative phase of synaptogenesis can reduce functional recovery, even within an adaptive environment. Similarly, non-injured (naïve) hippocampal slices treated with FN-439 failed to produce LTP induction and maintenance, further suggesting that inhibition of MMPs under normal conditions is also detrimental (Meighan et al., 2007). Thus, our collective data support a key role for MMPs in shaping the environment around reorganizing synapses to foster their growth, as well as support stabilization for synaptic efficacy in the new circuits generated. The findings also clarify the requirement for increased MMP activity during the more acute postinjury periods and the subsequent attenuation of this activity as synapses mature and regain their functional status.

In addition to LTP, we also investigated the effect of GM6001 treatment on LTD and PPF. Despite observing significant changes in LTP, we found no group differences in LTD and PPF measurements. Interestingly, PPF abnormalities have been observed within the central (Reeves et al., 2000) and lateral (Cao et al., 2006) fluid percussion (cFPI, lFPI), persisting for up to seven to nine days postinjury, respectively. Such model differences show that pathophysiological processes influencing pre-synaptic plasticity are altered when cFPI is combined with targeted deafferentation in the TBI+BEC model. This result provides further support for our hypothesis that neuroexcitation insult and deafferentation are interactive in the context of maladaptive synaptic reorganization.

Collectively, these electrophysiological data suggest that postsynaptic vulnerability may be a preferential contributor to deficits in synaptic efficacy following TBI+BEC. Further, by documenting that these deficits can be attenuated with MMP inhibition, we provide support for the hypothesis that MMPs and their synaptic substrates participate in the recovery of functional synapses following TBI.

The current LTP findings with GM6001 treatment point to several possible mechanisms by which MMPs might affect functional recovery during reactive synaptogenesis. One such LTP-associated synaptic mechanism may involve the adhesive and stabilization roles of N-cadherin. N-cadherin functions extracellularly to bind pre- and post-synaptic elements and establishing intracellular connections to stabilize the synapse and permit efficient function (Takeichi and Abe, 2005). Pre- and post-synaptic adhesion is essential for synaptic growth, maturation and resistance to disassembly (Bozdogi et al., 2004). Based on these roles, N-cadherin is linked to synapse potentiation and plasticity during early and late LTP (E-LTP, L-LTP), where *in vitro* blocking N-cadherin results in the failure to produce LTP induction and/or maintenance (Tang et al., 1998; Bozdogi et al., 2000). The current study shows that MMP inhibition mediates increased N-cadherin expression and attenuates E-LTP induction deficits at 15d after TBI+BEC insult. All LTP monitoring conducted in this study, and certainly the P1 period, would fall within the E-LTP phase which may last for ~1 to 3 h (Blitzer et al., 2005). Recall that, following GM6001 treatment 15d N-cadherin protein expression in TBI+BEC is very similar to what was seen at that time interval after UEC, a period which represents the onset of the synaptic stabilization. Similar levels of N-cadherin protein in these two groups suggests the potential for similar

maturation and stabilization of hippocampal synapses. Therefore, N-cadherin may directly influence the successful synapse stabilization or synaptic efficacy during E-LTP.

An additional N-cadherin associated mechanism that may be enhanced by MMP inhibition involves modification of the post-synaptic density (PSD) during E-LTP. E-LTP does not require new protein synthesis, but rather, relies on modification and re-organization of existing synapses using available stored proteins (Malenka and Bear, 2004; Issac et al., 1995; Liao et al., 1995). Modifications made to existing synapses include the trafficking and placement of additional AMPA receptors into the PSD, which is regulated by N-cadherin in cultured neurons, therefore indicating a link between structural and functional plasticity (Bredt and Nicoll, 2003; Malenka and Nicoll, 1999; Nuriya and Huganir, 2006). Based on current literature, the interaction between AMPA receptors and N-cadherin appears to enhance synaptic efficacy as measured by LTP. Our finding of functional improvement, associated with increased hippocampal N-cadherin following GM6001 treatment, would be consistent with prior reports of an N-cadherin role in receptor and PSD stabilization. A preservation of N-cadherin function, after GM6001 treatment, conceivably permitted enhanced synaptic transmission and LTP-associated plasticity in our maladaptive model.

In addition to its role in post-synaptic density organization and function, N-cadherin affects synaptic Ca^{2+} conductance through other binding partners at the synapse. In the previous chapter, we provided evidence that MMP lysis of the N-cadherin extracellular domain mediates the cleavage and release of an intracellular ~35-40 kDa cytoplasmic tail fragment-1 (CTF1). This 40 kDa N-cadherin fragment was detected in both the UEC and TBI+BEC models. Although we did not find significant

change in this fragment with GM6001 treatment, it is important to consider its possible influence on Ca^{2+} conductance on synaptic function. The intracellular release of CTF1 can indirectly affect Ca^{2+} conductance by interacting with one of its binding partners, p120 catenin, which subsequently releases and activates RhoA. Through interaction with myosin-actin cytoskeleton, soluble, active RhoA ultimately decreases synaptic Ca^{2+} influx through action on voltage activated Ca^{2+} channels (VACC) (Marrs et al., 2009). Therefore, extensive lysis of N-cadherin by a persistently activated ADAM-10 can serve as an upstream mediator of RhoA signaling, leading to decreased Ca^{2+} conductance and attenuated synaptic efficacy. Our LTP results suggest that MMP inhibition may limit N-cadherin cleavage, thereby preventing RhoA driven decrease in synaptic Ca2+ influx, and decreasing the injury-induced deficits seen during P1 of our LTP trials. Although the exact mechanism(s) are yet to be established, the relationship between N-cadherin and synaptic function is well established and further supported by our present molecular and electrophysiological data.

MMP Inhibition and Cognitive Recovery

One of the principal concerns following TBI is the presence of persistent cognitive impairment. To study the effect of MMP inhibition on cognitive recovery following injury, we used the Morris Water Maze (MWM) task, which is a reliable and sensitive measurement of cognitive function following TBI (Hamm, 2001). In these experiments, we did find a significant injury effect on MWM performance during 12-15d postinjury trials. Impaired latency to find the goal platform in the injured-vehicle group was consistent with our published studies (Phillips et al., 1994; Phillips and Reeves, 2001; Falo et al., 2006). However, using the present GM6001 treatment paradigm we

were unable to detect a drug effect on MWM performance. These results are in contrast to a prior TBI+BEC study where the MMP inhibitor FN-439 showed improved spatial learning over a five day trial period, utilizing both acute (1-2d) and delayed (6-7d) treatment paradigms (Falo et al., 2006). It is interesting that both studies applied MMP inhibitor at 6-7d postinjury, but only FN-439 showed attenuation of cognitive deficits. Both GM6001 and FN-439 inhibit MMPs through a common mechanism of binding divalent ions critical to engaging the active site of the enzyme. They do, however, exhibit specificity for different MMP family members. The FN-439 compound targets collagenase, gelatinase and stromelysin, while GM6001 more broadly inhibits a wide range of MMPs, inclusive of the MT-MMP family group. This difference in specificity may account for the presence or absence of behavioral effects in the MWM test, which would suggest that more specific targeting of MMPs is a better approach than using a general profile inhibitor. Unfortunately, no such inhibitor targeting membrane bound MMPs has been developed to test this possibility.

Despite the challenges of inhibitor specificity, we did find a positive relationship between GM6001 treatment and the modest reversal of injury-induced deficits within the inductive phase of LTP. Since LTP may serve as a cellular model for learning and memory, and the MWM task tests functional aspects of memory, the emergence of a reversal in LTP deficit with MMP inhibition supports the interaction between MMP function and behavioral recovery. The failure to detect attenuation of MWM deficits in our experimental paradigm may indicate that a more careful dose/delivery study is needed. For example, shifting to intra ventricular rather than intra peritoneal would likely improve delivery and facilitate any drug effect on CNS structures. It is also

important to recognize that while the hippocampus is an essential structure for the processing of learning and memory, MWM tested behavior involves the coordination of multiple nervous system circuits.

MMP Inhibition and Synapto-Dendritic Reorganization

Finally, we examined the effect of MMP inhibition on synaptic ultrastructure in the stratum radiatum of the hippocampal CA1 field and the dentate molecular layer at 15d postinjury. Sampling from each area allowed us to compare dendritic and synaptic cytoarchitecture in the region subjected to electrophysiological recording, as well as the principal deafferented zone undergoing reactive synaptogenesis. In the injured-vehicle animals we found abnormalities in synaptic structure that were consistent with maladaptive plasticity as previously described for the TBI+BEC model (Phillips et al., 1994; Falo et al., 2006). For example, injured-vehicle animals exhibited damaged dendrites, as well as atrophied and disorganized synaptic profiles in both the stratum radiatum and outer molecular layer when compared to control tissue. These observations are consistent with our prior TBI+BEC studies showing persistent axo-dendritic pathology and abnormal synaptic reorganization at 15d postinjury (Phillips et al., 1994; Gordon et al., 1996; Phillips and Reeves, 2001; Falo et al., 2006). By contrast, injured-treated animals exhibited robust reorganization of synaptic structure, with larger, well organized supportive dendrites. Post synaptic densities were larger and more complex in structure, often abutting axon terminals with well-organized pre-synaptic vesicles at the membrane surface. Although we did not use quantitative methods for analysis, we did observe that synapses appeared to be more abundant following MMP inhibition. Similar cytoarchitectural changes in synapse structure have

been reported following TBI+BEC treatment with the MMP inhibitor FN-439 (Falo et al., 2006).

The synapto-dendritic reorganization described here provides a structural correlate to the positive effects of MMP inhibition on synaptic function and support MMPs as mediators of improved outcome under conditions of maladaptive plasticity. Our collective results suggest that such inhibition stabilized synaptic structure which contributes to improved induction of LTP and synaptic efficacy after TBI+BEC. Again, these structural improvements can be directly linked to the functional properties of N-cadherin at the synaptic interface. N-cadherin mediates specific post-synaptic density organization and synaptic stabilization through AMPA receptor placement and actin cytoskeleton anchorage, respectively, each of which support the capacity for LTP (Nuriya and Huganir, 2006; Togashi et al., 2002; Lilien et al., 1999). Quantitative EM analysis of CA1 dendrites in hippocampal slices transfected with mutated N-cadherin constructs also revealed significantly smaller dendritic spines and post-synaptic densities and reduced spine stability, further illustrating N-cadherin's role in synaptic structural organization (Mendez et al., 2010). Our results support a role for N-cadherin in structural synaptic recovery. They tie together elevated MMP activity, N-cadherin lytic fragment production and intracellular signaling to alter synapse structure during maladaptive plasticity. Importantly, MMP inhibition at the onset of this process appears to facilitate structural recovery by generating a more adaptive environment for synaptogenesis.

SUMMARY

We have shown that MMP inhibition at 6 and 7d postinjury significantly alters the expression of hippocampal ADAM-10 and N-cadherin protein at 15d survival in the TBI+BEC model of maladaptive plasticity. This inhibition shifted the expression of ADAM-10 and N-cadherin to the pattern seen during adaptive plasticity. Targeted MMP inhibition also reversed deficits in LTP induction and stabilized synapto-dendritic integrity. However, the same treatment paradigm had no effect on cognitive performance. While these results suggest that MMP inhibition during reactive synaptogenesis promotes structural and functional recovery, there are important limitations to be considered. Foremost, GM6001 is a broad-spectrum MMP inhibitor, affecting multiple soluble and membrane-bound MMPs. Although we were able to show that ADAM-10 expression was altered by GM6001 treatment, we did not provide evidence that its enzyme activity was blocked by the compound. Moreover, the effects observed could be due to inhibition of other MMPs as well. Therefore, for future studies it will be important to specifically target ADAM-10 or MMPs activated by MT5-MMP (e.g.-MMP2) in order to directly link these enzymes to adaptive synaptic recovery. Further investigation is also needed to better define the molecular mechanisms that regulate MT-MMP expression and activity, as well as identify the downstream effects of their proteolytic products on the process of reactive synaptogenesis.

Chapter 4

General Discussion

DISCUSSION

Summary of Results

Chapters 2 and 3 presented the protein and mRNA profiles of membrane-type MMPs, MT5-MMP and ADAM-10, along with a shared substrate N-cadherin, within adult rat hippocampus following TBI. Expression profiles were compared in two models of TBI, one exhibiting adaptive synaptic plasticity (UEC) and the other maladaptive synaptic plasticity (TBI+BEC). We also presented the effects of MMP inhibition on molecular, electrophysiological, behavioral and structural outcome at 15d following TBI+BEC. MMP inhibition targeted elevated MT5-MMP and ADAM-10 expression during the axonal sprouting and synapse formation period of synaptogenesis. Collectively, our results provide evidence that membrane-bound MMPs and their constitutive substrates (e.g.-N-cadherin, pro-MMP-2) are influence both adaptive and maladaptive plasticity in a time and injury-dependent manner. Inhibition of membrane-bound MMPs during maladaptive plasticity leads to change in their protein expression and improved outcome with respect to synaptic efficacy and structure. Therefore, targeted MMP inhibition has the potential to translate maladaptive plasticity into a more adaptive process, facilitating an improved recovery.

In Chapter 2, MT5-MMP, ADAM-10 and N-cadherin expression was shown to differ between adaptive and maladaptive models of TBI as a function of postinjury survival, suggesting that their role(s) in the process are temporally regulated. Comparison of model profiles shows that MT5-MMP plays a more acute role during the degenerative and regenerative phases (2 and 7d) of injury-induced synaptogenesis, potentially through interaction with TIMP-2 and activation of proMMP-2. Our results

suggest that ADAM-10 is the preferred protease targeting N-cadherin during the phase of synapse reorganization and stabilization (7 and 15d) postinjury. Protein analysis at 15d after TBI+BEC specifically showed a temporal correlation between a persistent increase of ADAM-10 and decreased N-cadherin expression, contrasting with the opposite pattern of expression in adaptive UEC plasticity. Changes in hippocampal protein expression in both models were consistent with the pattern seen using immunohistochemistry, where signal increase was greater over the deafferented dentate molecular layer (ML), principally within reactive astrocytes. These results suggest a role for reactive astrocytes in the synthesis and/or processing of MT5-MMP, ADAM-10 and N-cadherin following injury. Synthesis of MT5-MMP by reactive astrocytes is further supported by our preliminary 7d *in situ* hybridization results, showing MT5-MMP mRNA signal within reactive astrocytes of both adaptive and maladaptive models. Finally, microarray results suggested the greatest change in ADAM-10 transcript post-UEC and TBI+BEC, matching our maximally elevated WB ADAM-10 protein expression between 7-15d postinjury. Preliminary quantitative RT-PCR (qRT-PCR) analysis on the same 7d ML samples revealed elevated ADAM-10 mRNA in both models and decreased N-cadherin transcript post-TBI+BEC. These 7d changes in ML mRNA track with ADAM-10 and N-cadherin protein expression during maladaptive plasticity. Taken together, MT5-MMP, ADAM-10 and N-cadherin protein and mRNA profiles revealed time and recovery-dependent changes which were correlated with extent of recovery. Such results led us to investigate the effect of MMP inhibition on not only protein expression, but also synaptic structure and function post-TBI+BEC.

The results presented in Chapter 3 demonstrated that the significant effect of MMP inhibition on ADAM-10 and N-cadherin protein expression likely influenced improvements in synaptic structure and function at 15d post-TBI+BEC. MMP inhibition by GM6001 at 6 and 7d after TBI+BEC targeted the period with greatest elevation of MT5-MMP and ADAM-10 protein, as well as the onset of axonal sprouting and synaptic reorganization. Our results showed that MMP inhibition had no effect on 15d hippocampal MT5-MMP expression, but significantly decreased ADAM-10 and increased N-cadherin expression, thereby shifting their profiles to those observed at 15d post-UEC. Changes in ADAM-10 and N-cadherin expression were accompanied by improvement in the capacity to induce hippocampal long-term potentiation (LTP), but failed to correlate with improved spatial learning and memory performance by injured-treated animals. Further, MMP inhibition improved dendritic and synaptic structure within the hippocampus and dentate gyrus at 15d post-TBI+BEC. Given the importance of N-cadherin to synapse stabilization, these improvements in synaptic function and structure could be influenced by a shift to increased N-cadherin expression following MMP inhibition. Collectively, the novel results presented in Chapters 2 and 3 are supported by the current literature and indicate roles for membrane-bound MMPs like MT5-MMP and ADAM-10, as well as N-cadherin in synaptic plasticity and recovery following TBI.

Roles of Membrane-Bound MMPs in Synaptogenesis

Due to their transmembrane position, membrane-bound MMPs serve a unique role in neuroplasticity by interacting with both cellular and extracellular substrates, often at very focused sites along the cell surface. Our results show that membrane-bound

MMPs, MT5-MMP and ADAM-10: 1) are expressed at high levels within the hippocampus under injury conditions that induce synaptogenesis, 2) are normalized in expression by 15d during adaptive synaptogenesis, 3) exhibit a time course of expression which is consistent with MMPs secreted during adaptive and maladaptive plasticity, 4) are highly localized to reactive astrocytes, not microglia, following injury, and 5) may influence postinjury recovery through individual interaction with TIMP-2/proMMP-2 and N-cadherin, respectively. The results presented in Chapters 2 and 3 are further supported by current literature that shows that MT5-MMP and ADAM-10 are highly expressed and active during development and disease processes that involve plasticity.

Our study investigated postinjury tissue expression and localization of MT5-MMP and ADAM-10 in the hippocampus, a structure known for its ability to exhibit properties of neuroplasticity. We showed a protein and mRNA expression of membrane-bound MMPs which is consistent with reported expression during CNS development. In the developing brain, hippocampal MT5-MMP and ADAM-10 are found primarily in neuronal axonal growth cones and/or dendritic spines, with some evidence of ADAM-10 glial localization. Based on these patterns, MT5-MMP and ADAM-10 are thought to facilitate the outgrowth of neurites and the formation of synapses (Hayashita-Kinoh et. al, 2001; Sekine-Aizawa et. al, 2001; Bernstein et al., 2003; Marcinkiewicz and Seidah, 2000). Specifically, *in vitro* developmental studies have shown that MT5-MMP and ADAM-10 are involved in neurite outgrowth through proteoglycan cleavage and axonal guidance through interaction with ephrin, respectively (Hayashita-Kinoh et al., 2001; Hattori et al., 2000). ADAM-10 is highly involved in Notch signaling which influences neurogenesis,

axonal and dendritic growth, synaptic plasticity, and neuronal death during both nervous system development and disease (Lathia et al., 2008). Additionally, MT5-MMP has been shown to facilitate the re-organization of Aβ fibers within the spinal cord following *in vivo* sciatic nerve injury (Komori et al., 2004). Together, these studies and our current results show that membrane-bound MT5-MMP and ADAM-10 are critical to success of the plasticity process in both developing and adult nervous systems.

Elevation of hippocampal MT5-MMP and ADAM-10 expression during reactive synaptogenesis does show some similarity to that of their secreted counterparts following TBI. For example, protein analysis revealed an acute upregulation of MT5-MMP and ADAM-10 at 2 and 7d post-UEC and TBI+BEC. MT5-MMP mRNA was moderately elevated at 7d for each model. These results indicate that MT5-MMP and ADAM-10 are temporally correlated with the degradation and regeneration of synapses during both adaptive and maladaptive plasticity. However, it is important to note that during adaptive recovery, MT5-MMP and ADAM-10 return to control levels by 15d. This shift in expression indicates that as adaptive plasticity proceeds into the synapse stabilization phase, high levels of membrane-bound MMPs are not required, perhaps due to a reduced need for local ECM and cell-cell modification. In previous studies we have shown similar 2-7d increases of MMP-2, -3, and -9 protein and mRNA for both models, however, these secreted MMPs were normalized to control expression by 15d (Phillips and Reeves, 2001; Kim et al., 2005; Falo et al., 2006). We also observed persistent elevation of ADAM-10 protein up to 15d post-TBI+BEC. Prior studies also show a persistent elevation of MMPs 2, 3 and 9 after TBI+BEC insult, but for this secreted MMP it occurs at 7d, not 15d (Falo et al., 2006). We have also shown 2 and

7d increases in MMP-2 and -9, and elevations in both MMP-2 mRNA and activity 7d following TBI+BEC (Phillips and Reeves, 2001). Other investigators have also shown elevation of secreted MMPs during plasticity in models of neurotrauma, including controlled cortical impact, lateral fluid percussion injury, olfactory bulb lesion, and cerebral ischemia (Wang et al., 2000; Truettner et al., 2005; Costanzo et al., 2006; Costanzo and Perrino, 2008; Romanic et al., 1998; Fujimoto et al., 2008). The fact that secreted and membrane-bound MMPs show similar expression patterns suggests that they each have important roles in postinjury recovery. However, the precise role(s) may be further dictated by their cellular localization and distribution.

Our current study showed pronounced upregulation of membrane-bound MT5-MMP and ADAM-10 in reactive astrocytes, not microglia. Astrocytic localization of secreted MMPs (i.e.-MMP3) has been shown in our previous studies as well (Kim et al., 2005; Falo et al., 2006). While soluble MMPs are released from astrocytes over a more diffuse area within the ECM, our current results suggest that membrane-bound MT5-MMP and ADAM-10 are primarily found within the membranes of ML reactive astrocytes. Localization and up regulation of MMP mRNA and protein within astrocytes are supported by several published *in vitro* and *in vivo* studies. For example, lipopolysaccaride (LPS) stimulated cultured astrocytes produce active MMP-2 and proMMP-9 protein (Gottschall and Yu, 1995; Rosenberg et al., 2001). LPS stimulated cultured astrocytes also express varying levels of mRNA for MMP-2, -3, -9, -10, -11, -12, -13 and MT1-MMP (Wells et al., 1996). Other studies show that, following *in vivo* spinal cord injury peri-lesion reactive astrocytes express MMP-1 (Buss et al., 2007). MMP-2, -3 and -9 display a temporal upregulation in reactive astrocytes following

middle cerebral artery occlusion (MCAO) in rats (Rosenberg et al., 2001). Additionally, ADAM-10 was found to be constitutively expressed in reactive astrocytes in multiple sclerosis patients (Kieseier et al., 2003). While our immunohistochemical results identified reactive astrocytes as sites of MT5-MMP and ADAM-10 localization, they failed to show MT5-MMP and ADAM-10 co-localization with microglial markers (CD-11, IBa-1), which is consistent with other CNS inflammation and injury studies (Toft-Hansen et al., 2007; Kieseier et al., 2003). Therefore, our results suggest that reactive astrocytes likely function as the primary sites for synthesis and recycling of MT5-MMP and ADAM-10, thus directly affecting the organization of the ECM during injury-induced synaptic plasticity.

Finally, the present study suggests that, of the two membrane-bound MMPs examined, N-cadherin may be preferentially targeted by ADAM-10 during the later stages of reactive synaptogenesis. *In vitro* studies indicate that N-cadherin can be processed by either MT5-MMP or ADAM-10 (Monea et al., 2005; Reiss et al., 2006). However, our *in vivo* results reveal temporal correlates between the levels of ADAM-10 and N-cadherin which suggest that their specific interaction during the phase of synapse stabilization is critical to synaptic recovery after TBI. Conversely, we found evidence for the principal expression of MT5-MMP as a TIMP-2 bound form following injury, opening the possibility that it may play a different role in the synaptogenic process. Specifically, TIMP-2 bound MT5-MMP may function to activate proMMP-2 (Sternlicht and Werb, 2001; Nagase et al., 2006), supporting synapse organization at local sites along the dendritic membrane. The reduction of its expression during the later stages of adaptive synaptogenesis points to a lesser role for MT5-MMP in N-cadherin processing during

synapse stabilization. Thus, the current study provides evidence that distinct enzyme/substrate relationships may exist for membrane-bound MMPs during the course of reactive synaptogenesis.

Understanding Maladaptive Synaptic Plasticity

How do our current findings add to what is already known about maladaptive plasticity following TBI? While previous studies have examined secreted MMPs in the UEC and TBI+BEC models, this is the first study to show that maladaptive plasticity may be influenced by membrane-bound MMP/substrate interaction, specifically during periods of synapse stabilization and maturation. ADAM-10, rather than MT5-MMP, emerged as the prominent player in the maladaptive response, persistently elevated up to 15d. Despite different responses at 15d, MT5-MMP and ADAM-10 were both similarly elevated at the acute postinjury intervals, much like the secreted MMPs MMP 2, 3 and 9. This common elevation of expression suggests that both secreted and membrane-bound MMPs contribute to different phases of reactive synaptogenesis. We posit that increased ADAM-10 expression and activity at 15d post-TBI+BEC prevents N-cadherin-dependent stabilization and organization of nascent synapses, resulting in a maladaptive form of synaptic plasticity. This is supported by our EM analysis in Chapter 3, which shows reversal of synaptic pathology after MMP inhibition. N-cadherin is also directly linked to both post-synaptic density (PSD) organization and synaptic adhesion, therefore proteolysis of N-cadherin would disrupt PSD structure, commonly seen in synapse pathology (Malenka and Nicoll, 1999; Takeichi and Abe, 2006; Nuriya and Huganir, 2006). The role of ADAM-10/N-cadherin in the generation of maladaptive plasticity is also supported by our observation that deficits in LTP induction can be

attenuated when MMPs are inhibited, particularly given that attenuation is temporally correlated increased in N-cadherin expression. These improvements in synaptic structure and function are consistent with earlier studies which showed that synapse reorganization develops concurrently with the re-emergence of LTP following UEC lesion (Reeves and Steward, 1986). Based on these observations, we conclude that maladaptive plasticity is generated, in part, by ADAM-10 and N-cadherin synaptic interaction, and that MMP inhibition has potential to prevent these impairments.

Potential benefits of MMP inhibition on Recovery

Results presented in Chapter 3 suggest the potential application of MMP inhibition as a treatment to improve maladaptive plasticity. Our results provide evidence that broad-spectrum MMP inhibition (GM6001) can alter expression of membrane-bound MMPs like ADAM-10, affecting the tissue level of its synapse-related substrate N-cadherin. Inhibition of enzyme activity may also reduce expression of MMP genes through a feedback mechanism which limits proteolysis of ECM-cell and cell-cell contacts, stimulating intracellular signaling pathways which alter downstream transcription and protein expression (Conant and Gottschall, 2005). In the TBI+BEC model this would offer the benefit of returning MMP protein levels to those more in line with adaptive recovery. We also report that deficits in the early induction phase of LTP were attenuated with GM6001 treatment. Other studies also show that MMP inhibition can affect hippocampal LTP following injury. MMP inhibition by FN-439 at 30 min postinjury suppressed the emergence of LTP when compared to controls, suggesting that inhibition of MMPs at an inappropriate postinjury period can be detrimental, even within an adaptive environment (Phillips and Reeves, 2001). A similar negative effect of

FN-439 on LTP was found using normal hippocampal slices, where both induction and maintenance were impaired (Meighan et al., 2007). Taken together with our data, these results suggest that the role of MMPs in synaptic activity is complex, and that the application of MMP inhibitors must be considered in the context of both time postinjury and tissue condition. The benefits of MMP inhibition during maladaptive plasticity were further strengthened by the observation that GM6001treatment improved dendritic and synaptic cytoarchitecture within the hippocampus. However, we were unable to show that MMP inhibition translated into improvements in cognitive performance in the MWM. This result emphasizes the importance of optimizing dose and delivery in order to confirm whether or not the physiological and structural improvements are translatable into behavioral protection. The inclusion of MMP inhibition in future studies will be discussed below. Our results have shown the beneficial effects of MMP inhibition on the expression of and potential interaction between ADAM-10 and N-cadherin, and synaptic structure and function. In addition to altering membrane-bound MMP/substrate expression and interaction, TBI and MMP inhibition can modify the downstream extracellular and intracellular signaling pathways involved in synaptic plasticity.

Signaling Pathways and Plasticity

Interaction between MMPs and their substrates is known to influence downstream signaling pathways to regulate neuroplasticity. Our study suggests that ADAM-10 and N-cadherin interact at the synaptic membrane, and that TIMP-2 bound MT5-MMP may potentially function as an activator of proMMP-2 at the same location. In the case of membrane-bound MMPs, interaction with substrates occurs at the cell membrane, often involving the cleavage and release of an extracellular molecular

fragment of their substrate. MMPs which perform this lysis are termed sheddases. This cleavage generates intracellular fragments as well, peptides that can influence downstream signaling to affect plasticity following TBI. These pathways are well characterized *in vitro*. They can involve the shedding of an N-terminal N-cadherin fragment (NTF) by ADAM-10, which leads to γ-secretase cleavage and release of the intracellular 40 kDa C-terminus fragment (CFT1) (Reiss et al., 2005; Uemura et al., 2006; Kohutek et al., 2009). CTF1 can also undergo further calpain proteolysis into a 35 kDa fragment (CTF2) (Jang et al., 2009). Each of these fragments has been shown to be involved with downstream regulation of neuroplasticity. For example, ADAM-10/MMP-mediated cleavage and release of NTF promotes neurite outgrowth in cultured cells (Paradies and Grunwald, 1993; Utton et al., 2001). Based on our results, the production of NTF by ADAM-10 sheddase activity may permit modulation at the synapse and promote collateral sprouting of spared axons into the damaged region during injury-induced synaptogenesis. In addition to NTF, release of other intracellular N-cadherin fragments has been implicated in synaptic function and plasticity.

Recall that, in Chapter 2, we demonstrated the presence of an N-cadherin 40 kDa intracellular protein fragment in both adaptive and maladaptive models. While a significant decrease in the 40 kDa fragment was observed only at 2d post-UEC, the presence of this fragment indicates that intracellular N-cadherin lysis occurred in both adaptive and maladaptive models. This 40 kDa fragment likely represents CTF1, generated through NTF production by ADAM-10. Increased CTF1 may mediate several downstream pathways invoked by injury-induced synaptogenesis. For example, the production of CFT1 influences synaptic structural stability and synaptic Ca^{2+}

conductance (Brusés, 2006; McCusker and Alfandari, 2009). Synapse structure is disrupted when CTF1 is released from the membrane due to the breakdown of N-cadherin/catenin/cytoskeleton connections, which are necessary to provide structural stability to the synapse (Jang et al., 2009). Our results suggest that persistent ADAM-10 may be an upstream regulator of the production and release of CTF1. In this way, MMPs may direct the evolution of abnormal synaptic cytoarchitecture which we documented in hippocampal stratum radiatum and dentate molecular layer after TBI+BEC insult.

Structural instability can also lead to the failure of synaptic function. Extracellular cleavage of N-cadherin by MMPs and the intracellular release of CTF1 not only alter connections to the actin cytoskeleton, but also change the relationship N-cadherin and subcellular PSD proteins, including AMPA receptors and p120 catenin. When binding between N-cadherin and these proteins changes, Ca^{2+} conductance is altered. These downstream effects may help to explain the injury-induced deficits we observed in our LTP experiment. N-cadherin has been found to mediate the placement and positioning of AMPA receptors into the post-synaptic membrane, which is necessary for synaptic transmission and activation of NMDA receptors which results in Ca^{2+} influx (Silverman et al., 2007; Malenka and Bear, 2004). During the early induction phase of LTP, AMPA receptors are inserted into the post-synaptic membrane, strengthening the synaptic response. Here we showed LTP deficits at 15d post-TBI+BEC, a time when high ADAM-10 levels were matched with decreased full length N-cadherin. Following MMP inhibition, full length N-cadherin was increased, along with a reduction in LTP deficit. Restoration of intact N-cadherin may have facilitated AMPA receptor membrane

placement, therefore increasing Ca^{2+} conductance and improved synaptic efficacy. Neuronal Ca^{2+} conductance may also be altered when p120 catenin dissociates from RhoA and binds the juxtamembrane domain (JMD) of CTF1. In this series of events, intracellular cleavage of N-cadherin produces a form of the molecule which recruits and binds to p120 catenin, releasing RhoA. Free RhoA is activated upon release from p120 catenin and can then modulate voltage activated Ca^{2+} channels (VACC) in both pre- and post-synaptic sites. Through interaction with myosin-actin cytoskeleton, soluble, active RhoA ultimately decreases synaptic Ca^{2+} influx (Marrs et al., 2009). Although the mechanism is different from N-cadherin/AMPA receptor interaction, CTF1/p120 catenin interaction has similar downstream effects on Ca^{2+} conductance which would also support a decrease in synaptic efficacy after TBI+BEC and our observed effects on LTP.

While we were unable to visualize hippocampal N-cadherin fragments smaller than 40 kDa following injury, it is important to consider the role that such fragments may play in neuroplasticity after TBI. Current literature shows that CTF1 can be further processed into a 35 kDa fragment (CTF2), which also may affect synaptogenesis through interaction with CREB and β-catenin (Reiss et al., 2005; Marambaud et al., 2003; McCusker and Alfandari, 2009). CTF2 binds CREB binding protein (CBP), targeting it for degradation, therefore interfering with downstream transcription of CREB-dependent genes. Many of these genes are critical for CNS plasticity, such as c-fos, synapsin I, K+ channels and the alpha subunit of Ca2+/calmodulin-dependent kinase II (Marambaud et al., 2003; Lonze and Ginty, 2002; Deisseroth et al., 1996). Additionally, CTF2 associates with the Wnt signaling molecule, β-catenin, promoting

transcription of genes important for cell proliferation and survival, as well as synaptic plasticity: cyclin D1, c-myc, c-jun, and N-cadherin (Reiss et al., 2005; McCusker and Alfandari, 2009). CFT2-dependent action on transcription of any of these plasticity-associated genes could play a role in synaptic reorganization following TBI. Clearly, both extracellular and intracellular N-cadherin fragments generated by ADAM-10 are capable of altering trauma-induced synaptic plasticity through different signaling pathways. While the role of MT5-MMP appears to be less clear, some reasonable predictions as to its effect on reactive synaptogenesis can be made based on our current results.

Our Western blot (WB) results showed that MT5-MMP was not detectable in its active 58 kDa form, but rather, predominantly seen as an 80 kDa band, likely bound to its endogenous inhibitor TIMP-2. As previously mentioned, MT5-MMP is capable of binding toTIMP-2 in a complex with proMMP-2. The formation of this complex occurs at the cell membrane, where the binding of TIMP-2 inhibits any catalytic activity of MT5-MMP, the enzyme functioning as a docking station. TIMP-2 possesses a C-terminal domain with a high affinity for the HLD domain of proMMP2. The proMMP-2 “substrate” docks to the C-terminus of TIMP-2 and forms the ternary complex (Strongin et. al, 1995; Maskos and Bode, 2003). The binding of these three proteins is insufficient to activate proMMP-2, thus an adjacent TIMP-free MT5-MMP is needed to initiate the first pro-MMP-2 cleavage. Following the initial cleavage, an additional MMP-2 molecule removes the remaining propeptide domain from the intermediate MMP-2 to yield a mature and fully-active MMP-2 molecule (Deryugina et. al, 2001). This series of downstream events is initiated by the placement of MT5-MMP into the cell membrane.

Based on results from our lab and others, all components of the MT5-MMP/TIMP-2/proMMP-2 complex are found to be expressed in astrocytes (Conant and Gottschall, 2005). This molecular localization and proximity further supports their interaction and possible influence on plasticity within the deafferented molecular layer. Our lab has previously demonstrated increases in MMP-2 gene expression and activity in the injured hippocampus, as well as increased localization of MMP-2 in the deafferented molecular layer 2 and 7d following both UEC and TBI+BEC (Phillips and Reeves, 2001). This data is consistent with our the hypothesis that a significant increase in hippocampal MT5-MMP expression at 2 and 7d postinjury may result in formation of the MT5-MMP/TIMP2/MMP-2 complex and local MMP-2 activation.

The results presented in this dissertation add to our understanding of how membrane-bound MMPs and N-cadherin might influence the efficacy of synaptic plasticity following TBI. Interpretation of these results in the context of TBI neuropathology and recovery did reveal possibilities for targeting MMP inhibition in developing new therapies to improve postinjury recovery. While many of our initial questions were answered, new ones arose during our investigation. The following section describes some of these questions and the future studies which could address them.

Future Directions

In our lab group the overall research goal is to gain greater understanding of TBI pathophysiology and design treatment paradigms translatable to the clinic for improved patient recovery and rehabilitation. This study expands our current understanding of

synaptic recovery and reveals that membrane-bound MMP/substrate interaction can positively or negatively influence this process following TBI. Our results provide evidence that spatio-temporal changes in MT5-MMP, ADAM-10 and N-cadherin expression correlate with functional and structural recovery, and differ in effect depending on the plasticity conditions. However, additional investigation is needed to confirm two missing aspects of MMP involvement: 1) to fully characterize MT5-MMP, ADAM-10, and N-cadherin mRNA expression, and 2) to confirm injury-dependent differences in proteolytic activity for these membrane-bound MMPs. To further examine the specific cellular localization of ADAM-10, MT5-MMP and N-cadherin we plan to use EM immunohistochemical techniques. We also plan to take a closer look at MMP-related molecular mechanisms guiding neuroplasticity and identify additional manipulations to more specifically inhibit MT5-MMP and ADAM-10. These future studies are needed to confirm the findings in the current study.

Although we have profiled hippocampal MT5-MMP, ADAM-10, and N-cadherin protein expression over the time course of reactive synaptogenesis, we have yet to fully document the transcript profiles of these genes. Our preliminary 7d qRT-PCR results provide useful information about mRNA expression in enriched ML samples, pointing to larger model shifts in ADAM-10 and N-cadherin transcription at the tissue site of synaptogenesis. Nevertheless, it will be important to examine mRNA expression at later postinjury intervals in order to further dissect the persistent ADAM-10 expression in the maladaptive model of TBI. Also, our results failed to show pronounced model differences in MT5-MMP mRNA expression, suggesting that we need to investigate MT5-MMP transcription at more acute postinjury periods.

Measurement of MT5-MMP and ADAM-10 proteolytic activity is also needed to fully understand the relationship between enzyme expression and function during postinjury recovery. Unfortunately, no commercial assays specific for either MT5-MMP or ADAM-10 are currently available. While we were able to assess the active 70 kDa ADAM-10 with Western blots, this only confirms the expression of active enzyme, not its endogenous activity. Nevertheless, we have worked with a commercial supplier of enzyme assays in an attempt to measure ADAM-10 specific lysis using hippocampal tissue samples from our models. The assay tested was designed for cultured cells and did not show the same specificity in extracts from fresh brain. A feasible indirect option for exploring MT5-MMP activity would be to first measure MMP-2 lysis in our samples. Changes in MMP-2 activity would further support the postulated role of MT5-MMP as a facilitator of proMMP-2 activation. While less quantitative in nature, gel zymography methods have been used to assay membrane-bound MMP activity (Wang, 2004), which is another option. In future studies, we will continue to investigate the different options for accurate measurement of MT5-MMP and ADAM-10 proteolytic activity.

In addition to above directions, we will focus on molecular mechanisms involving membrane-bound MMPs which might influence the postinjury plasticity process. For example, we are currently investigating the role of β-catenin in postinjury gene transcription. N-cadherin lysis by ADAM-10 results in intracellular processing of N-cadherin fragments and the release of binding partner β-catenin, leading to its nuclear translocation and altered gene transcription of plasticity pathways (McCusker and Alfandari, 2009; Reiss et al., 2005; Lyuksyutova, AI et al., 2003; Yu and Malenka, 2003; Gogolla et al., 2009). Our preliminary studies with hippocampal β-catenin protein show

a significant decrease of full-length (94 kDa) β-catenin and an increase in detection of fragments (90 and 75 kDa) across all post-TBI+BEC times (See Appendix Fig E-1). Interestingly, in molecular layer enriched samples, this pattern of fragment generation was detected only at the acute 2d postinjury interval (See Appendix Fig E-2). These results show that hippocampal β-catenin protein lysis occur throughout the time course of reactive synaptogenesis, with pronounced increases in a 75 kDa form. Overall, maladaptive recovery produces greater change in β-catenin at 2 and 7d postinjury, generating more of the 75 kDa fragment. Notably, these shifts are spatio-temporally correlated with elevation of ADAM-10 and reduction of N-cadherin. For future studies we posit that ADAM-10 proteolysis of N-cadherin alters β-catenin binding within the post-synaptic site, resulting in the generation of fragments which are translocated to the cell nucleus as transcription factors, targeting genes associated with synaptic plasticity. In the context of this β-catenin hypothesis, we will investigate changes in transcript and protein expression of plasticity associated genes. Manipulation of these molecules or the mechanism by which they act will also support our current findings.

In Chapter 3 we showed that broad-spectrum MMP inhibition improved synaptic structure and function in the maladaptive TBI+BEC model. While these effects were modest, we believe that inhibition of membrane-bound MMPs remains an important area of study with clinical relevance, not only for TBI, but also for additional pathologies that involve MMPs. We have traditionally used broad-spectrum MMP inhibitors, including FN-439 and GM6001, when characterizing MMP activity and role during injury-induced plasticity. A chief issue with these drugs is the lack of specificity for individual MMPs. Specific MT5-MMP and ADAM-10 inhibitors were not commercially available for

use in the present experiments. In the interim, new inhibitors have been developed that preferentially target ADAM-10. In several studies, the compound GI254023X has been shown to block *in vitro* ADAM-10 induced shedding of N-cadherin, L1, Fas-ligand, Pcdhγ, VE-cadherin, and CX3CL1 (Ludwig et al, 2005; Hoettecke et al., 2010; Hundhausen et al, 2003; as reviewed in Pruessmeyer and Ludwig, 2009). Specific pharmacological inhibitors of MT5-MMP have yet to be developed, therefore future MT5-MMP studies in TBI may involve knock down experiments employing siRNA or transgenic approaches. In a preliminary study, we have applied MT5-MMP siRNA *in vivo* 24h prior to UEC and successfully reduced injury-induced elevations in MT5-MMP protein at the 2d postinjury (Phillips, unpublished data). Additionally, both ADAM-10 and MT5-MMP knockout mice are commercially available for use in neuropathology research and will be a useful tool for TBI as well (Komori et al, 2003; Folgueras et al., 2009; Postina et al., 2004).

In addition to broad-spectrum MMP inhibition, we have used established neuroprotective treatments to determine their effect on MMP expression and activity. Drugs such as MK-801(NMDA antagonist) show tandem neuroprotection and altered expression of secreted MMPs (Phillips and Reeves, 2001; Falo et al., 2006). We will use such agents in future studies to determine how membrane-bound MMPs and their synaptic substrates respond to protective therapies. In the case of MT5-MMP activation of proMMP-2, we have already shown that MK-801 treatment results in reduction of MMP-2 activity at 7d post-TBI+BEC. Based on this data, we would predict that postinjury treatment with MK-801 may also result in significant effects on ADAM-10 and N-cadherin expression and/or function. Such experiments will further identify specific

role(s) of membrane-bound MMPs MT5-MMP and ADAM-10 and their substrates during injury-induced plasticity. Lastly, regardless of the method or target of manipulation, it is imperative to develop the appropriate dosing and delivery paradigm. Therefore, future manipulations will first require more complete pharmacological studies to characterize treatment response along the synaptogenic time course. This approach is particularly important with respect to our MWM experiments, where, using a single dosing paradigm for GM6001, we failed to detect significant effects on cognitive performance.

Final Remarks

Collectively, the series of experiments presented in this dissertation give greater insight into the role of membrane-bound MMPs and their substrates during synaptic plasticity induced by TBI. Through characterization and manipulation of these molecules, we also broadened our understanding of the process of maladaptive synaptic plasticity, and developed additional questions for future studies. Our lab continues to test the importance of matrix molecules such as MMPs in the process of synaptic recovery. We strive to develop treatment options that prevent the persistent impairments that ensue following TBI and promote successful recovery.

List of References

List of References

Abe, K., Chisaka, O., Van Roy, F., & Takeichi, M. (2004). Stability of dendritic spines and synaptic contacts is controlled by alpha N-catenin. *Nature Neuroscience, 7*(4), 357-363.

Ahmad, M., Takino, T., Miyamori, H., Yoshizaki, T., Furukawa, M., & Sato, H. (2006). Cleavage of amyloid-beta precursor protein (APP) by membrane-type matrix metalloproteinases. *Journal of Biochemistry, 139*(3), 517-526.

Amaducci, L., Forno, K. I., & Eng, L. F. (1981). Glial fibrillary acidic protein in cryogenic lesions of the rat brain. *Neuroscience Letters, 21*(1), 27-32.

Amantea, D., Russo, R., Gliozzi, M., Fratto, V., Berliocchi, L., Bagetta, G., et al. (2007). Early upregulation of matrix metalloproteinases following reperfusion triggers neuroinflammatory mediators in brain ischemia in rat. *International Review of Neurobiology, 82*, 149-169.

Amaral, D. G., Scharfman, H. E., & Lavenex, P. (2007). The dentate gyrus: Fundamental neuroanatomical organization (dentate gyrus for dummies). *Progress in Brain Research, 163*, 3-22.

Anders, A., Gilbert, S., Garten, W., Postina, R., & Fahrenholz, F. (2001). Regulation of the alpha-secretase ADAM10 by its prodomain and proprotein convertases. *The*

FASEB Journal : Official Publication of the Federation of American Societies for Experimental Biology, 15(10), 1837-1839.

Anderson, P., Morris, R., Amaral, D., Bliss, T., & O'Keefe, J. (Eds.). (2006). *The hippocampus book*. USA: Oxford University Press.

Anilkumar, N., Uekita, T., Couchman, J. R., Nagase, H., Seiki, M., & Itoh, Y. (2005). Palmitoylation at Cys574 is essential for MT1-MMP to promote cell migration. *The FASEB Journal : Official Publication of the Federation of American Societies for Experimental Biology, 19*(10), 1326-1328.

Araki, Y., Miyagi, N., Kato, N., Yoshida, T., Wada, S., Nishimura, M., et al. (2004). Coordinated metabolism of alcadein and amyloid beta-protein precursor regulates FE65-dependent gene transactivation. *The Journal of Biological Chemistry, 279*(23), 24343-24354.

Asahi, M., Asahi, K., Jung, J. C., del Zoppo, G. J., Fini, M. E., & Lo, E. H. (2000). Role for matrix metalloproteinase 9 after focal cerebral ischemia: Effects of gene knockout and enzyme inhibition with BB-94. *Journal of Cerebral Blood Flow and Metabolism : Official Journal of the International Society of Cerebral Blood Flow and Metabolism, 20*(12), 1681-1689.

Baldwin, S. A., & Scheff, S. W. (1996). Intermediate filament change in astrocytes following mild cortical contusion. *Glia, 16*(3), 266-275.

Bales, J. W., Wagner, A. K., Kline, A. E., & Dixon, C. E. (2009). Persistent cognitive dysfunction after traumatic brain injury: A dopamine hypothesis. *Neuroscience and Biobehavioral Reviews, 33*(7), 981-1003.

Ball, M. J., Fisman, M., Hachinski, V., Blume, W., Fox, A., Kral, V. A., et al. (1985). A new definition of alzheimer's disease: A hippocampal dementia. *Lancet, 1*(8419), 14-16.

Bandyopadhyay, S., Hartley, D. M., Cahill, C. M., Lahiri, D. K., Chattopadhyay, N., & Rogers, J. T. (2006). Interleukin-1alpha stimulates non-amyloidogenic pathway by alpha-secretase (ADAM-10 and ADAM-17) cleavage of APP in human astrocytic cells involving p38 MAP kinase. *Journal of Neuroscience Research, 84*(1), 106-118.

Bekirov, I. H., Needleman, L. A., Zhang, W., & Benson, D. L. (2002). Identification and localization of multiple classic cadherins in developing rat limbic system. *Neuroscience, 115*(1), 213-227.

Belanger, M., & Magistretti, P. J. (2009). The role of astroglia in neuroprotection. *Dialogues in Clinical Neuroscience, 11*(3), 281-295.

Bell, K. F., Zheng, L., Fahrenholz, F., & Cuello, A. C. (2008). ADAM-10 over-expression increases cortical synaptogenesis. *Neurobiology of Aging, 29*(4), 554-565.

Bendeck, M. P., Irvin, C., & Reidy, M. A. (1996). Inhibition of matrix metalloproteinase activity inhibits smooth muscle cell migration but not neointimal thickening after arterial injury. *Circulation Research, 78*(1), 38-43.

Benson, D. L., Schnapp, L. M., Shapiro, L., & Huntley, G. W. (2000). Making memories stick: Cell-adhesion molecules in synaptic plasticity. *Trends in Cell Biology, 10*(11), 473-482.

Benson, D. L., & Tanaka, H. (1998). N-cadherin redistribution during synaptogenesis in hippocampal neurons. *The Journal of Neuroscience : The Official Journal of the Society for Neuroscience, 18*(17), 6892-6904.

Bernal, F., Hartung, H. P., & Kieseier, B. C. (2005). Tissue mRNA expression in rat of newly described matrix metalloproteinases. *Biological Research, 38*(2-3), 267-271.

Bernstein, H. G., Bukowska, A., Krell, D., Bogerts, B., Ansorge, S., & Lendeckel, U. (2003). Comparative localization of ADAMs 10 and 15 in human cerebral cortex normal aging, alzheimer disease and down syndrome. *Journal of Neurocytology, 32*(2), 153-160.

Bird, C. M., & Burgess, N. (2008). The hippocampus and memory: Insights from spatial processing. *Nature Reviews.Neuroscience, 9*(3), 182-194.

Black, R. A., & White, J. M. (1998). ADAMs: Focus on the protease domain. *Current Opinion in Cell Biology, 10*(5), 654-659.

Bliss, T. V., & Collingridge, G. L. (1993). A synaptic model of memory: Long-term potentiation in the hippocampus. *Nature, 361*(6407), 31-39.

Bordey, A., Lyons, S. A., Hablitz, J. J., & Sontheimer, H. (2001). Electrophysiological characteristics of reactive astrocytes in experimental cortical dysplasia. *Journal of Neurophysiology, 85*(4), 1719-1731.

Bordey, A., & Sontheimer, H. (1998). Properties of human glial cells associated with epileptic seizure foci. *Epilepsy Research, 32*(1-2), 286-303.

Borggrefe, T., & Oswald, F. (2009). The notch signaling pathway: Transcriptional regulation at notch target genes. *Cellular and Molecular Life Sciences : CMLS, 66*(10), 1631-1646.

Bozdagi, O., Shan, W., Tanaka, H., Benson, D. L., & Huntley, G. W. (2000). Increasing numbers of synaptic puncta during late-phase LTP: N-cadherin is synthesized, recruited to synaptic sites, and required for potentiation. *Neuron, 28*(1), 245-259.

Bozdagi, O., Valcin, M., Poskanzer, K., Tanaka, H., & Benson, D. L. (2004). Temporally distinct demands for classic cadherins in synapse formation and maturation. *Molecular and Cellular Neurosciences, 27*(4), 509-521.

Bredt, D. S., & Nicoll, R. A. (2003). AMPA receptor trafficking at excitatory synapses. *Neuron, 40*(2), 361-379.

Brown, M. S., Ye, J., Rawson, R. B., & Goldstein, J. L. (2000). Regulated intramembrane proteolysis: A control mechanism conserved from bacteria to humans. *Cell, 100*(4), 391-398.

Brumwell, C. L., & Curran, T. (2006). Developmental mouse brain gene expression maps. *The Journal of Physiology, 575*(Pt 2), 343-346.

Bruses, J. L. (2006). N-cadherin signaling in synapse formation and neuronal physiology. *Molecular Neurobiology, 33*(3), 237-252.

Buckingham, S. D. (2003). Ripping and folding: Regulated intramembrane proteolysis. *Horizon Symposia,*

Buki, A., & Povlishock, J. T. (2006). All roads lead to disconnection?--traumatic axonal injury revisited. *Acta Neurochirurgica, 148*(2), 181-93; discussion 193-4.

Buss, A., Pech, K., Kakulas, B. A., Martin, D., Schoenen, J., Noth, J., et al. (2007). Matrix metalloproteinases and their inhibitors in human traumatic spinal cord injury. *BMC Neurology, 7*, 17.

Cao, J., Hymowitz, M., Conner, C., Bahou, W. F., & Zucker, S. (2000). The propeptide domain of membrane type 1-matrix metalloproteinase acts as an intramolecular chaperone when expressed in trans with the mature sequence in COS-1 cells. *The Journal of Biological Chemistry, 275*(38), 29648-29653.

Cao, R., Hasuo, H., Ooba, S., Akasu, T., & Zhang, X. (2006). Facilitation of glutamatergic synaptic transmission in hippocampal CA1 area of rats with traumatic brain injury. *Neuroscience Letters, 401*(1-2), 136-141.

Cawston, T. E., & Wilson, A. J. (2006). Understanding the role of tissue degrading enzymes and their inhibitors in development and disease. *Best Practice & Research.Clinical Rheumatology, 20*(5), 983-1002.

Cerretti, D. P., Poindexter, K., Castner, B. J., Means, G., Copeland, N. G., Gilbert, D. J., et al. (1999). Characterization of the cDNA and gene for mouse tumour necrosis factor alpha converting enzyme (TACE/ADAM17) and its location to mouse chromosome 12 and human chromosome 2p25. *Cytokine, 11*(8), 541-551.

Clausen, F., Lewen, A., Marklund, N., Olsson, Y., McArthur, D. L., & Hillered, L. (2005). Correlation of hippocampal morphological changes and morris water maze performance after cortical contusion injury in rats. *Neurosurgery, 57*(1), 154-63; discussion 154-63.

Clement, A. B., Hanstein, R., Schroder, A., Nagel, H., Endres, K., Fahrenholz, F., et al. (2008). Effects of neuron-specific ADAM10 modulation in an in vivo model of acute excitotoxic stress. *Neuroscience, 152*(2), 459-468.

Conant, K., & Gottschall, P. (Eds.). (2005). *Matrix metalloproteinases in the central nervous system*. London: Imperial College Press.

Costanzo, R. M., & Perrino, L. A. (2008). Peak in matrix metaloproteinases-2 levels observed during recovery from olfactory nerve injury. *Neuroreport, 19*(3), 327-331.

Costanzo, R. M., Perrino, L. A., & Kobayashi, M. (2006). Response of matrix metalloproteinase-9 to olfactory nerve injury. *Neuroreport, 17*(17), 1787-1791.

Cotman, C. W. (1979). Specificity of synaptic growth in brain: Remodeling induced by kainic acid lesions. *Progress in Brain Research, 51*, 203-215.

Creager, R., Dunwiddie, T., & Lynch, G. (1980). Paired-pulse and frequency facilitation in the CA1 region of the in vitro rat hippocampus. *The Journal of Physiology, 299*, 409-424.

Cunningham, L. A., Wetzel, M., & Rosenberg, G. A. (2005). Multiple roles for MMPs and TIMPs in cerebral ischemia. *Glia, 50*(4), 329-339.

D'Ambrosio, R., Maris, D. O., Grady, M. S., Winn, H. R., & Janigro, D. (1999). Impaired K(+) homeostasis and altered electrophysiological properties of post-traumatic hippocampal glia. *The Journal of Neuroscience : The Official Journal of the Society for Neuroscience, 19*(18), 8152-8162.

Daniel, J. M., & Reynolds, A. B. (1999). The catenin p120(ctn) interacts with kaiso, a novel BTB/POZ domain zinc finger transcription factor. *Molecular and Cellular Biology, 19*(5), 3614-3623.

Deisseroth, K., Bito, H., & Tsien, R. W. (1996). Signaling from synapse to nucleus: Postsynaptic CREB phosphorylation during multiple forms of hippocampal synaptic plasticity. *Neuron, 16*(1), 89-101.

Deller, T., & Frotscher, M. (1997). Lesion-induced plasticity of central neurons: Sprouting of single fibres in the rat hippocampus after unilateral entorhinal cortex lesion. *Progress in Neurobiology, 53*(6), 687-727.

Deller, T., Frotscher, M., & Nitsch, R. (1996). Sprouting of crossed entorhinodentate fibers after a unilateral entorhinal lesion: Anterograde tracing of fiber reorganization with phaseolus vulgaris-leucoagglutinin (PHAL). *The Journal of Comparative Neurology, 365*(1), 42-55.

Deryugina, E. I., & Quigley, J. P. (2006). Matrix metalloproteinases and tumor metastasis. *Cancer Metastasis Reviews, 25*(1), 9-34.

Deryugina, E. I., Ratnikov, B. I., Postnova, T. I., Rozanov, D. V., & Strongin, A. Y. (2002). Processing of integrin alpha(v) subunit by membrane type 1 matrix metalloproteinase stimulates migration of breast carcinoma cells on vitronectin and enhances tyrosine phosphorylation of focal adhesion kinase. *The Journal of Biological Chemistry, 277*(12), 9749-9756.

Deuss, M., Reiss, K., & Hartmann, D. (2008). Part-time alpha-secretases: The functional biology of ADAM 9, 10 and 17. *Current Alzheimer Research, 5*(2), 187-201.

D'Hooge, R., & De Deyn, P. P. (2001). Applications of the morris water maze in the study of learning and memory. *Brain Research.Brain Research Reviews, 36*(1), 60-90.

Dietrich, W. D., Alonso, O., & Halley, M. (1994). Early microvascular and neuronal consequences of traumatic brain injury: A light and electron microscopic study in rats. *Journal of Neurotrauma, 11*(3), 289-301.

Dixon, C. E., Kraus, M. F., Kline, A. E., Ma, X., Yan, H. Q., Griffith, R. G., et al. (1999). Amantadine improves water maze performance without affecting motor behavior following traumatic brain injury in rats. *Restorative Neurology and Neuroscience, 14*(4), 285-294.

Dixon, C. E., Lyeth, B. G., Povlishock, J. T., Findling, R. L., Hamm, R. J., Marmarou, A., et al. (1987). A fluid percussion model of experimental brain injury in the rat. *Journal of Neurosurgery, 67*(1), 110-119.

Duffy, M. J., McKiernan, E., O'Donovan, N., & McGowan, P. M. (2009). The role of ADAMs in disease pathophysiology. *Clinica Chimica Acta; International Journal of Clinical Chemistry, 403*(1-2), 31-36.

Dumur, C. I., Ladd, A. C., Wright, H. V., Penberthy, L. T., Wilkinson, D. S., Powers, C. N., et al. (2009). Genes involved in radiation therapy response in head and neck cancers. *The Laryngoscope, 119*(1), 91-101.

Edwards, D. R., Handsley, M. M., & Pennington, C. J. (2008). The ADAM metalloproteinases. *Molecular Aspects of Medicine, 29*(5), 258-289.

English, W. R., Holtz, B., Vogt, G., Knauper, V., & Murphy, G. (2001). Characterization of the role of the "MT-loop": An eight-amino acid insertion specific to progelatinase A (MMP2) activating membrane-type matrix metalloproteinases. *The Journal of Biological Chemistry, 276*(45), 42018-42026.

Erb, D. E., & Povlishock, J. T. (1991). Neuroplasticity following traumatic brain injury: A study of GABAergic terminal loss and recovery in the cat dorsal lateral vestibular nucleus. *Experimental Brain Research, 83*(2), 253-267.

Faden, A. I., Demediuk, P., Panter, S. S., & Vink, R. (1989). The role of excitatory amino acids and NMDA receptors in traumatic brain injury. *Science (New York, N.Y.), 244*(4906), 798-800.

Falo, M. C., Fillmore, H. L., Reeves, T. M., & Phillips, L. L. (2006). Matrix metalloproteinase-3 expression profile differentiates adaptive and maladaptive synaptic plasticity induced by traumatic brain injury. *Journal of Neuroscience Research, 84*(4), 768-781.

Falo, M. C., Reeves, T. M., & Phillips, L. L. (2008). Agrin expression during synaptogenesis induced by traumatic brain injury. *Journal of Neurotrauma, 25*(7), 769-783.

Fambrough, D., Pan, D., Rubin, G. M., & Goodman, C. S. (1996). The cell surface metalloprotease/disintegrin kuzbanian is required for axonal extension in drosophila. *Proceedings of the National Academy of Sciences of the United States of America, 93*(23), 13233-13238.

Farkas, O., Lifshitz, J., & Povlishock, J. T. (2006). Mechanoporation induced by diffuse traumatic brain injury: An irreversible or reversible response to injury? *The Journal of Neuroscience : The Official Journal of the Society for Neuroscience, 26*(12), 3130-3140.

Farkas, O., & Povlishock, J. T. (2007). Cellular and subcellular change evoked by diffuse traumatic brain injury: A complex web of change extending far beyond focal damage. *Progress in Brain Research, 161*, 43-59.

Faul, M., Xu, L., Wald, M., & Coronado, V. (2010). *Traumatic brain injury in the united states: Emergency department visits, hospitalizations, and deaths, 2002-2006.*. Atlanta, GA: Center for Disease Control and Prevention, National Center for Injury Prevention and Control.

Fawcett, J., Rosser, A., & Dunnett SB (Eds.). (2003). *Brain injury, brain repair*. New York: Oxford University Press.

Fernandez-Catalan, C., Bode, W., Huber, R., Turk, D., Calvete, J. J., Lichte, A., et al. (1998). Crystal structure of the complex formed by the membrane type 1-matrix metalloproteinase with the tissue inhibitor of metalloproteinases-2, the soluble progelatinase A receptor. *The EMBO Journal, 17*(17), 5238-5248.

Fillmore, H. L., VanMeter, T. E., & Broaddus, W. C. (2001). Membrane-type matrix metalloproteinases (MT-MMPs): Expression and function during glioma invasion. *Journal of Neuro-Oncology, 53*(2), 187-202.

Folgueras, A. R., Valdes-Sanchez, T., Llano, E., Menendez, L., Baamonde, A., Denlinger, B. L., et al. (2009). Metalloproteinase MT5-MMP is an essential modulator of neuro-immune interactions in thermal pain stimulation. *Proceedings of the National Academy of Sciences of the United States of America, 106*(38), 16451-16456.

Fujimoto, M., Takagi, Y., Aoki, T., Hayase, M., Marumo, T., Gomi, M., et al. (2008). Tissue inhibitor of metalloproteinases protect blood-brain barrier disruption in focal cerebral ischemia. *Journal of Cerebral Blood Flow and Metabolism : Official Journal of the International Society of Cerebral Blood Flow and Metabolism, 28*(10), 1674-1685.

Galliano, M. F., Huet, C., Frygelius, J., Polgren, A., Wewer, U. M., & Engvall, E. (2000). Binding of ADAM12, a marker of skeletal muscle regeneration, to the muscle-specific actin-binding protein, alpha -actinin-2, is required for myoblast fusion. *The Journal of Biological Chemistry, 275*(18), 13933-13939.

Gijbels, K., Galardy, R. E., & Steinman, L. (1994). Reversal of experimental autoimmune encephalomyelitis with a hydroxamate inhibitor of matrix metalloproteases. *The Journal of Clinical Investigation, 94*(6), 2177-2182.

Gilmer, L. K., Roberts, K. N., Joy, K., Sullivan, P. G., & Scheff, S. W. (2009). Early mitochondrial dysfunction after cortical contusion injury. *Journal of Neurotrauma, 26*(8), 1271-1280.

Gogolla, N., Galimberti, I., Deguchi, Y., & Caroni, P. (2009). Wnt signaling mediates experience-related regulation of synapse numbers and mossy fiber connectivities in the adult hippocampus. *Neuron, 62*(4), 510-525.

Goldshmit, Y., & Bourne, J. (2010). Upregulation of EphA4 on astrocytes potentially mediates astrocytic gliosis after cortical lesion in the marmoset monkey. *Journal of Neurotrauma,*

Good, M. (2002). Spatial memory and hippocampal function: Where are we now? *Psicológica, 23*, 109-138.

Gordon DE, Phillips, L., & Povlishock, J. (1996). The interaction of neuroexcitation and targeted deafferentation in the pathology of traumatic brain injury (TBI): An assessment of disordered recovery in the rat dentate gyrus. [Abstract]. *Society for Neuroscience, 22* 2153.

Gottschall, P. E., & Yu, X. (1995). Cytokines regulate gelatinase A and B (matrix metalloproteinase 2 and 9) activity in cultured rat astrocytes. *Journal of Neurochemistry, 64*(4), 1513-1520.

Graham, D. I., McIntosh, T. K., Maxwell, W. L., & Nicoll, J. A. (2000). Recent advances in neurotrauma. *Journal of Neuropathology and Experimental Neurology, 59*(8), 641-651.

Grobelny, D., Poncz, L., & Galardy, R. E. (1992). Inhibition of human skin fibroblast collagenase, thermolysin, and pseudomonas aeruginosa elastase by peptide hydroxamic acids. *Biochemistry, 31*(31), 7152-7154.

Gross, J., & Lapiere, C. M. (1962). Collagenolytic activity in amphibian tissues: A tissue culture assay. *Proceedings of the National Academy of Sciences of the United States of America, 48*, 1014-1022.

Gurkoff, G. G., Giza, C. C., & Hovda, D. A. (2006). Lateral fluid percussion injury in the developing rat causes an acute, mild behavioral dysfunction in the absence of significant cell death. *Brain Research, 1077*(1), 24-36.

Halbleib, J. M., & Nelson, W. J. (2006). Cadherins in development: Cell adhesion, sorting, and tissue morphogenesis. *Genes & Development, 20*(23), 3199-3214.

Hall, R. J., & Erickson, C. A. (2003). ADAM 10: An active metalloprotease expressed during avian epithelial morphogenesis. *Developmental Biology, 256*(1), 146-159.

Hamm, R. J. (2001). Neurobehavioral assessment of outcome following traumatic brain injury in rats: An evaluation of selected measures. *Journal of Neurotrauma, 18*(11), 1207-1216.

Hamm, R. J., O'Dell, D. M., Pike, B. R., & Lyeth, B. G. (1993). Cognitive impairment following traumatic brain injury: The effect of pre- and post-injury administration of scopolamine and MK-801. *Brain Research.Cognitive Brain Research, 1*(4), 223-226.

Hamori, J. (1990). Morphological plasticity of postsynaptic neurones in reactive synaptogenesis. *The Journal of Experimental Biology, 153*, 251-260.

Hattori, M., Osterfield, M., & Flanagan, J. G. (2000). Regulated cleavage of a contact-mediated axon repellent. *Science (New York, N.Y.), 289*(5483), 1360-1365.

Hayashita-Kinoh, H., Kinoh, H., Okada, A., Komori, K., Itoh, Y., Chiba, T., et al. (2001). Membrane-type 5 matrix metalloproteinase is expressed in differentiated neurons

and regulates axonal growth. *Cell Growth & Differentiation : The Molecular Biology Journal of the American Association for Cancer Research, 12*(11), 573-580.

Hayes, R. L., Jenkins, L. W., & Lyeth, B. G. (1992). Neurotransmitter-mediated mechanisms of traumatic brain injury: Acetylcholine and excitatory amino acids. *Journal of Neurotrauma, 9 Suppl 1*, S173-87.

He, T. C., Sparks, A. B., Rago, C., Hermeking, H., Zawel, L., da Costa, L. T., et al. (1998). Identification of c-MYC as a target of the APC pathway. *Science (New York, N.Y.), 281*(5382), 1509-1512.

Hernandez-Barrantes, S., Bernardo, M., Toth, M., & Fridman, R. (2002). Regulation of membrane type-matrix metalloproteinases. *Seminars in Cancer Biology, 12*(2), 131-138.

Heupel, W. M., Baumgartner, W., Laymann, B., Drenckhahn, D., & Golenhofen, N. (2008). Different Ca2+ affinities and functional implications of the two synaptic adhesion molecules cadherin-11 and N-cadherin. *Molecular and Cellular Neurosciences, 37*(3), 548-558.

Hicks, R., Soares, H., Smith, D., & McIntosh, T., (1996). Temporal and spatial charachterization of neuronal injury following lateral fluid-percussion brain injury in the rat. *Acta Neuropathol* (Berlin), 91(3), 236-246.

Hoettecke, N., Ludwig, A., Foro, S., & Schmidt, B. (2010). Improved synthesis of ADAM10 inhibitor GI254023X. *Neuro-Degenerative Diseases, 7*(4), 232-238.

Hooper, N. M., & Lendeckel, U. (Eds.). (2005). *The adam family of proteases*. The Netherlands: Springer.

Hotary, K., Allen, E., Punturieri, A., Yana, I., & Weiss, S. J. (2000). Regulation of cell invasion and morphogenesis in a three-dimensional type I collagen matrix by membrane-type matrix metalloproteinases 1, 2, and 3. *The Journal of Cell Biology, 149*(6), 1309-1323.

Howard, L., Lu, X., Mitchell, S., Griffiths, S., & Glynn, P. (1996). Molecular cloning of MADM: A catalytically active mammalian disintegrin-metalloprotease expressed in various cell types. *The Biochemical Journal, 317 (Pt 1)*(Pt 1), 45-50.

Howard, L., Nelson, K. K., Maciewicz, R. A., & Blobel, C. P. (1999). Interaction of the metalloprotease disintegrins MDC9 and MDC15 with two SH3 domain-containing proteins, endophilin I and SH3PX1. *The Journal of Biological Chemistry, 274*(44), 31693-31699.

Hsu, J. Y., Bourguignon, L. Y., Adams, C. M., Peyrollier, K., Zhang, H., Fandel, T., et al. (2008). Matrix metalloproteinase-9 facilitates glial scar formation in the injured spinal cord. *The Journal of Neuroscience : The Official Journal of the Society for Neuroscience, 28*(50), 13467-13477.

Huber, O., Korn, R., McLaughlin, J., Ohsugi, M., Herrmann, B. G., & Kemler, R. (1996). Nuclear localization of beta-catenin by interaction with transcription factor LEF-1. *Mechanisms of Development, 59*(1), 3-10.

Hundhausen, C., Misztela, D., Berkhout, T. A., Broadway, N., Saftig, P., Reiss, K., et al. (2003). The disintegrin-like metalloproteinase ADAM10 is involved in constitutive cleavage of CX3CL1 (fractalkine) and regulates CX3CL1-mediated cell-cell adhesion. *Blood, 102*(4), 1186-1195.

Isaac, J. T., Nicoll, R. A., & Malenka, R. C. (1995). Evidence for silent synapses: Implications for the expression of LTP. *Neuron, 15*(2), 427-434.

Israelsson, C., Bengtsson, H., Kylberg, A., Kullander, K., Lewen, A., Hillered, L., et al. (2008). Distinct cellular patterns of upregulated chemokine expression supporting a prominent inflammatory role in traumatic brain injury. *Journal of Neurotrauma, 25*(8), 959-974.

Itoh, Y., Ito, N., Nagase, H., Evans, R. D., Bird, S. A., & Seiki, M. (2006). Cell surface collagenolysis requires homodimerization of the membrane-bound collagenase MT1-MMP. *Molecular Biology of the Cell, 17*(12), 5390-5399.

Itoh, Y., & Seiki, M. (2006). MT1-MMP: A potent modifier of pericellular microenvironment. *Journal of Cellular Physiology, 206*(1), 1-8.

Itoh, Y., Takamura, A., Ito, N., Maru, Y., Sato, H., Suenaga, N., et al. (2001). Homophilic complex formation of MT1-MMP facilitates proMMP-2 activation on the cell surface and promotes tumor cell invasion. *The EMBO Journal, 20*(17), 4782-4793.

Janes, P. W., Saha, N., Barton, W. A., Kolev, M. V., Wimmer-Kleikamp, S. H., Nievergall, E., et al. (2005). Adam meets eph: An ADAM substrate recognition

module acts as a molecular switch for ephrin cleavage in trans. *Cell, 123*(2), 291-304.

Jang, Y. N., Jung, Y. S., Lee, S. H., Moon, C. H., Kim, C. H., & Baik, E. J. (2009). Calpain-mediated N-cadherin proteolytic processing in brain injury. *The Journal of Neuroscience : The Official Journal of the Society for Neuroscience, 29*(18), 5974-5984.

Jaworski, D. M. (2000). Developmental regulation of membrane type-5 matrix metalloproteinase (MT5-MMP) expression in the rat nervous system. *Brain Research, 860*(1-2), 174-177.

Jontes, J. D., Emond, M. R., & Smith, S. J. (2004). In vivo trafficking and targeting of N-cadherin to nascent presynaptic terminals. *The Journal of Neuroscience : The Official Journal of the Society for Neuroscience, 24*(41), 9027-9034.

Jungling, K., Eulenburg, V., Moore, R., Kemler, R., Lessmann, V., & Gottmann, K. (2006). N-cadherin transsynaptically regulates short-term plasticity at glutamatergic synapses in embryonic stem cell-derived neurons. *The Journal of Neuroscience : The Official Journal of the Society for Neuroscience, 26*(26), 6968-6978.

Kamal, A., Almenar-Queralt, A., LeBlanc, J. F., Roberts, E. A., & Goldstein, L. S. (2001). Kinesin-mediated axonal transport of a membrane compartment containing beta-secretase and presenilin-1 requires APP. *Nature, 414*(6864), 643-648.

Kang, T., Nagase, H., & Pei, D. (2002). Activation of membrane-type matrix metalloproteinase 3 zymogen by the proprotein convertase furin in the trans-golgi network. *Cancer Research, 62*(3), 675-681.

Karkkainen, I., Rybnikova, E., Pelto-Huikko, M., & Huovila, A. P. (2000). Metalloprotease-disintegrin (ADAM) genes are widely and differentially expressed in the adult CNS. *Molecular and Cellular Neurosciences, 15*(6), 547-560.

Katayama, Y., Becker, D. P., Tamura, T., & Ikezaki, K. (1990). Early cellular swelling in experimental traumatic brain injury: A phenomenon mediated by excitatory amino acids. *Acta Neurochirurgica.Supplementum, 51*, 271-273.

Kelley, B. J., Farkas, O., Lifshitz, J., & Povlishock, J. T. (2006). Traumatic axonal injury in the perisomatic domain triggers ultrarapid secondary axotomy and wallerian degeneration. *Experimental Neurology, 198*(2), 350-360.

Keppel, G. (1991). *Design and analysis: A Researcher's handbook* (3rd ed.). Englewood Cliffs, New Jersey: Prentice Hall.

Keyvani, K., & Schallert, T. (2002). Plasticity-associated molecular and structural events in the injured brain. *Journal of Neuropathology and Experimental Neurology, 61*(10), 831-840.

Kieseier, B. C., Pischel, H., Neuen-Jacob, E., Tourtellotte, W. W., & Hartung, H. P. (2003). ADAM-10 and ADAM-17 in the inflamed human CNS. *Glia, 42*(4), 398-405.

Kim, H. J., Fillmore, H. L., Reeves, T. M., & Phillips, L. L. (2005). Elevation of hippocampal MMP-3 expression and activity during trauma-induced synaptogenesis. *Experimental Neurology, 192*(1), 60-72.

Kline, A. E., Massucci, J. L., Ma, X., Zafonte, R. D., & Dixon, C. E. (2004). Bromocriptine reduces lipid peroxidation and enhances spatial learning and hippocampal neuron survival in a rodent model of focal brain trauma. *Journal of Neurotrauma, 21*(12), 1712-1722.

Komori, K., Nonaka, T., Okada, A., Kinoh, H., Hayashita-Kinoh, H., Yoshida, N., et al. (2004). Absence of mechanical allodynia and abeta-fiber sprouting after sciatic nerve injury in mice lacking membrane-type 5 matrix metalloproteinase. *FEBS Letters, 557*(1-3), 125-128.

Krebs, L. T., Xue, Y., Norton, C. R., Shutter, J. R., Maguire, M., Sundberg, J. P., et al. (2000). Notch signaling is essential for vascular morphogenesis in mice. *Genes & Development, 14*(11), 1343-1352.

Kuruba, R., Hattiangady, B., & Shetty, A. K. (2009). Hippocampal neurogenesis and neural stem cells in temporal lobe epilepsy. *Epilepsy & Behavior : E&B, 14 Suppl 1*, 65-73.

LaFerla, F. M., Green, K. N., & Oddo, S. (2007). Intracellular amyloid-beta in alzheimer's disease. *Nature Reviews.Neuroscience, 8*(7), 499-509.

Laird, M. D., Vender, J. R., & Dhandapani, K. M. (2008). Opposing roles for reactive astrocytes following traumatic brain injury. *Neuro-Signals, 16*(2-3), 154-164.

Langlois, J. A., Rutland-Brown, W., & Wald, M. M. (2006). The epidemiology and impact of traumatic brain injury: A brief overview. *The Journal of Head Trauma Rehabilitation, 21*(5), 375-378.

Lathia, J. D., Mattson, M. P., & Cheng, A. (2008). Notch: From neural development to neurological disorders. *Journal of Neurochemistry, 107*(6), 1471-1481.

Leib, S. L., Leppert, D., Clements, J., & Tauber, M. G. (2000). Matrix metalloproteinases contribute to brain damage in experimental pneumococcal meningitis. *Infection and Immunity, 68*(2), 615-620.

Lele, Z., Folchert, A., Concha, M., Rauch, G. J., Geisler, R., Rosa, F., et al. (2002). Parachute/n-cadherin is required for morphogenesis and maintained integrity of the zebrafish neural tube. *Development (Cambridge, England), 129*(14), 3281-3294.

Lenzlinger, P. M., Morganti-Kossmann, M. C., Laurer, H. L., & McIntosh, T. K. (2001). The duality of the inflammatory response to traumatic brain injury. *Molecular Neurobiology, 24*(1-3), 169-181.

Letourneau, P. C., Shattuck, T. A., Roche, F. K., Takeichi, M., & Lemmon, V. (1990). Nerve growth cone migration onto schwann cells involves the calcium-dependent adhesion molecule, N-cadherin. *Developmental Biology, 138*(2), 430-442.

Leung, L. S., & Fu, X. W. (1994). Factors affecting paired-pulse facilitation in hippocampal CA1 neurons in vitro. *Brain Research, 650*(1), 75-84.

Levine, G. (1991). *A guide to SPSS for analysis of variance*. Hillsdale, New Jersey: Lawrence Erlbaum Associates.

Liao, D., Hessler, N. A., & Malinow, R. (1995). Activation of postsynaptically silent synapses during pairing-induced LTP in CA1 region of hippocampal slice. *Nature, 375*(6530), 400-404.

Lifshitz, J., Friberg, H., Neumar, R. W., Raghupathi, R., Welsh, F. A., Janmey, P., et al. (2003). Structural and functional damage sustained by mitochondria after traumatic brain injury in the rat: Evidence for differentially sensitive populations in the cortex and hippocampus. *Journal of Cerebral Blood Flow and Metabolism : Official Journal of the International Society of Cerebral Blood Flow and Metabolism, 23*(2), 219-231.

Lilien, J., Arregui, C., Li, H., & Balsamo, J. (1999). The juxtamembrane domain of cadherin regulates integrin-mediated adhesion and neurite outgrowth. *Journal of Neuroscience Research, 58*(6), 727-734.

Liuzzi, F. J., & Lasek, R. J. (1987). Astrocytes block axonal regeneration in mammals by activating the physiological stop pathway. *Science (New York, N.Y.), 237*(4815), 642-645.

Llano, E., Pendas, A. M., Freije, J. P., Nakano, A., Knauper, V., Murphy, G., et al. (1999). Identification and characterization of human MT5-MMP, a new membrane-

bound activator of progelatinase a overexpressed in brain tumors. *Cancer Research, 59*(11), 2570-2576.

Lloyd, E., Somera-Molina, K., Van Eldik, L. J., Watterson, D. M., & Wainwright, M. S. (2008). Suppression of acute proinflammatory cytokine and chemokine upregulation by post-injury administration of a novel small molecule improves long-term neurologic outcome in a mouse model of traumatic brain injury. *Journal of Neuroinflammation, 5*, 28.

Loesche, J., & Steward, O. (1977). Behavioral correlates of denervation and reinnervation of the hippocampal formation of the rat: Recovery of alternation performance following unilateral entorhinal cortex lesions. *Brain Research Bulletin, 2*(1), 31-39.

Lomo, T. (1971). Potentiation of monosynaptic EPSPs in the perforant path-dentate granule cell synapse. *Experimental Brain Research.Experimentelle Hirnforschung.Experimentation Cerebrale, 12*(1), 46-63.

Lonze, B. E., & Ginty, D. D. (2002). Function and regulation of CREB family transcription factors in the nervous system. *Neuron, 35*(4), 605-623.

Ludwig, A., Hundhausen, C., Lambert, M. H., Broadway, N., Andrews, R. C., Bickett, D. M., et al. (2005). Metalloproteinase inhibitors for the disintegrin-like metalloproteinases ADAM10 and ADAM17 that differentially block constitutive and phorbol ester-inducible shedding of cell surface molecules. *Combinatorial Chemistry & High Throughput Screening, 8*(2), 161-171.

Lum, L., Reid, M. S., & Blobel, C. P. (1998). Intracellular maturation of the mouse metalloprotease disintegrin MDC15. *The Journal of Biological Chemistry, 273*(40), 26236-26247.

Luo, J. (2005). The role of matrix metalloproteinases in the morphogenesis of the cerebellar cortex. *Cerebellum (London, England), 4*(4), 239-245.

Luo, Y., Ferreira-Cornwell, M., Baldwin, H., Kostetskii, I., Lenox, J., Lieberman, M., et al. (2001). Rescuing the N-cadherin knockout by cardiac-specific expression of N- or E-cadherin. *Development (Cambridge, England), 128*(4), 459-469.

Lynch, G., Gall, C., Rose, G., & Cotman, C. (1976). Changes in the distribution of the dentate gyrus associational system following unilateral or bilateral entorhinal lesions in the adult rat. *Brain Research, 110*(1), 57-71.

Lyuksyutova, A. I., Lu, C. C., Milanesio, N., King, L. A., Guo, N., Wang, Y., et al. (2003). Anterior-posterior guidance of commissural axons by wnt-frizzled signaling. *Science (New York, N.Y.), 302*(5652), 1984-1988.

Malenka, R. C., & Bear, M. F. (2004). LTP and LTD: An embarrassment of riches. *Neuron, 44*(1), 5-21.

Malenka, R. C., & Nicoll, R. A. (1999). Long-term potentiation--a decade of progress? *Science (New York, N.Y.), 285*(5435), 1870-1874.

Manabe, T., Togashi, H., Uchida, N., Suzuki, S. C., Hayakawa, Y., Yamamoto, M., et al. (2000). Loss of cadherin-11 adhesion receptor enhances plastic changes in

hippocampal synapses and modifies behavioral responses. *Molecular and Cellular Neurosciences, 15*(6), 534-546.

Mann, B., Gelos, M., Siedow, A., Hanski, M. L., Gratchev, A., Ilyas, M., et al. (1999). Target genes of beta-catenin-T cell-factor/lymphoid-enhancer-factor signaling in human colorectal carcinomas. *Proceedings of the National Academy of Sciences of the United States of America, 96*(4), 1603-1608.

Marambaud, P., Wen, P. H., Dutt, A., Shioi, J., Takashima, A., Siman, R., et al. (2003). A CBP binding transcriptional repressor produced by the PS1/epsilon-cleavage of N-cadherin is inhibited by PS1 FAD mutations. *Cell, 114*(5), 635-645.

Marcello, E., Gardoni, F., Mauceri, D., Romorini, S., Jeromin, A., Epis, R., et al. (2007). Synapse-associated protein-97 mediates alpha-secretase ADAM10 trafficking and promotes its activity. *The Journal of Neuroscience : The Official Journal of the Society for Neuroscience, 27*(7), 1682-1691.

Marcinkiewicz, M., & Seidah, N. G. (2000). Coordinated expression of beta-amyloid precursor protein and the putative beta-secretase BACE and alpha-secretase ADAM10 in mouse and human brain. *Journal of Neurochemistry, 75*(5), 2133-2143.

Marrs, G. S., Theisen, C. S., & Bruses, J. L. (2009). N-cadherin modulates voltage activated calcium influx via RhoA, p120-catenin, and myosin-actin interaction. *Molecular and Cellular Neurosciences, 40*(3), 390-400.

Maskos, K., & Bode, W. (2003). Structural basis of matrix metalloproteinases and tissue inhibitors of metalloproteinases. *Molecular Biotechnology, 25*(3), 241-266.

Maskos, K., Fernandez-Catalan, C., Huber, R., Bourenkov, G. P., Bartunik, H., Ellestad, G. A., et al. (1998). Crystal structure of the catalytic domain of human tumor necrosis factor-alpha-converting enzyme. *Proceedings of the National Academy of Sciences of the United States of America, 95*(7), 3408-3412.

Massucci, J. L., Kline, A. E., Ma, X., Zafonte, R. D., & Dixon, C. E. (2004). Time dependent alterations in dopamine tissue levels and metabolism after experimental traumatic brain injury in rats. *Neuroscience Letters, 372*(1-2), 127-131.

Maxwell, W. L., Povlishock, J. T., & Graham, D. L. (1997). A mechanistic analysis of nondisruptive axonal injury: A review. *Journal of Neurotrauma, 14*(7), 419-440.

Mayer, J., Hamel, M. G., & Gottschall, P. E. (2005). Evidence for proteolytic cleavage of brevican by the ADAMTSs in the dentate gyrus after excitotoxic lesion of the mouse entorhinal cortex. *BMC Neuroscience, 6*, 52.

McCarthy, M. M. (2003). Stretching the truth. why hippocampal neurons are so vulnerable following traumatic brain injury. *Experimental Neurology, 184*(1), 40-43.

McCusker, C. D., & Alfandari, D. (2009). Life after proteolysis: Exploring the signaling capabilities of classical cadherin cleavage fragments. *Communicative & Integrative Biology, 2*(2), 155-157.

McIntosh, T. K. (1994). Neurochemical sequelae of traumatic brain injury: Therapeutic implications. *Cerebrovascular and Brain Metabolism Reviews, 6*(2), 109-162.

McWilliams, R., & Lynch, G. (1978). Terminal proliferation and synaptogenesis following partial deafferentation: The reinnervation of the inner molecular layer of the dentate gyrus following removal of its commissural afferents. *The Journal of Comparative Neurology, 180*(3), 581-616.

Mechtersheimer, S., Gutwein, P., Agmon-Levin, N., Stoeck, A., Oleszewski, M., Riedle, S., et al. (2001). Ectodomain shedding of L1 adhesion molecule promotes cell migration by autocrine binding to integrins. *The Journal of Cell Biology, 155*(4), 661-673.

Meighan, P. C., Meighan, S. E., Davis, C. J., Wright, J. W., & Harding, J. W. (2007). Effects of matrix metalloproteinase inhibition on short- and long-term plasticity of schaffer collateral/CA1 synapses. *Journal of Neurochemistry, 102*(6), 2085-2096.

Mendez, P., De Roo, M., Poglia, L., Klauser, P., & Muller, D. (2010). N-cadherin mediates plasticity-induced long-term spine stabilization. *The Journal of Cell Biology, 189*(3), 589-600.

Monea, S., Jordan, B. A., Srivastava, S., DeSouza, S., & Ziff, E. B. (2006). Membrane localization of membrane type 5 matrix metalloproteinase by AMPA receptor binding protein and cleavage of cadherins. *The Journal of Neuroscience : The Official Journal of the Society for Neuroscience, 26*(8), 2300-2312.

Moon, R. T., Kohn, A. D., De Ferrari, G. V., & Kaykas, A. (2004). WNT and beta-catenin signalling: Diseases and therapies. *Nature Reviews.Genetics, 5*(9), 691-701.

Mori, H., Tomari, T., Koshikawa, N., Kajita, M., Itoh, Y., Sato, H., et al. (2002). CD44 directs membrane-type 1 matrix metalloproteinase to lamellipodia by associating with its hemopexin-like domain. *The EMBO Journal, 21*(15), 3949-3959.

Morris, R. G., Garrud, P., Rawlins, J. N., & O'Keefe, J. (1982). Place navigation impaired in rats with hippocampal lesions. *Nature, 297*(5868), 681-683.

Muir, K.W. (2006). Glutamate-based therapeutic approaches: Clinical trials with NMDA antagonists. *Current Opinions in Pharmacology*, 6(1), 53-60.

Nadler, J. V., & Cuthbertson, G. J. (1980). Kainic acid neurotoxicity toward hippocampal formation: Dependence on specific excitatory pathways. *Brain Research, 195*(1), 47-56.

Nagase, H., Visse, R., & Murphy, G. (2006). Structure and function of matrix metalloproteinases and TIMPs. *Cardiovascular Research, 69*(3), 562-573.

Nagase, H., & Woessner, J. F.,Jr. (1999). Matrix metalloproteinases. *The Journal of Biological Chemistry, 274*(31), 21491-21494.

Nagy, V., Bozdagi, O., Matynia, A., Balcerzyk, M., Okulski, P., Dzwonek, J., et al. (2006). Matrix metalloproteinase-9 is required for hippocampal late-phase long-term potentiation and memory. *The Journal of Neuroscience : The Official Journal of the Society for Neuroscience, 26*(7), 1923-1934.

Nakahara, H., Howard, L., Thompson, E. W., Sato, H., Seiki, M., Yeh, Y., et al. (1997). Transmembrane/cytoplasmic domain-mediated membrane type 1-matrix metalloprotease docking to invadopodia is required for cell invasion. *Proceedings of the National Academy of Sciences of the United States of America, 94*(15), 7959-7964.

Naor, D., Sionov, R. V., & Ish-Shalom, D. (1997). CD44: Structure, function, and association with the malignant process. *Advances in Cancer Research, 71*, 241-319.

National Institute of Health Consensus Developmental Panel. Rehabilitation of persons with traumatic brain injury. *Journal of American Medical Association, 282*, 974-983.

Neurobehavioral Guidelines Working Group, Warden, D. L., Gordon, B., McAllister, T. W., Silver, J. M., Barth, J. T., et al. (2006). Guidelines for the pharmacologic treatment of neurobehavioral sequelae of traumatic brain injury. *Journal of Neurotrauma, 23*(10), 1468-1501.

Noble, L. J., Donovan, F., Igarashi, T., Goussev, S., & Werb, Z. (2002). Matrix metalloproteinases limit functional recovery after spinal cord injury by modulation of early vascular events. *The Journal of Neuroscience : The Official Journal of the Society for Neuroscience, 22*(17), 7526-7535.

Noe, V., Willems, J., Vandekerckhove, J., Roy, F. V., Bruyneel, E., & Mareel, M. (1999). Inhibition of adhesion and induction of epithelial cell invasion by HAV-containing E-cadherin-specific peptides. *Journal of Cell Science, 112 (Pt 1)*(Pt 1), 127-135.

Nuriya, M., & Huganir, R. L. (2006). Regulation of AMPA receptor trafficking by N-cadherin. *Journal of Neurochemistry, 97*(3), 652-661.

Oda, H., & Tsukita, S. (1999). Nonchordate classic cadherins have a structurally and functionally unique domain that is absent from chordate classic cadherins. *Developmental Biology, 216*(1), 406-422.

O'Keefe, J., & Nadel, L. (1978). *The hippocampus as a cognitive map*. Oxford: Clarendon Press.

Okonowo, D. O., & Povlishock, J. T. Immunosuppressants in traumatic brain injury. *Immunosuppressant analogs in neuroprotection* (pp. 263-281). New Jersey: Humana Press.

Okumura, Y., Sato, H., Seiki, M., & Kido, H. (1997). Proteolytic activation of the precursor of membrane type 1 matrix metalloproteinase by human plasmin. A possible cell surface activator. *FEBS Letters, 402*(2-3), 181-184.

Ortiz, R. M., Karkkainen, I., Huovila, A. P., & Honkaniemi, J. (2005). ADAM9, ADAM10, and ADAM15 mRNA levels in the rat brain after kainic acid-induced status epilepticus. *Brain Research.Molecular Brain Research, 137*(1-2), 272-275.

Osenkowski, P., Toth, M., & Fridman, R. (2004). Processing, shedding, and endocytosis of membrane type 1-matrix metalloproteinase (MT1-MMP). *Journal of Cellular Physiology, 200*(1), 2-10.

Palmer, A. M., Marion, D. W., Botscheller, M. L., Swedlow, P. E., Styren, S. D., & DeKosky, S. T. (1993). Traumatic brain injury-induced excitotoxicity assessed in a controlled cortical impact model. *Journal of Neurochemistry, 61*(6), 2015-2024.

Pan, D., & Rubin, G. M. (1997). Kuzbanian controls proteolytic processing of notch and mediates lateral inhibition during drosophila and vertebrate neurogenesis. *Cell, 90*(2), 271-280.

Paradies, N. E., & Grunwald, G. B. (1993). Purification and characterization of NCAD90, a soluble endogenous form of N-cadherin, which is generated by proteolysis during retinal development and retains adhesive and neurite-promoting function. *Journal of Neuroscience Research, 36*(1), 33-45.

Parks, W. C., & Mecham, R. P. (Eds.). (1998). *Matrix metalloproteinases*. San Diego: Academic Press.

Pasquale, E. B. (2005). Eph receptor signalling casts a wide net on cell behaviour. *Nature Reviews.Molecular Cell Biology, 6*(6), 462-475.

Pei, D. (1999). Identification and characterization of the fifth membrane-type matrix metalloproteinase MT5-MMP. *The Journal of Biological Chemistry, 274*(13), 8925-8932.

Pei, D., & Weiss, S. J. (1995). Furin-dependent intracellular activation of the human stromelysin-3 zymogen. *Nature, 375*(6528), 244-247.

Pettus, E. H., Christman, C. W., Giebel, M. L., & Povlishock, J. T. (1994). Traumatically induced altered membrane permeability: Its relationship to traumatically induced reactive axonal change. *Journal of Neurotrauma, 11*(5), 507-522.

Phillips, L. L., Lyeth, B. G., Hamm, R. J., Jiang, J. Y., Povlishock, J. T., & Reeves, T. M. (1997). Effect of prior receptor antagonism on behavioral morbidity produced by combined fluid percussion injury and entorhinal cortical lesion. *Journal of Neuroscience Research, 49*(2), 197-206.

Phillips, L. L., Lyeth, B. G., Hamm, R. J., & Povlishock, J. T. (1994). Combined fluid percussion brain injury and entorhinal cortical lesion: A model for assessing the interaction between neuroexcitation and deafferentation. *Journal of Neurotrauma, 11*(6), 641-656.

Phillips, L. L., Lyeth, B. G., Hamm, R. J., Reeves, T. M., & Povlishock, J. T. (1998). Glutamate antagonism during secondary deafferentation enhances cognition and axo-dendritic integrity after traumatic brain injury. *Hippocampus, 8*(4), 390-401.

Phillips, L. L., & Reeves, T. M. (2001). Interactive pathology following traumatic brain injury modifies hippocampal plasticity. *Restorative Neurology and Neuroscience, 19*(3-4), 213-235.

Pizzi, M. A., & Crowe, M. J. (2007). Matrix metalloproteinases and proteoglycans in axonal regeneration. *Experimental Neurology, 204*(2), 496-511.

Postina, R., Schroeder, A., Dewachter, I., Bohl, J., Schmitt, U., Kojro, E., et al. (2004). A disintegrin-metalloproteinase prevents amyloid plaque formation and hippocampal defects in an alzheimer disease mouse model. *The Journal of Clinical Investigation, 113*(10), 1456-1464.

Povlishock, J. T., & Christman, C. W. (1995). The pathobiology of traumatically induced axonal injury in animals and humans: A review of current thoughts. *Journal of Neurotrauma, 12*(4), 555-564.

Povlishock, J. T., Erb, D. E., & Astruc, J. (1992). Axonal response to traumatic brain injury: Reactive axonal change, deafferentation, and neuroplasticity. *Journal of Neurotrauma, 9 Suppl 1*, S189-200.

Povlishock, J. T., & Jenkins, L. W. (1995). Are the pathobiological changes evoked by traumatic brain injury immediate and irreversible? *Brain Pathology (Zurich, Switzerland), 5*(4), 415-426.

Povlishock, J. T., & Pettus, E. H. (1996). Traumatically induced axonal damage: Evidence for enduring changes in axolemmal permeability with associated cytoskeletal change. *Acta Neurochirurgica.Supplement, 66*, 81-86.

Pruessmeyer, J., & Ludwig, A. (2009). The good, the bad and the ugly substrates for ADAM10 and ADAM17 in brain pathology, inflammation and cancer. *Seminars in Cell & Developmental Biology, 20*(2), 164-174.

Quinn, T. M., Maung, A. A., Grodzinsky, A. J., Hunziker, E. B., & Sandy, J. D. (1999). Physical and biological regulation of proteoglycan turnover around chondrocytes in cartilage explants. implications for tissue degradation and repair. *Annals of the New York Academy of Sciences, 878*, 420-441.

Rasouli, A., Bhatia, N., Dinh, P., Cahill, K., Suryadevara, S., & Gupta, R. (2009). Resection of glial scar following spinal cord injury. *Journal of Orthopaedic Research : Official Publication of the Orthopaedic Research Society, 27*(7), 931-936.

Redies, C., & Takeichi, M. (1993). Expression of N-cadherin mRNA during development of the mouse brain. *Developmental Dynamics : An Official Publication of the American Association of Anatomists, 197*(1), 26-39.

Reeves, T. M., Prins, M. L., Zhu, J., Povlishock, J. T., & Phillips, L. L. (2003). Matrix metalloproteinase inhibition alters functional and structural correlates of deafferentation-induced sprouting in the dentate gyrus. *The Journal of Neuroscience : The Official Journal of the Society for Neuroscience, 23*(32), 10182-10189.

Reeves, T. M., & Smith, D. C. (1987). Reinnervation of the dentate gyrus and recovery of alternation behavior following entorhinal cortex lesions. *Behavioral Neuroscience, 101*(2), 179-186.

Reeves, T. M., & Steward, O. (1986). Emergence of the capacity for LTP during reinnervation of the dentate gyrus: Evidence that abnormally shaped spines can

mediate LTP. *Experimental Brain Research.Experimentelle Hirnforschung.Experimentation Cerebrale, 65*(1), 167-175.

Reeves, T. M., Zhu, J., Povlishock, J. T., & Phillips, L. L. (1997). The effect of combined fluid percussion and entorhinal cortical lesions on long-term potentiation. *Neuroscience, 77*(2), 431-444.

Reiss, K., Maretzky, T., Ludwig, A., Tousseyn, T., de Strooper, B., Hartmann, D., et al. (2005). ADAM10 cleavage of N-cadherin and regulation of cell-cell adhesion and beta-catenin nuclear signalling. *The EMBO Journal, 24*(4), 742-752.

Reiss, K., & Saftig, P. (2009). The "a disintegrin and metalloprotease" (ADAM) family of sheddases: Physiological and cellular functions. *Seminars in Cell & Developmental Biology, 20*(2), 126-137.

Roberts, C. M., Tani, P. H., Bridges, L. C., Laszik, Z., & Bowditch, R. D. (1999). MDC-L, a novel metalloprotease disintegrin cysteine-rich protein family member expressed by human lymphocytes. *The Journal of Biological Chemistry, 274*(41), 29251-29259.

Roelle, S., Grosse, R., Aigner, A., Krell, H. W., Czubayko, F., & Gudermann, T. (2003). Matrix metalloproteinases 2 and 9 mediate epidermal growth factor receptor transactivation by gonadotropin-releasing hormone. *The Journal of Biological Chemistry, 278*(47), 47307-47318.

Roghani, M., Becherer, J. D., Moss, M. L., Atherton, R. E., Erdjument-Bromage, H., Arribas, J., et al. (1999). Metalloprotease-disintegrin MDC9: Intracellular maturation and catalytic activity. *The Journal of Biological Chemistry, 274*(6), 3531-3540.

Romanic, A. M., White, R. F., Arleth, A. J., Ohlstein, E. H., & Barone, F. C. (1998). Matrix metalloproteinase expression increases after cerebral focal ischemia in rats: Inhibition of matrix metalloproteinase-9 reduces infarct size. *Stroke; a Journal of Cerebral Circulation, 29*(5), 1020-1030.

Rosenberg, G. A. (1995). Matrix metalloproteinases in brain injury. *Journal of Neurotrauma, 12*(5), 833-842.

Rosenberg, G. A. (2002). Matrix metalloproteinases in neuroinflammation. *Glia, 39*(3), 279-291.

Rosenberg, G. A. (2009). Matrix metalloproteinases and their multiple roles in neurodegenerative diseases. *Lancet Neurology, 8*(2), 205-216.

Rosenberg, G. A., Dencoff, J. E., Correa, N.,Jr, Reiners, M., & Ford, C. C. (1996). Effect of steroids on CSF matrix metalloproteinases in multiple sclerosis: Relation to blood-brain barrier injury. *Neurology, 46*(6), 1626-1632.

Rosenberg, G. A., Estrada, E. Y., & Mobashery, S. (2007). Effect of synthetic matrix metalloproteinase inhibitors on lipopolysaccharide-induced blood-brain barrier opening in rodents: Differences in response based on strains and solvents. *Brain Research, 1133*(1), 186-192.

Rosenberg, G. A., Navratil, M., Barone, F., & Feuerstein, G. (1996). Proteolytic cascade enzymes increase in focal cerebral ischemia in rat. *Journal of Cerebral Blood Flow and Metabolism : Official Journal of the International Society of Cerebral Blood Flow and Metabolism, 16*(3), 360-366.

Rosenberg, G. A., Sullivan, N., & Esiri, M. M. (2001). White matter damage is associated with matrix metalloproteinases in vascular dementia. *Stroke; a Journal of Cerebral Circulation, 32*(5), 1162-1168.

Rudge, J. S., & Silver, J. (1990). Inhibition of neurite outgrowth on astroglial scars in vitro. *The Journal of Neuroscience : The Official Journal of the Society for Neuroscience, 10*(11), 3594-3603.

Sabo, S. L., Ikin, A. F., Buxbaum, J. D., & Greengard, P. (2001). The alzheimer amyloid precursor protein (APP) and FE65, an APP-binding protein, regulate cell movement. *The Journal of Cell Biology, 153*(7), 1403-1414.

Saftig, P., & Hartmann, D. (2005). ADAM-10. In N. M. Hooper, & U. Lendeckel (Eds.), *The ADAM family of proteases* (pp. 85-121). Netherlands: Springer.

Sahin, U., Weskamp, G., Kelly, K., Zhou, H. M., Higashiyama, S., Peschon, J., et al. (2004). Distinct roles for ADAM10 and ADAM17 in ectodomain shedding of six EGFR ligands. *The Journal of Cell Biology, 164*(5), 769-779.

Sastre, M. (2010). Troubleshooting methods for APP processing in vitro. *Journal of Pharmacological and Toxicological Methods, 61*(2), 86-91.

Sato, H., Kinoshita, T., Takino, T., Nakayama, K., & Seiki, M. (1996). Activation of a recombinant membrane type 1-matrix metalloproteinase (MT1-MMP) by furin and its interaction with tissue inhibitor of metalloproteinases (TIMP)-2. *FEBS Letters, 393*(1), 101-104.

Sato, H., & Seiki, M. (1996). Membrane-type matrix metalloproteinases (MT-MMPs) in tumor metastasis. *Journal of Biochemistry, 119*(2), 209-215.

Scheff, S., Benardo, I., & Cotman, C. (1977). Progressive brain damage accelerates axon sprouting in the adult rat. *Science (New York, N.Y.), 197*(4305), 795-797.

Schultz, G. S., Strelow, S., Stern, G. A., Chegini, N., Grant, M. B., Galardy, R. E., et al. (1992). Treatment of alkali-injured rabbit corneas with a synthetic inhibitor of matrix metalloproteinases. *Investigative Ophthalmology & Visual Science, 33*(12), 3325-3331.

Seals, D. F., & Courtneidge, S. A. (2003). The ADAMs family of metalloproteases: Multidomain proteins with multiple functions. *Genes & Development, 17*(1), 7-30.

Sekine-Aizawa, Y., Hama, E., Watanabe, K., Tsubuki, S., Kanai-Azuma, M., Kanai, Y., et al. (2001). Matrix metalloproteinase (MMP) system in brain: Identification and characterization of brain-specific MMP highly expressed in cerebellum. *The European Journal of Neuroscience, 13*(5), 935-948.

Shan, W. S., Tanaka, H., Phillips, G. R., Arndt, K., Yoshida, M., Colman, D. R., et al. (2000). Functional cis-heterodimers of N- and R-cadherins. *The Journal of Cell Biology, 148*(3), 579-590.

Shigemori, Y., Katayama, Y., Mori, T., Maeda, T., & Kawamata, T. (2006). Matrix metalloproteinase-9 is associated with blood-brain barrier opening and brain edema formation after cortical contusion in rats. *Acta Neurochirurgica.Supplement, 96*, 130-133.

Shtutman, M., Zhurinsky, J., Simcha, I., Albanese, C., D'Amico, M., Pestell, R., et al. (1999). The cyclin D1 gene is a target of the beta-catenin/LEF-1 pathway. *Proceedings of the National Academy of Sciences of the United States of America, 96*(10), 5522-5527.

Sifringer, M., Stefovska, V., Zentner, I., Hansen, B., Stepulak, A., Knaute, C., et al. (2007). The role of matrix metalloproteinases in infant traumatic brain injury. *Neurobiology of Disease, 25*(3), 526-535.

Silverman, J. B., Restituito, S., Lu, W., Lee-Edwards, L., Khatri, L., & Ziff, E. B. (2007). Synaptic anchorage of AMPA receptors by cadherins through neural plakophilin-related arm protein AMPA receptor-binding protein complexes. *The Journal of Neuroscience : The Official Journal of the Society for Neuroscience, 27*(32), 8505-8516.

Sofroniew, M. V. (2005). Reactive astrocytes in neural repair and protection. *The Neuroscientist : A Review Journal Bringing Neurobiology, Neurology and Psychiatry, 11*(5), 400-407.

Sounni, N. E., & Noel, A. (2005). Membrane type-matrix metalloproteinases and tumor progression. *Biochimie, 87*(3-4), 329-342.

Squire, L. R. (1992). Memory and the hippocampus: A synthesis from findings with rats, monkeys, and humans. *Psychological Review, 99*(2), 195-231.

Stamenkovic, I. (2003). Extracellular matrix remodelling: The role of matrix metalloproteinases. *The Journal of Pathology, 200*(4), 448-464.

Sternlicht, M. D., & Werb, Z. (2001). How matrix metalloproteinases regulate cell behavior. *Annual Review of Cell and Developmental Biology, 17*, 463-516.

Steward, O., & Vinsant, S. L. (1983). The process of reinnervation in the dentate gyrus of the adult rat: A quantitative electron microscope analysis of terminal proliferation and reactive synaptogenesis. *J.Comp.Neurol., 214*, 370-386.

Steward, O. (1989). Reorganization of neuronal connections following CNS trauma: Principles and experimental paradigms. *Journal of Neurotrauma, 6*(2), 99-152.

Steward, O., Vinsant, S. L., & Davis, L. (1988). The process of reinnervation in the dentate gyrus of adult rats: An ultrastructural study of changes in presynaptic terminals as a result of sprouting. *The Journal of Comparative Neurology, 267*(2), 203-210.

Stone, J. R., Okonkwo, D. O., Dialo, A. O., Rubin, D. G., Mutlu, L. K., Povlishock, J. T., et al. (2004). Impaired axonal transport and altered axolemmal permeability occur in distinct populations of damaged axons following traumatic brain injury. *Experimental Neurology, 190*(1), 59-69.

Strongin, A. Y., Collier, I., Bannikov, G., Marmer, B. L., Grant, G. A., & Goldberg, G. I. (1995). Mechanism of cell surface activation of 72-kDa type IV collagenase. isolation of the activated form of the membrane metalloprotease. *The Journal of Biological Chemistry, 270*(10), 5331-5338.

Su, Z., Han, D., Sun, B., Qiu, J., Li, Y., Li, M., et al. (2009). Heat stress preconditioning improves cognitive outcome after diffuse axonal injury in rats. *Journal of Neurotrauma, 26*(10), 1695-1706.

Su, Z., Yuan, Y., Chen, J., Cao, L., Zhu, Y., Gao, L., et al. (2009). Reactive astrocytes in glial scar attract olfactory ensheathing cells migration by secreted TNF-alpha in spinal cord lesion of rat. *PloS One, 4*(12), e8141.

Suehiro, E., Fujisawa, H., Akimura, T., Ishihara, H., Kajiwara, K., Kato, S., et al. (2004). Increased matrix metalloproteinase-9 in blood in association with activation of interleukin-6 after traumatic brain injury: Influence of hypothermic therapy. *Journal of Neurotrauma, 21*(12), 1706-1711.

Suzuki, S. C., & Takeichi, M. (2008). Cadherins in neuronal morphogenesis and function. *Development, Growth & Differentiation, 50 Suppl 1*, S119-30.

Szklarczyk, A., Lapinska, J., Rylski, M., McKay, R. D., & Kaczmarek, L. (2002). Matrix metalloproteinase-9 undergoes expression and activation during dendritic remodeling in adult hippocampus. *The Journal of Neuroscience : The Official Journal of the Society for Neuroscience, 22*(3), 920-930.

Takeda, S. (2009). Three-dimensional domain architecture of the ADAM family proteinases. *Seminars in Cell & Developmental Biology, 20*(2), 146-152.

Takeichi, M., & Abe, K. (2005). Synaptic contact dynamics controlled by cadherin and catenins. *Trends in Cell Biology, 15*(4), 216-221.

Tanabe, K., Takeichi, M., & Nakagawa, S. (2004). Identification of a nonchordate-type classic cadherin in vertebrates: Chicken hz-cadherin is expressed in horizontal cells of the neural retina and contains a nonchordate-specific domain complex. *Developmental Dynamics : An Official Publication of the American Association of Anatomists, 229*(4), 899-906.

Tanaka, H., Shan, W., Phillips, G. R., Arndt, K., Bozdagi, O., Shapiro, L., et al. (2000). Molecular modification of N-cadherin in response to synaptic activity. *Neuron, 25*(1), 93-107.

Tang, K., & Zhang, J. T. (2002). The effects of (-)clausenamide on functional recovery in transient focal cerebral ischemia. *Neurological Research, 24*(5), 473-478.

Tang, L., Hung, C. P., & Schuman, E. M. (1998). A role for the cadherin family of cell adhesion molecules in hippocampal long-term potentiation. *Neuron, 20*(6), 1165-1175.

Taupin, P. (2006). Neurogenesis in the adult central nervous system. *Comptes Rendus Biologies, 329*(7), 465-475.

Teasdale, G., & Jennett, B. (1974). Assessment of coma and impaired consciousness. A practical scale. *Lancet, 2*(7872), 81-84.

Thiery, J. P. (2003). Cell adhesion in development: A complex signaling network. *Current Opinion in Genetics & Development, 13*(4), 365-371.

Toft-Hansen, H., Babcock, A. A., Millward, J. M., & Owens, T. (2007). Downregulation of membrane type-matrix metalloproteinases in the inflamed or injured central nervous system. *Journal of Neuroinflammation, 4*, 24.

Togashi, H., Abe, K., Mizoguchi, A., Takaoka, K., Chisaka, O., & Takeichi, M. (2002). Cadherin regulates dendritic spine morphogenesis. *Neuron, 35*(1), 77-89.

Truettner, J. S., Alonso, O. F., & Dalton Dietrich, W. (2005). Influence of therapeutic hypothermia on matrix metalloproteinase activity after traumatic brain injury in rats. *Journal of Cerebral Blood Flow and Metabolism : Official Journal of the International Society of Cerebral Blood Flow and Metabolism, 25*(11), 1505-1516.

Uchida, N., Honjo, Y., Johnson, K. R., Wheelock, M. J., & Takeichi, M. (1996). The catenin/cadherin adhesion system is localized in synaptic junctions bordering transmitter release zones. *The Journal of Cell Biology, 135*(3), 767-779.

Uemura, K., Kihara, T., Kuzuya, A., Okawa, K., Nishimoto, T., Bito, H., et al. (2006). Activity-dependent regulation of beta-catenin via epsilon-cleavage of N-cadherin. *Biochemical and Biophysical Research Communications, 345*(3), 951-958.

Uemura, K., Kihara, T., Kuzuya, A., Okawa, K., Nishimoto, T., Ninomiya, H., et al. (2006). Characterization of sequential N-cadherin cleavage by ADAM10 and PS1. *Neuroscience Letters, 402*(3), 278-283.

Utton, M. A., Eickholt, B., Howell, F. V., Wallis, J., & Doherty, P. (2001). Soluble N-cadherin stimulates fibroblast growth factor receptor dependent neurite outgrowth and N-cadherin and the fibroblast growth factor receptor co-cluster in cells. *Journal of Neurochemistry, 76*(5), 1421-1430.

Vajtr, D., Benada, O., Kukacka, J., Prusa, R., Houstava, L., Toupalik, P., et al. (2009). Correlation of ultrastructural changes of endothelial cells and astrocytes occurring during blood brain barrier damage after traumatic brain injury with biochemical markers of BBB leakage and inflammatory response. *Physiological Research / Academia Scientiarum Bohemoslovaca, 58*(2), 263-268.

Verweij, B. H., Amelink, G. J., & Muizelaar, J. P. (2007). Current concepts of cerebral oxygen transport and energy metabolism after severe traumatic brain injury.

Neurotrauma: New insights into pathology and treatment (1st ed., pp. 111-124). Oxford, UK: Elsevier Science.

Vilalta, A., Sahuquillo, J., Rosell, A., Poca, M. A., Riveiro, M., & Montaner, J. (2008). Moderate and severe traumatic brain injury induce early overexpression of systemic and brain gelatinases. *Intensive Care Medicine, 34*(8), 1384-1392.

Wagner, A. K., Kline, A. E., Ren, D., Willard, L. A., Wenger, M. K., Zafonte, R. D., et al. (2007). Gender associations with chronic methylphenidate treatment and behavioral performance following experimental traumatic brain injury. *Behavioural Brain Research, 181*(2), 200-209.

Wagner, A. K., Sokoloski, J. E., Ren, D., Chen, X., Khan, A. S., Zafonte, R. D., et al. (2005). Controlled cortical impact injury affects dopaminergic transmission in the rat striatum. *Journal of Neurochemistry, 95*(2), 457-465.

Wang, J., & Tsirka, S. E. (2005). Neuroprotection by inhibition of matrix metalloproteinases in a mouse model of intracerebral haemorrhage. *Brain : A Journal of Neurology, 128*(Pt 7), 1622-1633.

Wang, P., Wang, X., & Pei, D. (2004). Mint-3 regulates the retrieval of the internalized membrane-type matrix metalloproteinase, MT5-MMP, to the plasma membrane by binding to its carboxyl end motif EWV. *The Journal of Biological Chemistry, 279*(19), 20461-20470.

Wang, X., Jung, J., Asahi, M., Chwang, W., Russo, L., Moskowitz, M. A., et al. (2000). Effects of matrix metalloproteinase-9 gene knock-out on morphological and motor outcomes after traumatic brain injury. *The Journal of Neuroscience : The Official Journal of the Society for Neuroscience, 20*(18), 7037-7042.

Wang, X., & Pei, D. (2001). Shedding of membrane type matrix metalloproteinase 5 by a furin-type convertase: A potential mechanism for down-regulation. *The Journal of Biological Chemistry, 276*(38), 35953-35960.

Wang, X., Yi, J., Lei, J., & Pei, D. (1999). Expression, purification and characterization of recombinant mouse MT5-MMP protein products. *FEBS Letters, 462*(3), 261-266.

Warren, K. M., Colley, B. S., Reeves, T. M., & Phillips, L. L. (2009). Post-injury matrix metalloproteinase inhibition targeting the onset of synaptogenesis enhances synaptic efficacy and promotes long-term synapse stabilization [Abstract]. *Journal of Neurotrauma, 26* A-77.

Warren, K. M., Lee, N. N., Black, R. T., Reeves, T. M., & Phillips, L. L. (2008). Recovery dependent differences in membrane-type 5 matrix metalloproteinase and n-cadherin expression during injury-induced synaptogenesis [Abstract]. *Journal of Neurotrauma, 25* 900.

Wells, G. M., Catlin, G., Cossins, J. A., Mangan, M., Ward, G. A., Miller, K. M., et al. (1996). Quantitation of matrix metalloproteinases in cultured rat astrocytes using the polymerase chain reaction with a multi-competitor cDNA standard. *Glia, 18*(4), 332-340.

Westling, J., Gottschall, P. E., Thompson, V. P., Cockburn, A., Perides, G., Zimmermann, D. R., et al. (2004). ADAMTS4 (aggrecanase-1) cleaves human brain versican V2 at Glu405-Gln406 to generate glial hyaluronate binding protein. *The Biochemical Journal, 377*(Pt 3), 787-795.

White, J. M. (2003). ADAMs: Modulators of cell-cell and cell-matrix interactions. *Current Opinion in Cell Biology, 15*(5), 598-606.

White, R. E., & Jakeman, L. B. (2008). Don't fence me in: Harnessing the beneficial roles of astrocytes for spinal cord repair. *Restorative Neurology and Neuroscience, 26*(2-3), 197-214.

Wilby, M. J., Muir, E. M., Fok-Seang, J., Gour, B. J., Blaschuk, O. W., & Fawcett, J. W. (1999). N-cadherin inhibits schwann cell migration on astrocytes. *Molecular and Cellular Neurosciences, 14*(1), 66-84.

Wilhelmsson, U., Bushong, E. A., Price, D. L., Smarr, B. L., Phung, V., Terada, M., et al. (2006). Redefining the concept of reactive astrocytes as cells that remain within their unique domains upon reaction to injury. *Proceedings of the National Academy of Sciences of the United States of America, 103*(46), 17513-17518.

Wolf, J. A., Stys, P. K., Lusardi, T., Meaney, D., & Smith, D. H. (2001). Traumatic axonal injury induces calcium influx modulated by tetrodotoxin-sensitive sodium channels. *The Journal of Neuroscience : The Official Journal of the Society for Neuroscience, 21*(6), 1923-1930.

Wu, Y. I., Munshi, H. G., Snipas, S. J., Salvesen, G. S., Fridman, R., & Stack, M. S. (2007). Activation-coupled membrane-type 1 matrix metalloproteinase membrane trafficking. *The Biochemical Journal, 407*(2), 171-177.

Yamagata, M., Weiner, J. A., & Sanes, J. R. (2002). Sidekicks: Synaptic adhesion molecules that promote lamina-specific connectivity in the retina. *Cell, 110*(5), 649-660.

Yang, P., Baker, K. A., & Hagg, T. (2006). The ADAMs family: Coordinators of nervous system development, plasticity and repair. *Progress in Neurobiology, 79*(2), 73-94.

Yang, Y., Estrada, E. Y., Thompson, J. F., Liu, W., & Rosenberg, G. A. (2007). Matrix metalloproteinase-mediated disruption of tight junction proteins in cerebral vessels is reversed by synthetic matrix metalloproteinase inhibitor in focal ischemia in rat. *Journal of Cerebral Blood Flow and Metabolism : Official Journal of the International Society of Cerebral Blood Flow and Metabolism, 27*(4), 697-709.

Yong, V. W. (2005). Metalloproteinases: Mediators of pathology and regeneration in the CNS. *Nature Reviews.Neuroscience, 6*(12), 931-944.

Yong, V. W., Power, C., Forsyth, P., & Edwards, D. R. (2001). Metalloproteinases in biology and pathology of the nervous system. *Nature Reviews.Neuroscience, 2*(7), 502-511.

Yoshino, A., Hovda, D. A., Katayama, Y., Kawamata, T., & Becker, D. P. (1992). Hippocampal CA3 lesion prevents postconcussive metabolic dysfunction in CA1.

Journal of Cerebral Blood Flow and Metabolism : Official Journal of the International Society of Cerebral Blood Flow and Metabolism, 12(6), 996-1006.

Yu, X., & Malenka, R. C. (2003). Beta-catenin is critical for dendritic morphogenesis. *Nature Neuroscience, 6*(11), 1169-1177.

Zalewska, T., Ziemka-Nalecz, M., Sarnowska, A., & Domanska-Janik, K. (2003). Transient forebrain ischemia modulates signal transduction from extracellular matrix in gerbil hippocampus. *Brain Research, 977*(1), 62-69.

Zhu, J., Hamm, R. J., Reeves, T. M., Povlishock, J. T., & Phillips, L. L. (2000). Postinjury administration of L-deprenyl improves cognitive function and enhances neuroplasticity after traumatic brain injury. *Experimental Neurology, 166*(1), 136-152.

Zucker, R. S. (1989). Short-term synaptic plasticity. *Annual Review of Neuroscience, 12*, 13-31.

Appendix A

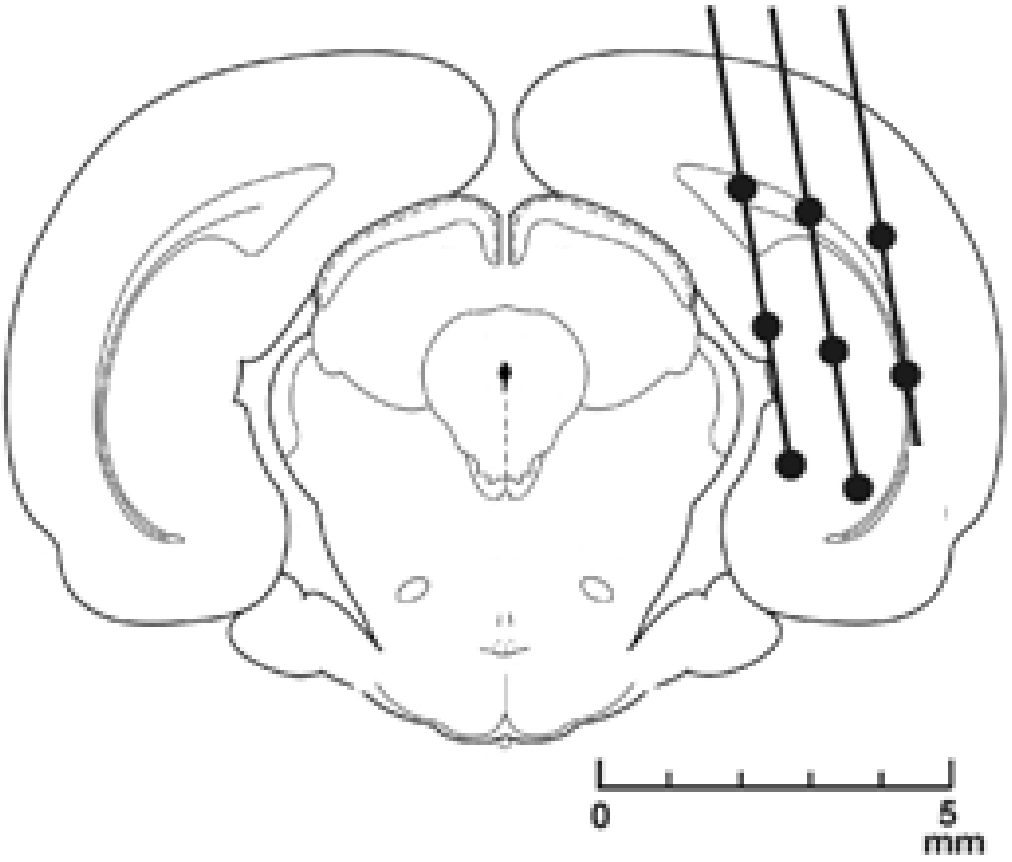

Figure A-1 Unilateral Entorhinal Cortex Lesion Stereotaxic Sites. Coronal section of rat brain with stereotaxic lesion sites indicated by black circles at 3, 4, and 5mm lateral to midline.

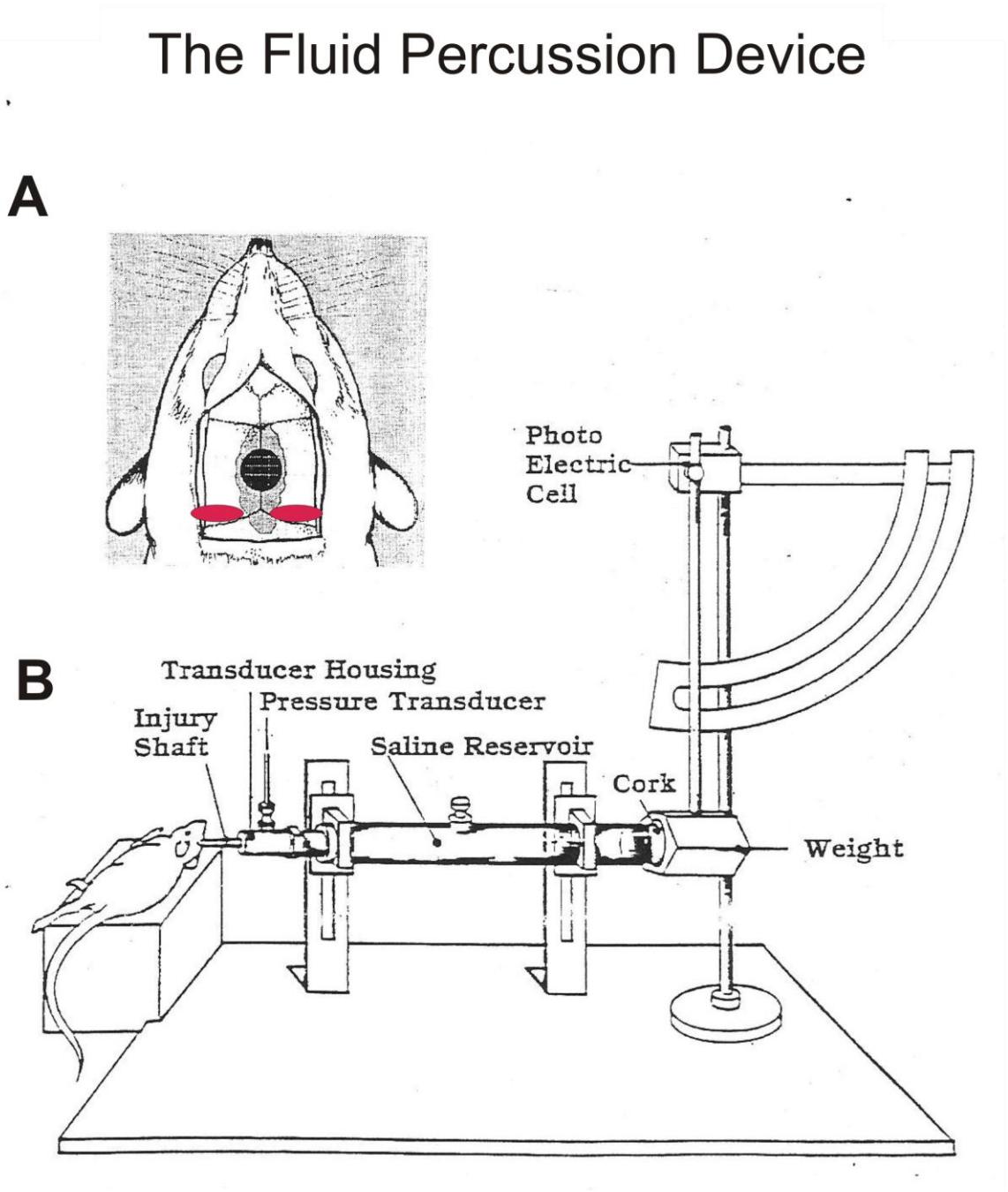

Figure A-2 Craniectomy Sites and Fluid Percussion Injury Device. (A) Craniectomy site (black) for central fluid percussion injury hub placement (located midway between bregma and lambda); Right and left craniectomy sites (red) for bilateral entorhinal cortex lesions (superior to entorhinal cortex).

Appendix B

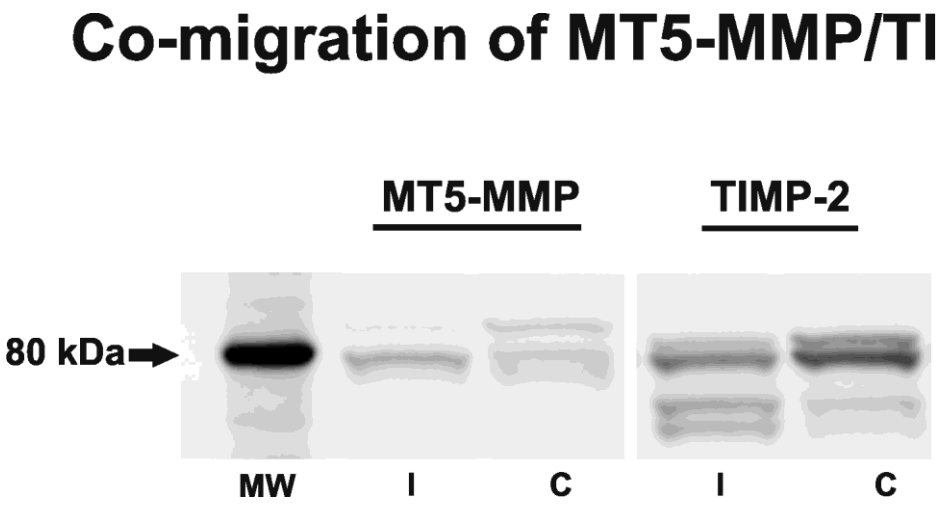

Figure B-1 Co-migration of MT5-MMP and TIMP-2 in Protein Analysis.
Representative gel blots illustrating co-migration of TIMP-2 with MT5-MMP within gel system, indicating potential MT5-MMP/TIMP-2 binding in hippocampal tissue.

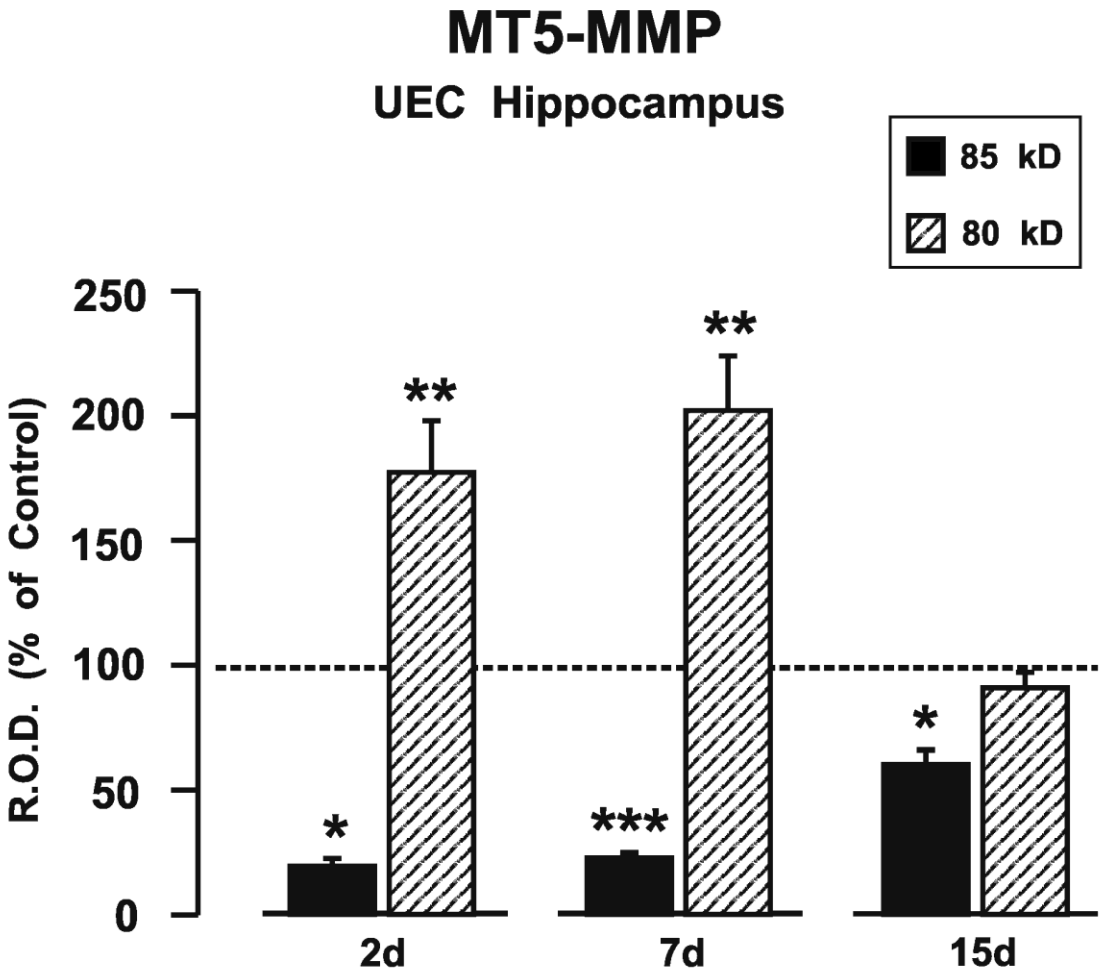

Figure B-2 Hippocampal Protein Expression of Additional MT5-MMP Forms following UEC. Values expressed as percent of contralateral hippocampus over 2, 7, and 15d postinjury time intervals. As indicated in Chapter 2, UEC insult produced significant increases in 80 kDa MT5-MMP (MT5) at 2 and 7d, however, an additional minor 85 kDa form was observed to decrease across all postinjury time intervals. 2d: n=7; 7d: n=4; 15d n=6. *p<0.05, **p<0.01, ***p<.001.

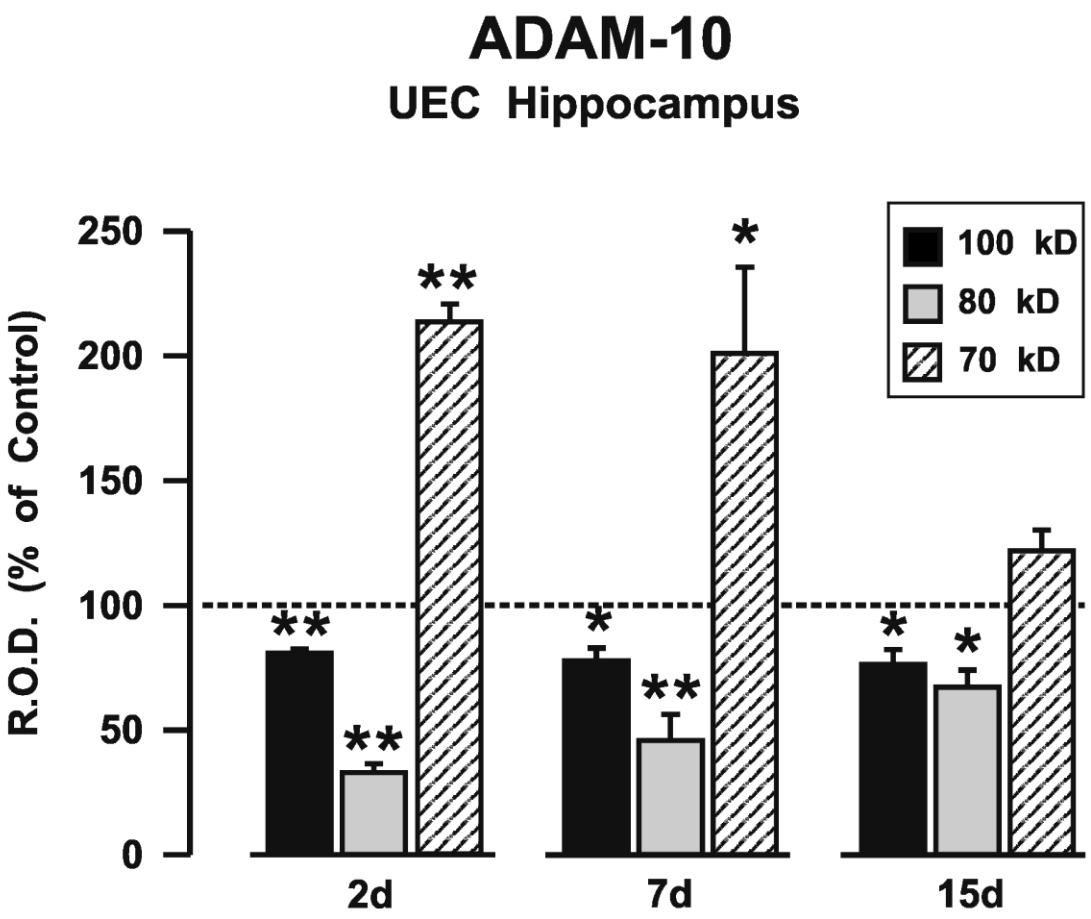

Figure B-3 Hippocampal Protein Expression of Additional ADAM-10 Forms following UEC. Values expressed as percent of contralateral hippocampus over 2, 7, and 15d postinjury time intervals. As indicated in Chapter 2, UEC insult induced a significant increase in 70 kDa ADAM-10 protein expression at 2 and 7d with a reduction to levels not different from controls at 15d. By contrast, 100 kDa and 80 kDa forms showed significant reductions across all postinjury time intervals. 2d: n=4; 7d: n=5; 15d n=4. *p<0.05, **p<0.01.

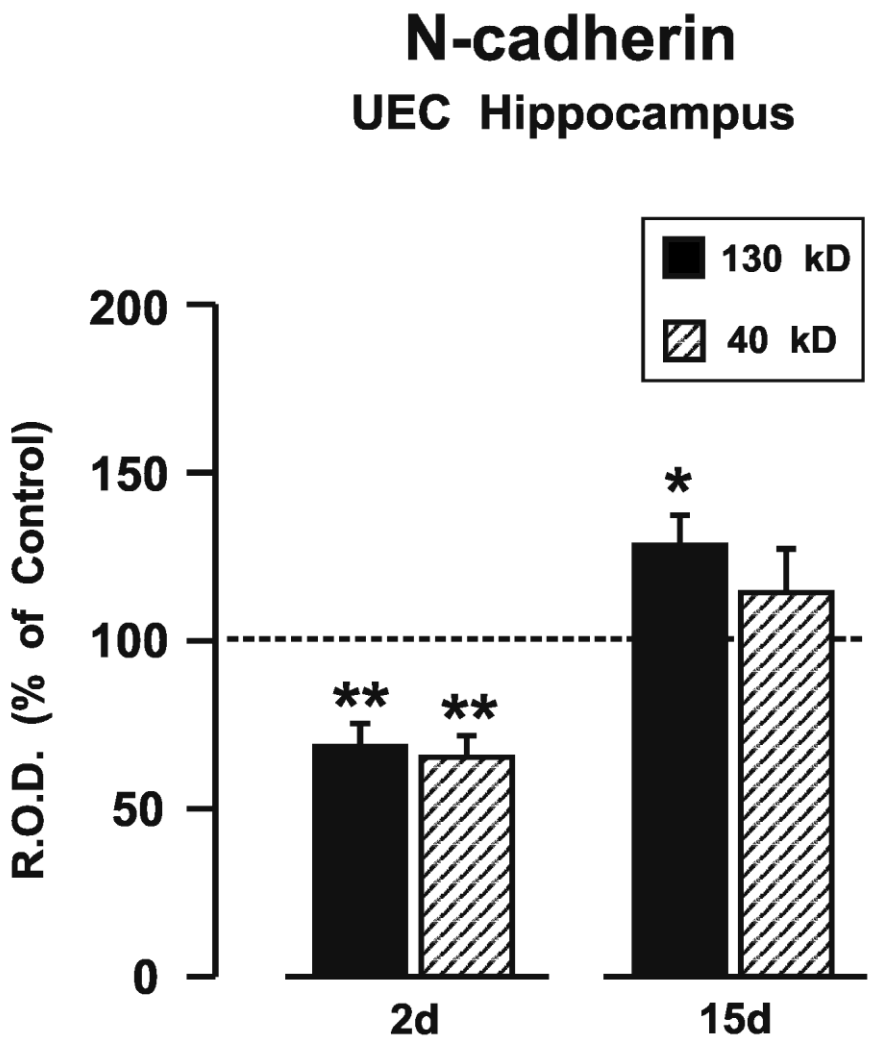

Figure B-4 Hippocampal Protein Expression of Additional N-cadherin Forms following UEC. Values expressed as percent of contralateral hippocampus over 2 and 15d postinjury time intervals. As indicated in Chapter 2, UEC insult produced a significant reduction at 2d for both 130 kDa and 40 kDa forms, and 15d elevation for the 130kDa form. The 40 kDa form was not measurable at 7d, therefore this time interval was not represented. 2d: n=7; 15d n=6. *p<0.05, **p<0.01.

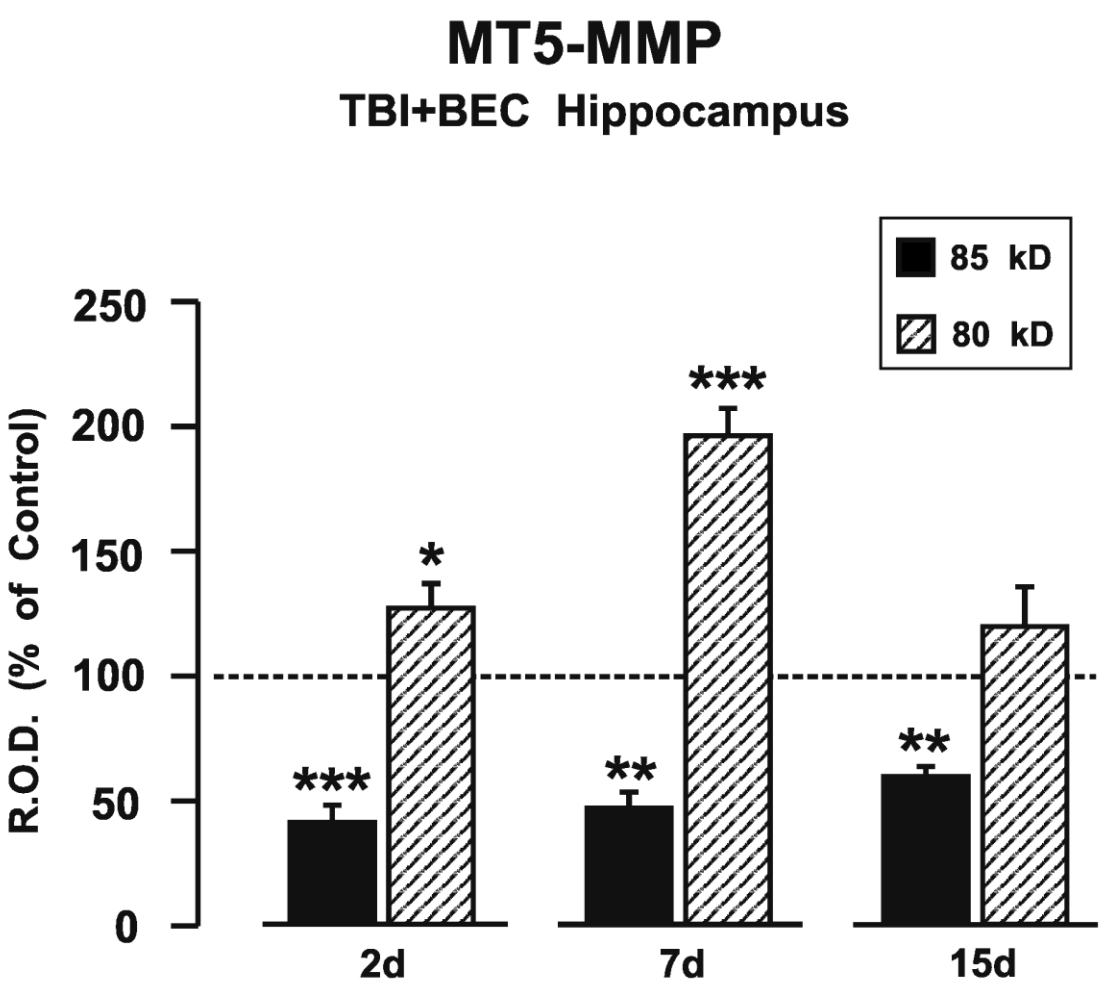

Figure B-5 Hippocampal Protein Expression of Additional MT5-MMP Forms following TBI+BEC. Values expressed as percent of sham controls over 2, 7, and 15d postinjury time intervals. As indicated in Chapter 2, TBI+BEC induced a significant increase in 80 kDa MT5-MMP (MT5) protein expression at 2 and 7d, with reduction to levels not different from controls at 15d. By contrast, the additional 85 kDa form showed significant reduction across all postinjury time intervals. Injured=I, Sham=S; 2d: I=10, S=8; 7d: I=16, S=10; 15d I=8, S=7; *p<0.05, **p<0.01, ***p<0.001.

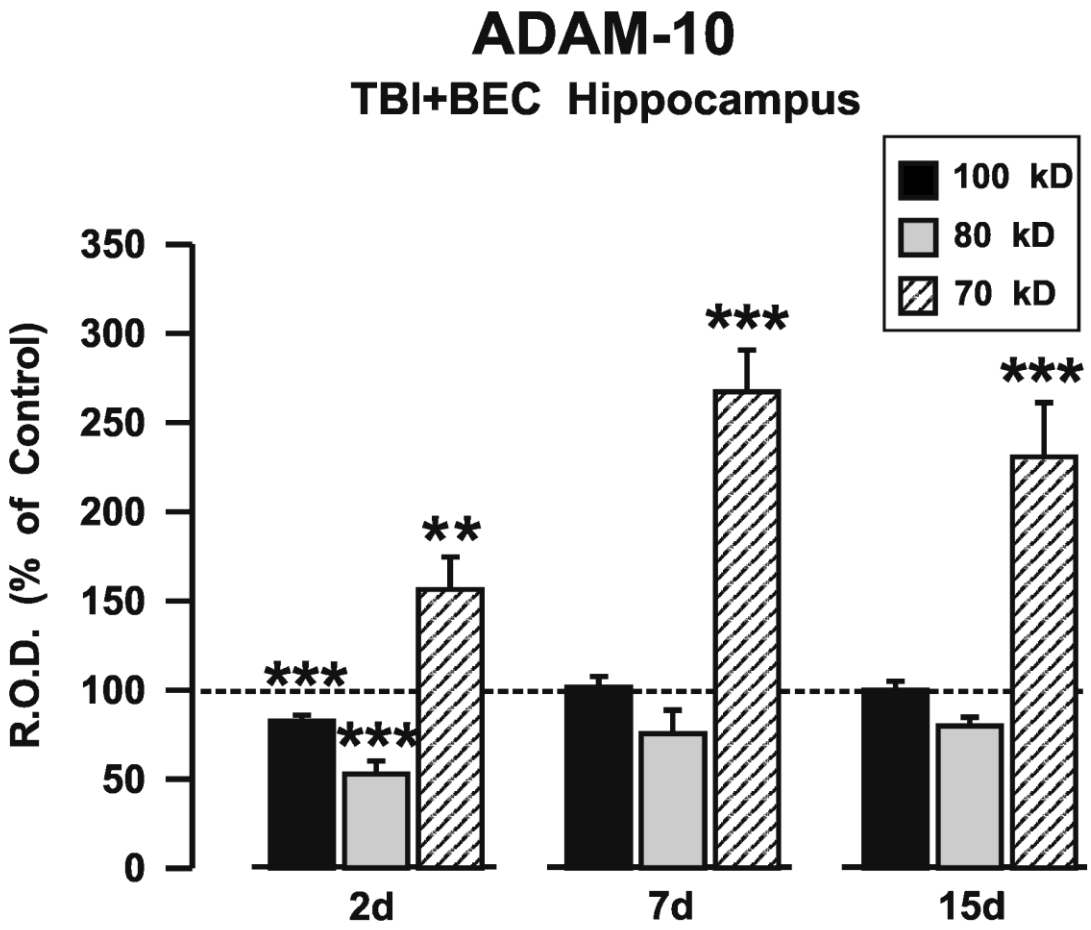

Figure B-6 Hippocampal Protein Expression of Additional ADAM-10 Forms following TBI+BEC. Values expressed as percent of sham controls over 2, 7, and 15d postinjury time intervals. As indicated in Chapter 2, TBI+BEC produced a significant increase in 70 kDa ADAM-10 over all postinjury time intervals. By contrast, 100 kDa and 80kDa showed a significant reduction at 2d only, and levels not different from controls at 7 and15d. Injured=I; Sham=S; 2d: I=6, S=8; 7d: I=7, S=9; 15d I=7, S=8; *p<0.05, **p<0.01, ***p<0.001.

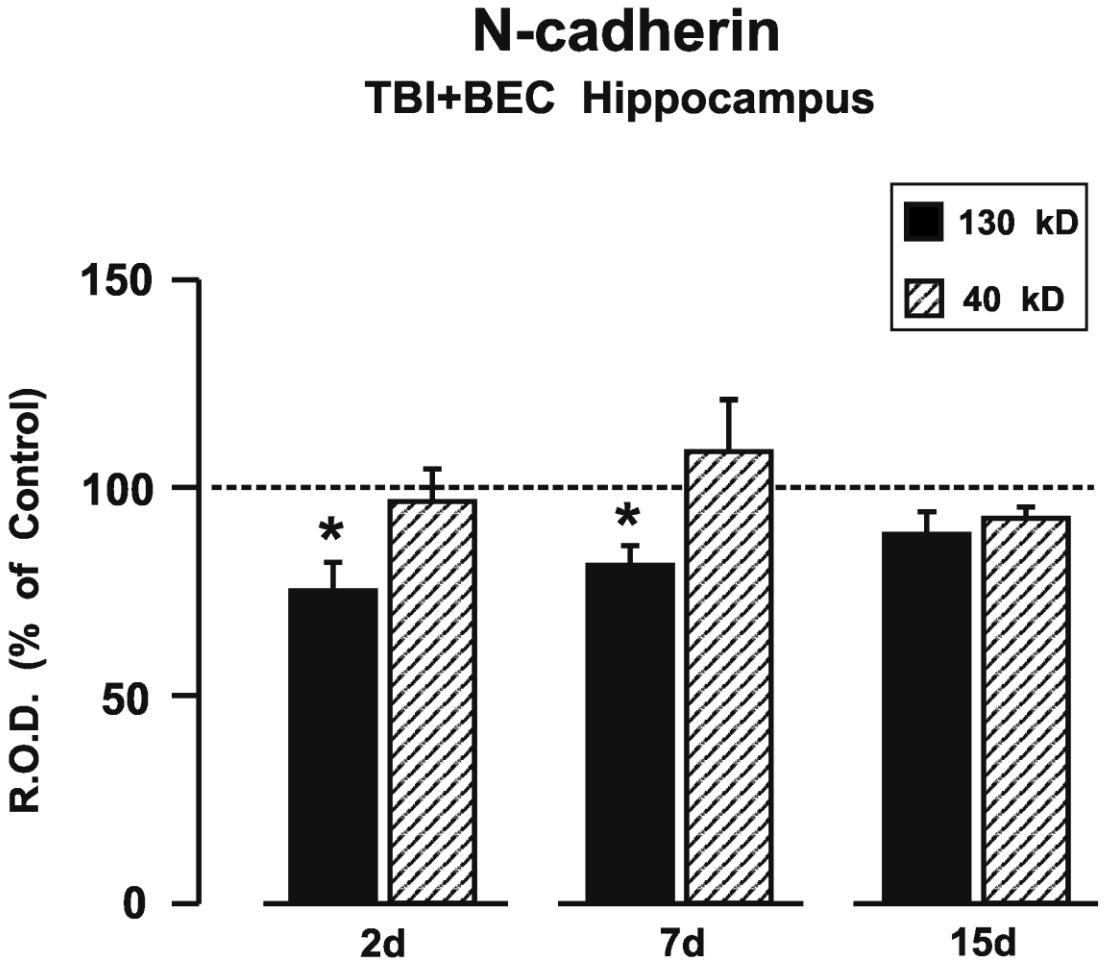

Figure B-7 Hippocampal Protein Expression of Additional N-cadherin Forms following TBI+BEC. Values expressed as percent of sham controls over 2, 7, and 15d postinjury time intervals. As indicated in Chapter 2, TBI+BEC produced a significant reduction at 2 and 7d in the 130 kDa form and levels not different from control in the 40 kDa form across all postinjury time intervals. Injured=I; Sham=S; 2d: I=9, S=8; 7d: I=15-16, S=10; 15d I=7, S=3-8; *p<0.05.

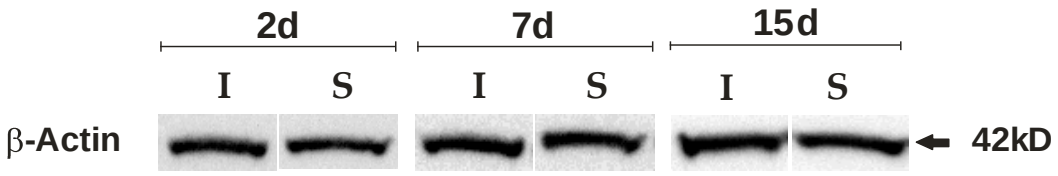

Figure B-8 Representative β-actin load control for Western blot Analysis. β-actin (42kDa) was selected as a load control for TBI+BEC Western blot analysis in Chapters 2 and 3. Representative samples from 2, 7, and 15d TBI+BEC blots show a typical pattern indicative of even loading in injured (I) and sham control (S) lanes across all postinjury time intervals.

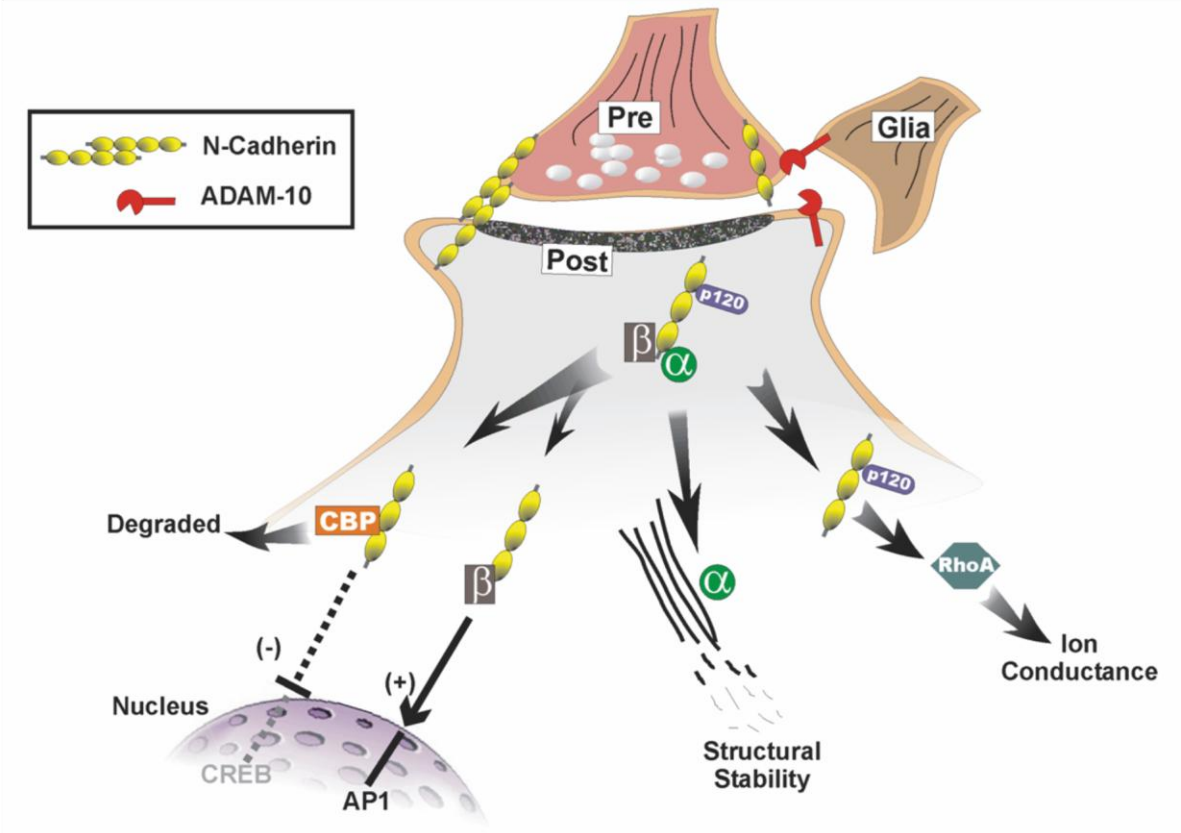

Figure B-9 Downstream Intracellular Signaling as a Result of N-cadherin Processing by ADAM-10. Schematic representation of ADAM-10 induced N-cadherin ectodomain shedding at the synaptic interface. N-cadherin processing and fragmentation may have downstream influence on ion conductance, structural integrity of the synapse, and β-catenin and CREB driven gene transcription. These events may potentially affect the plasticity process and recovery following TBI.

Appendix C

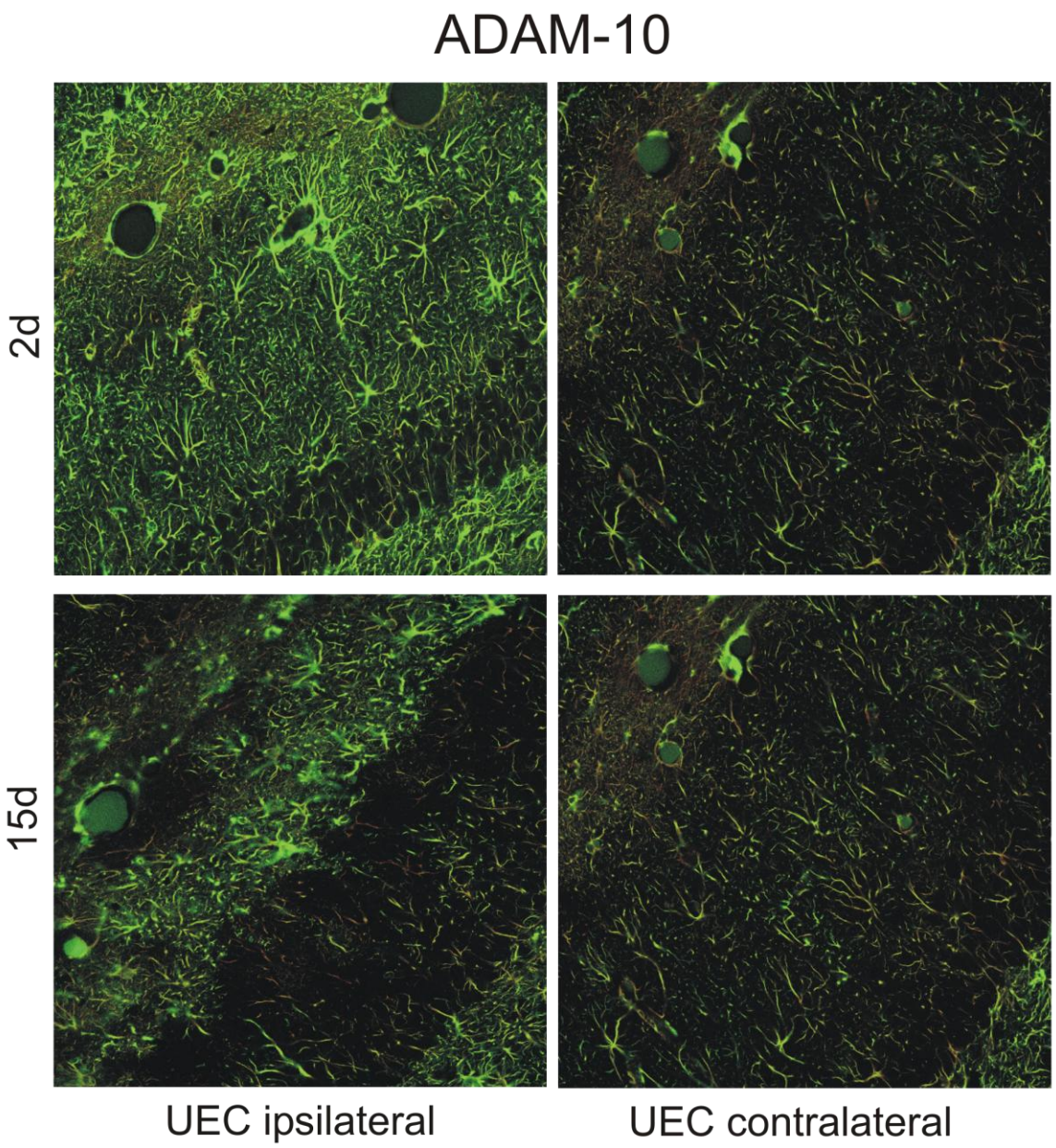

Figure C-1 Molecular Layer Localization of ADAM-10 with GFAP at 2 and 15d following UEC. Confocal overlay images showing ADAM-10 (green) and GFAP (red) co-localization (yellow) in ipsilateral (injured) and contralateral (control) dentate molecular layers at 2 and 15d postinjury. In ipsilateral images note increased ADAM-10 signal filling reactive astrocytes throughout molecular layer at 2d. By 15d, signal is concentrated in the outer molecular layer. Contralateral side shows ADAM-10 localization within non-reactive astrocytes, but with a much reduced level of signal. 40X magnification.

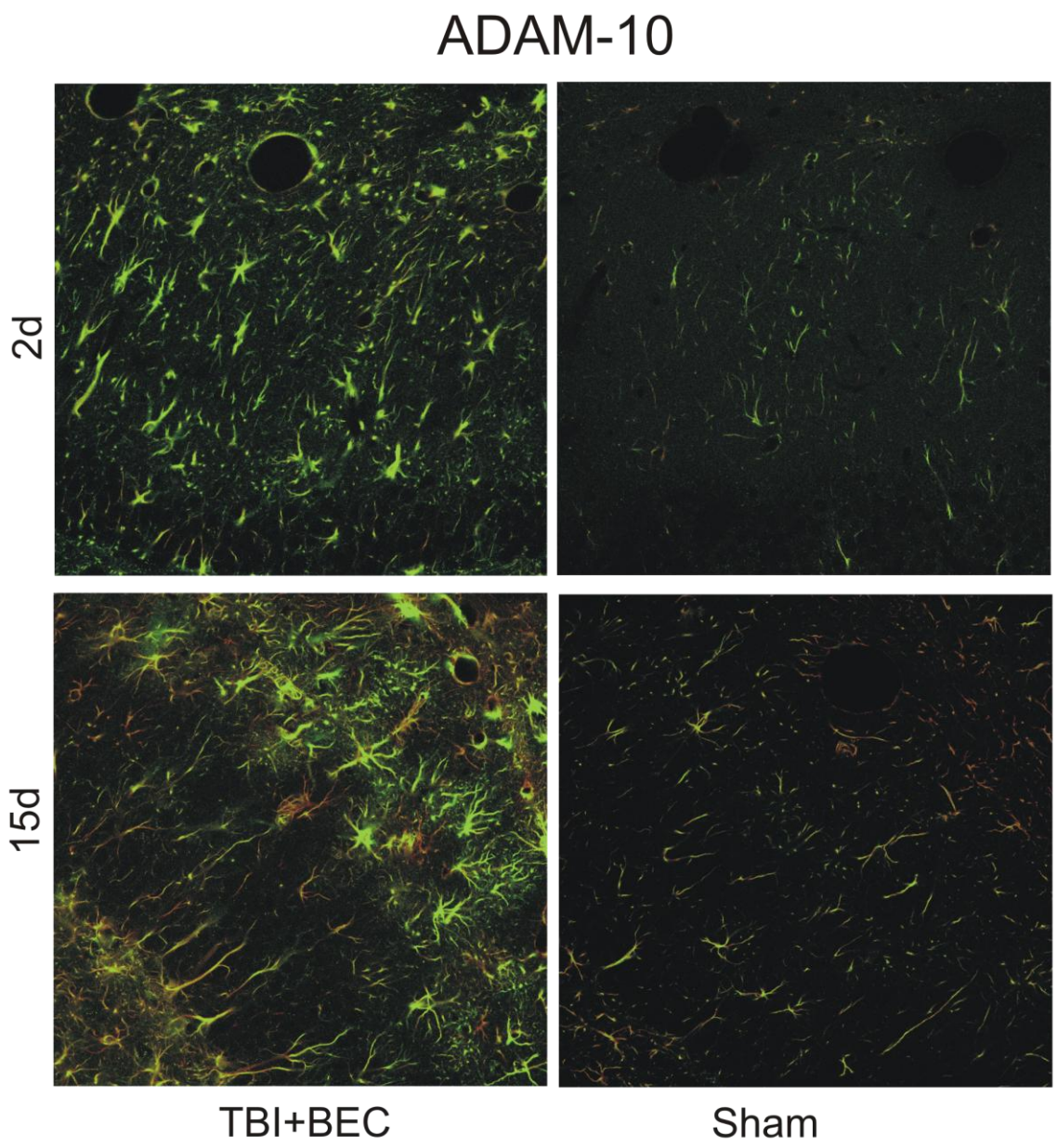

Figure C-2 Molecular Layer Localization of ADAM-10 with GFAP at 2 and 15d following TBI+BEC. Confocal overlay images showing ADAM-10 (green) and GFAP (red) co-localization (yellow) in combined-injured and sham dentate molecular layers at 2 and 15d survival. Note increased ADAM-10 signal filling reactive astrocytes throughout molecular layer at 2d postinjury. As in the UEC, ADAM-10 signal is concentrated in the outer molecular layer at 15d post-TBI+BEC. Sham shows reduced ADAM-10 signal within non-reactive astrocytes throughout molecular layer. 40X magnification.

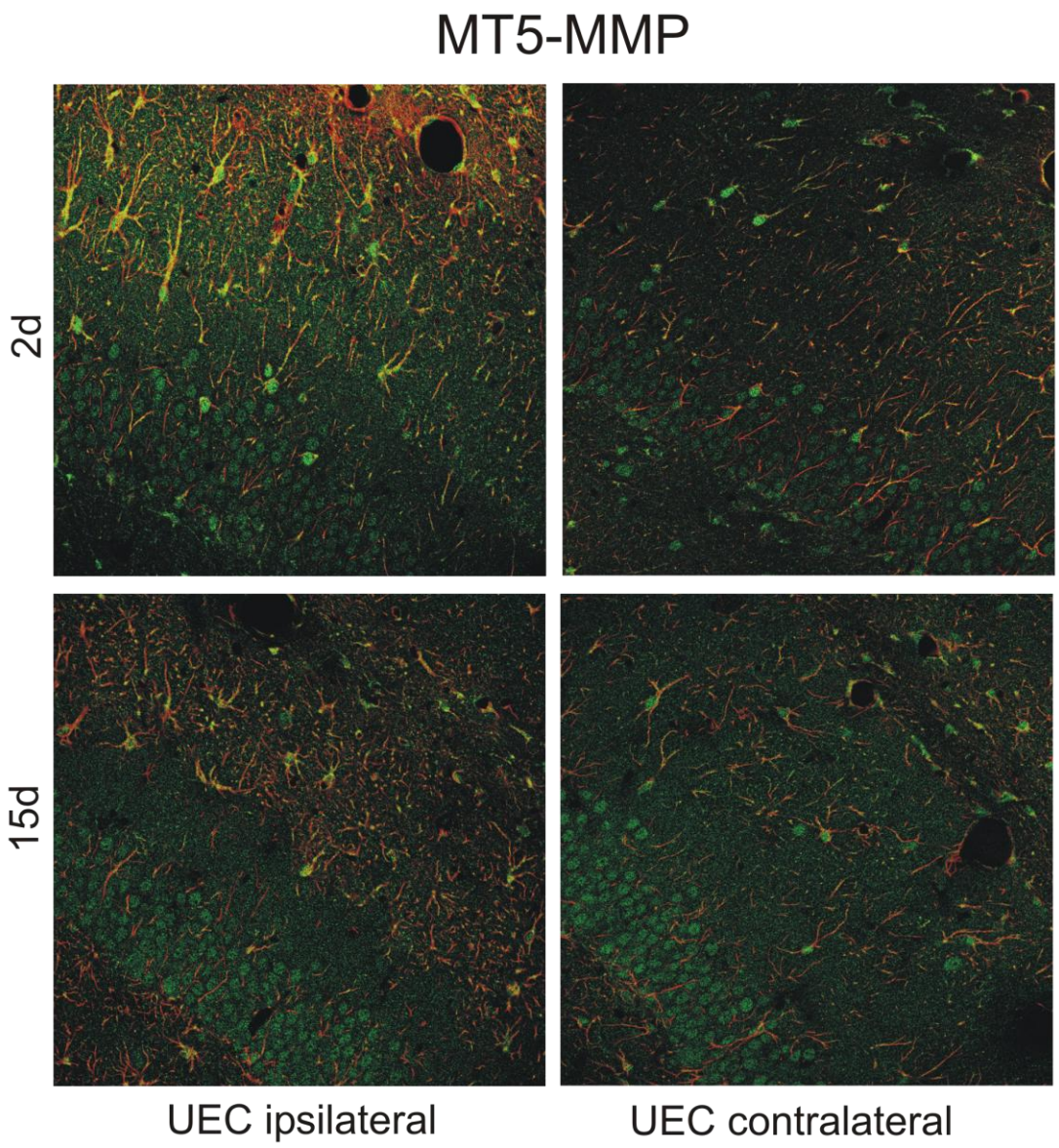

Figure C-3 Molecular Layer Localization of MT5-MMP with GFAP at 2 and 15d following UEC. Confocal overlay images showing MT5-MMP (green) and GFAP (red) co-localization (yellow) in ipsilateral (injured) and contralateral (control) dentate molecular layers. In the ipsilateral side, note increased outer molecular layer signal at 2d and 15d. MT5-MMP is clustered within reactive astrocyte cell bodies and extends into the glial processes. Neuronal labeling is seen as punctate signal in granule cell bodies and throughout molecular layer neuropil. At 15d ipsilateral and contralateral overlays show similar signal intensity and profile for MT5-MMP, despite differences in astrocytic response. MT5-MMP granule cell signal will need further confirmation with neuronal antibody markers. 40X magnification.

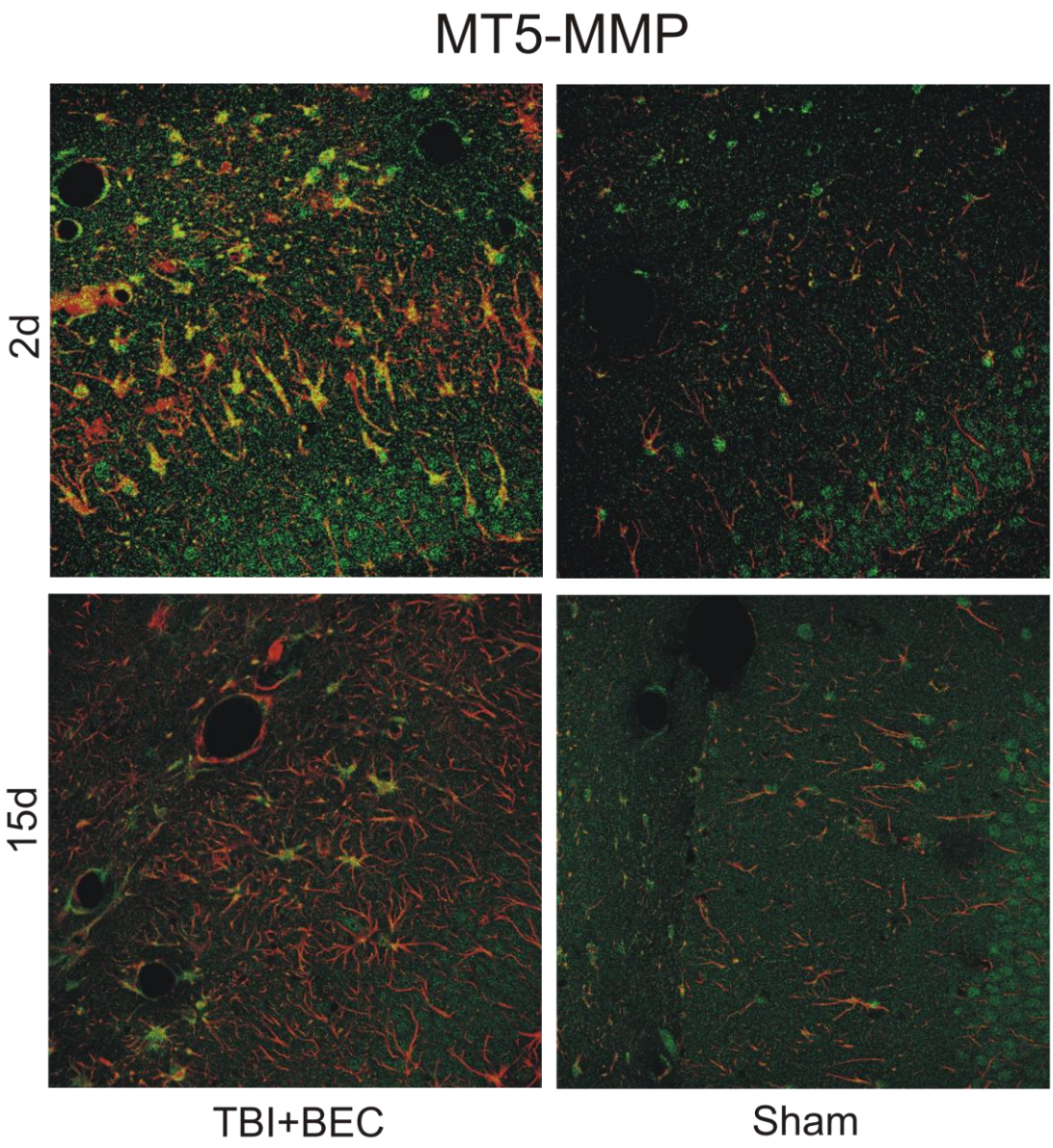

Figure C-4 Molecular Layer Localization of MT5-MMP with GFAP at 2 and 15d following TBI+BEC. Confocal overlay images showing MT5-MMP (green) and GFAP (red) co-localization (yellow) in injured and sham dentate molecular layers. In injured images, note increased in cluster-like MT5-MMPsignal within reactive astrocyte cell bodies and out into selective processes, as well as punctate signal throughout molecular layer and over granule cell bodies at 2d. At 15d injured and sham overlays show similar signal intensity and profile for MT5-MMP, despite the difference in astrocytic response. MT5-MMP granule cell signal will need further confirmation with neuronal antibody markers. 40X magnification.

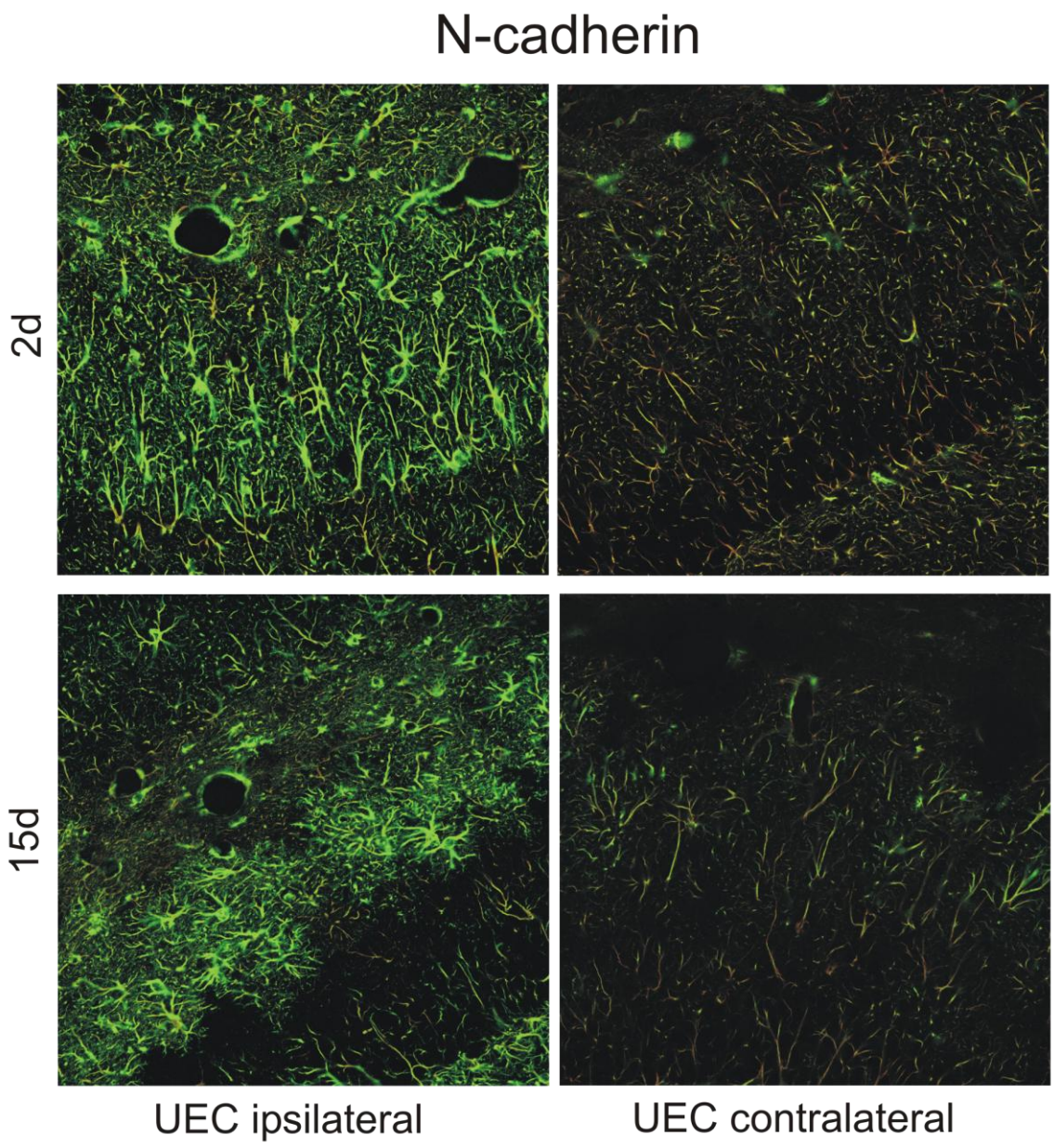

Figure C-5 Molecular Layer Localization of N-cadherin with GFAP at 2 and 15d following UEC. UEC confocal overlay images showing N-cadherin (green) and GFAP (red) co-localization (yellow) at 2 and 15d in ipsilateral (injured) and contralateral (control) dentate molecular layers. In ipsilateral images note increased N-cadherin signal filling reactive astrocytes throughout molecular layer at 2d and concentrated in the outer molecular layer at 15d. UEC contralateral side shows N-cadherin localization within non-reactive astrocytes, but with much reduced signal. 40X magnification.

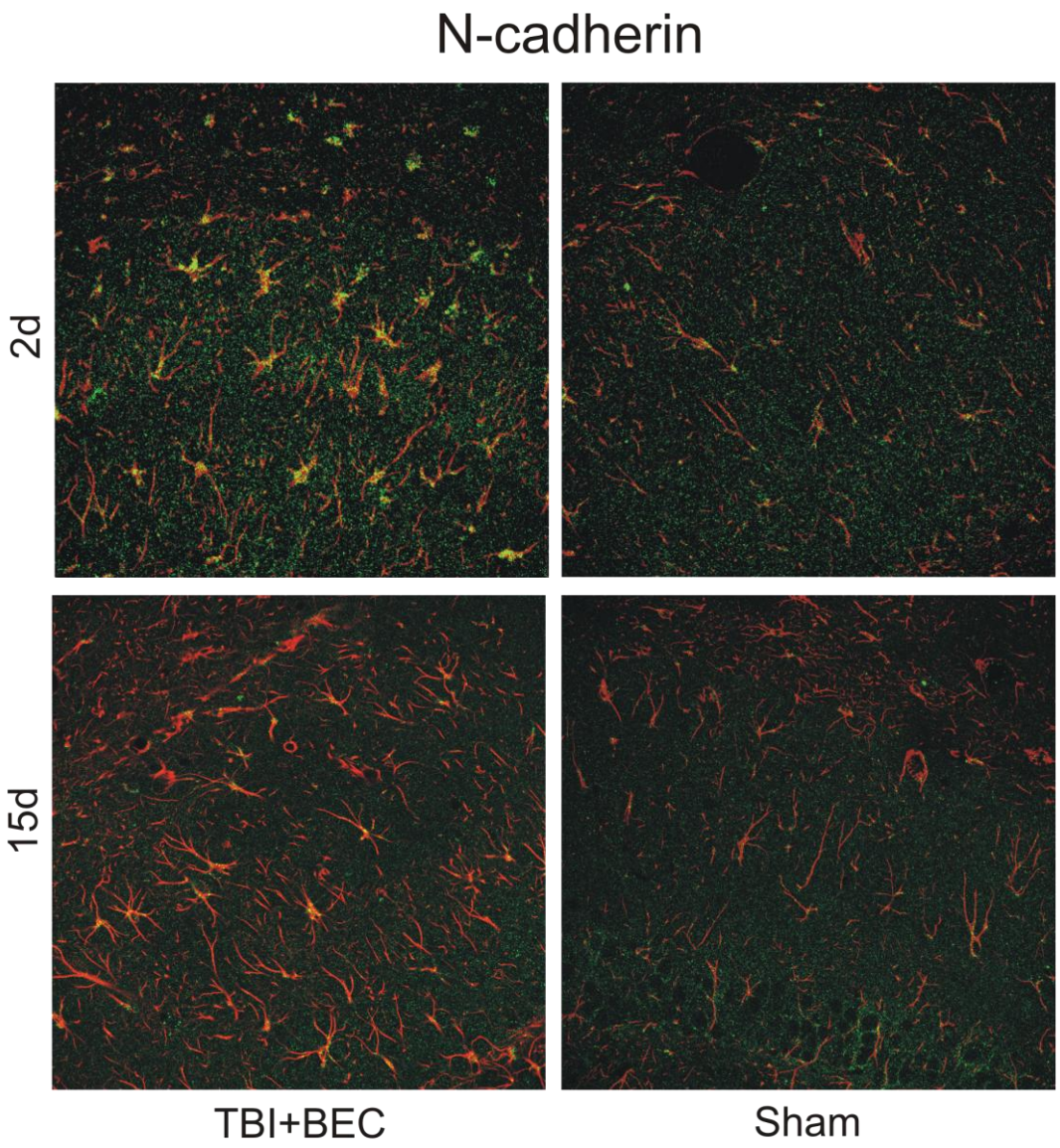

Figure C-6 Molecular Layer Localization of N-cadherin with GFAP at 2 and 15d following TBI+BEC. Confocal overlay images showing N-cadherin (green) and GFAP (red) co-localization (yellow) at 2 and 15d injured and sham dentate molecular layers. In 2d injured images, note increased N-cadherin signal primarily within reactive astrocyte cell bodies, as well as punctuate signal throughout molecular layer. At 2d, sham shows a much reduced N-cadherin signal and less reactive astrocytic labeling, although neuropil punctuate profile is similar. At 15d injured and sham overlays show similar signal intensity and profile for N-cadherin, despite the moderate difference in astrocytic response. Punctate N-cadherin signal is also visible throughout the molecular layer at 15d in both injured and sham. 40X magnification.

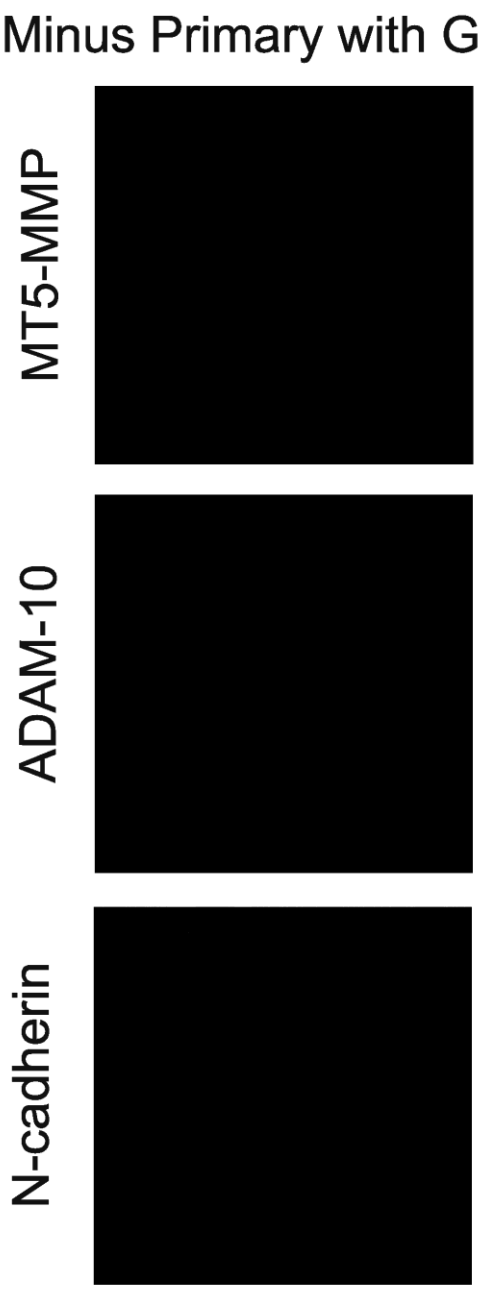

Figure C-7: Representative Minus Primary Controls for ADAM-10, MT5-MMP and N-cadherin immunostaining with GFAP. 7d UEC injured examples of tissue processed without the primary antibody show an absence of signal. Overlay images are representative of tissue for all immunohistochemical experiments in the study. From top to bottom: MT5-MMP/GFAP; ADAM-10/GFAP; and N-cadherin/GFAP confocal overlay images. 40X magnification.

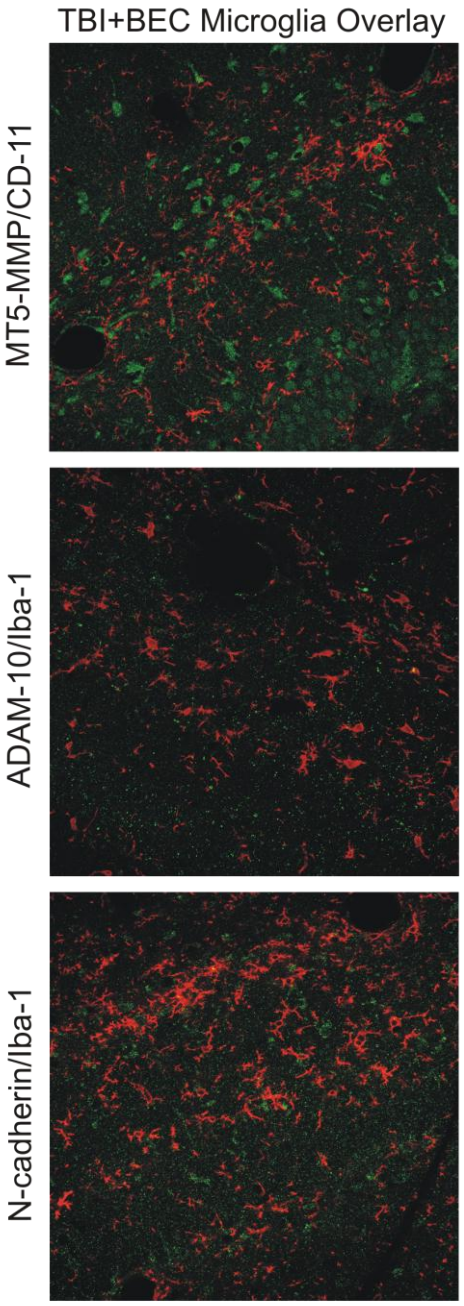

Figure C-8 Representative Molecular Layer Localization of MT5-MMP, ADAM-10, and N-cadherin with microglial markers CD-11/Iba-1. Co-localization of MT5-MMP with CD-11, and ADAM-10 and N-cadherin with Iba-1 in TBI+BEC injured tissue. Note no MT5-MMP, ADAM-10 and N-cadherin signal within molecular layer microglia following injury. MT5-MMP/ADAM-10/N-cadherin (green), CD-11/Iba-1 (red); 40X magnification.

Appendix D

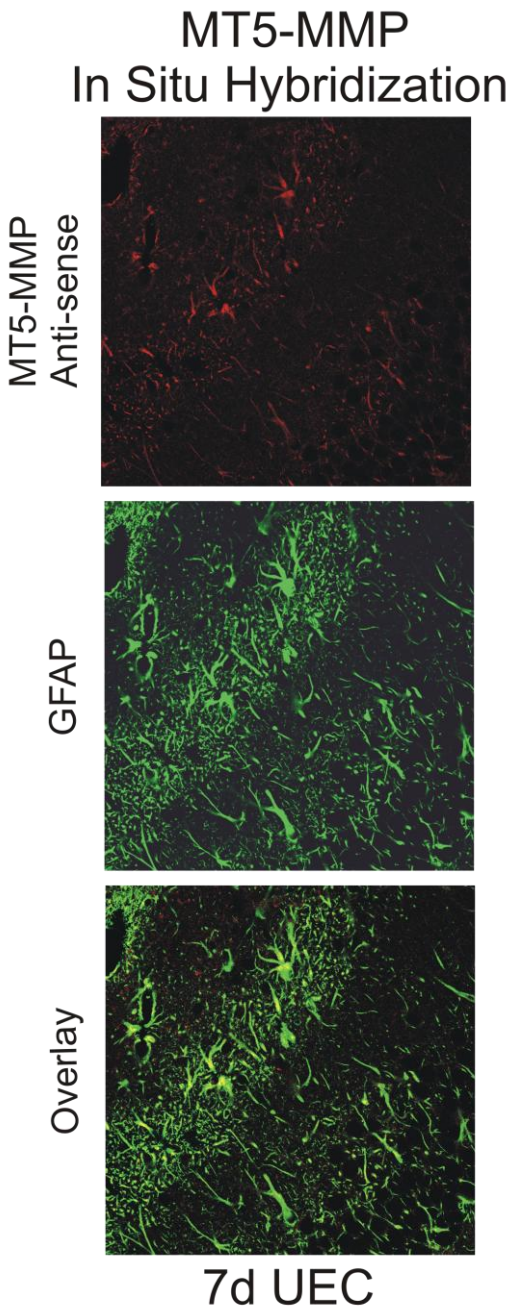

Fig. D-1 Molecular layer Co-localization of MT5-MMP RNA transcript with GFAP 7d post-UEC. Confocal images showing single channel MT5-MMP anti-sense ribroprobe (red) and reactive astrocytic marker GFAP (green) and overlay (yellow). Note increased co-labeling in outer molecular layer, primarily within astrocytic processes. 40X magnification.

Appendix E

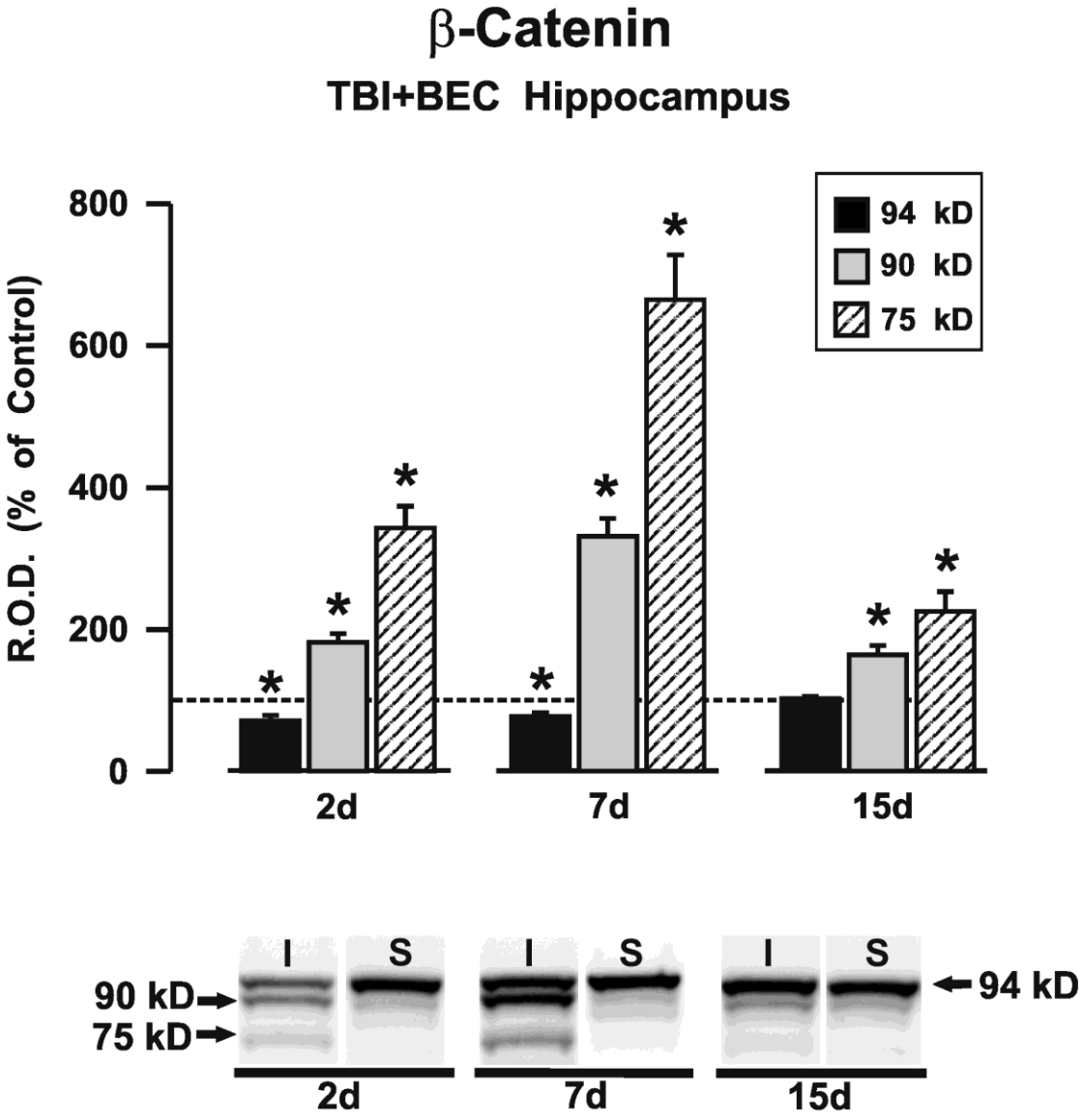

Figure E-1 Hippocampal Protein Expression of β-catenin following TBI+BEC. Values expressed as percent of sham controls. Significant increase of 90 kDa and 75kD β-catenin forms was seen at all time points, with significant decrease in 94 kDa at 2 and 7d. Greatest change in expression was found in the 75 kDa form, peaking at 7d. Representative blots shown below. I=Injured; S=Sham. 2d: Injured n=5, Sham n=3; 7d: Injured n=9, Sham n=4; 15d: Injured n=4, Sham n=3. *p<0.05.

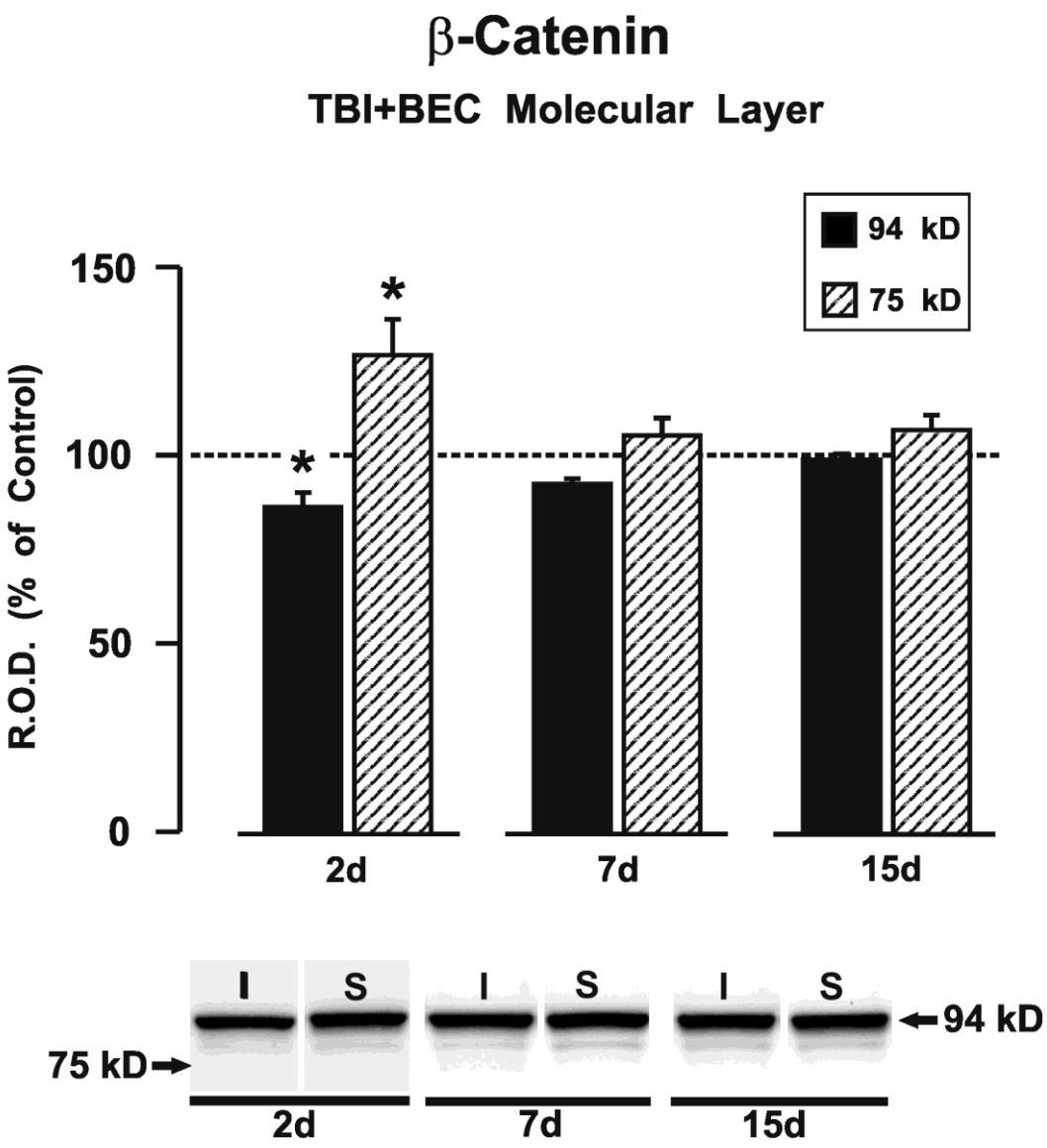

Figure E-2 Molecular Layer Protein Expression of β-catenin following TBI+BEC. Values expressed as percent of sham controls. Significant increase in 75 kDa form and decrease in 94 kDa form was seen only at 2d. No significant changes in β-catenin expression were found at 7 and 15d. A measurable 90 kDa form was not detectable in ML samples. Representative blots shown below. I=Injured; S=Sham; n-values: 2d I=4, S=6; 7d I=4, S=4; 15d I=3, S=3; *p<0.05.A

Vita

Kelly Michelle Warren was born on July 26, 1978 in Fairfax, VA, and is a citizen of the United States of America. She attended James Madison University in Harrisonburg, VA and earned a Bachelor of Science degree in Kinesiology. Kelly then attended the University of Saint Augustine for Health Sciences where she earned a Master's degree in Physical Therapy.